

**Differentiation between calcium antagonists *in vitro* and their effects in models of cerebral ischaemia.**

Thesis submitted for the degree of  
Doctor of Philosophy  
at the University of Leicester

by

Barry Kenny BSc (Hons).  
Department of Pharmacology  
Syntex Research, Edinburgh.  
Registered in conjunction with the  
Department of Pharmacology,  
University of Leicester

October, 1991.

UMI Number: U548339

All rights reserved

INFORMATION TO ALL USERS

The quality of this reproduction is dependent upon the quality of the copy submitted.

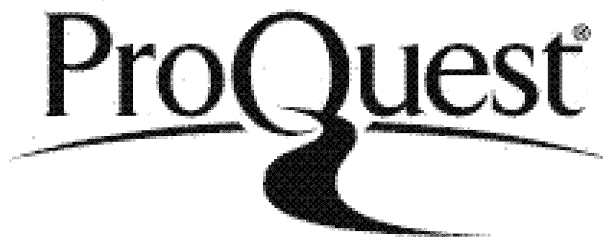
In the unlikely event that the author did not send a complete manuscript and there are missing pages, these will be noted. Also, if material had to be removed, a note will indicate the deletion.



UMI U548339

Published by ProQuest LLC 2015. Copyright in the Dissertation held by the Author.  
Microform Edition © ProQuest LLC.

All rights reserved. This work is protected against  
unauthorized copying under Title 17, United States Code.



ProQuest LLC  
789 East Eisenhower Parkway  
P.O. Box 1346  
Ann Arbor, MI 48106-1346



7501024235

X751901732

**Abstract of PhD thesis: The differentiation between calcium antagonists *in vitro* and their effects in models of cerebral ischaemia. Submitted by Barry Kenny, October 29, 1991.**

Different classes of calcium antagonist were defined *in vitro* using radioligand binding studies and the efficacy of the classes as neuroprotective agents was assessed *in vivo* using a novel model of cerebral ischaemia.

Radioligand binding studies indicated that the interactions of both class I (dihydropyridines) and class II (verapamil and diltiazem) calcium antagonists was temperature-, ligand- and tissue-dependent. Specific binding sites for class III antagonists (flunarizine, fluspirilene, etc.), labelled by [<sup>3</sup>H] fluspirilene in skeletal muscle, were not identified in brain membranes, although these compounds allosterically regulated [<sup>3</sup>H] dihydropyridine binding in brain. All class III compounds displayed high affinity for the [<sup>3</sup>H] fluspirilene site in skeletal muscle membranes and thus fluspirilene appeared to be prototypical of this class of compound. The calcium antagonist SR 33557 identified a novel high affinity binding site in brain membranes. This putative fourth site for a calcium antagonist appeared to be tightly coupled to the dihydropyridine site. Class III calcium antagonists displayed a range of affinities for other receptor and ion channel sites but all class III calcium antagonists showed high affinity for rat brain sodium channels labelled by [<sup>3</sup>H] batrachotoxinin-A-20- $\alpha$ -benzoate.

In the Mongolian gerbil, forebrain ischaemia (10 min but not 5 min) with 7 days recovery produced a significant reduction in the number of [<sup>3</sup>H] PN 200-110 binding sites in hippocampal membranes. However, an  $\omega_3$  ligand, [<sup>3</sup>H] PK 11195 was shown to be a better marker of ischaemic damage. Binding experiments and autoradiographic analysis demonstrated a significant ischaemia-induced increase in the density of  $\omega_3$  sites after 5 min forebrain ischaemia and 7 days recovery in the gerbil. The distribution and pharmacology of  $\omega_3$  sites was very species dependent.

[<sup>3</sup>H] PK 11195 was successfully used to establish a model of focal ischaemia in the mouse, in which a variety of class III calcium antagonists were found to be neuroprotective. The anticonvulsant phenytoin was active in the mouse focal ischaemia model and in an *in vitro* model of ischaemia (using the rat hippocampal slice). The interaction of calcium antagonists with both Na<sup>+</sup> and Ca<sup>2+</sup> channels is proposed to be important as a mechanism whereby these agents confer neuroprotection.

### **Acknowledgements.**

The work in this thesis was carried out in the Department of Pharmacology, Syntex Research, Edinburgh. This thesis, nor any part of it, has been submitted to any other university.

I would like to express my sincere thanks to several people for their help and advice during the course of this work. Firstly, I would like to thank my supervisors Dr. Mike Spedding and Prof. Steve Nahorski for their advice, support and encouragement. In particular, I am grateful for the amount of Mike's personal time generously offered during the course of this work. I would also like to thank several of my colleagues for their advice and help: Bob Sheridan, Alison MacKinnon, Chick Calder and Christine Brown. I would also like to extend my gratitude to other members of the laboratory for their support and encouragement, particularly Mike Stewart and Nick Manuel.

Finally, thanks to my wife Carolyn, whose support has been invaluable, especially in the last year since the arrival of our daughter.

## Abbreviations.

The abbreviations used in this thesis are in accordance with the guidelines set out in the *British Journal of Pharmacology* instructions to authors. Those not defined in the above publication are listed below.

$\text{Ca}^{2+}$ ,  $\text{Mg}^{2+}$ ,  $\text{Cd}^{2+}$ ,  $\text{Na}^{+}$ ,  $\text{K}^{+}$ ,  $\text{Mn}^{2+}$ ,  $\text{Gd}^{3+}$  refer to the free ionic species of calcium, magnesium, cadmium, sodium, potassium, manganese and gadolinium.

ACSF	artificial cerebrospinal fluid
AMPA	$\alpha$ -amino-3-hydroxy-5-methyl-4-isoxazoleproponic acid
2-APV	2-amino-5-phosphonopentanoic acid
Bay K 8644	(methyl-1,4-dihydro-2,6,-dimethyl-3-nitro-4-(2-trifluoromethylphenyl)-pyridine-5-carboxylate
BTX-B	batrachotoxinin-A-20- $\alpha$ -benzoate
$[\text{Ca}^{2+}]_i$	intracellular free $\text{Ca}^{2+}$
CaBP	calcium binding protein
CPP	3-[( $\pm$ )-2-carboxypiperazin-4-yl]propyl-1-phosphonic acid
CT	cranial computed X-ray tomography
DHP	dihydropyridine
EDTA	ethylenediaminetetraacetic acid
ER	endoplasmic reticulum
GppNHp	5'-guanylylimododiphosphate
GTP	guanosine 5'-triphosphate
HEPES	(N-[2-hydroxyethyl]piperazine-N'-[2-ethanesulfonic acid])
$\text{IP}_3$	inositol-1,4,5-trisphosphate
MCA	middle cerebral artery
MK 801	[(+)-5-methyl-10,11-dihydro-5H-dibenzo-[a,d]cyclohepten-5,10-imine] maleate.
MOPS	(3-[N-morpholino]propanesulfonic acid)
NMDA	N-methyl-D-aspartate

PET	positron emission tomography
PIP <sub>2</sub>	phosphatidylinositol-4,5-bisphosphate
PN 200-110	(isopropyl-4-(2,1,3-benzoxadiazol-4-yl)-1,4,-dihydro-2,6-dimethyl-5-methoxy-carbonylpyridine-3-carboxylate)
PK 11195	[1-(2-chlorophenyl-N-methyl-N-(1-methylpropyl)-3-isoquinolinecarboxamide]
PMSF	phenylmethanesulphonyl fluoride
PTB	peripheral-type benzodiazepine
RO 5-4864	4'-chlorodiazepam
SAH	subarachnoid haemorrhage
SCH 23390	(7-chloro-8-hydroxy-3-methyl-1-phenyl-2,3,4,5-tetrahydro-1H-3-benzamine hydrochloride)
SL 82.0715	[(±)-α-(4-chlorophenyl)-4-[(4-fluorophenyl)methyl]-1-piperidine ethanol]
SR 33557	[(2-isopropyl-1-((4-(3-(N-methyl-N-(3,4-dimethoxy-β-phenethyl)-amino)propyloxy)benzenesulfonyl))-indolizine]
t.i.d.	three times daily
Tris HCl	Tris[hydroxymethyl]aminomethane hydrochloride
VOC	voltage-operated calcium channel

---

## Contents.

### Chapter One.

General Introduction	Page
<b>1.1. Clinical Stroke.</b>	1
1.1.1. Distribution of stroke.	1
1.1.2. Detection of infarcted brain tissue.	3
1.1.3. Epidemiological studies and risk factors.	4
1.1.4. Drug treatment of clinical stroke.	6
<b>1.2. Cellular calcium control mechanisms.</b>	8
1.2.1. Intracellular calcium regulation.	9
1.2.2. Extrusion mechanisms.	12
1.2.3. Increases in intracellular $\text{Ca}^{2+}$ .	12
1.2.4. Different forms of voltage and receptor gated calcium entry.	13
1.2.5. Molecular biology.	16
1.2.6. N-methyl-D-aspartate mediated $\text{Ca}^{2+}$ entry.	19
<b>1.3. Experimental cerebral ischaemia: mechanisms and models.</b>	21
1.3.1. Evidence for an involvement of calcium ion homeostasis in cell ischaemia.	21
1.3.2. Ischaemic cell damage-selective neuronal vulnerability and relation to forebrain ischaemia.	24
1.3.3. Other models of forebrain ischaemia.	25
1.3.4. Focal ischaemia.	27
1.3.5. <i>In vitro</i> models of ischaemia.	28
1.3.6. NMDA antagonists protect against neuronal damage in focal and forebrain ischaemia models.	30

<b>1.4. Calcium antagonists form a heterogeneous group of compounds.</b>	<b>31</b>
1.4.1. Identification of calcium antagonist binding sites by radiolabelled calcium antagonists.	31
1.4.2. There are different classes of calcium antagonist.	33
1.4.3. Class I calcium antagonists.	33
1.4.4. Class II calcium antagonists.	36
1.4.5. Class III calcium antagonists.	37
1.4.6. Calcium channel activators.	39
1.4.7. Plasticity of L-type calcium channels labelled by [ <sup>3</sup> H] DHPs.	40
1.4.8. Evidence to suggest that calcium antagonists may confer protection in models of cerebral ischaemia.	42
1.4.9. Is there a clinical potential for calcium antagonists or NMDA antagonists.	44

<b>1.5. Experimental aims and thesis outline.</b>	<b>45</b>
---	-----------

## **Chapter Two.**

<b>Methods.</b>	<b>48</b>
2.1.1. Standard membrane preparation for [ <sup>3</sup> H] dihydropyridine binding assays.	48
2.1.2. Standard binding assay for [ <sup>3</sup> H] dihydropyridines and generalised assay protocols for competition, saturation and kinetic experiments.	48
2.1.3. Determination of assay protein.	51
2.2.1. Protocol for kinetic studies.	51
2.2.2. Determination of dissociation rate by infinite dilution.	52
2.3.1. Preparation and assay of cardiac tissue for [ <sup>3</sup> H] DHP binding.	53
2.3.2. Preparation of rabbit skeletal muscle membranes for [ <sup>3</sup> H] calcium antagonist binding studies.	53
2.3.3. [ <sup>3</sup> H] PN 200-110 and [ <sup>3</sup> H] fluspirilene binding to skeletal muscle membranes.	54

2.3.4. Preparation and assay of cardiac and cerebrocortical membranes for $\alpha_1$ binding studies.	55
2.3.5. Preparation of $\beta_1$ cardiac membranes.	56
2.3.6. [ $^3\text{H}$ ] Batrachotoxinin-A-20- $\alpha$ -benzoate binding assay in rat cortical synaptosomes.	56
2.3.7. Dopamine (D1 and D2) binding assays using rat corpus striatum.	58
2.3.8. [ $^3\text{H}$ ] Spiperone binding to 'spirodecanone' sites in hippocampal membranes.	59
2.3.9. [ $^3\text{H}$ ] PK 11195 binding assays.	59
2.3.10. [ $^3\text{H}$ ] SR 33557 binding to rat cerebral cortex membranes.	60
2.4. Experimental criteria and analysis of radioligand binding data.	61
2.5. Experimental validation of [ $^3\text{H}$ ] PN 200-110 binding assay.	63
2.6. <i>In vitro</i> receptor autoradiography studies.	66
2.6.1. [ $^3\text{H}$ ] PN 200-110 autoradiography.	67
2.6.2. [ $^3\text{H}$ ] PK 11195 autoradiography.	69
2.7. Experimental ischaemia.	69
2.7.1. Forebrain ischaemia in the Mongolian gerbil.	69
2.7.2. Standardised forebrain ischaemia by use of a 5 min isoelectric period.	70
2.7.3. Middle cerebral artery occlusion in the mouse.	72
2.7.4. [ $^3\text{H}$ ] PK 11195 binding assay on ischaemic mouse MCA samples.	74
2.8. Statistical analysis.	74
2.9. Drugs and chemicals used in the study.	74
2.10. Administration of drugs in mouse MCA model.	75

### **Chapter Three. The characterisation and differentiation between calcium antagonists in radioligand binding experiments.**

3.1. [ $^3\text{H}$ ] PN 200-110 binding to rat cerebral cortex.	76
3.1.1. [ $^3\text{H}$ ] PN 200-110 distribution of binding sites.	76
3.1.2. Pharmacological specificity of [ $^3\text{H}$ ] PN 200-110 binding to rat cerebral cortex at 25°C.	79

3.1.3. Interactions of palmitoyl carnitine at the [ <sup>3</sup> H] PN 200-110 site in rat cerebral cortex.	81
3.1.4. Effects of tissue, temperature and different radioligands on the allosteric regulation of [ <sup>3</sup> H] DHP binding, exemplified by d-cis diltiazem and verapamil.	85
3.2. Interaction of class III calcium antagonists with [ <sup>3</sup> H] DHP and Na <sup>+</sup> channel binding sites.	89
3.2.1. pH effects at the [ <sup>3</sup> H] PN 200-110 site in rat cerebral cortex.	90
3.2.2. Effects on [ <sup>3</sup> H] PN 200-110 saturation binding parameters.	93
3.2.3. Effects on [ <sup>3</sup> H] PN 200-110 dissociation kinetics.	93
3.2.4. Affinity of class III calcium antagonists for rat striatal dopamine D <sub>1</sub> and D <sub>2</sub> receptors.	96
3.2.5. Interaction of class III calcium antagonists with synaptosomal Na <sup>+</sup> channels labelled by [ <sup>3</sup> H] BTX.	98
3.2.6. Interaction of class III calcium antagonists with spirodecane binding sites labelled by [ <sup>3</sup> H] spiperone in rat hippocampus.	100
3.2.7. Comparative interaction of class III and other calcium antagonists at [ <sup>3</sup> H] PN 200-110 and [ <sup>3</sup> H] fluspirilene binding sites in skeletal muscle membranes.	102
3.3. Characterisation and identification of a novel high affinity binding site in rat cerebral cortex for [ <sup>3</sup> H] SR 33557.	107
3.3.1. Effects at the [ <sup>3</sup> H] PN 200-110 binding site in rat cortex.	107
3.3.2. Comparative reversal of calcium antagonism by d-cis diltiazem.	107
3.3.3. [ <sup>3</sup> H] SR 33557 binding to rat cerebral cortex.	112
3.3.4. Pharmacological specificity for other calcium channel activators and antagonists.	113
3.3.5. Effect of inorganic ions.	113
3.4. Discussion.	117

---

**Chapter Four. *In vivo* models of cerebral ischaemia: Effects on calcium channels and an assessment of calcium antagonists as potential neuroprotective agents.**

4.1.	The effect of forebrain ischaemia on [ <sup>3</sup> H] DHP antagonist binding parameters.	135
4.1.1.	The effect of 5 min forebrain ischaemia and 7 days recovery in the Mongolian gerbil on [ <sup>3</sup> H] PN 200-110 binding parameters.	135
4.1.2	[ <sup>3</sup> H] nitrendipine binding to ischaemic gerbil brain.	138
4.1.3.	The effect of reperfusion periods on [ <sup>3</sup> H] PN 200-110 binding parameters.	139
4.1.4.	Effects of 10 min forebrain ischaemia and various reperfusion times on [ <sup>3</sup> H] PN 200-110 binding site parameters.	139
4.2.	[ <sup>3</sup> H] PK 11195: Pharmacological characterisation.	143
4.2.1.	High affinity neuronal binding sites exist for [ <sup>3</sup> H] PK 11195.	143
4.2.2.	Selectivity of peripheral and non-peripheral benzodiazepines for $\omega_3$ sites.	146
4.2.3.	Effects of RO 5-4864 on [ <sup>3</sup> H] PK 11195 saturation binding parameters.	148
4.2.4.	Effect of RO 5-4864 on [ <sup>3</sup> H] PK11195 dissociation kinetics.	150
4.2.5.	[ <sup>3</sup> H] PK 11195 labelled subcellular fractions.	152
4.2.6.	Distribution of binding sites.	152
4.2.7.	[ <sup>3</sup> H] PK 11195 binding to purified mitochondria.	155
4.3.	[ <sup>3</sup> H] PK 11195 as a marker of ischaemic damage following forebrain ischaemia.	156
4.4.1.	[ <sup>3</sup> H] PK 11195 as a marker of neuronal damage in a mouse model of focal ischaemia.	159
4.4.2.	Post-ischaemic changes in cortical [ <sup>3</sup> H] PK 11195 binding parameters following middle cerebral artery occlusion.	159
4.4.3.	MK 801 and RS 87476 attenuate the ischaemia-induced increase in $\omega_3$ sites following left MCA occlusion in the mouse.	162

4.4.4. Comparative neuroprotection by other CEBs in the mouse MCA occlusion model.	166
4.4.5. Phenytoin is a potent neuroprotective agent in the mouse MCA occlusion model.	167
4.5. Discussion.	171

## **Chapter Five. An assessment of neuroprotection in the rat *in vitro* hippocampal slice.**

5.1. Introduction.	185
5.2. Methods.	188
5.2.1. Preparation of rat hippocampal slices.	188
5.2.2. Establishment of population spikes.	189
5.2.3. Establishment of a standard ischaemic protocol.	189
5.3. Results.	193
5.3.1. The effect of NMDA antagonists and calcium antagonists on population spikes during and after 10 min hypoxia.	193
5.3.2. The effect of phenytoin on population spike parameters and slice viability after 10 min hypoxia.	193
5.4. Discussion.	198

## **Chapter Six.**

Epilogue: Why are class III calcium antagonists neuroprotective?	204
--	-----

## **Appendix:**

Theoretical basis for the direct identification of receptors in competition, kinetic and saturation radioligand binding experiments.	i-iv
--	------

<b>References.</b>	210
--------------------	-----

## Tables and Figures.

<b>Chapter One.</b>	<b>Page</b>
Figure 1.1. The distribution of acute stroke.	i
Figure 1.2. Neurovasculature and the circle of Willis.	2
Figure 1.3. The subunit composition of the L-type calcium channel.	17
Figure 1.4. The putative structure of the $\alpha_1$ subunit and the transmembrane helices of the L channel.	18
Figure 1.5. Schematic role for calcium in the ischaemic cascade leading to neuronal death.	22
Figure 1.6. The structure of calcium antagonists.	35
Figure 1.7. Multiple allosterically coupled binding sites for different classes of calcium antagonist associated with the L-type calcium channel.	38
Table 1.1. Classification of calcium antagonist subgroups.	34
Table 1.2. Literature variation in the efficacy of nimodipine in experimental cerebral ischaemia.	43
 <b>Chapter Two.</b>	
Figure 2.1. Specific binding of [ $^3$ H] PN 200-110 as a function of assay protein.	65
Figure 2.2. EEG recordings before and during forebrain ischaemia in the Mongolian gerbil.	71
Table 2.1. The effect of membrane wash cycles on [ $^3$ H] PN 200-110 binding parameters in rat cerebral cortex.	64
Table 2.2. The effect of different storage and resuspension protocols on [ $^3$ H] PN 200-110 binding parameters in rat cerebral cortex.	64
 <b>Chapter Three.</b>	
Figure 3.1. Saturation binding isotherms of [ $^3$ H] PN 200-110 binding to rat cerebral cortex.	77
Figure 3.2. Kinetics of [ $^3$ H] PN 200-110 binding to rat cerebral cortex membranes.	77

Figure 3.3 (i-iii). The effect of palmitoyl carnitine on [ <sup>3</sup> H] PN 200-110 binding in i) competition experiments, ii) kinetic experiments and iii) saturation experiments.	82
Figure 3.4. The effect of palmitoyl carnitine on $\alpha_1$ , $\beta_1$ and DHP receptor densities in heart and cerebral cortex membranes.	83
Figure 3.5. Comparative allosteric properties of verapamil and diltiazem.	88
Figure 3.6. Allosteric regulation of [ <sup>3</sup> H] PN 200-110 binding by <i>cis</i> and <i>trans</i> diclofurime.	90
Figure 3.7. The effect of calcium antagonists on [ <sup>3</sup> H] PN 200-110 dissociation in rat cortex.	95
Figure 3.8. Displacement of [ <sup>3</sup> H] spiperone from spirodecane sites in rat hippocampus.	101
Figure 3.9. Displacement of [ <sup>3</sup> H] fluspirilene from skeletal muscle membranes by calcium antagonists.	104
Figure 3.10. Comparative displacement studies for class III calcium antagonists at [ <sup>3</sup> H] PN 200-110 and [ <sup>3</sup> H] fluspirilene sites.	105
Figure 3.11. Scatchard transformation of [ <sup>3</sup> H] PN 200-110 binding in the presence of SR 33557.	108
Figure 3.12. The effect of SR 33557 on [ <sup>3</sup> H] PN 200-110 dissociation kinetics.	108
Figure 3.13. Comparative reversal by d- <i>cis</i> diltiazem of the inhibition of [ <sup>3</sup> H] nitrendipine binding by calcium antagonists.	110
Figure 3.14. Comparative reversal by d- <i>cis</i> diltiazem of the inhibition of [ <sup>3</sup> H] nitrendipine by SR 33557 and flunarizine.	111
Figure 3.15. Comparative dissociation of [ <sup>3</sup> H] SR 33557 from rat cortex by infinite dilution and excess unlabelled SR 33557.	115
Figure 3.16. A proposal for allosterically coupled binding sites for calcium antagonists.	134
Table 3.1. Tissue distribution of [ <sup>3</sup> H] PN 200-110 binding sites.	76
Table 3.2. Affinity of calcium antagonists at the [ <sup>3</sup> H] PN 200-110 binding site in rat cerebral cortex.	78

Table 3.3. Effect of GppNHp on the displacement of [ <sup>3</sup> H] PN 200-110 by Bay K 8644 in rat cerebral cortex.	79
Table 3.4. The effect of increasing acyl chain length on the ability of acyl carnitines to displace [ <sup>3</sup> H] PN 200-110 in rat cerebral cortex.	81
Table 3.5. The effect of palmitoyl carnitine on $\alpha_1$ , $\beta_1$ , and DHP saturation binding parameters in cerebral cortex and heart.	85
Table 3.6. The effect of temperature on the displacement of [ <sup>3</sup> H] PN 200-110 by diltiazem and verapamil.	86
Table 3.7. The effect of decreasing pH on calcium antagonist affinity.	91
Table 3.8. Comparative saturation shifts of [ <sup>3</sup> H] PN 200-110 binding in rat cerebral cortex by fluspirilene and nifedipine.	92
Table 3.9. The effect of calcium antagonists on the rate of dissociation of [ <sup>3</sup> H] PN 200-110.	94
Table 3.10. The affinity of class III calcium antagonists at dopamine D <sub>1</sub> and D <sub>2</sub> receptors.	97
Table 3.11. The affinity of calcium antagonists for [ <sup>3</sup> H] BTX labelled Na <sup>+</sup> channels.	99
Table 3.12. Affinities of calcium antagonists for [ <sup>3</sup> H] PN 200-110 and [ <sup>3</sup> H] fluspirilene sites in skeletal muscle membranes.	106
Table 3.13. Comparative affinities of calcium antagonists and ions at the [ <sup>3</sup> H] SR 33557 and [ <sup>3</sup> H] PN 200-110 binding sites in rat cortex.	116

## Chapter Four.

Figure 4.1. The effect of forebrain ischaemia in the gerbil on [ <sup>3</sup> H] PN 200-110 autoradiography.	137
Figure 4.2. Scatchard transformation of [ <sup>3</sup> H] PK 11195 binding to rat, gerbil and mouse cerebral cortex membranes.	144
Figure 4.3. Scatchard transformation of [ <sup>3</sup> H] PK 11195 binding to rat and gerbil cortical membranes in the presence of RO 5-4864.	149

Figure 4.4. The effect of RO 5-4864 on [ <sup>3</sup> H] PK 11195 dissociation kinetics from rat and gerbil cortex.	151
Figure 4.5. Subcellular distribution of [ <sup>3</sup> H] PK 11195 in rat and gerbil brain.	153
Figure 4.6. The effect of 5 min forebrain ischaemia and 7 days recovery in the gerbil on [ <sup>3</sup> H] PK 11195 autoradiography.	158
Figure 4.7. Temporal increase in the density of [ <sup>3</sup> H] PK 11195 binding sites following MCA occlusion in the mouse.	161
Figure 4.8. The effect of MCA occlusion in the mouse on [ <sup>3</sup> H] PK 11195 autoradiography.	163
Figure 4.9. Comparative neuroprotective potency of calcium antagonists in the mouse MCA model.	169
Figure 4.10. The protective effect of phenytoin in the mouse MCA model.	170
Table 4.1. The effect of 5 min forebrain ischaemia and 7 days recovery on [ <sup>3</sup> H] PN 200-100 binding parameters in gerbil brain.	136
Table 4.2. Autoradiographic parameters for [ <sup>3</sup> H] PN 200-110 binding to gerbil brain sections following 5 min forebrain ischaemia.	138
Table 4.3. The effect of 5 min forebrain ischaemia and 7 days recovery on [ <sup>3</sup> H] nitrendipine binding in the gerbil.	140
Table 4.4. The effect of reperfusion on [ <sup>3</sup> H] PN 200-110 binding following 5 min forebrain ischaemia in the gerbil.	141
Table 4.5. The effect of various reperfusion times on [ <sup>3</sup> H] PN 200-110 binding in the gerbil following 10 min forebrain ischaemia.	142
Table 4.6. Saturation binding parameters for [ <sup>3</sup> H] PK 11195 binding to rat and gerbil brain membranes.	145
Table 4.7. Affinities of $\omega_3$ and non- $\omega_3$ compounds for the [ <sup>3</sup> H] PK 11195 binding site in hippocampal and cortical membranes from rat and gerbil.	147
Table 4.8. The effect of RO 5-4864 on [ <sup>3</sup> H] PK 11195 saturation binding parameters in rat and gerbil cortex.	148
Table 4.9. The effect of RO 5-4864 on [ <sup>3</sup> H] PK 11195 dissociation kinetics in rat, gerbil and mouse cortical membranes.	150

Table 4.10. Displacement of [ <sup>3</sup> H] PK 11195 from purified mitochondria from rat and gerbil cortex.	154
Table 4.11. The effect of 5 min forebrain ischaemia on [ <sup>3</sup> H] PK 11195 binding parameters in gerbil brain membranes.	156
Table 4.12. The effect of 5 min forebrain ischaemia and 7 days recovery on [ <sup>3</sup> H] PK 11195 autoradiography parameters in gerbil brain.	157
Table 4.13. Temporal [ <sup>3</sup> H] PK 11195 binding changes to cortical brain tissue following MCA occlusion in the mouse.	160
Table 4.14. Ischaemia-induced increases in cortical $\omega_3$ sites after MCA occlusion and 7 days recovery in the mouse.	162
Table 4.15. The effect of MK 801, RS 87476 and nimodipine on the ischaemia-induced increase in $\omega_3$ site following MCA occlusion in the mouse.	164
Table 4.16. The effect of flunarizine, SR 33557, nimodipine and (+) butaclamol on the ischaemia-induced increase in $\omega_3$ sites following MCA occlusion in the mouse.	167

## Chapter Five.

Figure 5.1. The <i>in vitro</i> rat hippocampal slice.	186
Figure 5.2. Hypoxic changes in the population spike at 32°C with 10 mM glucose.	190
Figure 5.3. Hypoxic changes in the population spike at 35°C with 4 mM glucose.	191
Figure 5.4. The effect of hypoxia on population spikes and DC potential in the presence and absence of phenytoin.	196
Figure 5.5. The effect of phenytoin on population spike amplitude during and after hypoxia.	197
Table 5.1. The effect of drugs on population spike parameters during and after hypoxia.	194

Table 5.2. The effect of hypoxia on population spike parameters in the presence and absence of phenytoin.	195
--	-----

**Appendix.**

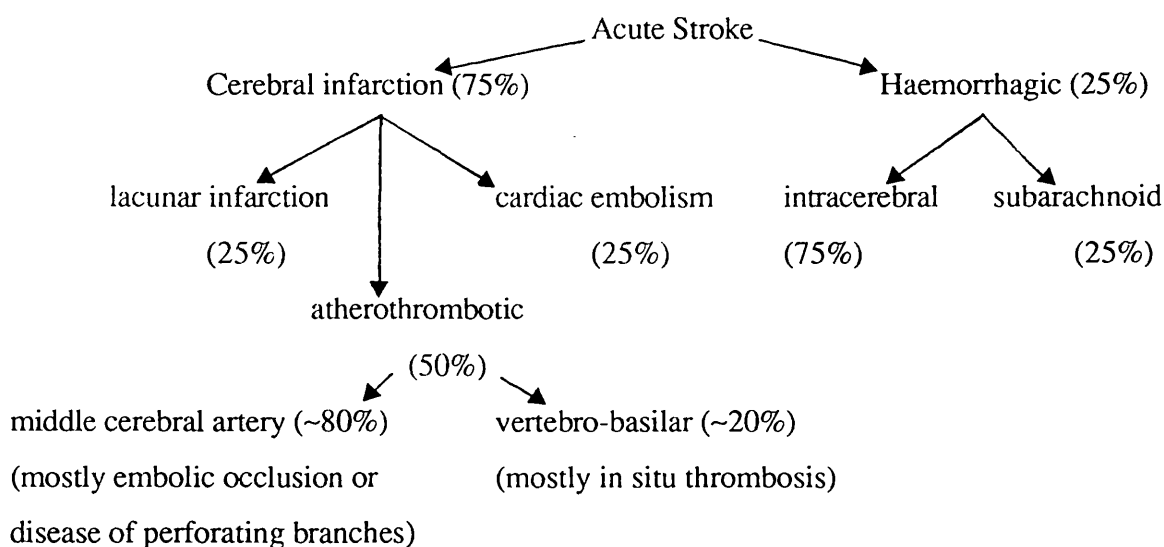
Figure 1. The hyperbolic relationship of mass action.	i-iv
---	------

## 1.1 CLINICAL STROKE

### 1.1.1. Distribution of strokes.

'Stroke' is a generalised term for vascular diseases affecting the brain, the outcome of which is a severe reduction or complete cessation of blood flow, depriving tissue of metabolic support (cerebral ischaemia), and ultimately resulting in cell death. In the western world stroke is the third highest cause of mortality (in the U.S.A. the annual occurrence rate is 250,000), and its consequences are the leading cause of physical disablement. The sequence of events leading to cerebral infarction occurs as a direct result of a reduction or cessation of blood supply whether it be general or localised. However, as a disease, stroke is heterogeneous in nature such that the extent of the interruption in cerebral blood flow can vary, and the episode can be transient or permanent. A reduction in global blood flow is less common (although it could for example be associated with cardiac failure followed by pulmonary resuscitation). The majority (about 75-80 %) of strokes are infarctions or ischaemic in nature (see Figure 1.1), the remainder mostly being haemorrhagic (intracerebral or subarachnoid). Ischaemic stroke most frequently results from atherothrombotic infarcts, less common are lacunar infarcts and those arising from cardiac emboli.

**Figure 1.1.** Distribution of acute stroke. (From Allen *et al.*, 1988)



In atherothrombotic stroke the occlusion of a cerebral artery results in an area of infarcted tissue and in three quarters of acute strokes this occurs in the territory of the middle cerebral artery (MCA). The MCA supplies the lateral parts of the cerebral hemispheres and perforating arteries from it, such as the lenticulostriate artery, also supply the basal ganglia. Damage to sub-cortical structures will affect the overlying cortical function, and depending on the structure involved, gives rise to clinical syndromes associated with stroke such as sensory loss, motor loss or hemiplegia and aphasia. These syndromes are often indicative of the location of the infarcted tissue. Thus, for example, lesions in the internal capsule (the area where motor fibres are bounded by the thalamus and basal ganglia) can give rise to pure motor deficit or hemiplegia without higher dysfunction (Allen *et al.*, 1984). Another characteristic syndrome is Broca aphasia (associated with slurred speech and loss of voluntary mouth control) which is associated with lesions in Broca's area, an area of premotor cortex controlling speech (Allen *et al.*, 1988). However, such diagnoses represent gross simplifications representative of the pathological lesion, the extent of which can vary to a large extent within a population. This is largely due to variations between individuals in the extent to which anterior and posterior parts of the cerebral circulation are complete (the circle of Willis, Figure 1.2); this is incomplete in more than half the population (Allen *et al.*, 1988) such that collateral blood supply also varies.

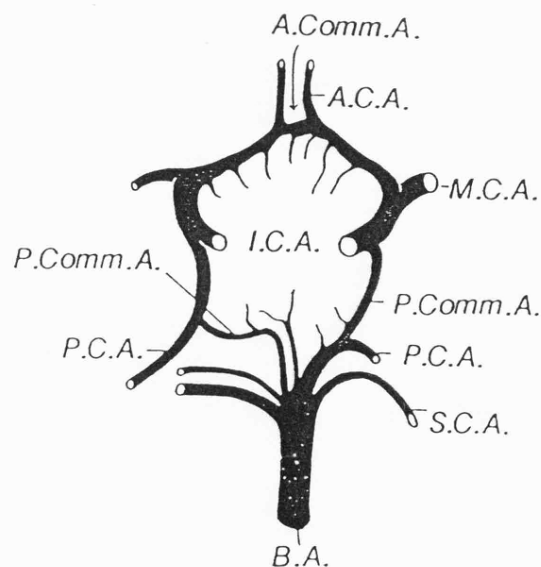


**Figure 1.2.** Neurovasculature and the circle of Willis.

*A.comm.A.*-anterior communicating artery, *A.C.A.*- anterior cerebral artery, *M.C.A.*- middle cerebral artery, *P.comm.A.*-posterior communicating artery, *S.C.A.* superior cerebellar artery, *P.C.A.*- posterior cerebral artery, *B.A.*- basilar artery, *I.C.A.*-internal carotid artery (From Allen *et al.*, 1988).

### 1.1.2. Detection of infarcted brain tissue.

The clinical distinction of pathological lesions based on associated symptoms is clearly unreliable and inaccurate (Harrison, 1980). However, in the last decade such confirmation has been readily made with advances in neuro-imaging technology. The most useful of these has been cranial computed X-ray tomography (CT scans). CT scans are radiodensity maps taken through slices of the brain, the density of each cylindrical brain area represented by 'grey density'. Lesions are detected by changes in tissue radiodensity (partly as a result of changes in calcium and water content) or by lack of contrast compared to normal brain tissue. Iodine contrast media can enhance a scan and is of particular use in detecting abnormal blood vessels. The primary use of CT scanning, especially at short post-ischaemic time intervals, is to resolve whether the vascular lesion is due to haemorrhage or infarction (Sandercock *et al.*, 1985), especially as the full resolution of infarcted tissue does not become apparent until longer post ischaemic periods. Such differential diagnoses have important implications for therapy with anti-platelet agents.

Another useful neuro-imaging technique is positron emission tomography (PET scans). PET scans are quantitative measurements of positron emitting radiomolecules of metabolic significance, used as indicators of cerebral blood volume (CBV), regional cerebral blood flow (rCBF), oxygen consumption (CMR<sub>O<sub>2</sub></sub>), oxygen extraction (OEF), glucose utilisation (CMR gl) and pH. Following initial arterial occlusion, the brain is seen to undergo cerebral arteriole vasodilation (increased CBV) in an attempt to restore flow (local CBF increases), associated with an attempt to increase O<sub>2</sub> extraction (regional OEF increases). However, if cells are necrotic following ischaemia, then-oxygen and glucose utilisation (CMR<sub>O<sub>2</sub></sub> and CMR gl) decrease regardless of changes in blood flow or volume.

The use of such techniques has illustrated that a zone surrounds the ischaemic core consisting of tissues that are oedematous and functionless, but have not reached the threshold for complete infarction. This area is referred to as the ischaemic penumbra, and although the zone of dead tissue increases with time, it is this damaged zone that therapeutic intervention may protect when administered after the occurrence of stroke. One of the best examples where the use of CT scanning has been particularly useful is in the detection of lacunar infarctions (which constitute about 25% of all cerebral infarcts).

In the 1960s, Fisher and colleagues described a clinical syndrome associated with minor stroke deficit, thought to be linked to small 'lacunes' (small fluid filled lesions)

usually found deep in the brain (e.g. basal ganglia) caused by the occlusion of a perforating artery (Fisher, 1982). The affected arteries are more susceptible to injury because they are high pressure arteries responsible for a large component of the cerebrovascular resistance (Ross Russell, 1984), and thus the syndrome is often associated with hypertension (Bamford & Warlow, 1988). However, while CT scanning has confirmed the lacunar syndrome to be associated with such infarcts, the pathophysiology of these lesions is far from clear.

Occlusions in these small resistance arteries can result from a process of lipohyalinosis, the walls of the artery being disrupted by segmental necrosis in which fatty macrophages appear (similar to that occurring in large vessel atherosclerosis, Allen *et al.*, 1988), often described by the term microatheroma. This distinction is made because patients may present with lacunar infarcts in the absence of larger vessel atherosclerosis, and thus the exact relationship between microatheroma and lipohyalinosis of small vessels and larger vessel atheromatous plaques is uncertain (Bamford & Warlow, 1988), as even Fisher (1982) who first used the term microatheroma described it as atherosclerosis of the smaller arteries. At best then, it is not clear as to whether this represents two distinct pathological processes or just the differing responses of different arterial vessels to hypertension. This is adequately described by Allen *et al.* (1988) who postulated that "small vessel lacunar disease is atherosclerosis pushed into smaller arteries by raised blood pressure".

### *1.1.3. Epidemiological studies and risk factors.*

Extensive epidemiological studies have assessed many of the proposed risk factors associated with the occurrence of cerebral infarction. These studies involve large numbers of patients with continual monitoring and follow up after initial selection, often so that groups can be age- and sex- matched. They are often community based studies or collective data from multi-centre studies. The advantage of the community-based studies is that the study population is not a random sample but a representative distribution of a population. The Framingham study and, recently, the more pertinent Oxford Community Stroke Project (Bamford *et al.*, 1988) are prime examples.

Such studies led Fisher (1985) to demonstrate the magnitude of systolic blood pressure to be directly proportional to the risk of stroke, as hypertension also presents as a

risk factor in heart disease possibly resulting in cerebral embolism. More recently, MacMahon *et al.* (1990) demonstrated that a prolonged but modest decrease in diastolic blood pressure substantially reduced the risk of stroke (by nearly 50%) and this has important preventive implications.

The risk of stroke is proportionate to age. Incidence is slightly higher in men, and after the age of 55 it doubles every ten years. After a first stroke there is a 10% risk of recurrence within a year (Allen *et al.*, 1988; Malmgren *et al.*, 1987).

Recent studies (Shinton & Beevers, 1989; Donnan, 1989) have now confirmed that smoking does present a substantial risk for stroke, secondary to thromboembolic arterial disease. Cardiac diseases, such as left ventricular hypertrophy, arrhythmias and atrial fibrillation represent significant risk factors, especially for embolic stroke (Dyken *et al.*, 1984). Incidence of stroke is also increased in diabetes as this causes cerebral thrombosis and increased cerebral atheroma. Infarcts due to emboli may also result from heart failure which is also increased in diabetes (Allen *et al.*, 1988). The evidence for a direct causative effect of other factors is somewhat less clear.

Chen *et al.* (1989) could derive no relationship between the level of cholesterol and stroke incidence (further supported by Donnan, 1989). However Khaw & Rose (1989) showed quite clearly that by reducing the level of cholesterol the risk of stroke was attenuated. An interpretation of these findings could be that the reduced risk was secondary to a reduction in those aspects of coronary heart disease that risk factors per se. The effects of ethanol consumption are also unclear. Donnan (1989) showed no risk factor associated with ethanol, whilst Gill *et al.* (1986) demonstrated that alcoholism represents a significant risk factor in its own right. Similarly, many other studies have indicated an association with oestrogen levels resulting from oral contraceptives. In these cases a risk may only be shown when other factors co-exist such as hyperlipidaemia, diabetes and hypertension (see Dyken *et al.*, 1984). High levels of haemoglobin (high haematocrit) have been shown to represent a substantial risk (Allen *et al.*, 1988). Many other factors have been postulated such as race and genetic disposition. However, it is well established that hypertension is a genetic phenomenon, and the adverse disposition of certain races may be due to dietary habits.

Transient ischaemic attacks (TIAs) are periods of focal ischaemia resulting from a deficit in the arterial vessels to the brain, normally lasting less than 24hr. By implication, TIAs represent a risk factor although patients with TIAs also have an increased incidence of

associated conditions such as hypertension, coronary heart disease, left ventricular hypertrophy and diabetes. As these represent the possibility of impending stroke, treating associated conditions may represent substantial benefit since only 10% of all strokes are preceded by TIAs (Weinfeld, 1981).

#### *1.1.4. Drug treatment of clinical stroke.*

There are extensive literature reports on a variety of approaches used in the treatment of stroke either as preventive agents (e.g. after the occurrence of TIAs), or as treatment of cerebral infarction and progressing stroke. As about 75% of strokes are due to atherothrombotic brain infarction or cardiac emboli (the remainder lacunar) their prevention with agents interfering with thrombo-embolic events has been investigated. Perhaps the most widely studied, on the basis of its anti-platelet properties, has been aspirin.

Aspirin inhibits cyclo-oxygenase and therefore the formation of the products of arachidonic acid metabolism, thromboxane A<sub>2</sub> (TXA<sub>2</sub>) and prostacyclin. The former compound is a potent platelet aggregator, the latter being one of the most potent vasodilators and platelet inhibitors known. The Antiplatelet Trials Corporation (1988) compiled and reviewed data from 25 separate studies on aspirin and found a reduction in the occurrence of stroke by 30%. It would also appear that there is a strong case for the examination of low selective doses of aspirin because inhibition of cyclo-oxygenase in platelets is achieved far more effectively than in the endothelial cell (platelets are anuclear and cyclo-oxygenase cannot be resynthesised after inhibition), thus the balance would be in favour of prostacyclin production from endothelial cells with a net effect of platelet inhibition and vasodilation (see Weissman, 1991). It is important to note, however, that in non CT-diagnosed patients (unfortunately by far the majority) aspirin can precipitate or worsen haemorrhagic stroke (Lowe, 1990). Data for other anti-platelet agents, such as ticlopidine, have demonstrated these agents to have a similar efficacy to aspirin in preventing secondary stroke (Gent *et al.*, 1989).

Anti-coagulants have also been postulated to work in secondary prevention on the basis of their ability to interfere with the coagulation cascade mechanism thereby reducing embolism. Studies have been carried out with heparin (Cerebral Embolism Group, 1983; Lodder & van der Lugt, 1983) but these failed to show great efficacy and have now been largely abandoned due to haemorrhagic complications with associated risk far outweighing

any conferred benefit (Grotta, 1987; Sila & Furlan, 1988). It is possible that tissue-specific plasminogen activators represent a more useful class of agent with reduced inherent haemorrhagic properties, as these agents promote the conversion of plasminogen to plasmin which subsequently degrades fibrin and fibrinogen and inactivates clotting factors such as prothrombin (Sila & Furlan, 1988). However, this therapy has also been shown to have associated problems of oedema and haemorrhage (Koudstaal *et al.*, 1988).

Intravenous prostacyclin causes systemic vasodilation and potently inhibits platelet aggregation. In small initial trials, in patients with acute stroke, results were encouraging. However, in larger randomised trials, confirmed by CT, no benefit was conferred (Martin *et al.*, 1985; Hsu *et al.*, 1987). More stable analogues, with less side effects on peripheral vasculature for a given anti-platelet effectiveness may be worthy of consideration.

As previously outlined, an increased haematocrit represents a risk factor. However, large randomised trials assessing the use of haemodilution with dextran 40 showed no overall protection against acute cerebral infarction (Heros & Korosue, 1989).

Corticosteroids have been tested on the basis of their ability to reduce cerebral oedema. However, no difference between drug treatment with dexamethasone or placebo was found, indeed only serious side effects were confirmed (Norris & Hachinski, 1986). A role for the involvement of 5-HT<sub>2</sub> receptors in cerebral infarction has been postulated, as this receptor subtype mediates vasoconstriction, activation of platelets, and increases oedema. Naftidrofuryl is a 5-HT<sub>2</sub> antagonist, also affecting cellular metabolic parameters (increasing ATP and decreasing lactate in ischaemic tissue and therefore creating greater oxygen efficiency) but the results with this agent, at best, are inconclusive (Lowe, 1990).

Two other established classes of drug have been tested: opiates and barbiturates. Naloxone is a non-selective opiate receptor antagonist, which at high concentrations also possesses properties as a calcium antagonist (Faden, 1984). Naloxone is widely reported to be well tolerated and may be of benefit if excitatory peptides and other transmitters promote cellular damage through calcium influx, or damage is exacerbated through opiate-mediated post-ischaemic depression of cellular metabolism. However, no benefit for naloxone has been shown in clinical studies (Fallis *et al.*, 1984). Although relatively non-specific and with other actions, such as blockade of neuronal calcium channels, the proposed use of barbiturates as anti-ischaemic agents is based on their ability to suppress neuronal metabolism and decrease seizure activity (Safer, 1980) thereby decreasing the formation of damaging products of anaerobic metabolism such as lactate. Clinical studies

with these agents have shown no effect (Rockoff *et al.*, 1979).

In summary, there are no agents where neuroprotection has been demonstrated clinically, although this may partly reflect the difficulty of demonstrating a positive effect in a condition which is heterogeneous in nature.

## 1.2. CELLULAR CALCIUM CONTROL MECHANISMS.

Intracellular calcium ( $[Ca^{2+}]_i$ ) plays a key role as a second messenger in the regulation of many cell functions, a role which is normally afforded by exquisite control over the concentration of intracellular free  $Ca^{2+}$ . The total concentration of  $Ca^{2+}$  in nerve cells is around 1.5 mM and yet the portion of free ionic  $Ca^{2+}$  in the cytosol is in the region of 0.1  $\mu$ M, thus the difference in the relative proportions of ionic calcium between the internal and external milieu promotes a large electrochemical gradient for  $Ca^{2+}$  entry across the cell membrane. The cytosolic levels of free  $Ca^{2+}$  are maintained at this level firstly by having  $Ca^{2+}$  specific transport proteins in the normally impermeable plasma membrane, and secondly by means of a highly efficient intracellular "buffering" mechanism whereby the majority of  $Ca^{2+}$  ions are bound and sequestered at a number of sites including the sarcoplasmic (in muscle cells) and endoplasmic (in non-muscle cells) reticulum, mitochondria, and intracellular binding proteins such as calmodulin and parvalbumin (see Meldolesi *et al.*, 1990). Increases in the concentration of intracellular free  $Ca^{2+}$  give rise to important events such as excitation-contraction coupling, enzyme-regulation and in neuronal cells, transmitter release. The importance of controlling the level of intracellular free  $Ca^{2+}$  has prompted extensive studies over recent years as to how calcium enters the cell and how this entry can be regulated, since a growing body of evidence in the last ten years has postulated a role for calcium in neuronal cell death following ischaemia (e.g. Siesjo, 1981; Hass, 1981; Rothman, 1984; Hossmann *et al.*, 1985; Deshpande *et al.*, 1987; Siesjo & Bengtsson, 1989a; 1989b). This has led to a variety of pharmacological manipulations, including the proposed use of calcium antagonists, designed to reduce cellular calcium entry whereby potential therapeutic benefit may be conferred in cerebral ischaemia; such mechanisms are the focus of this thesis. Thus, a more appropriate title to this thesis may have been 'Are calcium antagonists of any use in ischaemic stroke?' - And,

if so, why ?' Before evidence is presented suggesting a role for  $\text{Ca}^{2+}$  in the ischaemic process, the normal physiological mechanisms of cellular  $\text{Ca}^{2+}$  entry and control will be overviewed.

### ***1.2.1. Intracellular calcium regulation.***

The amount of free cellular  $\text{Ca}^{2+}$  will ultimately be controlled by  $\text{Ca}^{2+}$  movement across the plasma membrane (see below). However, within the cell there are other key elements which control the concentration of  $\text{Ca}^{2+}$ .

In neuronal cells the endoplasmic reticulum (ER) is an important regulator of  $[\text{Ca}^{2+}]_i$ . This structure contains an ATPase with high affinity for  $\text{Ca}^{2+}$  externally, which when bound, promotes ATP-dependent phosphorylation and changes the enzyme into a conformation that has low affinity for calcium internally. This mechanism allows the ER to take up large amounts of  $\text{Ca}^{2+}$  and the ATPase may be regulated by calmodulin (Carafoli, 1987). The ER, however, is probably not the main buffering mechanism in cases of transient increases in  $[\text{Ca}^{2+}]_i$  as it is unable to sequester  $\text{Ca}^{2+}$  at the required rate, since  $\text{Ca}^{2+}$  will enter the cell during an action potential at a rate greater than the capacity of the ER for uptake (Blaustein, 1988). Thus, intracellular binding proteins account for rapid calcium removal with the ER increasingly involved on a slower time scale following neuronal activity. Under constant neuronal activity the ER will mainly contribute to changes in  $[\text{Ca}^{2+}]_i$  when, during depolarisation it will be steadily loading  $\text{Ca}^{2+}$  for subsequent release, since the endoplasmic reticulum or a closely related site is thought to be synonymous with the  $\text{Ca}^{2+}$  release site at which myo-inositol (1,4,5) trisphosphate ( $\text{IP}_3$ ) acts (Berridge & Irvine, 1989). Meldolesi *et al.* (1988) speculated that this  $\text{Ca}^{2+}$  release site for  $\text{IP}_3$  may be discrete localised structures, referred to as calciosomes, structures enriched with  $\text{Ca}^{2+}$  ATPase and calreticulin (high affinity calcium binding protein), although there is uncertainty if these sites represent the  $\text{IP}_3$  release sites since calreticulin is not always associated with calciosomes (see Meldolesi *et al.*, 1990). However, the receptor site for  $\text{IP}_3$  has now been characterised (see Nahorski, 1988; Pietrobon *et al.*, 1990) which appears to have nanomolar affinity for  $\text{IP}_3$ , with  $\text{Ca}^{2+}$  release channel gating occurring within 20 ms of  $\text{IP}_3$  addition (Spat *et al.*, 1986).

Mitochondria have a large capacity for sequestering  $[\text{Ca}^{2+}]_i$  by carrying  $\text{Ca}^{2+}$

electrophoretically via a uniport mechanism into the matrix by means of the difference in potential across the inner mitochondrial membrane set up through  $H^+$  extrusion by the respiratory chain. It has a low rate of uptake and affinity for  $[Ca^{2+}]_i$  in the resting state and the inner membrane also has egress mechanisms, in particular a  $Na^+/Ca^{2+}$  exchanger, to ensure that matrix  $Ca^{2+}$  concentration is kept around the same as that in the cytosol (See McCormack *et al.*, 1990). However, during excessive neuronal activity when  $[Ca^{2+}]_i$  is  $>1\mu M$ , or during pathophysiological conditions,  $Ca^{2+}$  will be continuously accumulated by the mitochondria as the normal egress mechanisms become saturated, since their overall  $V_{max}$  is around ten fold less than the uptake mechanism with the system balance around  $1\mu M$ . Despite their low affinity for  $Ca^{2+}$ , mitochondria have a large capacity for total  $Ca^{2+}$  accumulation (by co-accumulating phosphate and precipitating hydroxyapatite deposits in the matrix) (Carafoli, 1987). Thus, under some conditions mitochondria will continuously store excessive amounts of cytosolic  $Ca^{2+}$  without significant detrimental effects and accordingly, it has been suggested that the ability of mitochondria to sequester large amounts of  $Ca^{2+}$  will determine whether injured cells survive or not (Carafoli, 1987).

*In vitro* studies have shown that under physiological cellular calcium loads, uptake into the endoplasmic reticulum predominates, whilst under excessive calcium loading the mitochondria become the predominant calcium pool (Rasmussen & Barrett, 1984). Other evidence suggests, however, that under normal conditions mitochondria only regulate their own level of matrix  $Ca^{2+}$ , and not  $[Ca^{2+}]_i$ , excessive sequestration of  $Ca^{2+}$  only occurring pathologically and associated with damaged cells and impaired function (Rasmussen & Barrett, 1984). Thus, mitochondria are able to prevent  $[Ca^{2+}]_i$  rising above  $3-5\mu M$  (see McCormack *et al.*, 1990), allowing the cell time to correct the abnormal  $Ca^{2+}$  load. Mitochondria thus act as a "bale out" mechanism whereby they function as a safety device against toxic increases in  $Ca^{2+}$  (Richter *et al.*, 1990). This ability of mitochondria to sequester  $Ca^{2+}$  is, however, limited, and continual overloading results in a disturbance of functional integrity, e.g. the uncoupling of oxidative phosphorylation (Siesjo, 1981) and leads to the opening of a protein pore, opened by and permeable to matrix  $Ca^{2+}$ , with deleterious consequences for the cell under ischaemic/reperfusion conditions (e.g. Crompton *et al.*, 1988). Cyclosporine has recently been shown to block this pore (Richter *et al.*, 1990).

In more recent years, the role of intracellular binding proteins (CaBP) has received growing attention since some of these proteins mediate  $Ca^{2+}$  signal-transduction

mechanisms whilst others appear to act as discretely localised  $\text{Ca}^{2+}$  buffers. CaBP exist primarily as two subfamilies: firstly the EF-hand proteins (so called because of the conformational shape of the  $\text{Ca}^{2+}$  binding site) and the annexins which bind little  $\text{Ca}^{2+}$  alone, but in the presence of phospholipid containing membranes are capable of forming  $\text{Ca}^{2+}$  complexes.

The EF-hand proteins include calmodulin, parvalbumin, calretinin and calbindin, which have all been identified in the CNS (Persechini *et al.*, 1989). Some EF-hand proteins, on binding  $\text{Ca}^{2+}$ , trigger cellular events due to changes in their conformation, and calmodulin is the most widely characterised in this respect. In mammalian tissues the concentration of calmodulin is highest in the brain (Cheung, 1988), and in resting cells will buffer more than 0.1 mM  $\text{Ca}^{2+}$ . Activation of calmodulin has been shown to modulate enzyme activity (Cheung, 1980; Cheung, 1988; Pietrobon *et al.*, 1990). The buffer proteins (parvalbumin, calretinin and calbindin) play a more passive role as intracellular  $\text{Ca}^{2+}$  buffers but their heterogeneous distribution in neuronal cells may give rise to highly localised role. Parvalbumin appears to be prevalent in certain high frequency bursting GABAergic neurones, but not in others of lower frequency. Thus, it may be present in certain neurones to reduce the  $\text{Ca}^{2+}$  activated  $\text{K}^{+}$  conductances that would reduce neuronal excitability (see Blaustein, 1988). Furthermore, in the gerbil hippocampus, it has been shown that only the perforant path contains parvalbumin (Scotti & Nitsch, 1991). Other CaBP also show a discrete localisation, for example being absent in neurones containing peptides (Nitsch *et al.*, 1990). Such a distribution for CaBP may be an important feature in the selective neuronal loss that occurs as a result of some pathological seizure states (e.g. Kirino, 1982; Griffiths *et al.*, 1982; sections 1.3.1. and 1.3.2.) and this is supported by more recent experimental evidence. Lowenstein *et al.* (1991) demonstrated that seizure activity up-regulated the expression of hippocampal calbindin and calbindin mRNA, and in human epileptic hippocampi only seizure-resistant CA2 cells express calbindin (Sloviter *et al.*, 1991). In culture, those subpopulations of hippocampal neurones expressing calbindin have been shown to be more resistant to excitotoxicity following exposure to excitatory amino acids than those where calbindin is absent (Mattson *et al.*, 1991) and thus the discrete distribution of CaBP may be one of the determining factors for some neuronal populations surviving ischaemic insults and epileptic seizures. Furthermore, in other neurodegenerative diseases, such as Alzheimer's, calbindin levels are dramatically reduced in those affected brain areas (Iacopino & Christakos, 1990).

The various members of the annexin family, termed annexin I-VII (Crumpton & Dedman, 1990) bind  $\text{Ca}^{2+}$  in the presence of phospholipid containing membranes, forming a complex of up to eight  $\text{Ca}^{2+}$  ions per protein molecule (Bazzi & Nelsestuen, 1991) and represent a further means of cellular  $\text{Ca}^{2+}$  buffering.

### *1.2.2. Extrusion mechanisms.*

$[\text{Ca}^{2+}]_i$  can be extruded principally in two ways. Firstly by way of energy expenditure (ATP) that drives a  $\text{Ca}^{2+}$ -activated, calmodulin-regulated ATPase located on the cell membrane (Penniston 1983 ; Meyer, 1989). Secondly, there is an electrogenic, high capacity (but importantly, not unidirectional)  $\text{Na}^+/\text{Ca}^{2+}$  exchange mechanism, regulated by the  $\text{Na}^+$  gradient across the cell membrane. The stoichiometry of this system is  $3\text{Na}^+:1\text{Ca}^{2+}$  (Reeves & Hale, 1984). This mechanism is dependent on the  $\text{Na}^+$  gradient across the plasma membrane (normally higher out than in) and if this falls (associated with increasing levels of intracellular  $\text{Na}^+$  on depolarisation), the transporter can carry  $\text{Ca}^{2+}$  into the cell. Upon cellular repolarisation and activation of the  $\text{Na}^+/\text{K}^+$  ATPase pump,  $\text{Ca}^{2+}$  extrusion would occur.

### *1.2.3 Increases in intracellular $\text{Ca}^{2+}$ .*

$\text{Ca}^{2+}$  can enter into cells via an increase in the permeability of the plasma membrane (normally impermeable to  $\text{Ca}^{2+}$ ) by the selective opening of channels whereby  $\text{Ca}^{2+}$  can enter the cell along its electrochemical gradient. There are principally two types of calcium channel: firstly, many cells including neuronal, smooth muscle and secretory cells, possess channels that are dependent on the membrane potential. These channels can either be open, closed or inactivated, though  $\text{Ca}^{2+}$  entry is associated with the open form when the cell is depolarised. Consequently when the cell is resting, with a membrane potential around -70mV, these channels will be impermeable to  $\text{Ca}^{2+}$ . The amount of  $\text{Ca}^{2+}$  entry via these voltage-sensitive or voltage-operated calcium channels (VOCs) in any cell will therefore depend ultimately on the extent and time to which the cell is depolarised. As will be discussed later, this is one of the main reasons for the selectivity expressed by agents that modify VOC function. The second type of channel permeable to  $\text{Ca}^{2+}$  is one where channel

opening results from the action of an agonist, even though cellular depolarisation may subsequently follow and promote further  $\text{Ca}^{2+}$  entry via VOCs. The receptor operated ion channel (ROC) for the excitatory amino acid N-methyl-D-aspartate (NMDA) is a prime example of ROC mediated  $\text{Ca}^{2+}$  entry.

The intracellular level of calcium can also rise in neuronal tissue as a result of activation of a variety of different receptors (e.g. Nahorski, 1988), linked via a G protein, to phosphoinositidase C (phospholipase C) that acts on phospholipids in the plasma membrane. This action hydrolyses phosphatidyl inositol (4,5)-bisphosphate ( $\text{PIP}_2$ ) into diacylglycerol (which subsequently acts on protein kinase C) and myo-inositol (1,4,5)-trisphosphate ( $\text{IP}_3$ ) which can release  $\text{Ca}^{2+}$  from non-mitochondrial stores, possibly from a membrane associated with the endoplasmic reticulum. The associated activation of protein kinase C by the other product of this phospholipase, diacylglycerol, can result in the phosphorylation of calcium channels and modify calcium currents (Barbaran *et al.*, 1985; Tsien *et al.*, 1988).  $\text{Ca}^{2+}$  can also enter the cell non selectively through the plasma membrane if it is damaged, and in some pathological situations  $\text{Ca}^{2+}$  is thought to enter via other voltage-sensitive ion channels (e.g. for  $\text{Na}^+$ ) for which there is a close structural homology and which, under certain conditions, may become less discriminatory ( Jacques *et al.*, 1981; Nachshen *et al.*, 1986)

#### 1.2.4. *Different forms of voltage and receptor gated calcium entry.*

VOCs have been shown on the basis of electrophysiological experiments to consist of at least three forms (Nowycky *et al.*, 1985 ; Tsien *et al.*, 1988):

T (transient, small conductance, activated by weak depolarisation);

L (long lasting, large conductance, activated by strong depolarisation);

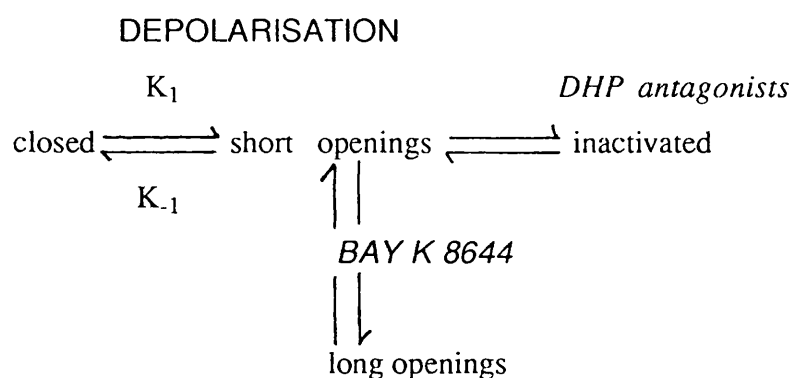
N (neuronal - coupled to transmitter release, intermediate conductance and kinetics).

These three distinct forms of VOC can be distinguished both in terms of their electrophysiological characteristics, and their sensitivity to pharmacological manipulation. L- type channels are extensively regulated by the various classes of agent described as calcium antagonists (Fleckenstein, 1983). The cellular location, duration and voltage over which the channel opens will probably define channel function. N channels are potentially

blocked by the inorganic ion  $Gd^{3+}$  (Docherty, 1988) and  $\omega$ -conotoxin (Olivera *et al.*, 1985), with a subsequent block of transmitter release. L channels are also sensitive to  $\omega$ -conotoxin (Suzuki & Yoshioka, 1987), but to a much more variable extent. Thus, Tsien *et al.* (1988) consider  $\omega$ -conotoxin to block L currents although Anderson & Harvey (1987) could find no effect in mouse motor nerve terminals. Furthermore, Owen *et al.* (1989) demonstrated that noradrenaline release from chromaffin cells was sensitive to DHPs but  $\omega$ -conotoxin insensitive. T channels are insensitive to  $\omega$ -conotoxin, but may be sensitive to some types of calcium channel antagonists e.g. amiloride (Tang *et al.*, 1988) but the selectivity shown for these channels is poor. T channels are likely to play a role in the pacemaker activity of cells (e.g. sino-atrial cells) because they are opened by small depolarisations in well polarised cells, but their voltage characteristics allow them to rapidly recover from inactivation for further opening during hyperpolarisation. Within the CNS they may therefore play an important role in bursting and oscillatory activity (Llinas, 1988). More recently, other DHP and  $\omega$ -conotoxin insensitive high threshold channels have been identified (Llinas *et al.*, 1989) and termed 'P' because of their identification in Purkinje cells, although this channel may be similar to other  $\omega$ -conotoxin insensitive N channels such as the B1 channel cloned and expressed by Numa's group (Mori *et al.*, 1991). The P channel seems to be selectively blocked by funnel web spider toxin (Llinas *et al.*, 1989). It is probable that a large family of channels exists within this broad classification; for example there are differences in the electrophysiological properties of L channels in cardiac and skeletal muscle (see McKenna *et al.*, 1990) and in rat brain Snutch *et al.* (1990) demonstrated that four distinct classes of L channel may exist based on differences in cDNA. Neuronal L channels also exhibit a slower rate of inactivation than in cardiac cells, and as noted, there is inconsistency in the sensitivity of L channels to  $\omega$ -conotoxin.

In neuronal tissue the density of  $\omega$ -conotoxin sites is ten-twenty fold higher than DHP sites (Wagner *et al.*, 1988) and it is probable that N-type channels are located on or close to the nerve terminal and are thus believed to play a role in neurotransmitter release (Hirning *et al.*, 1988; Tsien *et al.*, 1988). Whilst L type channels are preferentially located on the cell body, playing a role in excitation-contraction coupling in smooth and cardiac muscle, in some circumstances they may play a role in membrane excitability and transmitter release (see Spedding *et al.*, 1989). Thus, in recent studies (Westenbroek *et al.*, 1990) using monoclonal antibodies to detect DHP sensitive L channels, the location of

these sites was found to be associated with the cell soma and proximal dendrites. Although somewhat over-simplified, this hypothesis explains some fundamental observations, such as the relative insensitivity of some preparations to calcium antagonists in blocking depolarisation-induced transmitter release, whilst still being sensitive to  $\omega$ -conotoxin. Thus the selective enhancement of the L type component in further increasing transmitter release beyond that of the depolarising stimuli can be demonstrated by use of calcium channel activators and blocked by the respective antagonist (Middlemiss & Spedding, 1985). A second reason as to why neuronal transmitter release is insensitive to calcium antagonists is that the calcium channel does not exist in a single state or form, and as such can be explained in the kinetics described below where at any given time channels could exist in either the closed, open or inactivated state:-



The kinetics of this equilibrium are such that depolarisation will shift the equilibrium to the right, away from the closed form, and thus promote calcium entry. Calcium antagonists have high affinity for the inactivated state and when bound under such conditions stabilise this state of the channel and prevent calcium entry. DHP antagonists have a thousand fold greater affinity for depolarised compared to polarised cells (Bean, 1984; Sanguinetti & Kass, 1984). The calcium channel activator Bay K 8644 has been claimed to induce a mode of gating of L channels that exhibits long openings, by decreasing the rate of deactivation ( $K_{-1}$ ) of the open state (Sanguinetti *et al.*, 1986; Janis & Triggle, 1990). Armstrong & Kalman (1990) proposed that the voltage dependence of DHP binding was determined by voltage-dependent dephosphorylation, since channel inactivation was reversed by cAMP-dependent phosphorylation, whereby calcium channel activators may inhibit dephosphorylation and antagonists bind to the inactivated

dephosphorylated form reducing the probability of channel opening. Consequently, since neurones are not extensively depolarised and channels spend little time in the open or inactive state, as compared to smooth muscle or heart, much higher concentrations of calcium antagonist are needed to affect neuronal transmitter release. This may also explain why some of the effects of calcium antagonists are more readily demonstrated in cultured neuronal cells subjected to a different level of depolarisation (see Spedding *et al.*, 1989).

#### 1.2.5. *Molecular biology.*

In the last 2-3 years the application of molecular biology has rapidly advanced the understanding of calcium channel structure and has resulted in the definition of the primary structure of channel subtypes and the receptor sites on the channel proteins for those agents classed as calcium antagonists.

The high density of L channels in skeletal muscle and the availability of high affinity probes has led to L channels being the first to be sequenced. As illustrated in Figure 1.3, purification of the membrane fractions revealed that the skeletal muscle L channel consists of at least five subunits designated  $\alpha_1$ ,  $\alpha_2$ ,  $\beta$ ,  $\gamma$ , and  $\delta$ . The  $\alpha_1$  subunit is a 175 kDa polypeptide and contains phosphorylation sites and receptor sites for DHPs, phenylalkylamines and benzothiazepines. It also forms the ion selective pore and voltage sensor for the channel as shown in Figure 1.4, based on the original proposal by Tanabe *et al.* (1987), with strong resemblance to other voltage operated ion channels e.g. for  $\text{Na}^+$ . The  $\alpha_1$  subunit consists of a single polypeptide chain with four repeating units of homology (termed motifs, I-IV). Each motif consists of six  $\alpha$ -helical trans-membrane spanning regions (termed S1-S6). The amino acid composition of the S4 segment (positively charged lysine or arginine at every third or fourth residue, residing opposite negatively charged amino acids) is responsible for the voltage sensing mechanism detecting changes in membrane potential (see Tsien *et al.*, 1991). Mikami *et al.* (1989) expressed the cardiac  $\alpha_1$  subunit in *Xenopus* oocytes and demonstrated properties of L-type VOCs.

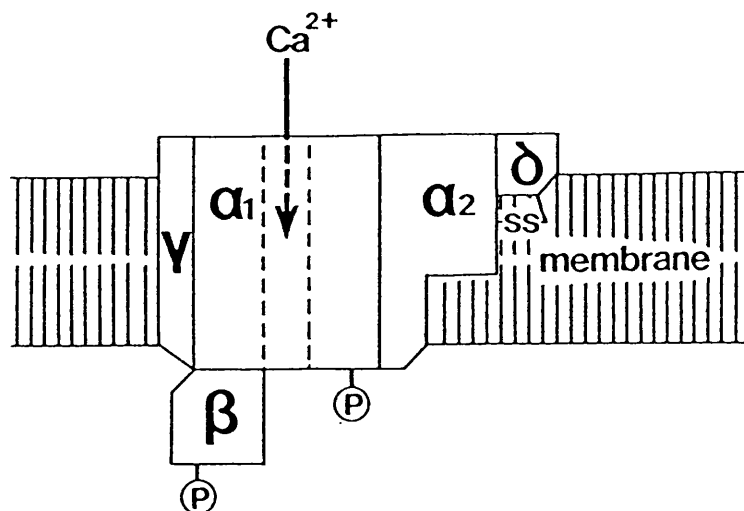
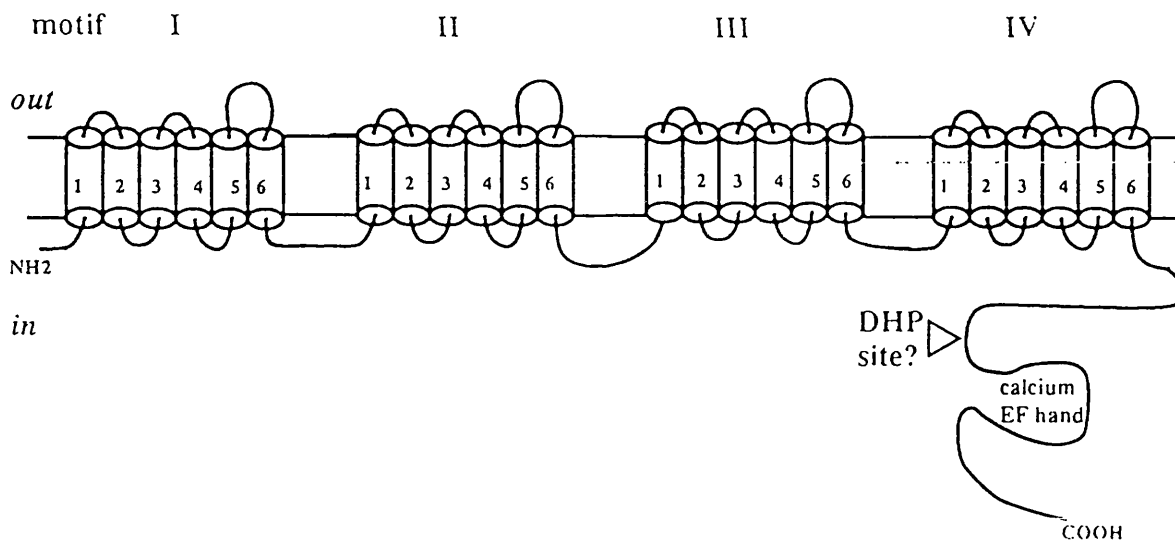


**Figure 1.3.** The subunit composition of the L-type VOC (from Seagar *et al.*, 1988)

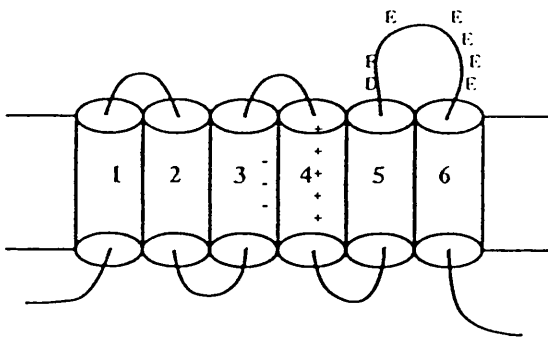
Further confirmation that the  $\alpha_1$  subunit carried the voltage sensor was demonstrated by Tanabe *et al.* (1988) in dysgenic mice which lack the  $\alpha_1$  subunit and show abnormal excitation-contraction coupling and when the normal form of the  $\alpha_1$  subunit was expressed in myotubules in dysgenic mice, re-expression of  $\text{Ca}^{2+}$  current was achieved. The same group (Tanabe *et al.*, 1990) have also expressed the cardiac  $\alpha_1$  subunit in dysgenic mice myotubules and this isoform of the  $\alpha_1$  subunit functioned as a 'cardiac-like' voltage sensor. Other similar studies (e.g. Perez-Reyes *et al.*, 1989) where the  $\alpha_1$  subunit has been expressed and shown to exhibit DHP sites and  $\text{Ca}^{2+}$  current have confirmed the  $\alpha_1$  subunit as being the voltage sensor and ion pore. It is now apparent that different isoforms of the L channel exist, resulting in different properties (McKenna *et al.*, 1990; Snutch *et al.*, 1990) and whilst it appears that the negatively charged amino acid sequence is highly conserved in S3, variations in S4 may result in different properties (for reviews see Tsien *et al.*, 1991; Spedding & Kenny, 1991).

Recently, Regulla *et al.* (1991) using photoactive DHPs to covalently bind to the  $\alpha_1$  subunit from skeletal muscle, after digestion and sequencing of the peptides, demonstrated that the DHP site was primarily located on the cytosolic tail beyond IV S6 between amino acids 1390 and 1477 on the C-terminus (see Figure 1.4), an area highly conserved in a variety of tissues. It would appear that this region does not bind DHPs exclusively as Streissnig *et al.* (1990) demonstrated phenylalkylamine binding to a site

# PUTATIVE STRUCTURE OF $\alpha_1$ -SUBUNIT OF L CHANNEL



## THE S 1-6 TRANSMEMBRANE HELICES



**CARDIAC IV S3:**  
D-AWNTFD-ALIVVGSIVD-IAI

**CARDIAC IV S4:**  
TFFR+LFR+UMR+LUK+LLSR+G

**Figure 1.4.** The putative structure of the  $\alpha_1$  subunit of the L channel and the cardiac motif IV( S3-S4) transmembrane helices (taken from Spedding & Kenny, 1991). Based on the proposal of Regulla *et al.* (1991) the DHP binding site might be located on the cytosolic tail beyond IV S6 between amino acids 1390 and 1437, closely associated with the cytosolic Ca<sup>2+</sup> EF-hand (Babitch, 1990). The structure of the cardiac IV transmembrane helices shows the conserved nature of repeating negatively charged amino acids in S3 coupled to positively charged amino acids in S4 (every third of fourth repeating residue being arginine or lysine) which might constitute the voltage-sensing apparatus for the channel.

close to this domain. Such a location for these sites would be close to the putative cytoplasmic EF-hand, the  $\text{Ca}^{2+}$  binding domain for the channel (Babitch, 1990). A possibility exists therefore that  $\text{Ca}^{2+}$  binding to this domain induces a conformational change to allow DHP binding (Tsien *et al.*, 1991) and possibly explains the requirement for  $\text{Ca}^{2+}$  in the detection of [ $^3\text{H}$ ] DHP binding sites (see 1.4.3.), although the relationship between the binding of  $\text{Ca}^{2+}$  and DHPs to their respective domains with changes in channel gating/membrane potential remains intriguing.

The role of the other channel subunits is less clear. For example, the  $\gamma$  subunit has only been demonstrated in skeletal muscle thus far although they do appear to play a regulatory role. Thus, expression of  $\alpha_2$  with  $\alpha_1$  increases  $\text{Ca}^{2+}$  current, and the presence of the  $\beta$  subunit modifies DHP binding to  $\alpha_1$  and increases the rate of activation and inactivation of the channel (Varadi *et al.*, 1991).

#### 1.2.6. *N-methyl-D-aspartate receptor mediated $\text{Ca}^{2+}$ entry.*

Receptor-mediated  $\text{Ca}^{2+}$  entry, evoked by the excitatory amino acid glutamate, is an important mechanism leading to increased  $[\text{Ca}^{2+}]_i$  in the context of the present work since growing evidence indicates a role for this transmitter and associated  $\text{Ca}^{2+}$  entry in excitotoxic cell death following ischaemia (see below). This neurotransmitter is widely employed in the CNS producing changes in intracellular  $\text{Ca}^{2+}$  following activation of postsynaptic membranes. The receptors which mediate the effects of glutamate have been characterised thus far in terms of the selectivity expressed by the prototypical agonists N-methyl-D-aspartate (NMDA), kainic acid and quisqualic acid (e.g. Foster & Fagg, 1984).

The NMDA receptor gates a channel permeable to both  $\text{Na}^+$  and  $\text{Ca}^{2+}$  and agonist-induced depolarisation results in large increases in  $[\text{Ca}^{2+}]_i$  (e.g. Miller, 1989). A variety of different regulatory sites for agonists, antagonists, ions and regulatory endogenous polyamines has been described on the NMDA-channel complex. The NMDA response can be blocked by a range of antagonists both competitive (e.g. D-2-amino-5-phosphonopentanoate) and non-competitive, which block the open state of the channel, including MK-801 and phencyclidine (e.g. Watkins, 1989). Indeed, many phencyclidine-like agents (e.g. ketamine), which have affinity for sigma receptors, also act as NMDA antagonists through an interaction at the ion channel (see Wong & Kemp, 1991). It is now apparent that a number of regulatory sites exist on the NMDA channel complex for ions,

such as  $Mg^{2+}$  which under normal conditions blocks the channel through an interaction at a distinct recognition site (Reynolds & Miller, 1988), but is relieved on membrane depolarisation.  $Zn^{2+}$  also acts at a distinct site to block NMDA responses by interfering with agonist binding, rather than by a direct effect in the channel (Reynolds & Miller, 1988; Wong & Kemp, 1991).

A distinct site also exists on the NMDA channel complex for another agonist, glycine, which markedly potentiates NMDA responses (Johnson & Ascher, 1987) so that antagonists at this site such as 7-chlorokynurenic acid produce depression of NMDA responses in a glycine reversible manner (Ascher & Johnson, 1989). More recently, evidence for the regulation of NMDA responses by endogenous polyamines and antagonism by agents such as ifenprodil have been reported (Carter *et al.*, 1989) although the precise location of these sites and the mechanism of antagonism is unclear.

Activation of kainate receptors also results in increased  $[Ca^{2+}]_i$  due to both  $Na^+$  influx and its resulting depolarisation, and possibly via a direct  $Ca^{2+}$  gated mechanism (see Miller, 1989). These receptors, however, are difficult to distinguish from quisqualate receptors because of the poor pharmacological specificity (Monaghan *et al.*, 1989).

Activation of quisqualate receptors by either quisqualate or its analogue AMPA, can mediate responses similar to kainate, i.e.  $Ca^{2+}$  entry following  $Na^+$  dependent depolarisation (Fagg, 1985). However, Murphy & Miller (1989) demonstrated increases in  $[Ca^{2+}]_i$  following exposure to quisqualate in cells that were pre-loaded with  $Ca^{2+}$ , and that the effect was lost on further stimulation unless internal stores were refilled. This effect was blocked by treating the cells with pertussis toxin, suggesting that the effect was due to the receptor being G protein linked. To distinguish between these different receptor sites and remove ambiguity, those receptors linked to inositol trisphosphate and diacylglycerol metabolism are referred to as "metabotropic receptors" at which AMPA is ineffective, and those that mediate  $Na^+$  gated events mediated by this agonist can be classified as distinct "AMPA" receptors (Watkins, 1989; Monaghan *et al.*, 1989).

Having thus established a role for these receptors mediating increases in  $[Ca^{2+}]_i$  in response to glutamate, the effects of various NMDA and non-NMDA receptor antagonists in models of cerebral ischaemia are overviewed below in sections 1.3.5. and 1.3.6.)

### 1.3. EXPERIMENTAL CEREBRAL ISCHAEMIA: MECHANISMS AND MODELS.

#### *1.3.1. Evidence for an involvement of calcium ion homeostasis in cell ischaemia.*

In 1977, by use of ion sensitive microelectrodes, Nicholson and co-workers (Nicholson *et al.*, 1977) demonstrated that in anoxic cerebral cortex marked decreases in the concentration of extracellular  $\text{Ca}^{2+}$  were accompanied with associated increases in extracellular  $\text{K}^{+}$ . In an experimental model of cerebral ischaemia (Harris *et al.*, 1981) similar reductions in extracellular calcium were also demonstrated. A role for increased cytosolic  $\text{Ca}^{2+}$  as the cause of cell death was demonstrated in non neuronal cells (Farber, 1981). Hass (1981) first postulated a similar role for  $\text{Ca}^{2+}$  in the death of neuronal cells following experimental cerebral ischaemia. Evidence from other studies indicated that this reduction in extracellular  $\text{Ca}^{2+}$  was not exclusive to the ischaemic brain and was observed in other states of neuronal hyperexcitability (Hansen & Zeuthen, 1981; Harris *et al.*, 1984). Such a hypothesis (Siesjo, 1981; 1988) is based on the probability that excessive calcium entry results from increased extracellular  $\text{K}^{+}$  and from the action of certain neurotransmitters, in particular activation of NMDA receptors by glutamate, proposed to induce two types of damage through osmolytic and  $\text{Ca}^{2+}$  related mechanisms (Rothman & Olney, 1986).  $\text{Ca}^{2+}$  related events are proposed to be responsible for the irreversible neuronal damage that occurs following cerebral ischaemia (Figure 1.5 ).

A consequence of a reduction in the supply of ATP would be the failure of the  $\text{Na}^{+}/\text{K}^{+}$  ATPase. An important role for  $\text{Na}^{+}/\text{K}^{+}$  ATPase in relation to the loss of synaptic activity during ischaemia has been demonstrated (Lipton & Whittingham, 1982). Intracellular pH in neurones is maintained through a  $\text{Na}^{+}/\text{H}^{+}$  exchange mechanism, the  $\text{Na}^{+}$  gradient for which is maintained by the  $\text{Na}^{+}/\text{K}^{+}$  ATPase. Acidosis would thus result from ischaemia, at a time when lactic acid is being produced because of compromised ATP supply with consequential detrimental effects on various cell functions. Reduced ATP would also result in a further loss of ionic homeostasis due to reduced  $\text{Ca}^{2+}$  extrusion through the  $\text{Ca}^{2+}$  activated ATPase. Experimental evidence would tend to support this proposed sequence of events. As a result of ischaemia a marked reduction in ATP occurs

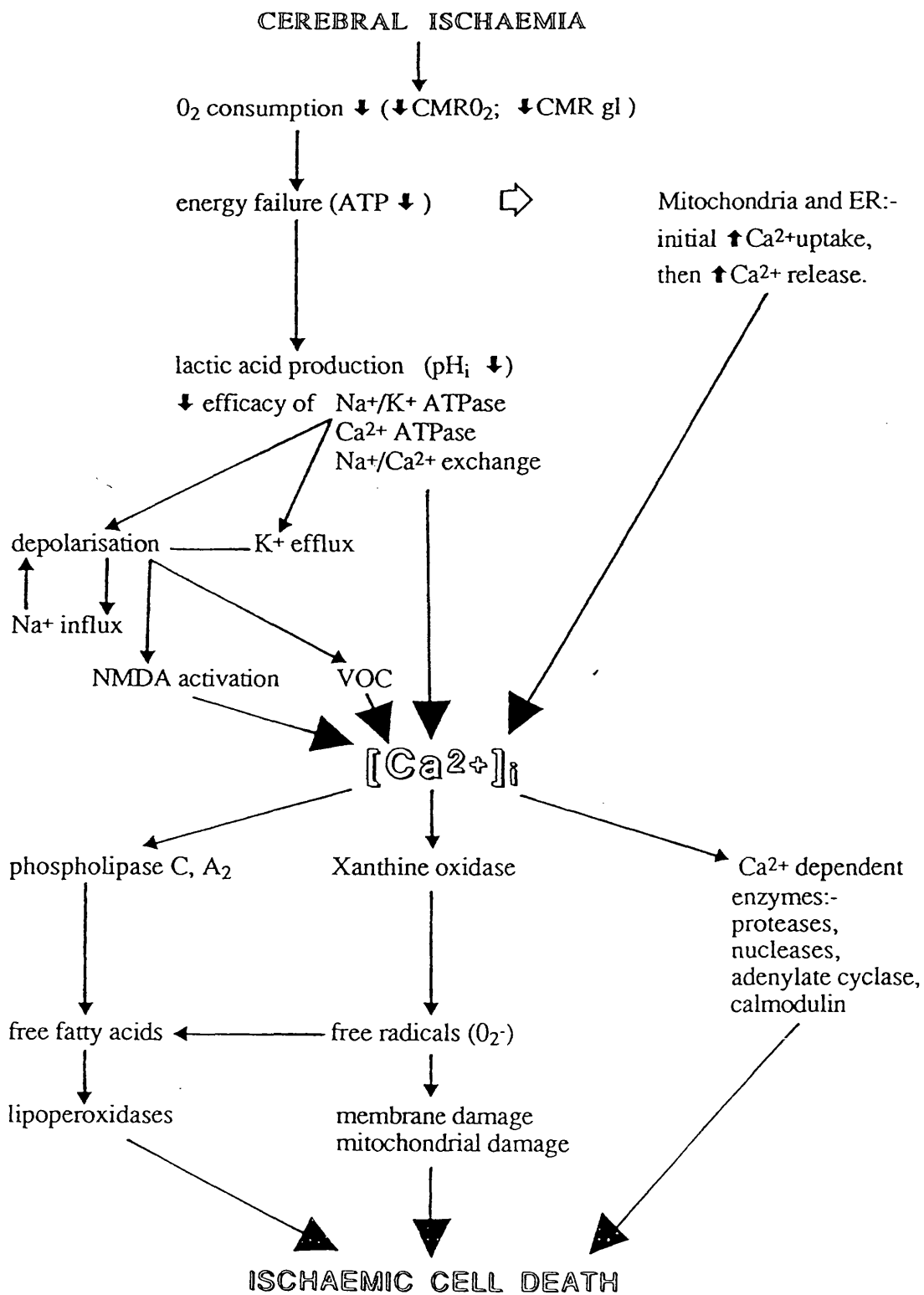


**Figure 1.5.** Schematic role for calcium in the ischaemic cascade leading to neuronal cell death

(Welch, 1982), reduced intracellular pH occurs as a result of lactic acid production (Siesjo, 1981; Smith *et al.*, 1986; Meyer, 1989). Intracellular acidosis increases  $\text{Ca}^{2+}$  release from intracellular sequestration sites (Abercrombie & Hart, 1986), since increased  $[\text{H}^+]_i$  would compete for carboxyl residues which normally form  $\text{Ca}^{2+}$  complexes. Increased cytosolic  $\text{Ca}^{2+}$  levels have adverse effects on mitochondrial function (Griffiths *et al.*, 1982; Simon *et al.*, 1984; Hillered *et al.*, 1984), in particular the uncoupling of oxidative phosphorylation (Siesjo, 1981), with the eventual release of  $\text{Ca}^{2+}$  through a  $\text{Ca}^{2+}$  operated pore (McCormack *et al.*, 1990).

During the early ischaemic period there is a large increase in extracellular potassium (up to 50 mM), due to leakage from energy-compromised cells (Nedergaard, 1988).  $\text{Ca}^{2+}$  entry through presynaptic channels as a result of depolarisation would result in increased neurotransmitter release, including excitatory amino acids, which on relief of the  $\text{Mg}^{2+}$  block, would cause further  $\text{Ca}^{2+}$  entry on postsynaptic activation (Miller, 1989). In addition, the uptake of glutamate by glial cells is inhibited by high potassium concentrations (Barbour *et al.*, 1988). Furthermore, depletion in the level of a variety of neurotransmitters following cerebral ischaemia is well documented (Welch *et al.*, 1978; Alps *et al.*, 1985). It is, however, the excessive release of excitatory amino acids that forms the basis for the excitotoxic theory of calcium-mediated cell death (see Choi, 1985; Rothman & Olney, 1986) in which the important distinction was made between rapid cell death being  $\text{Na}^+$  dependent (accompanied by osmolysis because of  $\text{Cl}^-$  entry) (Rothman, 1985), and delayed neuronal cell death which was  $\text{Ca}^{2+}$  dependent (Choi, 1988b).

The role of cellular  $\text{Ca}^{2+}$  and the relationship to neuronal death following activation of NMDA receptors has been demonstrated in tissue culture with the use of electron microscopy (Garthwaite & Garthwaite, 1986). Early exposure to NMDA agonists caused a substantial influx of calcium, but this was buffered by the Golgi apparatus and nucleus, with the cytoplasm relatively unaffected and the neurones capable of survival on removal of the agonist. Longer periods of NMDA exposure, however, caused  $\text{Ca}^{2+}$  deposits in the mitochondria and cytoplasm with the neurones becoming necrotic on removal of the agonist. The temporal relationship between irreversible damage and  $\text{Ca}^{2+}$  loading of intracellular buffering sites is very close (Hajos *et al.*, 1986), associated with swelling of the Golgi apparatus and aggregation of chromatin in the nucleus. The mitochondria become swollen in proportion to the amount of  $\text{Ca}^{2+}$  accumulated because of associated phosphate deposits (Kariman, 1985). However, unlike the osmolytic swelling that occurs on

NMDA exposure, none of the pathological changes occur in  $\text{Ca}^{2+}$  free media (Garthwaite, 1989). When intracellular buffering mechanisms fail to halt these increases in intracellular  $\text{Ca}^{2+}$  levels, many  $\text{Ca}^{2+}$ - dependent destructive enzymes will be activated (Figure 1.5). Activation of phospholipases leads to membrane breakdown and the production of arachidonic acid, metabolism of which gives rise to free radical formation (Siesjo, 1981; White *et al.*, 1984; Siesjo, 1988). Activation of proteases such as calpain causes cytoskeletal breakdown due to degradation of microtubules and filaments and a vesicular appearance or blebbing of the cell surface (Nicotera *et al.*, 1986; Garthwaite, 1989).

### ***1.3.2 Ischaemic cell damage- selective neuronal vulnerability and relation to forebrain ischaemia.***

Rothman (1983) demonstrated that glutamate toxicity was enhanced under anoxic conditions *in vitro*. In the hippocampus, large increases in the level of glutamate measured by microdialysis have been detected following forebrain ischaemia (Benveniste *et al.*, 1984; Hagberg *et al.*, 1985). It is now also clear that a selective pattern of neuronal damage in experimental animals occurs following a period of forebrain ischaemia.

Meldrum & Brierley (1973) first demonstrated the loss of pyramidal neurones in the CA1 and CA3 subfields of the hippocampus following experimentally-induced status epilepticus. In the gerbil, neurological deficit leading to neuronal loss has been demonstrated following cerebral ischaemia (Levine & Payan, 1966), and in the same model Kirino (1982) used the term 'delayed neuronal death' to describe the very selective loss of certain neuronal cells that occurred following experimentally induced forebrain ischaemia. This is a widely used model of ischaemia, occlusion of both common carotid arteries producing complete forebrain ischaemia in most animals because of the lack of connection between carotid and vertebro-basilar circulations (Levine & Payan, 1966 ; Kahn, 1972).

It is a feature of this model that the morphological cell change is gradual and takes several days to become apparent (Kirino, 1982). This principle is now established in other experimental models including the rat (Pulsinelli *et al.*, 1982b; Kirino *et al.*, 1984) where in all cases the CA1 pyramidal cells of the hippocampus are the most selectively vulnerable, with the involvement of other neuronal areas dependent on the severity and duration of the ischaemic period. Those brain areas shown to be selectively vulnerable have excitatory

amino acid input (see Garthwaite, 1989). Furthermore, lesions of these glutaminergic afferents projecting to the hippocampus attenuate ischaemia-induced neuronal damage (Pulsinelli, 1985; Wieloch, 1985). These areas are also rich in calcium channels. Such neurones show a tendency to burst fire (Wong & Prince, 1978), with neurones in CA1 being predisposed to epileptiform activity and suggesting that they may be involved in neuronal vulnerability (see Siesjo, 1988). It is interesting to note that in the gerbil model further pathological processes occur following forebrain ischaemia involving other areas such as deep cortical layers and the paramedian area of the hippocampus (Brown *et al.*, 1979) with reactive changes occurring similar to those previously described (Ito *et al.*, 1975). However, these changes were as a result of epileptic seizures following the ischaemic insult consistent with this animal being susceptible to convulsions. It has been postulated that neuronal hyperexcitability may be the cause for selective neuronal loss (see Meyer, 1989), arising during ischaemia due to the release of excitatory amino acids acting at post-synaptic sites, thus providing further *in vivo* evidence for excitotoxic cell death.

An important feature of the hippocampus is its neuronal circuitry: the perforant path is the major excitatory input to the hippocampus and an increased transmitter release in CA1 could result from the pathway directly or from the multi-synaptic pathway via the dentate gyrus and CA3 pyramidal cells. Similarly, damage in CA1 has been shown to result from excessive activity in CA3 (Suzuki *et al.*, 1983), and lesioning the pathway from CA3 results in protection of CA1 neurones (Onodera *et al.*, 1986). Furthermore, lesioning the input to CA1 also causes a significant decrease in the release of glutamate in CA1 as a result of ischaemia without effect on NMDA receptor density (Diemer *et al.*, 1989).

### ***1.3.3. Other models of forebrain ischaemia.***

Occlusion of bilateral carotid arteries in the rat has been described in a so called '2 vessel occlusion model' (Eklof & Siesjo, 1973). When combined with hypotension reversible forebrain ischaemia is produced. Also in the rat, a 4 vessel occlusion model has been described. This is a somewhat more complicated model as it is produced in two stages, by permanent vertebral artery occlusion followed by transient carotid artery occlusion (Pulsinelli & Brierley, 1979). The histology of this model resembles that of the two vessel model (Ginsberg & Busto, 1989) with ischaemic cell changes in selectively

vulnerable structures including CA1 pyramidal neurones of the hippocampus, caudate putamen, neocortex and purkinje cells of the cerebellum. As with the gerbil, this model has been extensively used in the characterisation of potential neuroprotective agents, and as such, several points are noteworthy.

Following electrocautery of the vertebral arteries, ischaemia is not induced until 24 hours later and a complete lack of vertebral flow must be attained in order to successfully achieve complete ischaemia following carotid artery occlusion (Ginsberg & Busto, 1989). Within the 72 hour recovery period, 40% of rats will convulse and should not be used for further analysis (Pulsinelli & Brierley, 1979). There is also considerable variability between the results of various laboratories in this model (Pulsinelli & Brierley, 1979; Pulsinelli & Buchan, 1988, Ginsberg & Busto, 1989) as to the severity and outcome of the ischaemic insult. Although differences between and within strains have been noted, it is possible that inherent differences in blood glucose are an important variable as hyperglycaemia markedly exacerbates damage in global ischaemia models (Welsh *et al.*, 1980; Pulsinelli *et al.*, 1982a). Furthermore, inconsistency in brain temperature may account for variations between laboratories (Busto *et al.*, 1987) as brain temperature during and after forebrain ischaemia in rats cannot be predicted from rectal temperature. Taken together, such findings indicate that the 4 vessel occlusion model does not represent an easy means of quantifying neuronal damage and detecting neuroprotective agents.

Other rat models include the model initially introduced by Levine (1960) and modified by Salford & Siesjo (1974) combining unilateral occlusion with hypoxemia resulting in tissue acidosis and a unilateral selective pattern of damage to hippocampus and striatum. As with other models of selective vulnerability models there is evidence for an involvement of the glutaminergic input into CA1 via the Schaffer collateral pathway from CA3 in the neurotoxic mechanism leading to CA1 neuronal death, since selective lesioning of CA3 neurones with kainic acid protects CA1 neurones against ischaemic damage in this model (Benveniste *et al.*, 1989). Models of forebrain ischaemia are relevant to the human in situations where there is a rapid failure of cerebral perfusion and oxygenation, thus manifesting as global ischaemia. Thus, following cardiac arrest, selective damage to hippocampal pyramidal neurones has been shown (Petito *et al.*, 1987).

#### 1.3.4. Focal ischaemia.

Models of middle cerebral artery (MCA) occlusion have gained increasing acceptance over recent years, being more pertinent to the human condition as the resultant infarct is more focal in nature (Garcia, 1984). The first attempts in this area were aimed at inducing infarction by embolising an intracranial artery (with homologous blood) and met with some success when the technique was adapted with the use of silicone spheres and other silastic material (Molinari & Laurent, 1976). The majority of approaches now use a transorbital approach to surgically manipulate the initial segment of the MCA. Initially described in the monkey, the first well documented procedure of proximal MCA occlusion (following zygoma removal between rhinal branch and lateral striate arteries) in the rat was described by McCulloch's group (Tamura *et al.*, 1981a; 1981b). The same workers later modified this model and replaced electrocautery with snare ligation and thus introduced reperfusion aspects into the model (Shigeno *et al.*, 1985). Transorbital occlusion leads to total interruption of anterograde cerebral blood flow and establishes retrograde flow through anastomoses of anterior and posterior cerebral arteries (Garcia, 1984).

A close correlation exists between the extent of histological abnormality and the area of decreased regional blood flow, although there is a large change in flow on the edge of the ischaemic lesion (Tyson *et al.*, 1984), often referred to as the ischaemic 'penumbra'. In this model the caudate putamen and olfactory cortex were consistently found to be infarcted, the involvement of the frontoparietal cortex was more variable (Duverger & MacKenzie, 1988). As in forebrain ischaemia models there is strong evidence for the involvement of  $\text{Ca}^{2+}$  in the ischaemic damage.

Following focal ischaemia Rappaport *et al.* (1987) demonstrated that significant amounts of  $\text{Ca}^{2+}$  had accumulated in the ischaemic zone by 4hr. By 24hr this had reached 17 times the amount of pre-ischaemia tissue  $\text{Ca}^{2+}$  content, indicating large  $\text{Ca}^{2+}$  shifts as a result of ischaemia, and demonstrating the capacity of brain tissue to act as a ' $\text{Ca}^{2+}$  sink'. Evidence also exists for an involvement of excitatory amino acids as *in vivo* microdialysis shows marked elevations of released glutamate (Benveniste *et al.*, 1984) and increases in the level of [ $^3\text{H}$ ] MK 801 binding (enhanced by glutamate) have been demonstrated in the zone of ischaemic tissue in autoradiographic studies (Wallace *et al.*, 1989). As in global models, the presence of experimentally-induced hypotension increases the infarct (Osbourne *et al.*, 1987). The severe infarct observed in striatum following focal ischaemia

is probably a reflection of a greater reduction in blood flow in this area compared to cortex, arising because of the lack of collateral supply to the basal ganglia.

An interesting variation of this model has been described (Watson *et al.*, 1985; Nakayama *et al.*, 1988) in which an occlusive thrombus of aggregated platelets is induced by means of photothrombotic occlusion of the MCA. Infarction is generated by the intravenous injection of the dye rose bengal and activation by light of a specific wavelength which induces a photochemical reaction to produce singlet oxygen which peroxidises lipid molecules and causes microvascular platelet aggregation, thus representing a potentially useful model for the study of compounds interfering with thromboembolic processes.

Another rodent model of cerebral ischaemia is the stroke-prone spontaneously hypertensive rat established by Okamoto *et al.* (1974). The affected sites in this model include the occipital cortex and basal ganglia (Yamori *et al.*, 1976). Ischaemic damage occurs in this model because of elevated vascular resistance in the large cerebral arteries, an inherent feature of the model representing a compensation mechanism to decreased pressure in smaller vessels during hypertensive episodes, thus differing from other strains of animals. This is a difficult model to work with in practice because of the resulting temporal and geographical variability of infarct occurrence.

#### *1.3.5. In vitro models of ischaemia.*

The excitotoxic theory of  $\text{Ca}^{2+}$  mediated neuronal cell death has largely been substantiated by *in vitro* studies using primary cultures of central neurones. These are generally neonatal or embryonic brain fragments, which after dissociation, are developed in growth factor supplemented media such that they quickly form active excitatory and inhibitory synaptic connections. These cultures can be made hypoxic/ischaemic by exposure to a  $\text{CO}_2/\text{N}_2$  environment, exposure to cyanide or by glucose deprivation. Two pieces of evidence suggest a role for glutamate involvement in producing *in vitro* neuronal damage. Firstly, Rothman and co-workers (Rothman, 1983; Rothman & Samaie, 1985) noted that exposure of hippocampal neurones to either hypoxia or sodium cyanide only produced cell death when the cultures were established, i.e. having excitatory glutamatergic synapses. Cell death did not occur when the cells were first put into culture. Other studies have shown that exposure to low levels of excitatory amino acids causes neuronal injury with no effect on glial cells (Choi, 1988a). Secondly, competitive and non-competitive

NMDA antagonists and high levels of magnesium have all been shown to attenuate neuronal loss in a variety of hypoxic cultures (Rothman, 1984; Weiloch, 1985; Goldberg *et al.*, 1988; Choi *et al.*, 1989; Choi & Rothman, 1990). Furthermore, in cultures of rat basal ganglia, with fewer glutamatergic neurones, NMDA antagonists were ineffective.

An important feature of *in vitro* cell loss is that neurotoxicity can be separated into two components of initial neuronal swelling (associated with Na<sup>+</sup> and Cl<sup>-</sup> uptake) caused by neuronal depolarisation, followed by the delayed degeneration of the neurones, which is calcium dependent. The second component can be attenuated by reduced levels of Ca<sup>2+</sup> (see Garthwaite, 1989) and mimicked by calcium ionophores, with the calcium component being more important at low levels of toxic exposure (Choi *et al.*, 1989). Thus, antagonism of L-type VOCs does not attenuate NMDA mediated toxicity but recent evidence (Weiss *et al.*, 1990) suggests that DHPs may reduce neuronal loss caused by low level exposure to some glutamate agonists. The concentrations required to do this are high, although this may be consistent with the high concentrations required to block L channel mediated calcium current, but as significant effects were only obtained at concentrations >10µM, protection via other mechanisms cannot be excluded, as high concentrations of other agents such as morphinans are protective in this model (Choi *et al.*, 1989).

Another *in vitro* approach has been the use of hippocampal slice preparations. *In vivo*, one of the first consequences of ischaemia is the loss of electrical activity (as measured by EEG). Similarly *In vitro*, by means of a hippocampal slice preparation (Lipton & Whittingham, 1979), it has been demonstrated that the loss of electrical activity (assessed by evoked potentials) was due to hypoxia-induced depolarisation of neuronal membranes, presumably because under excessive depolarisation the membrane would not be able to repolarise sufficiently to activate further action potentials. Using ouabain, the same workers implicated a role for the failure of the Na<sup>+</sup>/K<sup>+</sup> ATPase, as it caused similar effects to hypoxia and the process was found to be enhanced by increased levels of extracellular K<sup>+</sup>. In a later study (Lipton & Whittingham, 1982), the failure of synaptic transmission was shown to be through a reduction in ATP subsequently affecting Na<sup>+</sup>/K<sup>+</sup> ATPase and as this is one of the first effects of ischaemia it may well explain rapid synaptic failure. This model therefore represents a potential functional model for the study of *in vitro* hypoxia, of particular relevance because of the excitatory amino acid involvement in hippocampal synaptic transmission. The use of this model is described in more detail in Chapter 5 of this thesis.

### ***1.3.6. NMDA antagonists protect against neuronal damage in focal and forebrain ischaemia models.***

Originally designed as an anti-convulsant, the non-competitive NMDA antagonist MK-801 has been shown to be a potent neuroprotective agent in reducing hippocampal cell loss following cerebral ischaemia in the gerbil (Gill *et al.*, 1987) and neocortical cells in the rat (MacDonald *et al.*, 1987). Neuroprotection was found to be dose-dependent and protection was still conferred when the drug was administered post-ischaemia. Gill *et al.* (1988) demonstrated that neuroprotection was still conferred when administered up to 24 hrs post ischaemia. In a more severe ischaemia in the gerbil, induced by 10 min bilateral carotid occlusion, MK 801 was still neuroprotective when administered pre-ischaemia (see Iversen *et al.*, 1989). Neuroprotection has also been demonstrated for other NMDA antagonists. 3-(2-carboxypiperazin-4-yl)propyl-1-phosphonate (CPP) has been shown to be protective in gerbil forebrain ischaemia (Boast *et al.*, 1988) and both 2-APV and CPP are neuroprotective in gerbil brain (Swan *et al.*, 1988). The neuroprotective effects of MK-801 in this model have been attributed to a hypothermic effect since Pulsinelli (see Meldrum & Swan, 1989) has shown the compound to be ineffective where efforts have been made to maintain brain temperature. However, this finding must be taken in context, since as already noted, protection with MK-801 is still conferred in this model when administered up to 24 hrs post-ischaemia, and increasing brain temperature to compensate for any drug effect may result in exacerbating CA1 neuronal damage beyond the level of drug protection.

Nevertheless, protection in forebrain ischaemia has also been shown with competitive and non-competitive NMDA antagonists following 2 vessel occlusion in the rat (Meldrum *et al.*, 1989). However, in the rat 4 vessel occlusion model, neither class of NMDA antagonist offers significant protection (Swan & Meldrum, 1989; Wieloch *et al.*, 1988) and in the monkey, following complete forebrain ischaemia, MK-801 is ineffective (Lanier *et al.*, 1989). The findings with all classes of NMDA antagonist in models of focal ischaemia are somewhat more consistent. All classes of antagonist (competitive antagonists, channel blockers, glycine and polyamine site antagonists) have been shown to be active in focal ischaemia models reducing the infarct volume following MCA occlusion in the rat or cat. In a cat MCA model, MK-801 was effective in reducing infarct volume pre- or post-ischaemia (Park *et al.*, 1988a). Similar findings have been confirmed in the rat

MCA model (Gill *et al.*, 1991). The competitive antagonist, 2-APV, is also active in the rat (Roman *et al.*, 1989) as is the glycine antagonist kynureate (Germano *et al.*, 1988). The polyamine regulatory site antagonists, ifenprodil and SL 82.0715, are active in rat, cat and mouse MCA occlusion models (Gotti *et al.*, 1988; Gotti *et al.*, 1990).

#### **1.4. Calcium antagonists form a heterogeneous group of compounds**

Given this evidence for neuroprotection by agents active at the NMDA receptor complex, the present work aims to establish whether those compounds classified as calcium antagonists show similar neuroprotective potency in models of experimental cerebral ischaemia. As already noted in part 1.2.4. there are several different forms of VOCs. However, it is the L channel that forms the basis for the interaction of calcium antagonists used in the present work. Characterisation of these interactions in the last decade has revealed that these compounds form a heterogeneous group, and several proposals have been made to classify them accordingly. As the main thrust of this thesis is to differentiate these compounds *in vitro* in an attempt to define which, if any, of these agents represent potential neuroprotective agents, the background to the classification of these compounds will now be overviewed.

##### ***1.4.1. Identification of calcium antagonist binding sites by radiolabelled calcium antagonists.***

The term 'calcium antagonist' was first coined by Fleckenstein in 1966 to describe the action of certain verapamil-like compounds of unknown mechanism whose action appeared to mimic the effect of calcium withdrawal reducing cardiac contractility through an action on cardiac excitation-contraction coupling without any major effect on the Na<sup>+</sup>-dependent upstroke of the action potential (for a review see Fleckenstein, 1988). These studies were followed by the identification of other more potent compounds (including D-600 or methoxyverapamil and the first 1,4-dihydropyridine, nifedipine) which again inhibited Ca<sup>2+</sup>-dependent contractility but did not affect Na<sup>+</sup> dependent action potentials. At the same time as Fleckenstein's seminal studies, other workers (Paton & Rang, 1965) initiated experiments with the aim of labelling drug receptor sites with radiolabelled

compounds. These workers attempted to label muscarinic binding sites on slices of guinea pig ileum but failed to observe workable amounts of specific binding because of the low incorporation of tritium into the atropine used (thus resulting in low specific activity of the ligand). However, with the introduction of higher specific activity ligands, binding studies have revolutionised receptor pharmacology in the identification of receptors and their subtypes.

Well documented examples include the first demonstration of the opiate receptor in nervous tissue (Pert & Snyder, 1973), muscarinic receptors in brain (Yamamura & Snyder, 1974) and  $\alpha$ -adrenoceptors (Williams *et al.*, 1976). Lesser known examples include the specific binding of [ $^{125}$ I] insulin to talcum powder (Cuatrecasas & Hollenberg, 1975) and the binding of some radiolabelled opiates to glass fibre filters (Snyder *et al.*, 1975)!! These last two cases highlight some of the problems of analysing ligand binding data, and as this is becoming increasingly computerised, care must be taken to avoid experimental artifacts such as non-equilibrium, use of impure ligands, improper definition of non-specific binding, poor recovery of unfiltered media in measuring the amount of assay [ $^3$ H] and displaced non-specific binding (could be interpreted as heterogeneity of binding sites in Scatchard plots of saturation data). An extensive account of these artifacts and the computerised approach in their resolve has been described (Kermode, 1989) and overviewed in relation to the quantification of the affinity of calcium antagonists (Kenny *et al.*, 1991).

The first demonstration of high affinity binding for a radiolabelled calcium antagonist was carried out by Glossmann and co-workers using [ $^3$ H] nitrendipine (see Glossmann *et al.*, 1982). These and other studies rapidly confirmed that the affinity of these agents was similar to the potency of inhibition of  $\text{Ca}^{2+}$  contraction of smooth muscle. Furthermore, the binding of these agents was shown to be calcium-dependent, with no detectable binding in the absence of divalent cations (Glossmann *et al.*, 1982). Sites for these agents were found to be similar in brain, heart and smooth muscle (Ferry *et al.*, 1985). In parallel functional experiments, it appeared that these agents formed a heterogeneous group of compounds, and on the basis of functional studies and binding experiments, could be subclassified accordingly.

#### 1.4.2. *There are different classes of calcium channel antagonists.*

It is now quite apparent that those compounds classed as calcium antagonists (Figure 1.6) acting at L-type VOCs can be separated into at least three groups based on site of action and pharmacological specificity, and for the purpose of this thesis the definition of Spedding (1985b) will be referred to. The classification is as follows:-

I. Dihydropyridines (e.g. nifedipine, isradipine, nicardipine)

II. Hydrophilic basic compounds (e.g. verapamil, diltiazem, diclofurime)

III. Lipophilic diphenylalkylamines (e.g. cinnarizine, flunarizine, lidoflazine, pimozide).

This classification is different to that claimed by other workers based on antagonist potency and selectivity (Fleckenstein, 1983), or allosteric properties in binding experiments (Glossmann *et al.*, 1982; Glossmann & Ferry, 1985). A current subclassification has been proposed by the World Health Organisation (Table 1.1).

#### 1.4.3. *Class I calcium antagonists.*

Dihydropyridines (DHPs) preferentially bind to the inactivated state of the VOC (high affinity state associated with depolarisation), or in membrane preparations where the membrane fractions are 'infinitely' depolarised since there is no membrane potential. Thus, in radioligand binding assays where the reaction is terminated by filtration only high affinity components ( $<1\text{nM}$ ) will be easily detected, and high affinity binding sites have been demonstrated in a number of tissues (Glossmann *et al.*, 1982).

Furthermore, it has been shown that the voltage dependence of VOC activity will determine DHP density. Consequently, resting channels at  $-80\text{mV}$  (Bean 1984, Sanquinetti & Kass, 1984) would not be detected in filtration assays as the affinity of this state is only in the order of  $1\mu\text{M}$  (Janis *et al.*, 1985). This also explains the relative weakness of DHPs as cardiac suppressants since they only inhibit contractility in the heart by binding to the inactivated form of the channel, which exists only for very short periods. Conversion to high affinity on depolarisation ( $<0.3\text{nM}$ ) would allow detection, as shown in cardiac

**Table 1.1. Classification of calcium antagonist subgroups**

<b>Fleckenstein (1983):</b>	Group A DHPs (nifedipine) verapamil, diltiazem, methoxyverapamil
	Group B prenylamine, fendiline, perhexiline, bepridil (+flunarizine, cinnarizine)

**Glossmann (1982; 1984)**

CLASS I	DHPs (nifedipine), fendiline, tiapamil, flunarizine
CLASS II	verapamil, methoxyverapamil
CLASS III	diltiazem

**Spedding (1982; 1985)**

CLASS I	DHPs (nifedipine etc.)
CLASS II	verapamil, diltiazem
CLASS III	flunarizine, cinnarizine, lidoflazine, bepridil, perhexiline, prenylamine

**WHO classification (Vanhoutte & Paoletti, 1987)**

CLASS I	Verapamil, methoxyverapamil
CLASS II	DHPs (nifedipine etc.)
CLASS III	diltiazem
CLASS IV	flunarizine
CLASS V	prenylamine, fendiline
CLASS VI	perhexiline

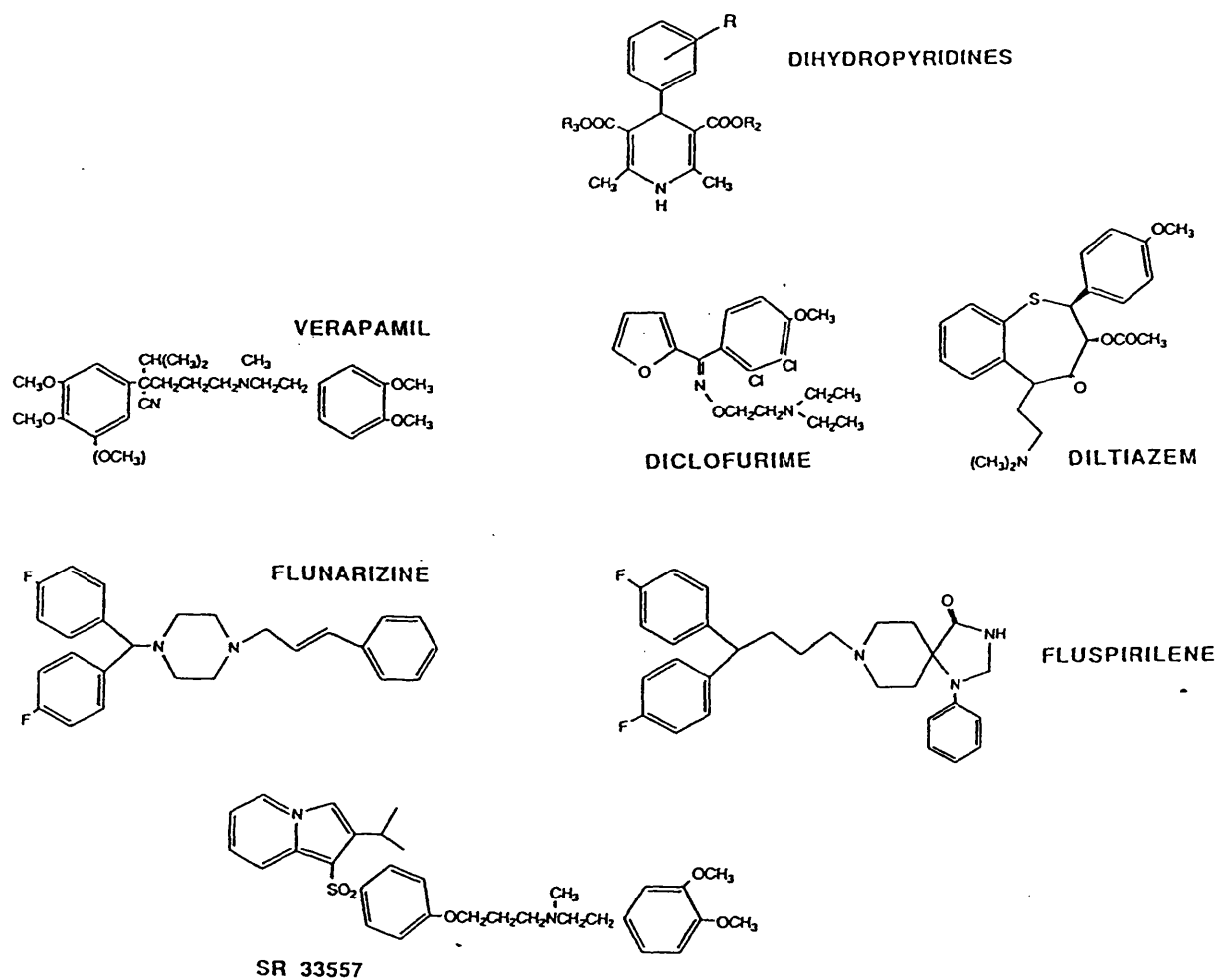


**Figure 1.6.** The structure of class I (DHPs with substitution points R, R<sub>2</sub> and R<sub>3</sub>), class II (verapamil, diclofurime and diltiazem) and class III (flunarizine and fluspirilene) calcium antagonists. SR 33557, an indolizine sulfone, is a novel high affinity calcium antagonist that labels a site in cardiac and skeletal muscle membranes distinct from the sites of action of class I, II and III compounds (Chatelain et al, 1991).

myocytes (Green *et al.*, 1985). Equilibrium dissociation constants ( $K_d$ ) and the number of sites ( $B_{max}$ ) in radioligand binding assays show considerable tissue variability, although a single class of binding sites is always labelled. Differences in the effects within the class of DHP molecules will relate to their kinetics, which will be dependent on the relative lipophilicity of the DHP, although this does not explain how certain [ $^3H$ ] DHPs have affinity constants that show tissue variation. [ $^3H$ ] isradipine (PN 200-110) binds with an affinity constant of 0.03 nM in brain, but only 1.4 nM in skeletal t-tubule membrane fractions (the richest known source of calcium channels) (Glossmann & Ferry, 1985).

The binding of [ $^3H$ ] DHPs is very temperature dependent, and the presence of divalent cations is a requisite. DHP binding is pH dependent, being stable and maximal in brain over the range 6.5-8.0 (Glossman *et al.*, 1985; Janis *et al.*, 1985) and is lost on heat treatment of the membranes (Glossman *et al.*, 1982). The binding site for [ $^3H$ ] DHP antagonists is so exquisitely sensitive to  $Ca^{2+}$  that high affinity binding occurs even in low contaminating concentrations of  $Ca^{2+}$  (present in extensively washed membrane preparations using non ion supplemented buffer). After depletion of cations with chelating agents such as EDTA, or the more calcium specific EGTA, high affinity binding isotherms can be established by the addition of cations, so called 'refill' curves, with the cations having  $EC_{50}$  values in the  $\mu M$  range for reconstitution (Glossmann *et al.*, 1982). The increase in detectable binding resulting from cation readdition is due to an increased receptor number, with no change in affinity (Bolger & Skolnick, 1986). Structurally related DHPs displace [ $^3H$ ] DHP ligands from their binding sites through a competitive interaction.

Class I compounds are reversible competitive antagonists of  $K^+$  depolarised smooth muscle and their effects are fully reversed by Bay K 8644 (Spedding, 1985a). They are predominantly vasodilators because of their selectivity for vascular smooth muscle, without direct effects on the myocardium, but can therefore precipitate reflex tachycardia.

#### ***1.4.4. Class II calcium antagonists.***

Class II agents (as typified by verapamil and diltiazem) modulate [ $^3H$ ] DHP binding in a negative and positive allosteric manner respectively, the extent of which is thermodynamically dependent (Glossmann & Ferry, 1985). It is likely that this modulation

is induced by an interaction at two distinct sites that are tightly linked, but each coupled to the DHP site so as to increase or decrease [ $^3\text{H}$ ] DHP binding (Galizzi *et al.*, 1985; Mir & Spedding, 1987). This effect is multi-directional as occupation of the DHP site also regulates binding of [ $^3\text{H}$ ] verapamil and [ $^3\text{H}$ ] diltiazem (Ferry *et al.*, 1984).

Class II agents differ from DHPs in that the regulation of binding by divalent cations is inhibitory. The binding of both [ $^3\text{H}$ ] diltiazem (in skeletal muscle t-tubules) and [ $^3\text{H}$ ] verapamil (in brain) is inhibited by mM concentrations of divalent cations. When the positive and negative allosteric effects of diltiazem and verapamil on [ $^3\text{H}$ ] DHP were investigated, it was found that the effect of  $\text{Ca}^{2+}$  was to decrease the affinity of the compounds in their interaction without any effect on maximal potency (Schoemaker & Langer, 1989), suggesting an interaction at the  $\text{Ca}^{2+}$  recognition site. In functional studies, the effects of class II agents are reversed by Bay K 8644 and the compounds are reversible competitive calcium antagonists in  $\text{K}^+$  depolarised smooth muscle. Although the interaction of these agents is also voltage-dependent, they have direct effects on the myocardium causing bradycardia and AV block. These effects may relate to different kinetics of these drugs, and a dependence on stimulation frequency (Spedding, 1985a).

#### 1.4.5. Class III calcium antagonists.

Class III agents show lower affinity and selectivity for VOCs. They affect  $\text{Na}^+$  channels with similar affinity (Grima *et al.*, 1986) and interact with the intracellular binding proteins such as calmodulin at similar concentrations (Spedding, 1983). Thus, it is possible that these compounds may have other non-specific effects because of their lipophilicity. The potency of some of these agents is decreased in the presence of  $\text{Ca}^{2+}$  (Spedding, 1982) and this class of agent may also affect T-type  $\text{Ca}^{2+}$  channels (Tang *et al.*, 1988). In functional studies Bay K 8644 does not reverse the effects of class III agents (Spedding & Berg, 1984). These agents have slow kinetics *in vitro* and *in vivo*, and although they behave like antiarrhythmics, many of their effects may be due to interactions other than at calcium channels.

Unlike class I and II agents, distinct binding sites for these and other agents have not been directly demonstrated in brain tissues, although it is apparent that distinct sites exist for a variety of compounds in skeletal muscle and cardiac membrane preparations (e.g. Qar *et al.*, 1987; King *et al.*, 1989; Chatelain *et al.*, 1991, Figure 1.7). However, it

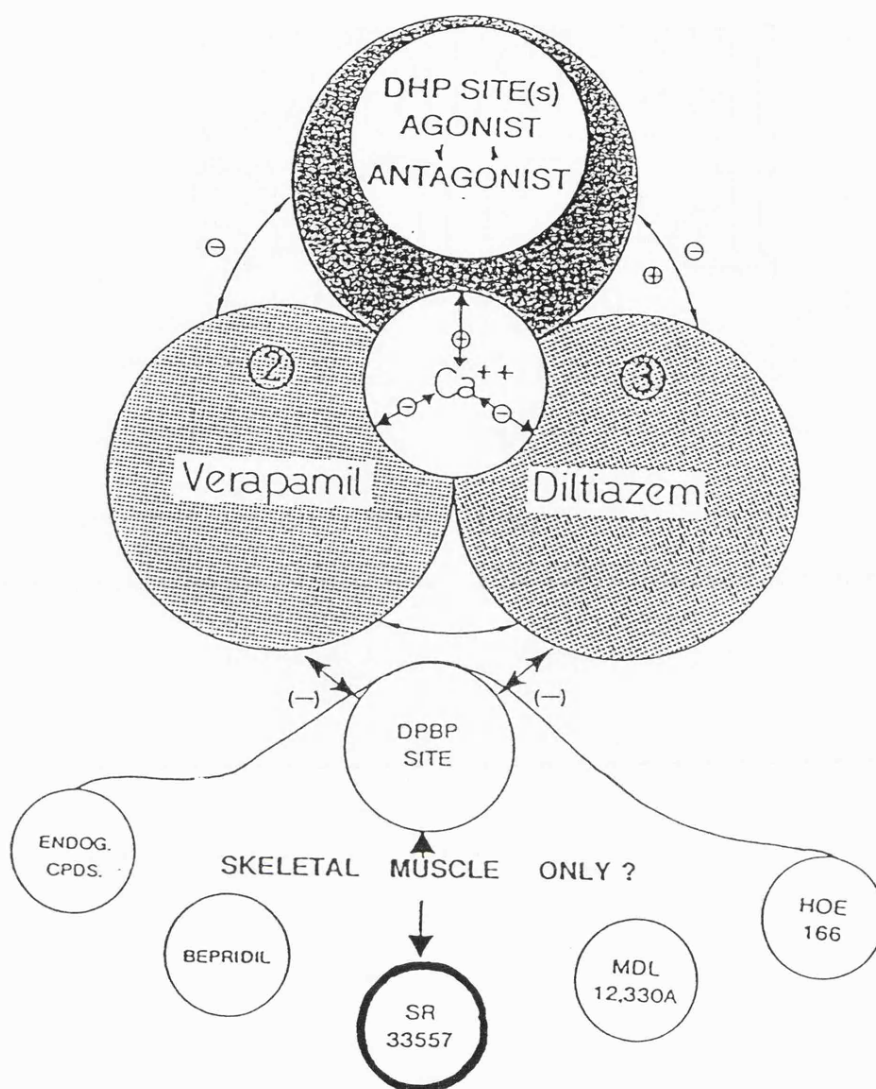


**Figure 1.7.** Multiple allosterically coupled binding sites for different classes of calcium antagonist associated with the L-type calcium channel. Definitive sites for the prototypical agents dihydropyridines, phenylalkylamines (verapamil) and benzothiazepines (diltiazem) have been demonstrated in brain membranes. Note the positive allosteric coupling between the DHP and diltiazem sites. Sites for other calcium antagonists have only been demonstrated in skeletal muscle or cardiac membranes thus far.

is the interaction of these compounds in brain tissue that will be the focus of attention in the present work.

#### 1.4.6. Calcium channel activators.

Minor modification to the DHP structure *per se* has resulted in agents which bind at the same site as DHP antagonists, but activate VOCs, increasing calcium entry. Such an agent is Bay K 8644 and this compound stabilises the prolonged open form of the channel, enhancing inward  $\text{Ca}^{2+}$  current (Reuter *et al.*, 1988). Some limited experiments have shown that Bay K 8644 binds to both a high and low affinity state (Lee *et al.*, 1987) although it has been demonstrated that low affinity sites are not associated with  $\text{Ca}^{2+}$  channels (Sarmiento *et al.*, 1987). Indeed, the binding site for activators has been widely reported to be the same as that for DHP antagonists (for a review see Triggle & Rampe, 1989). In a similar fashion to antagonist binding, increased binding affinity is expressed by activators on depolarisation, conditions upon which activators might possess blocking properties (Kokubun *et al.*, 1986). At negative membrane potentials in polarised cells, activators are capable of exerting positive allosteric interactions at DHP binding sites as measured by [ $^3\text{H}$ ] DHP antagonist binding in cultured cells from rat heart (Reuter *et al.*, 1988). It is possible that across the spectrum of DHP agents varying degrees of agonism and antagonism will be expressed by any given molecule and this is reflected by the range of affinities expressed by [ $^3\text{H}$ ] DHPs in various tissues (Glossmann *et al.*, 1985).

There is increasing evidence that calcium channel function can be modulated by endogenous calcium channel activators. Palmitoyl carnitine is a lipid metabolite which accumulates in high concentrations in the sarcolemma and cytosol during myocardial ischaemia (Corr *et al.*, 1984), and a direct interaction of palmitoyl carnitine has been shown in  $\text{K}^+$  depolarised smooth muscle (Spedding & Mir, 1987) with similar effects to Bay K 8644. Furthermore, an interaction has also been demonstrated at the [ $^3\text{H}$ ] nitrendipine binding site in rat cortex membranes (Spedding & Mir, 1987). In a later study (Patmore *et al.*, 1989a), these findings were further supported in that a positive inotropic effect for palmitoyl carnitine in cultures of cardiac myocytes was demonstrated. Such findings may therefore indicate a role for endogenous calcium channel activators at VOCs, at least during myocardial ischaemia. The interaction of palmitoyl carnitine with [ $^3\text{H}$ ] DHP binding sites in brain membranes will be examined in detail in the first experimental chapter of this

thesis.

#### ***1.4.7. Plasticity of L-type calcium channels labelled by [<sup>3</sup>H] DHPs.***

An important feature of L channels labelled by [<sup>3</sup>H] DHPs in the context of the present work is the plasticity that VOCs display. As earlier described, neurones have the ability to control the level of [Ca<sup>2+</sup>]<sub>i</sub> by means of pumps and exchanger mechanisms and by means of VOCs, and there is considerable evidence that the number and function of L type VOCs can change in certain conditions, possibly as a mechanism of avoiding or attenuating the consequence of some pathological conditions. Evidence certainly exists that VOCs can be modified by receptor-mediated events, including direct activation by intracellular messengers through protein kinase-mediated channel phosphorylation and direct interactions with G proteins (Hofmann *et al.*, 1987; Dolphin, 1991). Such modifications are likely to be important in the heterologous regulation of channel number and function, although the mechanism of homologous drug and disease-induced changes in [<sup>3</sup>H] DHP sites are less clear. It has been postulated that ion-channels may be regulated in a similar manner to conventional receptor systems, changes being controlled by the rate of receptor synthesis, membrane insertion, internalisation and degradation (Hollenberg, 1985). In some disease-induced changes in neuronal [<sup>3</sup>H] DHP sites it is clear that the reduction is a reflection of the loss of neuronal populations on which the binding sites were located. However, shorter term up- or down-regulation of [<sup>3</sup>H] DHP sites more likely reflects modification of the membrane lipid environment, receptor distribution and phosphorylation state (Ferrante & Triggle, 1990).

Despite the fact that the total number of DHP sensitive L channels is some 10-20 fold lower than ω-conotoxin-sensitive N channels in neuronal tissue (Wagner *et al.*, 1988), L channel plasticity has been demonstrated in many situations within the CNS. This thesis will examine this property of [<sup>3</sup>H] DHP binding sites following cerebral ischaemia. If such a role is to be examined it seems justified to review some important previous findings in relation to the present work.

The ontogeny of L channel appears to be tissue specific (Janis *et al.*, 1985), and whilst certain peripheral tissues show high densities and rate of appearance of sites after birth (rat heart and skeletal muscle) the rate is much slower in brain (Kazazoglou *et al.*, 1983). In chick heart, binding densities are maximal at 4-8 days but virtually undetectable

in the brain (Marangos *et al.*, 1984). In the rat, maximal levels of binding are seen post-natal in the heart at day 5, and in the brain at day 20 (Janis *et al.*, 1985).

In rodents, chronic *in vivo* exposure to calcium antagonists leads to a reduction in the subsequent number of detectable [ $^3\text{H}$ ] DHP binding sites (Panza *et al.*, 1985; Ferrante & Triggle, 1990). Chronic treatment with calcium antagonists is also capable of heterologous regulation of other binding sites: for example rat striatal dopamine ( $\text{D}_2$ ) receptors have been shown to be up-regulated following treatment with either flunarizine or nimodipine (Govoni *et al.*, 1988b).

Chronic treatment with the neuroleptic, chlorpromazine, and subsequent withdrawal increases [ $^3\text{H}$ ] DHP binding (Ramkumar & El-Fakahany, 1985). These workers also demonstrated a selective decrease in the number of neuronal [ $^3\text{H}$ ] nimodipine binding sites following morphine treatment in rat (Ramkumar & El-Fakahany, 1984), with nimodipine being as effective as clonidine in withdrawal, a drug classically used to attenuate the naloxone-precipitated withdrawal syndrome following morphine administration (Ramkumar & El-Fakahany, 1984).

Little and co-workers (Dolin *et al.*, 1987) demonstrated that the development of ethanol dependence was associated with increased number and function of DHP sensitive VOCs, and DHP antagonists were effective in preventing withdrawal (Little *et al.*, 1986). The up-regulation, and subsequent reversal, of brain DHP binding sites has been shown to be extremely rapid following ethanol treatment (Govoni *et al.*, 1988a). On the other hand, some workers (Lucchi *et al.*, 1985) have shown that chronic ethanol reduces the number of DHP binding sites in brain. The reasons for this discrepancy are unknown.

In hypertension, the number of brain DHP binding sites is increased, as demonstrated in the SHR (Ishii *et al.*, 1983). In rats, some brain areas show increased levels of [ $^3\text{H}$ ] DHP binding sites after exposure to lead in early life (Rius *et al.*, 1986). An *in vitro* selective effect of this cation for certain brain areas has also been shown in binding studies to membrane homogenates (Govoni *et al.*, 1988a). Furthermore, some of these changes have been shown to occur in clinical situations. For example, decreases in [ $^3\text{H}$ ] DHP binding have been shown in brains from Parkinson's patients in those areas where degeneration of nigro-striatal neurones occurs (Nishini *et al.*, 1986).

Whilst there are several reports of ischaemia-induced changes in the properties of [ $^3\text{H}$ ] calcium antagonist binding sites in the myocardium (Nayler *et al.*, 1985; Matucci *et al.*, 1987; Dillon & Nayler, 1987), in neuronal tissue there is little and conflicting

evidence as to the effect of cerebral ischaemia. A preliminary study in gerbils showed changes in frontal cortex [ $^3\text{H}$ ] DHP sites following ischaemia (Kenny *et al.*, 1986), whilst in the rat, increases in hippocampal [ $^3\text{H}$ ] DHP binding have been shown following forebrain ischaemia (Magnoni *et al.*, 1988).

#### *1.4.8. Evidence to suggest that calcium antagonists may confer protection in models of cerebral ischaemia.*

The overall aim of this thesis is to assess the efficacy of, and mechanism whereby, calcium antagonists might be neuroprotective. This has largely been prompted by initial experimental evidence indicating that some calcium antagonists conferred benefit in models of experimental cerebral ischaemia. However, across the literature, reported findings are not consistent, even with the same compound in essentially similar models. Nimodipine has been one of the most widely studied agents and an example of the inconsistency in published findings with this compound in different ischaemic models is shown in Table 1.2.

The first studies in this area were carried out by Kazda *et al.* (1979), who demonstrated that nimodipine could reduce mortality incidence and improve post-ischaemic hypofusion. Most subsequent studies have attempted to measure parameters such as brain morphology, neurological deficit and EEG, whilst trying to separate direct protective effects from those secondary to an alteration of haemodynamic parameters. Nimodipine has been shown to be ineffective against the loss of CA1 neurones in the gerbil hippocampus (Alps *et al.*, 1988; Pashen *et al.*, 1988) and rat hippocampus (Vibrulst *et al.*, 1987). No effect was seen in monkey brain (Steen *et al.*, 1985) although beneficial effects have been reported for nimodipine reducing the incidence of lesions in the striate nucleus (Pashen *et al.*, 1988). Nicardipine, also a dihydropyridine, is effective in the gerbil (Alps *et al.*, 1988) but conflicting results have been obtained in rat following different protocols (Grotta *et al.*, 1986; Alps *et al.*, 1987).

The efficacy of calcium antagonists on post-ischaemic hypofusion has been found to differ between studies (see Hossmann, 1989), although with some agents that have similar effects on cerebral blood flow, a different protective effect is observed in their ability to protect hippocampal CA1 neurones. This suggests a direct interaction with the ischaemic mechanism for some, but not other agents. Calcium antagonists appear to have

Model	Effect	Reference
gerbil, 5 min bilateral carotid artery occlusion (BLO)	no protection of CA1 500 µg/ kg pre- and post-ischaemia.	<i>Alps et al., 1988.</i>
gerbil, 10 min BLO	protection of CA1 1.5 mg/ kg post-ischaemia	<i>Hossmann, 1989.</i>
rat MCA	no effect on infarct size 20 µg/ kg pre- and during ischaemia	<i>Kobayashi et al., 1988.</i>
rat MCA	decrease in infarct volume, 20 µg/ kg pre- and during ischaemia	<i>Obana et al., 1985.</i>
rat MCA	improvement of neurological deficit, 20 µg/ kg pre- and post- ischaemia	<i>Germano et al., 1987.</i>
rat MCA	no improvement in neurological deficit, 20 µg/ kg post-ischaemia	<i>Kobayashi et al., 1988.</i>

**Table 1.2.** Literature variation in the reported efficacy of nimodipine in experimental cerebral ischaemia.

little effect on the recovery of energy metabolism or oxygen/glucose metabolism following global ischaemia (Steen *et al.*, 1983, Newberg *et al.*, 1984). Furthermore, collated results from more than ten studies of focal and global ischaemia (Hossmann, 1989) show calcium antagonists to be mainly ineffective in their ability to improve post-ischaemic EEG, however, EEG pattern cannot be considered as a measure of neuronal integrity, since it is generally correlated with improved cerebral blood flow (Wauquier *et al.*, 1988) and correlates poorly with histological outcome.

In focal ischaemia models, nimodipine has been reported to increase infarct size following MCA occlusion (Obana *et al.*, 1985), although this has been attributed to an effect on cerebral blood flow (Hossmann, 1989). However, of considerable interest was the finding that both nimodipine and flunarizine showed beneficial effects in photochemically-induced infarction models (Van Reempts *et al.*, 1987; Nakayama *et al.*, 1988).

#### ***1.4.9. Is there a clinical potential for calcium antagonists or NMDA antagonists?***

The effectiveness of the above agents in various animal models of cerebral ischaemia has already been overviewed and will form the focus of attention for later aspects in this work, but the relevance of these models must be put into perspective in relation to the clinical condition of stroke. Recently, Pulsinelli & Buchan (1989) highlighted the poor clinical efficacy of over 25 compounds whose effectiveness was statistically proven over placebo using behavioural or histopathological end-point criteria. Whilst these authors comment on lack of clinical efficacy, it is true to say that in some cases, such as cerebral infarction, insufficient data. As recently highlighted (Molinari, 1988), clinical tests in humans must be relevant to the outcome in animal models and on this basis much data obtained in forebrain ischaemia models may not be relevant to atherothrombotic or lacunar infarction.

In a recent editorial, Wiebers *et al.* (1990) postulated that improved clinical outcome was the only relevant measure of stroke therapy, such that a compound showing quantitative improvement on CT scans or other laboratory parameters without clinical improvement hardly represents therapy of great promise. At the present time there are no substantial data to justify the use of NMDA antagonists.

The first relevant clinical studies describing the use of calcium antagonists were carried out with nimodipine in the treatment of subarachnoid haemorrhage (SAH) performed by Allen *et al.* (1983), investigating the potential use in treating vasospasm following SAH. This, and other studies (Petruk *et al.*, 1988; Pickard *et al.*, 1989) have confirmed beneficial effects of nimodipine in SAH but have indicated that the drug seemed to have little effect on vasospasm directly, and that the beneficial effect was through attenuation of ischaemic events following vasospasm. Thus, there appeared to be indirect evidence for a therapeutic potential using nimodipine in non-haemorrhagic cerebral infarction. In a large study (Gelmers, 1988), performed double blind and placebo-controlled, treatment was commenced within 24 hours of cerebral infarction only selective beneficial effects were found. In men, nimodipine decreased mortality by 58%, and it appeared that the drug was more effective in those patients presenting with severe deficit at the start of treatment. However, more recently, a number of larger, double-blind studies have indicated nimodipine to be ineffective (e.g. Martinez-Vila *et al.*, 1990). Furthermore, similar studies with another dihydropyridine, PY 108-068, have not demonstrated any benefit in patients with acute ischaemic cerebral infarction (Oczkowski *et al.*, 1989). These findings therefore raise the important question as to whether any benefit is conferred with other classes of calcium antagonist.

### ***1.5. Experimental aims and thesis outline.***

The thesis will attempt to examine the role of L-type VOCs and calcium antagonists in the ischaemic brain and determine the efficacy of these agents in a model of cerebral ischaemia. In this respect, one of the principal aims was to characterise the changes in [<sup>3</sup>H] DHP binding parameters in brain regions following ischaemia in an attempt to use [<sup>3</sup>H] DHP ligands as neuronal markers, against which comparative neuroprotective properties of various compounds can be assessed. Particular attention was made to the establishment of a focal ischaemia model, as a variety of different global ischaemia models have been previously established in which both calcium antagonists and NMDA antagonists have been characterised as being neuroprotective, based on the attenuation of damage to selectively vulnerable neurones (e.g. Alps *et al.*, 1988; Gill *et al.*, 1988). The methodology used in the first two experimental chapters is described in Chapter 2. Experimental results and discussion in relation to other published work will be described

in Chapters 3-6.

Chapter 3 will deal with the interaction of the various classes of calcium antagonist in radioligand binding experiments. The aim of this chapter was to enlarge on and characterise the original observation that the lipid metabolite produced in ischaemia, palmitoyl carnitine, selectively interacts with [ $^3\text{H}$ ] DHP binding sites (Spedding & Mir, 1987). The interactions of calcium antagonists in brain membranes will be examined using a range of different experimental protocols including competition, saturation and kinetic analyses. The interaction of some calcium antagonists at other receptors and ion channels will be described in an attempt to identify common mechanistic features for the various classes of calcium antagonist. For such experiments the initial distinction between calcium antagonist subgroups was based on the classification of Spedding (1985b), with the assumption that class II agents (verapamil and diltiazem) bind to separate, allosterically coupled binding sites (Glossmann *et al.*, 1985). Throughout the course of this work, a large number of compounds interacting with [ $^3\text{H}$ ] calcium channel ligands has been described in the literature, notably in skeletal muscle and cardiac membranes, and the characterisation of the interaction at neuronal binding sites will be described for some of these compounds. As a consequence of these studies, the final section of this chapter will describe a binding site for a novel calcium antagonist, SR 33557, which appears to be distinct, but tightly coupled to DHP binding sites in brain tissue.

*In vivo* aspects of cerebral ischaemia are dealt with in Chapter 4. An extensive series of experiments examining the effect of forebrain ischaemia on [ $^3\text{H}$ ] DHP binding parameters will be described. In the same forebrain ischaemia model the use of [ $^3\text{H}$ ] PK 11195 will also be characterised. It will be shown that this marker of  $\omega_3$  sites is a sensitive, indirect index of neuronal damage and using this ligand, a novel focal ischaemia model in the mouse will be described. The attenuation of the ischaemia-induced increase in  $\omega_3$  sites will be used to assess the comparative neuroprotective potencies of different compounds and the mechanisms whereby these agents are neuroprotective will be discussed.

The fifth chapter of this thesis describes a series of experiments carried out using an *in vitro* model of cerebral ischaemia: the rat hippocampal slice preparation. Using this model, an experimental protocol will be established for an hypoxic insult resulting in non-recovery of synaptic transmission as measured extracellularly in the CA1 region of the hippocampus. Using this protocol, the protective effect of a variety of different compounds will be described in terms of their ability to attenuate the extent of anoxic damage as

measured by recovery of synaptic transmission. This chapter will contain separate introduction and methodology sections pertaining to that series of experiments.

The principal conclusion derived from the thesis will be discussed in Chapter 6.

## Chapter Two.

### Methods.

#### *2.1.1. Standard membrane preparation for [<sup>3</sup>H] dihydropyridine binding assays.*

Male Sprague-Dawley rats (200-350g) were killed by cervical dislocation. The optic nerves were severed and the brain carefully removed from the skull cavity. The brain was immediately placed on a glass petri dish over a bed of ice. The cerebral cortex was dissected free from remaining tissue and placed in ice cold 50 mM Tris HCl buffer (pH 7.4 at 4 °C). Tissues were homogenised in 30 vol. buffer using a Polytron tissue disruptor (Kinematica, PT 10, setting 10) with two bursts of 10s duration. Following the homogenisation of individual samples, the tissue disruptor was washed in order to avoid cross contamination between samples (an important step when preparing membranes for quantitative binding analysis from animals subject to various experimental procedures). Tissue homogenate was then centrifuged in a cooled (4°C) centrifuge (Sorvall, RC 5B) at 48,000g for 15 min. The resulting pellet was resuspended by homogenisation (Polytron, setting 10) with one burst of 10s duration and the homogenate centrifuged at 48,000g for 15 min. This step was repeated twice to produce the final membrane pellet. This pellet was resuspended by homogenisation in 4-5 ml ice cold 50 mM Tris HCl at a protein concentration of 2-3 mg/ml. Final membrane pellets were stored in liquid nitrogen until required for assay.

#### *2.1.2. Standard binding assay for [<sup>3</sup>H] dihydropyridines and generalised assay protocols used for competition, saturation and kinetic experiments.*

Membrane pellets were thawed (at 25°C) and resuspended by Polytron homogenisation in assay buffer (setting 10, one burst > 5s duration). Assays were carried out in 50 mM Tris HCl (pH 7.4 at 25°C) in a total volume of 2.0 ml using disposable

polypropylene assay tubes (Sterlin, 4.9 ml) to incubate the assay constituents. Reactions were initiated by addition of membrane homogenate followed by rapid vortex mixing. Assay tubes were then incubated to equilibrium at the desired temperature in a thermostatically controlled water bath. For competition assays [ $^3\text{H}$ ] (+) PN 200-110 was used at a ligand concentration of 0.03 nM (in corresponding experiments [ $^3\text{H}$ ] nitrendipine was used at 0.2 nM).

In saturation experiments eight concentrations of radioligand were generally used between 0.005 and 1.0 nM. Serial dilutions of radioligand were made by sequential 1:1 dilutions of a stock radioligand solution by initial removal of stock radioligand with a Hamilton syringe and dilution into assay buffer. The appropriate dilution of the commercial stock radioligand solution was calculated from a knowledge of the specific activity, and the concentration of the radioactivity. The specific activity for all ligands was expressed as Ci/mmol, and the concentration of all ligands used in this study was 1  $\mu\text{Ci}/\mu\text{l}$ . For a ligand with a specific activity of 50 Ci/mmol, 1 Ci would contain 1 / 50 mmol and  $\therefore$  1  $\mu\text{Ci}$  would contain 1 / 50 nmol in 1  $\mu\text{l}$ . Thus, 1  $\mu\text{Ci}$  = 1 / 50 mmol/litre ( $2 \times 10^{-5}$  M). From a knowledge of this stock ligand concentration, a working ligand solution for assay additions was made by an appropriate dilution of the commercial radioligand stock into assay buffer as described. Sequential dilutions of radioligand solutions were made with an Eppendorf pipette, radioligand solution being aspirated and expelled several times to ensure the appropriate dilution was made and to reduce the effect of adherence of any radioligand to the pipette tip. If a ligand was suspected to bind to the pipette tip, then the tip was left to equilibrate between dilutions to reduce carry over.

In competition assays, drug dilutions were made with a change of tip after every dilution to ensure accurate serial dilutions. In assays with [ $^3\text{H}$ ] (+) PN 200-110, non-specific binding was determined in the presence of 1  $\mu\text{M}$  nitrendipine (or 1  $\mu\text{M}$  nifedipine in [ $^3\text{H}$ ] nitrendipine experiments) and the specific binding was calculated as the total binding minus that in the presence of nitrendipine. At least ten (and normally twelve) concentrations of competing drug were used in competition assays. In order to maximally cover the inhibition of binding between total and non-specific levels, a range of drug concentrations

were constructed by serial 1 : 10 dilutions, each interspaced by a serial 3 :10 dilution, such that when drug concentrations were expressed logarithmically, log and half-log concentrations gave an optimum spread of data points over the competition curve. Data points for competition experiments were determined in duplicate, and in saturation experiments, quadruplicate total and duplicate non-specific determinations were made at each ligand concentration.

Following the addition of membrane homogenate (60-80  $\mu$ g protein), incubations were carried out under subdued light by means of aluminium foil over the water bath. [ $^3$ H] DHP ligands were incubated for 30 min at 37°C, 120 min at 25°C and 180 min at 4°C (Mir & Spedding, 1987). Binding reactions were terminated by rapid filtration of assay samples over Whatman GF/B glass fibre filters using a Brandel 24 place cell harvester, under a constant vacuum of 23 mm Hg. The filters were washed once with washing buffer (50 mM Tris HCl, pH 7.4 at 4°C) immediately prior to sample filtration, and then washed twice with 5 ml of ice cold buffer immediately after sample filtration. Residual buffer and unbound radioligand was removed by application of the vacuum for a further 5 s, after which the filters were removed and left to dry. Bound radioactivity was determined by placing individual filter disks in 5 ml scintillation cocktail (LKB 'optiphase' Hisafe II). Filters were left in scintillant overnight to fully equilibrate and counted for bound [ $^3$ H] in a scintillation counter (Beckman LS 5000 or 1700 series). Samples were counted for a total of 3 min, over which time the sample radioactivity was expressed as mean DPM (disintegrations per minute) for a series of 10 s counts over the 3 min period. DPM could be calculated directly in these machines due to the presence of a [ $^3$ H] quench curve library, thus allowing DPM to be calculated directly from counts per minute (CPM) based on counting efficiency (40-45 %) after quench correction. In all assays, at the time of addition of radioligand to test tubes, in order to check the concentration of radioligand used, the same addition was also made directly to scintillation vials. This value was compared to an aliquot taken from an 'unfiltered' assay tube. If a discrepancy existed between these two values, after correction for the aliquot volume, then this indicated that the radioligand was adhering to the test tube or pipette tip and that a modification to the assay procedure was

necessary to reduce the adsorption of the radioligand to plastic surfaces and other non-receptor material as much as possible.

### ***2.1.3. Determination of assay protein.***

Assay protein was determined using a Pierce BCA assay reagent kit (Smith *et al.*, 1985) with plastic cuvettes. A standard protein curve (using bovine serum albumin) was constructed over the range 10-800  $\mu\text{g/ml}$  by incubating 100  $\mu\text{l}$  samples in 2 ml BCA reagent for 2 hr at 25°C. This protocol is linear for standard curves up to 1 mg/ml and is sensitive down to 5  $\mu\text{g/ml}$ . Sample absorbance (100  $\mu\text{l}$  sample) was read at 562 nm in a Pye Unicam SP 1800 UV spectrophotometer against a blank containing BCA reagent and 100  $\mu\text{l}$  assay buffer. A standard curve of absorbance vs protein concentration was constructed using the Cricket Graph application on a Macintosh SE microcomputer. A knowledge of the standard linear curve fitting parameters, calculated with Cricket Graph, allowed the subsequent construction of a Microsoft Excel file from which protein concentrations were calculated from test sample absorbances.

### ***2.2.1. Protocol for kinetic studies.***

These experiments were carried out with several ligands in order to determine the rate of association of radioligand with the receptor under study, and therefore the time to equilibrium. They were also used to determine the rate of dissociation of the ligand from the receptor at equilibrium, experiments often being performed in the presence of other drugs to characterise the nature of drug interaction with a [ $^3\text{H}$ ] ligand-receptor complex.

To determine the association rate, assay tubes were set up for duplicate total and non-specific binding determinations and all assay constituents were added to the tubes except for the membrane suspension. Before the addition of membranes, tubes were equilibrated to the required temperature, and the reaction started by addition of membranes. Since more than 24 samples (the number of tubes simultaneously filtered) were normally

assayed, incubation times were staggered to allow for the time difference between the successive filtering of 24 tube batches. Thus, the reactions in each 24 tube batch were initiated at time T-2 min relative to the previous 24 tube batch.

A similar protocol was used for the determination of dissociation rates. Total and non-specific replicates were set up as for association determinations and left to reach equilibrium. Dissociation was initiated by the addition of an excess of unlabelled high affinity drug. In [ $^3\text{H}$ ] PN 200-110 dissociation rate experiments 1  $\mu\text{M}$  nitrendipine was used. A one way process of dissociation can be initiated as re-association of the radioligand to the binding site is very unlikely because of occupation of the site by unlabelled DHP present in excess. For each set of tubes measuring dissociation as a function of time, a set of control tubes were filtered simultaneously to ensure that the level of equilibrium was unchanged throughout the duration of the dissociation experiment. As for association rate determinations, additions to tubes were staggered at T-2 min relative to the previous 24 samples to account for filtration times between batches of tubes.

### *2.2.2. Determination of dissociation rate by infinite dilution.*

In experiments where the rate of dissociation of the radioligand was not independent of occupation of the receptor sites with excess unlabelled ligand (e.g. in a negatively co-operative system), monitoring the rate of dissociation by adding excess unlabelled ligand was not appropriate. Therefore, dissociation was initiated by 'infinite dilution' of an equilibrated assay mixture. In practice, this was a hundred fold dilution. Using this method, a one way process of dissociation can be initiated since re-association is unlikely because of the very low concentration of radioligand resulting from the dilution process. It also has the advantage of monitoring dissociation independently of receptor occupation by unlabelled molecules. The large volume resulting from a typical dilution of 50 ml into 5 litres meant that sample volumes had to be increased accordingly, such that 50 ml aliquots had to be removed from the diluted reaction mixture and individually filtered. This was achieved using Millipore 12 well manifolds under vacuum (22 mm Hg), each

well containing individual Whatman GF/B filters. With assistance, it was therefore possible to filter four samples (total and non-specific replicates) simultaneously for each time point. A different manifold was used for each time point, so that the four samples were filtered uniformly, rather than leaving filters containing bound radioligand on the manifold before later filtrations, since uneven dissociation of bound radioligand may have occurred if filters were left for a period of time under several applications of the vacuum.

### *2.3.1. Preparation and assay of cardiac tissue for [<sup>3</sup>H] DHP binding.*

Hearts from male Sprague-Dawley rats were cleaned of blood vessels and connective tissue. The atria were cut free and discarded. Ventricular tissue was finely minced with scissors and homogenised as described for cerebral cortex. Following the homogenisation step, the homogenate was filtered through a single layer of muslin, before proceeding identically as described for cerebral cortex. The final pellet was resuspended at a protein concentration of 6 mg/ml.

Aliquots of membrane homogenate (180-250 µg protein/assay) were assayed for [<sup>3</sup>H] (+) PN 200-110 binding parameters as described for [<sup>3</sup>H] DHP binding in cerebral cortex. Pretreatment experiments with palmitoyl carnitine were carried out by incubating the tissue homogenates with 10 µM palmitoyl carnitine for 30 min at 37°C after the second stage of the membrane preparation, after which membranes were cooled and washed in the usual way, thereby washing out palmitoyl carnitine during the remaining preparation stages.

### *2.3.2. Preparation of rabbit skeletal muscle membranes for [<sup>3</sup>H] calcium antagonist binding studies.*

Male New Zealand rabbits (1.5-2.5 kg) were killed by cervical dislocation and the hind skeletal muscle dissected free. Due to the high tissue yield (more than 250g from each animal) freshly dissected tissue was frozen in liquid nitrogen and re-thawed as required for

preparation. Tissues were homogenised in ice cold 0.3 M sucrose / 40 mM MOPS, pH 7.5, containing 0.1 mM phenylmethylsulphonylfluoride (PMSF) and 1  $\mu$ M pepstatin, using a Waring commercial blender. Four 20s bursts (each separated by 10s to allow the tissue to re-settle) were used to homogenise the tissue, using a ratio of 1g tissue to 5 ml buffer. The homogenised tissue was filtered through a single layer of muslin and centrifuged at 3,500g for 30 min at 4°C. The supernatant was carefully decanted and the pH measured, and (if necessary) readjusted to pH>7.0 using 2.0 M KOH. The supernatant was centrifuged at 10,000g for 20 min. The supernatant from this step was carefully decanted and adjusted to 0.5 M KCl by addition of the solid salt under gradual stirring, and then centrifuged at 100,000g in an ultracentrifuge (Beckman, L8-M using an SW 28 rotor) for 2 hr. The resulting pellet was resuspended by Polytron homogenisation (setting 5, one 10s burst) and centrifuged at 100,000g for 30 min to produce the final pellet. This was resuspended in 50 mM Tris HCl (pH 7.4 at 25°C) at a protein concentration of approximately 0.2-0.5 mg/ml and stored in liquid nitrogen.

### ***2.3.3. [<sup>3</sup>H] (+) PN 200-110 and [<sup>3</sup>H] fluspirilene binding to skeletal muscle membranes.***

[<sup>3</sup>H] DHP and [<sup>3</sup>H] fluspirilene binding in skeletal muscle membranes was carried out using generalised assay procedures as described in section 2.1.2. Aliquots of skeletal muscle homogenate (10-20  $\mu$ g protein) were incubated with 0.1 nM [<sup>3</sup>H] fluspirilene or 0.2 nM [<sup>3</sup>H] (+) PN 200-110 in 50 mM Tris HCl (pH 7.4 at 25°C) in a total volume of 1.0 ml. For [<sup>3</sup>H] fluspirilene binding the assay buffer also contained 0.01 % bovine serum albumin and 0.1 mM PMSF. Incubations were carried out for 60 min after which time [<sup>3</sup>H] DHP assay samples were filtered as described (section 2.1.2.). [<sup>3</sup>H] fluspirilene assay samples were filtered over Whatman GF/B filters that had been pre-treated with 0.05 % polyethylenimine in order to reduce filter binding of the radioligand. Pre-treatment of filters was achieved by soaking filter mats for 45-60 min in polyethylenimine prior to filtration. In these experiments the filters were not pre-soaked with washing buffer as previously

described but assay constituents were filtered immediately after application of the vacuum and then filters were washed in the usual manner.

#### ***2.3.4. Preparation and assay of cardiac and cerebrocortical membranes for $\alpha_1$ binding sites.***

Rat hearts were dissected free of blood vessels and connective tissue, the atria removed, and the left ventricle was dissected free from the remaining cardiac tissue. Left ventricular tissue was homogenised as described for cardiac [ $^3\text{H}$ ] DHP membranes, with the exception that the first two preparative stages were carried out in 50 mM Tris HCl, 5 mM EDTA (pH 7.4 at 40°C) with the homogenate filtered through a double layer of muslin after initial homogenisation. The final two washing stages were then carried out using 50 mM Tris HCl, 0.5 mM EDTA (pH 7.4 at 40°C). This buffer was also used to resuspend the final pellet as described for cardiac [ $^3\text{H}$ ] DHP membranes.

Cerebrocortical membranes were prepared exactly as described for [ $^3\text{H}$ ] DHP binding with the exception that 50 mM Tris HCl, 5 mM EDTA (pH 7.4 at 40°C) was used for the first two washes, and 50 mM Tris HCl, 0.5 mM EDTA (pH 7.4 at 40°C) was used for the final two washes and final membrane pellet.

Aliquots of tissue homogenate (80-140  $\mu\text{g}$  protein/assay for cerebral cortex assays, 150-210  $\mu\text{g}$  protein/assay for left ventricular membranes) were incubated in 50 mM Tris HCl, 0.5 mM EDTA (pH 7.4) in a total volume of 0.5 ml for 30 min at 25°C. Saturation experiments were carried out with [ $^3\text{H}$ ] Prazosin over the concentration range 0.02-4.0 nM. Non-specific binding was determined in the presence of 10  $\mu\text{M}$  phentolamine. In this series of experiments, membranes were incubated with 10  $\mu\text{M}$  palmitoyl carnitine (10  $\mu\text{M}$ ) for 30 min at 37°C) following re-homogenisation of the tissue pellet after the second centrifugation step. Palmitoyl carnitine was then washed out by carrying out the final two washes as described (section 2.3.1.). Control membranes were incubated as described, but in buffer only.

### 2.3.5. Preparation of $\beta$ cardiac membranes.

These were prepared as for cardiac [ $^3\text{H}$ ] DHP membranes with the exception that left ventricular tissue was used as described for cardiac  $\alpha_1$  membranes. The preparation buffer was 50 mM Tris HCl throughout all preparative stages. Aliquots of membrane homogenate (290-310  $\mu\text{g}$  protein/assay) were incubated in a 50 mM Tris HCl (pH 7.4 at 25°C) in a total volume of 0.5 ml for 30 min at 25°C. Saturation experiments were carried out with [ $^3\text{H}$ ] dihydroalprenolol (0.02-5.0 nM). Non-specific binding was determined in the presence of 0.2 mM (-) isoprenaline bitartrate. *In vitro* incubations with palmitoyl carnitine (10  $\mu\text{M}$ ) were carried out after the second wash exactly as described for  $\alpha_1$  membranes.

### 2.3.6. [ $^3\text{H}$ ] Batrachotoxinin A-20- $\alpha$ -benzoate (BTX-B) binding assay in rat cortical synaptosomes.

#### a) Rat cortical synaptosome preparation.

Rat cortical synaptosomes were prepared essentially as previously described (Gordon-Weeks, 1987). Cerebral cortices were removed from Sprague-Dawley rats, cross chopped with a scalpel and homogenised in a hand held Teflon-glass homogeniser in 10 vol. ice cold 0.3 M sucrose, 5 mM  $\text{K}_2\text{HPO}_4$  (pH 7.4 at 4°C with 0.5 M HCl). Tissue was homogenised with 5-6 strokes and centrifuged at 1,000g for 10 min. The supernatant was retained, and the pellet (P1) resuspended by vortex mixing, and centrifuged at 1,000g for 10 min. The combined supernatants were then spun at 20,000g to produce pellet (P2). This pellet was found to be buff coloured with a lighter fraction above. By gentle vortexing it was possible to resuspend the light fraction containing the majority of the synaptosomes, whilst leaving the darker pellet, mainly composed of mitochondria undisturbed. The P2 fraction was resuspended in assay buffer for binding studies (section b) and used directly, or was further purified by sucrose gradient. In this instance, the P2 pellet was resuspended

as described in 8-10 ml homogenisation buffer and was layered on top of a sucrose gradient. The sucrose gradient consisted of three equi-volumetric layers of 0.8, 1.0 and 1.2 M sucrose. It was found that the best separation between layers could be achieved by the successive underlaying of each sucrose layer, and then leaving the gradient to settle in the centrifuge tube for at least 1 hr at 4°C. When layered over the gradient in this manner, after centrifugation at 100,000g in an ultracentrifuge (SW 28 rotor) for 2 hrs, the synaptosomes were recovered with a Pasteur pipette from the 1.0/1.2 M sucrose interface. The synaptosomes were transferred to an ice cold beaker and made up to a 30 ml volume by the addition of Krebs buffer (NaCl 145 mM, KCl 5 mM, CaCl<sub>2</sub> 1.2 mM, MgCl<sub>2</sub> 1.3 mM, NaH<sub>2</sub>PO<sub>4</sub> 1.2 mM, glucose 10 mM and HEPES 20 mM, pH 7.4) dropwise whilst stirring. This suspension was then centrifuged at 20,000g to form a pure synaptosomal pellet which was lifted off the bottom of the tube with a 'jet' of appropriate assay media, and dispersed by a small hand held Teflon-glass homogeniser. This synaptosomal preparation was kept on ice until required for assay.

***b) [<sup>3</sup>H] BTX-B binding assay.***

Aliquots of synaptosomes (equivalent to 10 mg original tissue wt/assay) were incubated in assay buffer (5.4 mM KCl, 0.8 mM MgSO<sub>4</sub>, 5.5 mM glucose, 50 mM HEPES, 130 mM choline chloride, pH 7.4 at 25°C with Tris base) in a total volume of 350 µl, containing 1 µM tetrodotoxin, 25 µg scorpion venom (*Leiurus quinquestriatus*), and [<sup>3</sup>H] BTX-B (2 nM). Incubations were carried out for 30 min at 37°C and terminated by rapid filtration over Whatman GF/B filters (soaked in ice cold washing buffer) under vacuum filtration followed by two washes in buffer composed of 130 mM choline chloride, 5 mM HEPES, 1.8 mM CaCl<sub>2</sub>, 0.8 mM MgSO<sub>4</sub> and bovine serum albumin (0.1 mg/ml). Non-specific binding was determined in the presence of 300 µM veratridine.

### ***2.3.7. Dopamine ( $D_1$ and $D_2$ ) binding assays using rat corpus striatum membranes.***

#### ***a) Rat corpus striatum membrane preparation***

Paired striata were obtained from the brains of male Sprague-Dawley rats by making two vertical cuts, rostral and caudal to the optic chiasma, thus enabling the striata to be easily identified and dissected from the area bounded medially by the lateral ventricle. Pooled striata were homogenised in 50 vol. ice cold Tris HCl (pH 7.4 at 4°C) by Polytron homogenisation (setting 10, two bursts of 10s duration). Homogenised tissue was centrifuged at 48,000g for 15 min. The resultant pellet was washed by resuspension and centrifugation a further three times as described for [ $^3$ H] DHP membrane preparations. For  $D_2$  binding assays the pellet was resuspended in ice cold 50 mM Tris HCl, and for  $D_1$  assays the final pellet was resuspended in 50 mM Tris HCl, 120 mM NaCl, 5 mM KCl, 2 mM  $\text{CaCl}_2$  and 1 mM  $\text{MgCl}_2$  prior to storage in liquid nitrogen.

#### ***b) Dopamine $D_2$ binding assay.***

Dopamine  $D_2$  binding assays were carried out with aliquots of striatal homogenate (100  $\mu\text{g}$  protein/assay) incubated in 50 mM Tris HCl (pH 7.4 at 25°C), in a total volume of 1.0 ml containing 0.06 nM [ $^3$ H] spiperone. Ketanserin (0.1  $\mu\text{M}$ ) was present in all assay tubes to prevent the binding of [ $^3$ H] spiperone to any 5-HT $_2$  sites present. Incubations were carried out for 45 min at 25°C and reactions were terminated by vacuum filtration over Whatman GF/B filters and washed with ice cold Tris HCl as described for general assay procedures. Non-specific binding was determined in the presence of 1  $\mu\text{M}$  (+) butaclamol.

**c) Dopamine D<sub>1</sub> binding assay.**

Dopamine D<sub>1</sub> binding assays were carried out as a modification of Billard *et al.* (1984). Striatal homogenate (100 µg protein/assay) was incubated in 50 mM Tris HCl (pH 7.4 at 25°C), in a total volume of 1.0 ml containing 0.3 nM [<sup>3</sup>H] SCH 23390. Assays were incubated for 15 min at 37°C prior to rapid filtration over Whatman GF/B filters and washed with ice cold Tris HCl as described. Non-specific binding was determined in the presence of 0.1 µM unlabelled SCH 23390.

**2.3.8. [<sup>3</sup>H] Spiperone binding to 'spirodecane' sites in hippocampal membranes.**

[<sup>3</sup>H] spiperone binding was carried out as described (Howlett *et al.*, 1979). Hippocampi were dissected from the brains of male Sprague-Dawley rats and homogenised in 80-100 vol. ice cold 50 mM Tris HCl (pH 7.4 at 4°C). Membrane washing and resuspension parameters were as described for [<sup>3</sup>H] DHP binding.

Aliquots of hippocampal homogenate (80-120 µg protein/assay) were incubated in 50 mM Tris HCl in a total volume of 1.0 ml, containing 0.2 nM [<sup>3</sup>H] spiperone, in the presence of 1 µM (+) butaclamol to exclude binding to dopamine D<sub>2</sub> sites, and 0.1 µM ketanserin to exclude binding to 5-HT<sub>2</sub> sites. Incubations were carried out at 25°C for 45 min and samples were filtered with ice cold 50 mM Tris HCl as previously described for [<sup>3</sup>H] DHP binding.

**2.3.9 [<sup>3</sup>H] PK 11195 binding assays.**

[<sup>3</sup>H] PK 11195 binding to brain tissue homogenates was carried out essentially as previously described (Benavides *et al.*, 1987). This assay was used for a variety of brain tissues from rats, gerbils and mice, and with the exception of homogenisation volumes (30

vol for cerebral cortices, 100 vol for hippocampi, and >100 vol for ischaemic mouse brain samples) assay procedures were identical for all tissues (see section 2.6.4. for ischaemic mouse sample assay). Tissues were homogenised in ice cold 50 mM Tris HCl and centrifugation and wash parameters were as described for [ $^3$ H] DHP assays.

Subcellular fractionation studies on brain tissues were carried out using the method described in section 2.3.6. for the preparation of rat cortical synaptosomes, with the exception that purified mitochondria, obtained as a pellet during the sucrose gradient spin, were resuspended by Polytron homogenisation (setting 5, one 10s burst) prior to assay.

Aliquots of tissue homogenate (100-200  $\mu$ g protein/assay for rat and mouse tissue homogenates, 25-80  $\mu$ g protein/assay for assay of gerbil brain tissues) were incubated with [ $^3$ H] PK 11195 (0.2 nM for competition experiments, 0.01-2.0 nM for saturation experiments) in a total volume of 1.0 ml. Incubations were carried out for 30 min at 25°C, and filtered with ice cold Tris HCl as described for [ $^3$ H] DHP binding. Stock ligand solutions for competition assays and serial dilutions for saturation experiments were made in 50 mM Tris HCl containing 1% (v/v) ethanol to reduce binding of the radioligand to pipette tips. Non-specific binding in all [ $^3$ H] PK 11195 assays was determined in the presence of 10  $\mu$ M RO 5-4864.

#### **2.3.10. [ $^3$ H] SR 33557 binding to rat cerebral cortex membranes.**

Rat cerebral cortex membranes were prepared as described for [ $^3$ H] DHP binding. Aliquots of tissue homogenate (80-100  $\mu$ g protein/assay) were incubated with [ $^3$ H] SR 33557 (0.2 nM for competition assays, and 0.005-1.0 nM for saturation studies) in a 50 mM Tris HCl buffer (pH 7.4 at 25°C) containing 0.01 % bovine serum albumin in a total volume of 1.0 ml at 25°C for 120 min in the dark (by means of a foil covered water bath). Assays were terminated by rapid filtration as described for [ $^3$ H] DHP binding over Whatman GF/B filters previously treated with 0.05% polyethylenimine for 60 min, followed by two 5 ml washes of ice cold 50 mM Tris HCl (pH 7.4 at 4°C). Non-specific binding was determined in the presence of 1  $\mu$ M SR 33557.

#### 2.4. *Experimental criteria and analysis of radioligand binding data.*

Data output from scintillation counters was transferred directly to floppy disk on Cromemco 64 K and IBM-PC computers for the construction of saturation data files. These files were then transferred to a HP 3000 mainframe system, on which analysis programs were run. Competition data files were also generated on floppy disk for analysis on a BBC model B microcomputer.

Binding isotherms of competition data, in the form of displacement curves, were analysed using a non-linear least squares parametric curve fitting program capable of defining  $IC_{50}$  (concentration of drug inhibiting 50% of specific binding) as described by Michel & Whiting, (1988). This program was also capable of iterative curve fitting to a single (with defined Hill slope,  $nH$ ) or two site model, and provided a sum of the square error for both models. The single site and two site models for each isotherm were compared, if appropriate, using the differential F value defined by the following equation:

$$F = (SS_1 - SS_2) / (df_1 - df_2)$$

---


$$SS_2 / df_2$$

where  $SS_1$  is the sum of the squares error for the single site,  $SS_2$  is the sum of the squares error for the two site model,  $df_1$  is the degrees of freedom for the single site model and  $df_2$  the degrees of freedom for the two site model. A two site fit was assumed to be significantly better than a single site fit if the determined F value had a  $p < 0.05$ .

The  $IC_{50}$  value obtained was converted to the inhibitory constant  $K_i$  using the equation of Cheng and Prusoff (1973):

$$K_i = \frac{IC_{50}}{1 + \frac{[L]}{K_d}}$$

where  $[L]$  represents the free concentration of radioligand, and  $K_d$  is the equilibrium dissociation constant.

This equation can be used under certain criteria;

- i) That the concentration of radioligand is not limiting, i.e. <10 % of the total radioligand is bound.
- ii) The assay is carried out at a protein concentration where the protein-dependence of binding is linear.
- iii) The concentration of radioligand used is not  $\gg K_d$ , thus amplifying conversion errors.
- iv) Labelled and unlabelled compound have the same affinity for the site.
- v) The action is competitive within the laws of mass action.

An important criterion to be fulfilled, especially in saturation experiments, is an accurate definition of non-specific binding. In a competition curve, with the selected compound to define non-specific binding, the binding should be seen to clearly plateau at the higher drug concentrations used. Improper definition of non-specific binding in saturation experiments can give rise to curvilinear Scatchard plots, which could be misinterpreted as complex binding, such as co-operativity or heterogeneity of binding sites.

Saturation binding isotherms of total, specific, and non-specific binding were created and analysed visually using an IBM PC. Graph plots of the data files allowed the detection of single assay points and allowed the elimination of rogue points prior to further analysis. These data files were transferred to a HP 3000 mainframe computer system, and equilibrium binding parameters  $K_d$  and  $B_{max}$  were obtained by analysis of the files using the iterative non-linear least square fitting program LIGAND (Munson & Rodbard, 1980). Throughout this thesis, saturation data will be presented in the form of Scatchard plots. These plots are linear transformations of saturation data and represent  $B/F$  on the ordinate axis versus  $B$  on the abscissa. These will be presented for graphical illustration only, as analysis of transformed data by least-squares linear regression introduces error in the estimation of binding parameters (e.g. when low levels of specific binding occur at low ligand concentrations or insufficient saturating concentrations of radioligand are used). Kermode, (1989) described a variety of experimental conditions leading to non-linear

Scatchard plots and conditions which introduce error in binding parameter calculations. To this end, non-linear regression analysis of specific binding data was used for all saturation data in the present studies.

Association and dissociation rates from kinetic experiments were determined as described by Weiland & Molinoff, (1981). With less than 10 % of the total radioligand bound, a plot of specific binding against time ( $\ln B_t/B_e$  vs  $t$ ) yielded the pseudo first order rate constant  $K_{obs}$  from the slope ( $B_t$  and  $B_e$  represent specifically bound ligand at time  $t$  and equilibrium respectively). The association rate constant  $K_1$  was calculated indirectly from the pseudo first order rate constant since:

$$K_1 = (K_{obs} - K_{-1}) / [L]$$

where  $K_{-1}$  is the first order dissociation rate constant, and  $[L]$  is the total assay radioligand.

$K_{-1}$  was determined directly from the slope of the plot of  $\ln B_t/B_e$  vs  $t$  after dissociation, allowing  $K_d$  to be derived thus,

$$K_d = \frac{K_{-1}}{K_1}$$

This method does, however, have the inherent disadvantage that any error in the determination of  $K_{-1}$  will be propagated into determination of  $K_1$  and  $K_d$ .

## 2.5. Experimental validation of [ $^3H$ ] (+) PN 200-110 binding assay.

The effect of the number of wash cycles in this assay was examined by assaying the membrane homogenate at each stage of the membrane preparation for specific [ $^3H$ ] (+) PN 200-110 binding (Table 2.1.).

**Table 2.1.**

Number of wash cycles	Specifically bound ligand (fmol/mg protein)	%non-specific binding (range)
0 (homogenised tissue only)	113 ± 6	4.3 (3.1 - 8.4)
1	164 ± 4	5.4 (4.8 - 8.1)
2	185 ± 9	7.6 (5.9 - 10.2)
3	176 ± 2	5.8 (2.9 - 9.8)
4	175 ± 4	6.1 (3.3- 10.1)

**Table 2.1.** The effect of membrane wash cycles on [<sup>3</sup>H] (+) PN 200-110 binding parameters in rat cerebral cortex. Membranes were assayed with 0.1 nM [<sup>3</sup>H] (+) PN 200-110. Values represent the mean ± s.e. mean of four determinations.

The effect of different membrane storage and resuspension procedures on [<sup>3</sup>H] (+) PN 200-110 binding was investigated in order to achieve reliable and reproducible assays from different batches of membranes (Table 2.2.).

**Table 2.2.**

Protocol	Kd (nM)	Bmax (fmol/mg protein)
Fresh tissue homogenate, resuspended for assay by Polytron homogenisation.	0.04 ± 0.005	202 ± 9
Homogenates, stored in liquid nitrogen for >3 months and resuspended by vortex mixing.	0.03 ± 0.004	109 ± 14
Homogenates, stored in pellet form for <3 months and resuspended by Polytron homogenisation	0.05 ± 0.003	196 ± 8

**Table 2.2.** The effect of different storage and resuspension protocols on [<sup>3</sup>H] PN 200-110 binding parameters in rat cerebral cortex. Values represent mean ± s.e.mean (n=4).

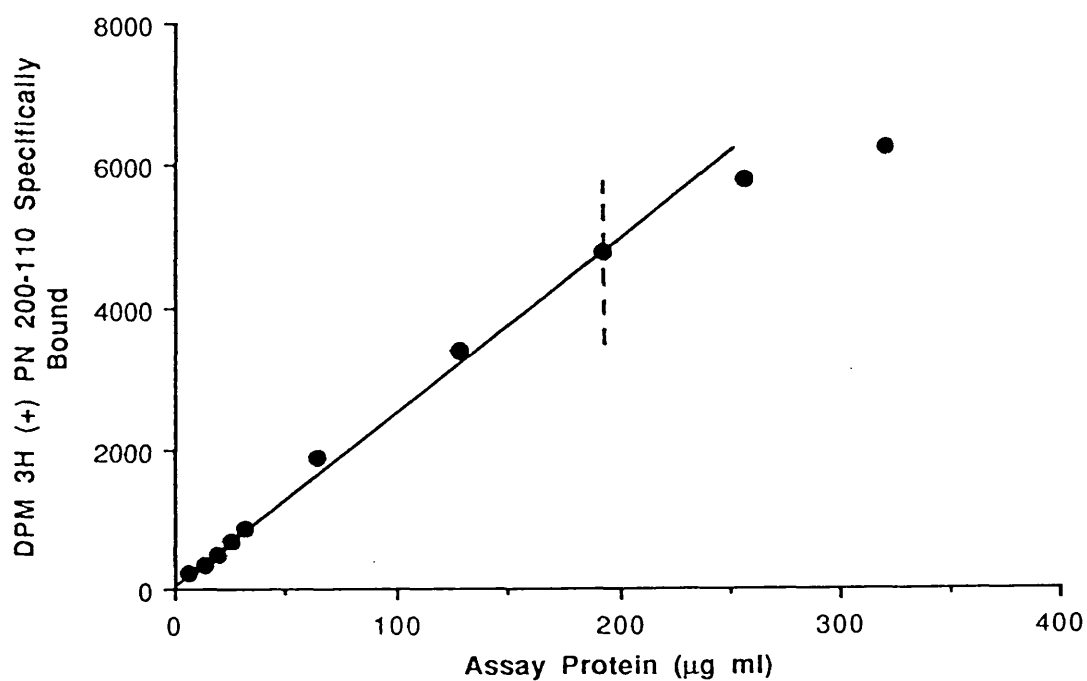


**Figure 2.1.** Specific binding of [ $^3\text{H}$ ] PN 200-110 (0.1nM) as a function of increasing assay protein. A representative experiment of one other is shown.

Specific binding was maximal after three wash cycles and thereafter all membrane preparations were carried out with four wash cycles. The percent specific binding was unaffected by the number of wash cycles, and was a reflection of ~~very low non-specific~~ binding properties of the ligand, even in homogenised non-washed tissue. It was found that storage of membrane homogenates for long periods and resuspension of membranes by vortex mixing resulted in a reduction in the amount of detectable binding sites of nearly 50%. This could be due to deterioration of membrane pellets over time, especially if thawing and re-freezing was suspected, and the likely occurrence of vesiculation or clumping of membranes on dilution in buffer, such that optimum dispersion of binding sites in suspension was only achieved by Polytron homogenisation. Consequently, all membrane homogenates (including those used in all other binding assays encompassed in this work) were stored in liquid nitrogen in pellet form for less than three months prior to assay and were resuspended in assay buffer by Polytron homogenisation (setting 10, one burst of >5s duration).

It was found that specific [ $^3\text{H}$ ] PN 200-110 increased as a function of increasing assay protein. This relationship was linear, but high protein concentrations became limiting such that a linear relationship was only observed up to 200  $\mu\text{g}$  protein/assay at a ligand concentration of 0.1 nM (+) PN 200-110 (Figure 2.1.). Higher protein concentrations were limiting with increasing ligand concentrations. However, the protein concentration of 80  $\mu\text{g}$  used in [ $^3\text{H}$ ] DHP assays was well within the linear part of the curve.

## 2.6. *In Vitro receptor autoradiography studies.*

Gerbils and mice were killed by cervical dislocation and decapitation. The brains were carefully removed, ensuring that the dura, optic nerves and any connective tissue were severed, enabling the brain to be easily removed from the skull cavity. Brains were immediately placed in isopentane maintained at  $-50^\circ\text{C}$  with dry ice. A vertical cut was made at the level of the cerebellum and cerebral cortex interface and the brains mounted onto

orientating microtome chucks with Tissue Tek and embedded in Lipshaw Embedding Matrix. Following a brief dip in isopentane (-50°C) the frozen brains were equilibrated at -30°C for 20 min in a cryostat (Bright Instruments), prior to sectioning. Glass slides were prepared in advance by rinsing initially in distilled water and then by brief immersion in a solution of 1% gelatin, 0.05% chromic potassium sulphate (previously heat stirred to fully solubilise the gelatin, filtered and left to cool), drip dried and left to dry thoroughly in a dessicated oven at 60°C. Sections were cut in the rostrocaudal plane, thaw-mounted onto the prepared slides, and stored in a sealed desiccated container at -20°C for 48-72 hours prior to assay to facilitate adhesion to the slide. Previous studies had shown that sections could be stored up to 7 days without any deterioration of binding activity (Glossmann & Ferry, 1985).

#### **2.6.1. [<sup>3</sup>H] (+) PN 200-110 autoradiography studies.**

Binding of [<sup>3</sup>H] (+) PN 200-110 to gerbil coronal brain sections was carried out essentially as previously described for rat brain sections (Glossmann & Ferry, 1985). Sections were pre-equilibrated with buffer (0.17M Tris HCl, pH 7.4 at 25°C) and then incubated in buffer containing 0.1 nM [<sup>3</sup>H] (+) PN 200-110 (71 Ci/mmol). Parallel sections were also incubated in an identical buffer containing 1 µM nitrendipine to define non-specific binding. Incubations were carried out at 25°C for 2 hrs. Unbound radioactivity was washed away by a short dip in ice cold 0.17 M Tris HCl (pH 7.4), followed by a 30 min wash in ice cold 0.17 M Tris HCl, (containing 0.25 mg/ml bovine serum albumin). The sections were then dipped briefly in ice cold distilled water to remove salts and dried under a stream of cold air for 60 min. Sections were then left to dry for 12 hrs at room temperature. Dried sections were placed in a Harvard Cassette, with each cassette containing RPA 507 standard microscaler (Amersham, activity 1.3 - 32 nCi/mg) and exposed to 24 x 30 cm [<sup>3</sup>H] sensitive Hyperfilm (Amersham). Exposure was carried out for 6 weeks at 4°C. After this period, films were carefully removed from the cassettes under safelight conditions and developed in Agfa X-ray developer (Diluted 1:6 with H<sub>2</sub>O)

at room temperature for 4 min. Following a brief wash in H<sub>2</sub>O the films were fixed with Agfa X-ray fixer (diluted 1:5 with H<sub>2</sub>O), rinsed in running water for 10 min and left to dry overnight in a drying cabinet at 30°C).

Autoradiograms were analysed using a Quantimet 920 image analysis system essentially as described (Sharif & Hughes, 1989). Light transmission through the film was corrected for background by a matrix shading corrector. Transmission of light through the autoradiograph was converted to optical density, and the OD of section images was generated by reference to the microscale standards, the OD of which was measured in relation to an Ilford neutral density filter of known OD. A calibration graph was thus produced of the standard's OD against the radioactivity per unit area of radioligand, and linear transformation of this data gave a plot of Ln OD vs Ln radioactivity, stored by the computer. The calibration curve for the standard microscale was established from the known radioactivity of the standards and the specific activity of the radioligand. Thus, the highest microscale standard of 32 nCi/mg corresponded to 450 fmol/mg tissue for [<sup>3</sup>H] (+) PN 200-110, with a specific activity of 71 Ci/mmol, and the standard curve was over the range 17.2 - 450 fmol/mg tissue. OD measurements of the required brain structures from the autoradiograms were performed by selecting a measuring box of appropriate dimensions over the appropriate structure, and the OD of that area measured. This procedure defined an area over which the OD was measured for conversion to radioactive concentration, and the image area was stored, such that after edge enhancement and alignment of the corresponding non-specific image over the total binding image, the OD of the defined structure was made automatically, with subtraction of the non-specific from the total yielding the specific binding for that structure. Collated data, usually for several measurements on each section were automatically stored on disk, and later printed to give the mean specific binding for the defined brain area. In the same way, it was possible to produce colour coded images for sections when total and non-specific sections were aligned and corrected as described, allowing a better visual differentiation to be made of areas that appeared less distinct on the monochrome monitor.

### 2.6.2. [<sup>3</sup>H] PK 11195 autoradiography.

[<sup>3</sup>H] PK 11195 binding to rat and gerbil brain sections was carried out essentially as described for [<sup>3</sup>H] (+) PN 200-110 binding studies. Sections were pre-incubated for 30 min in 0.17 M Tris HCl buffer (pH 7.4 at 25°C) and then in buffer containing 1.0 nM [<sup>3</sup>H] PK 11195 for gerbil brain sections and 0.2 nM [<sup>3</sup>H] PK 11195 for mouse brain sections. Parallel sections were incubated in an identical buffer containing 10 µM RO 5-4864 to define non-specific binding. Sections were incubated for 30 min at 25°C. Unbound radioactivity was removed by briefly dipping the sections in ice cold 0.17 M Tris HCl, followed by a 5 min wash in the same buffer. The sections were then briefly dipped in ice cold distilled water, and dried under a stream of cool air. Sections were exposed to [<sup>3</sup>H] sensitive hyperfilm for 6 weeks at 4°C. Sections were developed and analysed as described for [<sup>3</sup>H] (+) PN 200-110, the highest microscale standard for [<sup>3</sup>H] PK 11195 (81 Ci/mmol) being 395 fmol/ mg tissue and the range for the standard curve being 1.4 - 395 fmol/mg tissue.

## 2.7. Experimental ischaemia

### 2.7.1. Forebrain ischaemia in the Mongolian gerbil.

Male Mongolian gerbils weighing 60-90g were anaesthetised with 5% halothane (Halothane B.P, May & Baker) in a 30% oxygen / 70 % nitrous oxide mixture, delivered via a facemask. Following induction of anaesthesia, the halothane concentration was reduced to 1.5 % and maintained at this level throughout remaining surgical procedures. Fur was removed and skin surface cleaned with an alcoholic Hibitane solution. A skin incision was made by means of a ventral cut made in the paratracheal region, through which the right and left common carotid arteries were identified. The arteries were freed from the accompanying vagosympathetic nerve trunks and isolated by means of loose

ligatures, thus allowing quick identification and a means of easily clamping the arteries. Forebrain ischaemia was induced by clamping the arteries with microvascular clips (Ackland 2CV, Weiss, London, U.K.). During surgical procedures, animals were kept at a warm (37-38°C) temperature under operative arc lamps and core temperature, recorded via a rectal probe, was found to remain constant before, during and after surgical procedures. Following the required occlusion period (5 or 10 min) the clips were released and blood flow was restored (checked by observation of the arteries). The wound was dusted with antibiotic powder and repaired by means of five or six single stitches. During the recovery period, animals were housed singly and allowed free access to food and water.

After the appropriate post-occlusion period, brains were removed for binding analysis by cervical dislocation of the animals, followed by rapid decapitation. Brains were dissected over ice and the relevant brain structures dissected free, placed in cryotubes and immediately frozen in liquid nitrogen and stored until required for assay and analysis. Sham control animals were subject to identical procedures, with the exception of artery occlusion.

#### *2.7.2. Standardised forebrain ischaemia by use of a 5 min isoelectric period.*

For several experiments quantifying [<sup>3</sup>H] DHP parameter changes following forebrain ischaemia, in order to assess changes due to a 'standard' ischaemic insult and to rule out non-ischaemic animals, a period of 5 min isoelectricity was selected as the criteria for a standard ischaemic insult. Animals where isoelectricity of the EEG was resistant to artery occlusion, even after readjustment of the artery clips, were not included for subsequent experimental analysis of brain samples. EEG recordings were made by means of two electrodes attached in the forebrain region, midway between the eye and ear, and two electrodes behind the hind limbs for grounding. Forebrain recording electrodes corresponded to positions 13 and 14 in the 10-20 electrode system (input positions T4 and T3 on the lead terminator box). Recordings were made with a Mingograph EEG 10 eight

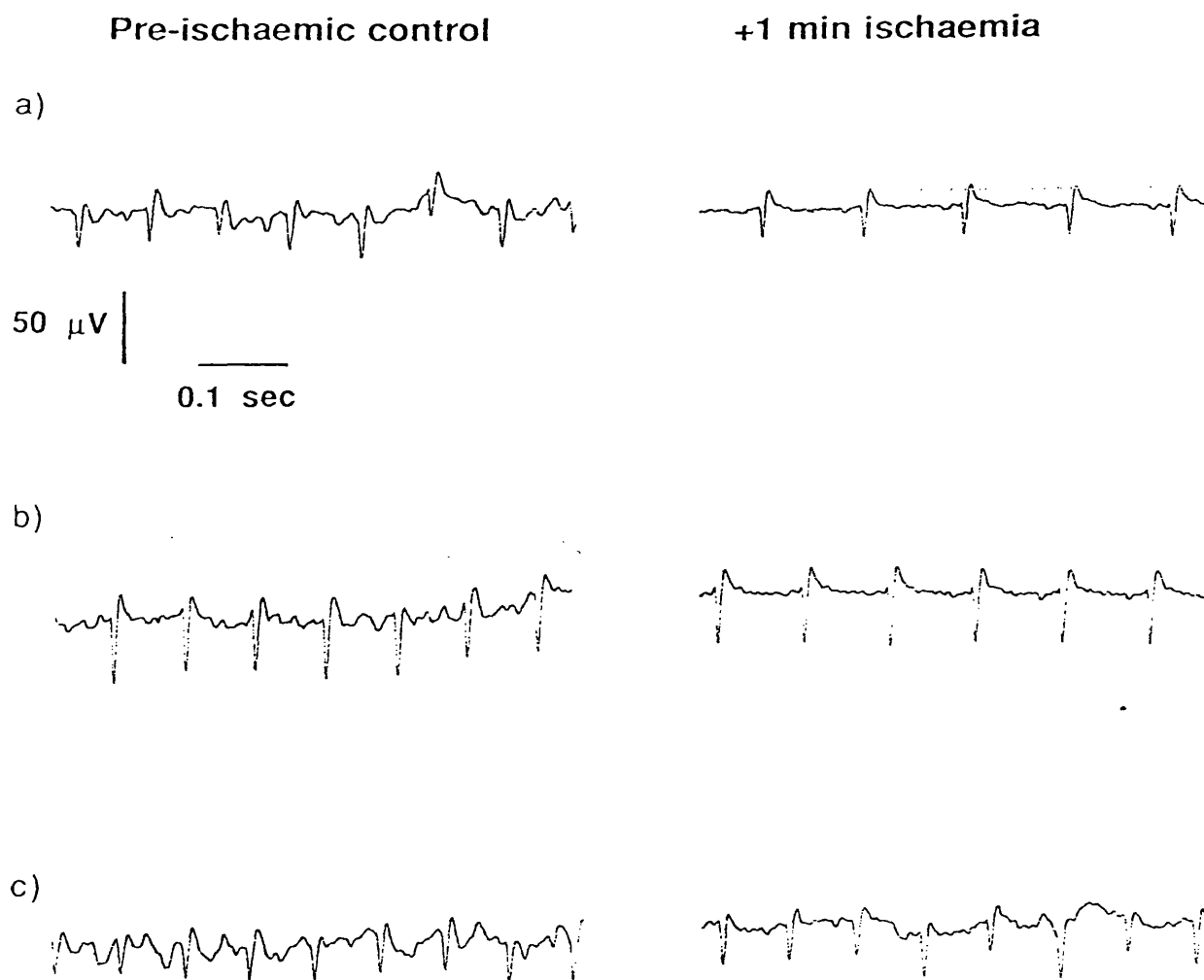


**Figure 2.2.** EEG recordings before and during (1 minute after artery occlusion) forebrain ischaemia in the mongolian gerbil.

a). Isoelectricity of the EEG on occlusion.

b). Isoelectricity of the EEG, but AC noise interference.

c). An animal where the EEG was not isoelectric during the ischaemic period, even after artery clip adjustment. Animals resistant to artery occlusion were not used for subsequent analysis.

channel recorder on a sensitivity of  $50 \mu\text{V cm}^{-1}$  and a variable chart speed between 6 and  $60 \text{ mm sec}^{-1}$ . Control recordings were established after the onset of anaesthesia, prior to any surgical manipulation, and a recording was made prior to artery occlusion to ensure a full EEG was obtainable. In some cases it was necessary to readjust the electrode positions to obtain a steady recording before proceeding with artery occlusion. Examples of recordings are shown in Figure 2.2 and illustrates recordings made from animals that were resistant to artery occlusion, susceptible to occlusion and a case where the EEG was flat but trace was masked with AC noise interference.

### 2.7.3. *Middle cerebral artery occlusion in the mouse.*

Adult male mice (Swiss, CD-1), weighing 30-50g were anaesthetised with pentobarbitone (pentobarbitone sodium, 0.1 ml of a 30 mg/ml solution) i.p. and exposure of the left middle cerebral artery was carried out as initially described (Welsh *et al.*, 1987). A skin incision was made between the orbit and the ear, and the skin reflected to expose the superior pole of the parotid gland and temporalis muscle. These were retracted to expose the cranium, through which the distal course of the left MCA could be seen through the translucent skull in the region of the foramen. A 1mm burr-hole craniectomy was performed with a dental drill to expose the left MCA. The left MCA was coagulated by bipolar diathermy and the burr-hole packed and sealed with bone wax. The temporalis muscle and parotid gland were replaced and closed with a single cat gut suture. The wound was dusted with antibiotic powder and surgically closed with five or six stitches. Animals were left to recover on a heated blanket, and for the remainder of the recovery period were housed singly with free access to food and water. After the appropriate recovery period animals were decapitated and the brains placed on a petri dish over ice. The ischaemic tissue, from the outer penumbra inwards, located in the parietal cortex, was dissected free from other cortical and striatal tissue and immediately frozen in liquid nitrogen. The corresponding cortical area from the contralateral hemisphere was dissected and frozen in an identical manner. Brain tissues were kept in liquid nitrogen until required for assay.

In experiments involving the assessment of potential neuroprotective agents, drugs or their appropriate vehicles were administered i.p. or i.v. in doses of 0.1 ml. Normally, stock solutions of drugs would be made at a concentration of 0.2 mg/ml, the effective dose being 500 µg/kg. Drugs were administered either pre- or post-ischaemia. Dosing schedules are given in the appropriate results section, drugs and their vehicles are given in sections 2.9 and 2.10.

#### ***2.7.4. [<sup>3</sup>H] PK 11195 binding assay on ischaemic mouse MCA samples.***

Mouse cortical brain tissues were homogenised individually in >100 vol. ice cold 50 mM Tris HCl (pH 7.4 at 4°C) using a Polytron tissue disruptor (setting 10, two 10s bursts). Homogenised tissue was centrifuged at 48,000g for 15 min at 4°C. Tissue pellets were washed a further two times by homogenisation (Polytron, setting 10, one 10s burst) and centrifugation. Final pellets were resuspended in Tris HCl buffer in a total volume of 4 ml and stored in liquid nitrogen until required for assay.

Aliquots of tissue homogenate (50-80 µg protein/assay) were incubated in 50 mM Tris HCl (pH 7.4 at 25°C) in a total volume of 1.0 ml. Assays were incubated for 30 min at 25°C. Reactions were terminated by filtration over Whatman GF/B filters, with two 5 ml washes of ice cold 50 mM Tris HCl washing buffer. Saturation binding parameters for [<sup>3</sup>H] PK 11195 were determined over the concentration range 0.005 -1.0 nM, each stock ligand concentration being made up in 1 % ethanol as described for earlier [<sup>3</sup>H] PK 11195 binding studies. Non-specific binding was determined in the presence of 10 µM RO 5-4864. Ischaemic and non-ischaemic samples from the same animal were generally assayed in parallel to account for any assay variation.

Protein determinations were carried out as described for generalised assay procedures and saturation binding parameters, K<sub>d</sub> and B<sub>max</sub>, were determined as described for generalised assay procedures.

## 2.8. Statistical analysis.

Data presented in this thesis are represented by mean  $\pm$  s.e. mean for  $n$  experimental determinations. Statistical comparisons between groups of data were made using the Student's  $t$ -test for unpaired data, where appropriate. In experiments in which multi-sample comparisons were made, data were analysed using analysis of variance (ANOVA) with Dunnett's  $t$ -test using the 'Statview' application on a Macintosh SE microcomputer. A level of probability of  $p < 0.05$  was taken as the level of statistical significance.

## 2.9. Drugs and chemicals used in the study.

The following radioligands with specific activities (SA, Ci/mmol) were used:-

[ $^3\text{H}$ ] (+) PN 200-110 (SA, 71- 86 ), [ $^3\text{H}$ ] nitrendipine (SA, 86-87), [ $^3\text{H}$ ] fluspirilene (SA, 67), [ $^3\text{H}$ ] BTX-B (SA, 55-60), [ $^3\text{H}$ ] dihydroalprenolol (SA, 111.2), [ $^3\text{H}$ ] PK 11195 (SA, 81-86) and [ $^3\text{H}$ ] prazosin (SA, 76.2) were obtained from Du pont (UK) Ltd. [ $^3\text{H}$ ] spiperone (SA, 105) and [ $^3\text{H}$ ] SCH 23390 (SA, 80.4) were obtained from Amersham International plc. [ $^3\text{H}$ ] SR 33557 (SA, 83) was custom synthesised by Amersham International and was kindly donated as a gift by Dr. A. Chatelain (Sanofi-Labaz Research Center, Bejar, Belgium).

The following drugs (and their sources) were used : flunarizine, lidoflazine, fluspirilene, cinnarizine, pimozide, spiperone, haloperidol and ketanserin from Janssen; phenytoin sodium from Parke Davies; Bay K 8644, nimodipine and nisoldipine from Bayer AG; Gallapomil (or D 600) from Knoll AG; dipyridamole from Boehringer Ingelheim; prenylamine from Hoechst; bepridil from Wallace Laboratories; phentolamine from Ciba Giegy, sodium pentobarbitone from May & Baker, (+), (-) butaclamol, MK 801, SCH 23390, and CPP from Research Biochemicals Inc. (Natick, MA, U.S.A.); GppNHp, GTP, aconitine, verapamil, veratrine, veratridine, palmitoyl DL carnitine, scorpion venom (*Leiurus quinquestriatus* V-5251), tetrodotoxin, isoprenaline, lorazepam,

clonazepam, diazepam, flunitrazepam and trifluoperazine from Sigma (Poole, Dorset, U.K.); SR 33557 from Sanofi. The following compounds were synthesised by Syntex laboratories (Research Syntex France or Palo Alto): PK 11195, RO 5-4864, (+), (-), PN 200-110, nitrendipine, nifedipine *d-cis* and *l-cis* diltiazem, RS 30026, acyl-carnitine analogues (decanoyl-arachidoyl), *cis* and *trans* diclofurime and RS 87476. Drug solutions were prepared on a daily basis.

Initially drugs were dissolved in a minimal concentration of solvent (ethanol, citric acid or H<sub>2</sub>O) and made up to a stock solution of 1 or 10 mM with ultra pure, reverse osmosis H<sub>2</sub>O. Subsequent dilutions were made in H<sub>2</sub>O or buffer as appropriate.

All other chemicals, biochemicals and reagents used were of the highest grade available and were obtained from Sigma (Poole, Dorset, U.K.), B.D.H Chemicals Ltd. (Poole, U.K.) or FSA laboratory supplies (Loughborough, England).

#### ***2.10. Administration of drugs in MCA model.***

Drugs were administered either i.p. or i.v. (0.1 ml injection volume) as indicated in the appropriate results sections. The dose of all compounds is expressed in terms of base substance. The following compounds were dissolved in either sterile H<sub>2</sub>O only or initially in ethanol and then in sterile H<sub>2</sub>O as stock solution of 0.2 mg/ml (final solution containing less than 0.1 % ethanol v/v): MK 801, RS 87476, flunarizine, (+) butaclamol and SR 33557. Nimodipine (0.2 mg/ml) and phenytoin (11.2 mg/ml) were made up in the following vehicle solution: 40 % polyethyleneglycol 300; 10 % ethanol; 50% H<sub>2</sub>O. All solutions were prepared daily for the period of dosing (normally 7 days).

---

## **Chapter 3**

**The characterisation and differentiation between calcium antagonists in radioligand binding experiments**

### 3.1. [ $^3\text{H}$ ] (+) PN 200-110 binding to rat cerebral cortex.

[ $^3\text{H}$ ] (+) PN 200-110 binding to rat cerebral cortex membranes at 25°C was saturable, reversible and of high affinity. Iterative non-linear analysis of the data indicated a single class of binding sites with an equilibrium dissociation constant,  $K_d$ , of  $0.03 \pm 0.008$  nM, and a density of binding sites,  $B_{\text{max}}$ , of  $221 \pm 20$  fmol/mg protein. Scatchard transformation of the specific saturation data are shown in Figure 3.1. In kinetic studies ( $n=4$ , mean ligand concentration 0.045 nM), the observed rate of association ( $K_{\text{obs}}$ ) at 25°C was  $0.022 \pm 0.002$  min $^{-1}$ , and the first order dissociation rate constant  $K_{-1}$  was  $0.0078 \pm 0.001$  min $^{-1}$ . Thus, the kinetically derived  $K_d$  of 0.026 nM (Figure 3.2) was similar to that derived from equilibrium binding studies.

#### 3.1.1. [ $^3\text{H}$ ] (+) PN 200-110 distribution of binding sites.

The binding of [ $^3\text{H}$ ] (+) PN 200-110 to rat brain tissues (Table 3.1) indicated that in those brain areas examined, all tissues were labelled with similar affinity at a single class of binding site.

**Table 3.1.**

TISSUE (n)	$B_{\text{max}}$ (fmol/mg protein)	$K_d$ (nM)
Rat cerebral cortex (6)	$221 \pm 20$	$0.03 \pm 0.008$
Rat hippocampus (4)	$248 \pm 23$	$0.04 \pm 0.01$
Rat striatum (4)	$191 \pm 10$	$0.04 \pm 0.004$
Rat cerebellum (4)	$77 \pm 12$	$0.05 \pm 0.01$
Rat cardiac left ventricle (4)	$214 \pm 21$	$0.07 \pm 0.005$
Rabbit purified skeletal muscle (2)	13.6 pmol/mg protein	0.24

**Table 3.1** The tissue distribution of [ $^3\text{H}$ ] (+) PN 200-110 binding sites. Values represent the mean  $\pm$  s.e. mean of (n) determinations.

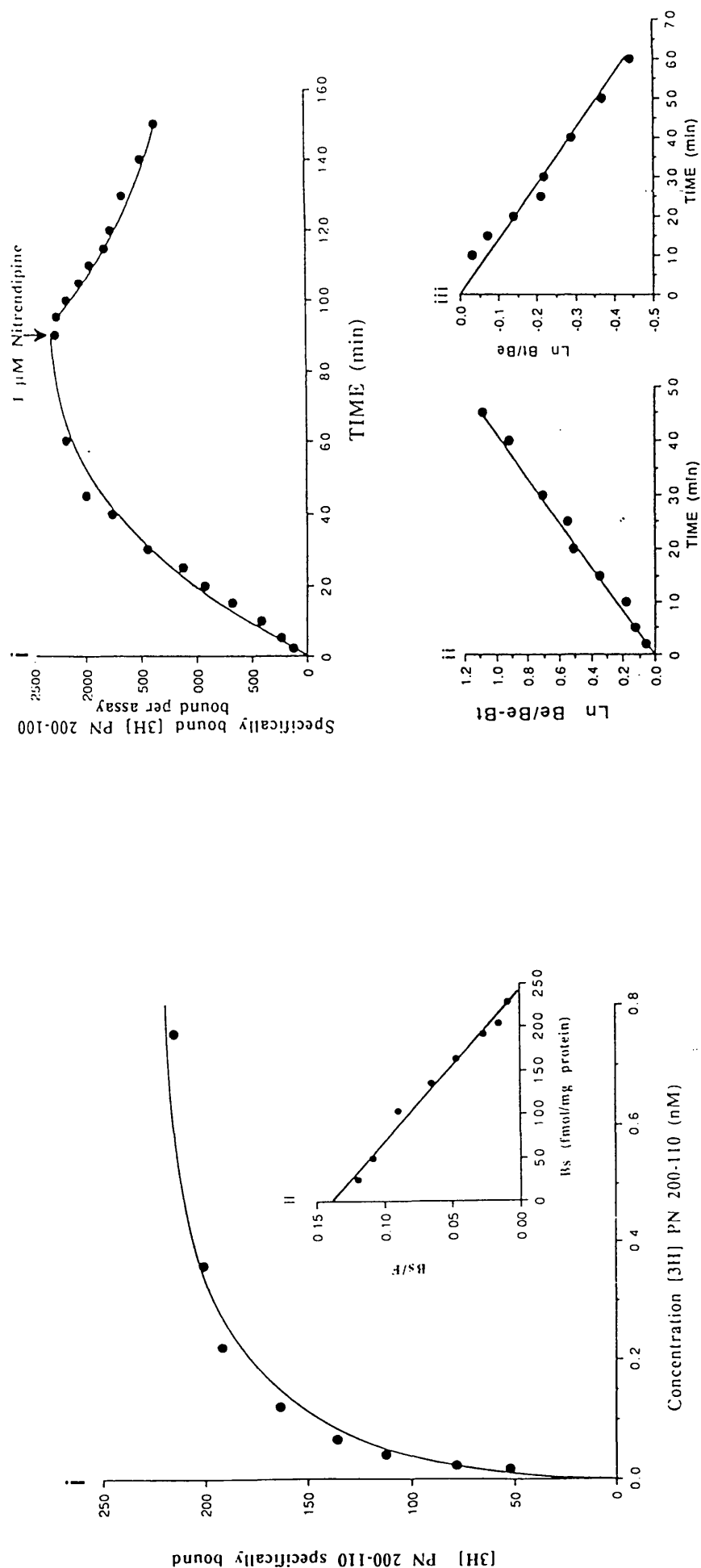


**Figure 3.1** i) Specific  $[3H]$  PN 200-110 saturation binding (fmol/mg protein) to rat cerebral cortex membranes as a function of ligand concentration at 25°C. ii) Linear transformation of the saturation data in the form of a Scatchard plot, where  $B$  represents specifically bound ligand (fmol/mg protein), and  $f$  is the free ligand concentration. The bound axis intercept indicates receptor density ( $B_{max}$ ), and the slope is equivalent to  $1/K_d$ .

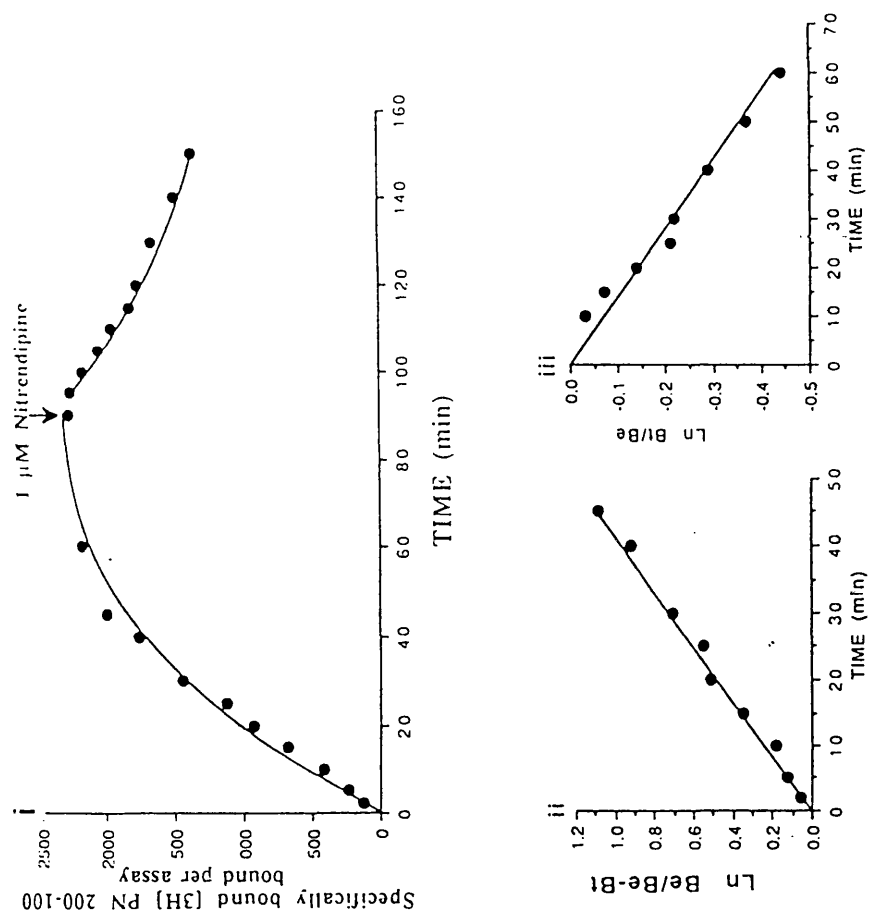


**Figure 3.2** Kinetics of  $[3H]$  PN 200-110 binding to rat cerebral cortex membranes at 25°C.

i) After equilibrium to 100 min dissociation was initiated by the addition of  $1 \mu M$  nitrendipine.  
ii & iii) The inserts show the log linear transformation of the association and dissociation data

---

**CALCIUM ANTAGONIST**

	pKi *(pIC <sub>50</sub> )	nH	%max
<b>CLASS I</b>			
(+) PN 200-110	10.1 ± 0.15	1.06	100
(-) PN 200-110	7.92 ± 0.02	1.14	100
Nitrendipine	9.67 ± 0.15	0.94	100
Nifedipine	8.97 ± 0.25	0.89	100
Bay K 8644	8.43 ± 0.21	0.96	100
RS 30026	8.28 ± 0.09	1.01	100
<b>CLASS II</b>			
Verapamil	7.69 ± 0.09*	0.92	42
D-cis-diltiazem	7.58 ± 0.13*	1.00	37
L-cis-diltiazem	not effective		
<b>CLASS III</b>			
Pimozide	7.72 ± 0.13	1.00	100
Fluspirilene	7.69 ± 0.01*	0.66	100
Flunarizine	6.10 ± 0.20*	1.28	92
Lidoflazine	6.44 ± 0.06*	0.84	90
Bepridil	5.53 ± 0.10*	1.00	68
Trifluoperazine	5.31* (n=1)	1.04	70
Prenylamine	6.90* (n=1)	0.81	100

---

**Table 3.2** Calcium antagonist affinity values at the [<sup>3</sup>H] PN 200-110 binding site in rat cerebral cortex at 25°C. Values represent the mean ± s.e. mean of 3-7 experiments. Affinities are represented by pKi or by \*pIC<sub>50</sub> where inhibition of binding is incomplete or where the Hill slope (nH) <1.0. % max is the maximal amount of specific binding displaced up to a drug concentration of 10 μM.

The highest number of sites was detected in the hippocampus and cerebral cortex with lower levels detected in straitum, and the cerebellum having the lowest density of sites. Other experiments indicated that this profile was not consistent in all tissues examined, as the affinity in rat left ventricular cardiac tissue ( $K_d$   $0.07 \pm 0.005$ ,  $n=4$ ) was lower than that in brain tissues and the affinity in purified rabbit skeletal muscle membranes almost a log order less potent ( $K_d$   $0.24$  nM), but the highest density of binding sites was labelled (13.6 pmol/ mg protein).

### ***3.1.2. Pharmacological specificity of [ $^3$ H] PN 200-110 binding to rat cerebral cortex at 25°C.***

The selectivity of a range of different calcium antagonists for the [ $^3$ H] PN 200-110 site in rat cerebral cortex is shown in Table 3.2. Class I calcium antagonists and activators (dihydropyridine related analogues) were potent inhibitors of [ $^3$ H] PN 200-110 binding. All agents displaced specific binding to the level of non-specific binding (defined by  $1\text{-}\mu\text{M}$  nitrendipine) and with Hill slopes close to unity. The potent dihydropyridine (DHP) PN 200-110 showed stereoselectivity for the site with the (+) isomer more than one hundred fold more potent than the (-) isomer. The calcium channel activators Bay K 8644 and RS 30026 displayed similar affinities for the site, and displaced the ligand in a similar manner to other agents of the class with Hill slopes close to unity.

<b>Table 3.3</b>	COMPETITOR	pIC50	nH
	Bay K 8644	$8.49 \pm 0.09$	1.04
	Bay K 8644 + $10\text{ }\mu\text{M}$ GppNHp	$8.47 \pm 0.04$	0.89
	Bay K 8644 + $100\text{ }\mu\text{M}$ GppNHp	$8.45 \pm 0.06$	1.02

**Table 3.3** Effects of GppNHp on the displacement of  $0.03$  nM [ $^3$ H] PN 200-110 from rat cerebral cortex membranes by Bay K 8644. Values represent the mean  $\pm$  s.e. mean of 4-5 experiments each carried out against control.

There was no evidence for a G protein involvement in the regulation of agonist

interaction at the [ $^3\text{H}$ ] DHP binding site on the basis of competition experiments with Bay K 8644. Displacement experiments carried out in the presence of GppNHp, a non-hydrolysable GTP analogue, showed that the affinity and Hill slope for competition curves generated to Bay K 8644 were unaffected by the presence of GppNHp (Table 3.3). With 100  $\mu\text{M}$  GppNHp a reduction of  $8.1 \pm 2.2\%$  in the amount of specific binding was observed. In other preliminary experiments, consistent with previously reported data (Glossmann *et al.*, 1982), only high concentrations of these agents were found to have an effect at [ $^3\text{H}$ ] DHP binding sites; GTP (0.5 and 5 mM) caused a 25% and 56% decrease in the specific binding of [ $^3\text{H}$ ] nitrendipine to rat cerebral cortex membranes respectively, and GppNHp (0.2 and 2 mM) inhibited binding by 27% and 51%. The effects of 0.5 mM GTP were partially reversed (to 90 % of control) by  $\text{Mg}^{2+}$  (1mM). The decrease in specific binding in the presence of high concentrations of guanine nucleotide binding proteins may result from the chelation of divalent cations, the presence of which are a requisite for high affinity binding.

The Class II agents verapamil and diltiazem both displaced [ $^3\text{H}$ ] PN 200-110 incompletely, the maximal inhibition of binding at concentrations up to 10  $\mu\text{M}$  were 42 % and 37 % respectively. These data indicated that both compounds interacted in a complex manner with the [ $^3\text{H}$ ] DHP site, although through such an action, stereoselectivity was retained as L-cis diltiazem was ineffective at concentrations up to 10  $\mu\text{M}$ .

The heterogeneous group of class III agents displayed a range of differences in their interaction with the DHP site, consistent with complex binding interactions. Several of these agents failed to inhibit binding fully at concentrations up to 10  $\mu\text{M}$  although this may be a reflection of low affinity in some cases (Table 3.2). Displacement of [ $^3\text{H}$ ] PN 200-110 by fluspirilene resulted in competition curves that exhibited low Hill slopes. Statistically, although the slope was low, the displacement isotherm was better fitted to a single rather than a two site model, and therefore the nature of the slope suggested that either the selectivity between sites was small, or more likely, that heterogeneity or multiple binding sites did not exist. To examine the possibility that this was a feature of the compound's interaction with the [ $^3\text{H}$ ] PN 200-110 site, similar experiments were carried

out with 0.2 nM [ $^3\text{H}$ ] nitrendipine. In these experiments similar results were obtained ( $\text{pIC}_{50}$  7.27,  $\text{nH}$  0.47). These results indicated that the interaction of this group of compounds, for which fluspirilene appeared typical, was not through a simple competitive interaction. However, if conclusions were to be made on the basis of these displacement studies alone, pimozone, which is a close structural analogue of fluspirilene, did not appear to act through a complex mechanism as the compound was potent and displaced binding maximally with a Hill slope close to unity. Displacement studies alone did not sufficiently describe the interaction of a given compound.

**3.1.3. Interactions of palmitoyl carnitine, a putative calcium channel activator, and related acyl carnitines at the [ $^3\text{H}$ ] PN 200-110 site in rat cerebral cortex.**

Displacement studies carried out with a range of acyl carnitines were carried out at the [ $^3\text{H}$ ] PN 200-110 binding site in rat cerebral cortex (Figure 3.3.i). The acyl carnitines examined were a series of structurally related compounds, differing in alkyl chain length. The affinities of these compounds at the [ $^3\text{H}$ ] DHP binding site are shown in Table 3.4.

**Table 3.4** Acyl carnitine analogue IC<sub>50</sub> ( $\mu\text{M}$ ) nH

(CH <sub>2</sub> ) <sub>8</sub> (decanoyl)	>100	-
(CH <sub>2</sub> ) <sub>10</sub> (lauroyl)	>100	-
(CH <sub>2</sub> ) <sub>12</sub> (myristoyl)	73	1.7
(CH <sub>2</sub> ) <sub>14</sub> (palmitoyl)	19 $\pm$ 5	1.8
(CH <sub>2</sub> ) <sub>16</sub> (stearoyl)	9.2	2.2
(CH <sub>2</sub> ) <sub>18</sub> (arachidoyl)	4.0	1.4

**Table 3.4** The effect of increasing acyl carnitine chain length on the ability of acyl carnitines to displace 0.03 nM [ $^3\text{H}$ ] PN 200-110 from rat cerebral cortex membranes. C-14 represents palmitoyl DL carnitine, and values represent the mean of 2 or 3 separate determinations each carried out in duplicate.

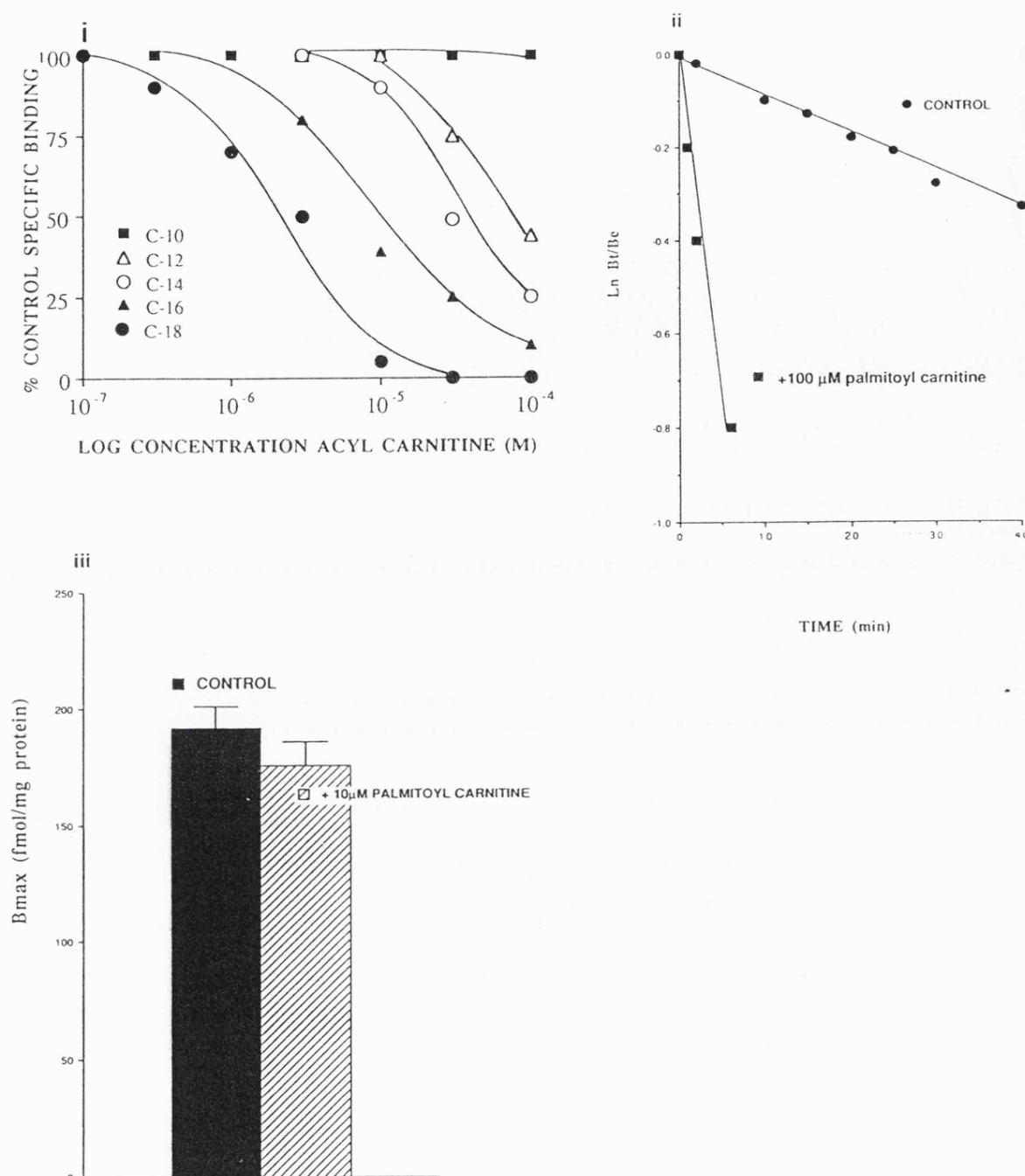


**Figure 3.3 i).** The effect of increasing acyl carnitine chain length (C-n is the number of carbon molecules in acyl carnitine chain) on the ability to displace [3H] PN 200-110 from rat cerebral cortex membranes.

**ii).** The effect of palmitoyl carnitine (100 $\mu$ M) on the dissociation of the [3H] PN 200-100 receptor complex from equilibrium. Dissociation was initiated by 1  $\mu$ M nitrendipine alone (control) and in the presence of palmitoyl carnitine.

**iii).** The effect of palmitoyl carnitine (10 $\mu$ M) inclusion during membrane preparation on [3H] PN 200-110 binding density in rat cerebral cortex. Palmitoyl carnitine was present during the first three washes prior to resuspension and washout in the final preparation step. Values represent the mean  $\pm$  s.e. mean for three different preparations prepared in parallel with and without palmitoyl carnitine prior to assay with [3H] PN 200-110.

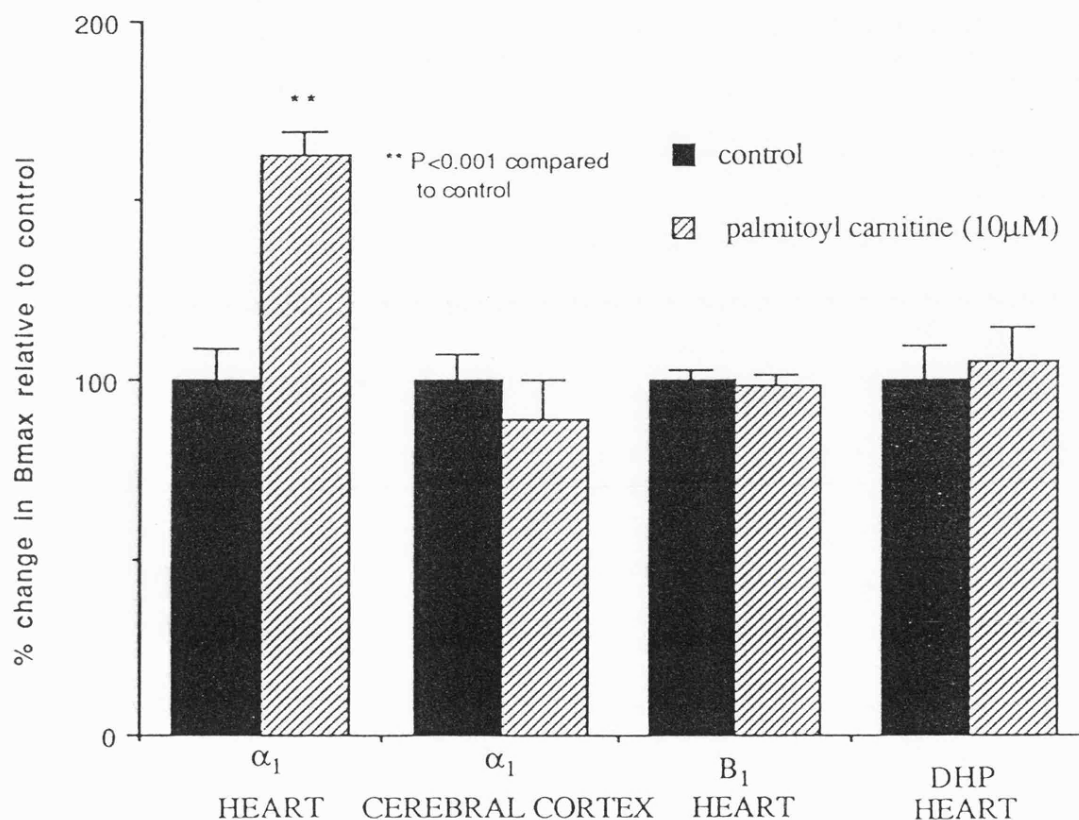


**Figure 3.4** The effect of pre-incubating membrane homogenates with palmitoyl carnitine on saturation binding parameters. Membranes were resuspended and incubated with palmitoyl carnitine (10μM) for 30 min at 37°C after the second centrifugation, after which they were washed by centrifugation and resuspension a further two times in buffer only. In all experiments binding assays were carried out on homogenates immediately after the last preparation stage. Values represent the mean  $\pm$  s.e.mean for 4 separate determinations for the % change in Bmax relative to their own control (taken as 100%).

α<sub>1</sub> parameters were established with [<sup>3</sup>H] prazosin, β<sub>1</sub> with [<sup>3</sup>H] dihydroalprenolol and [<sup>3</sup>H] PN 200-110 for DHP sites.

\*\*p<0.001 compared to control, students unpaired t-test.

These displacement studies indicated that the ability to inhibit specific binding was directly related to the chain length of the molecule. High Hill slopes, however, and the greater inhibition of binding observed at high concentrations of these agents suggested that the displacement was not as a result of competition for the radioligand binding site.

That the displacement of specific binding was not through competitive inhibition was further demonstrated when the effect of palmitoyl carnitine was examined on the rate of dissociation of [ $^3\text{H}$ ] PN 200-110 from rat cortex from equilibrium (Figure 3.3 ii). Palmitoyl carnitine (100 $\mu\text{M}$ ) caused a complete and rapid dissociation of the receptor complex, indicating that the agent decreased the amount of binding by a non-competitive interaction. However, although this decrease probably resulted from a disruption or change in membrane integrity, the effect was reversible. Incubations with palmitoyl carnitine during membrane preparation, followed by washout, had no effect on the density or affinity of [ $^3\text{H}$ ] PN 200-110 binding sites on subsequent analysis (Figure 3.3 iii).

This finding was somewhat surprising as it was envisaged that a change in binding parameters may have resulted from exposure to acyl carnitines analogous to a deleterious effect *in vivo* following the accumulation of acyl carnitines during ischaemia. Were these experiments not indicative or characteristic of effects following accumulations of acyl carnitines *in vivo*? Experimental evidence had demonstrated changes in the density of  $\alpha_1$  adrenoceptors following a period of myocardial ischaemia (Heathers *et al.*, 1987) and therefore the effects of acyl carnitine exposure were examined in a variety of other tissue homogenates and other receptor types to examine the possibility that these effects may be more selective. It was found that incubation of membrane homogenates with 10  $\mu\text{M}$  palmitoyl carnitine during the preparation stages was also without effect on myocardial [ $^3\text{H}$ ] DHP sites, but a marked and selective effect was found for up-regulation of left ventricular  $\alpha_1$  adrenoceptors. This effect was selective for myocardial  $\alpha_1$  adrenoceptors as no effect was found on  $\alpha_1$  adrenoceptors in the cerebral cortex, or myocardial  $\beta_1$  adrenoceptors (Table 3.5, Figure 3.4). Receptor binding affinities for all ligands were unaffected by the incubations with palmitoyl carnitine.

**Table 3.5**

RECEPTOR / TISSUE	CONTROL		PALMITOYL CARNITINE	
	Bmax	Kd	Bmax	Kd
$\alpha_1$ / Rat left ventricle	$36.0 \pm 3.1$	$0.30 \pm 0.006$	$59.6 \pm 3.7^{**}$	$0.31 \pm 0.01$
$\alpha_1$ / Rat cerebral cortex	$154 \pm 11$	$0.05 \pm 0.004$	$137 \pm 18$	$0.05 \pm 0.003$
$\beta_1$ / Rat left ventricle	$37.3 \pm 4$	$0.31 \pm 0.02$	$36 \pm 3$	$0.29 \pm 0.03$
DHP / Rat left ventricle	$214 \pm 21$	$0.07 \pm 0.005$	$223 \pm 22$	$0.08 \pm 0.01$
DHP / Rat cerebral cortex	$192 \pm 9$	$0.03 \pm 0.002$	$176 \pm 10$	$0.03 \pm 0.003$

**Table 3.5** The effect of palmitoyl DL carnitine exposure ( $10\mu\text{M}$  for 30 min at  $37^\circ\text{C}$ ) during membrane preparations on saturation binding parameters. Binding parameters represent Bmax (fmol/mg protein) and Kd (nM) for four separate experiments each compared against a parallel control. Values are the mean  $\pm$  s.e. mean. Assays were carried out using [ $^3\text{H}$ ] prazosin to label  $\alpha_1$  adrenoceptors, [ $^3\text{H}$ ] Dihydroalprenolol to label  $\beta_1$  adrenoceptors, and [ $^3\text{H}$ ] PN 200-110 to label DHP binding sites (\*\* $P < 0.001$  compared to control, unpaired t-test).

#### *3.1.4. Effects of tissue, temperature, and different radioligands on the allosteric modulation of [ $^3\text{H}$ ] DHP binding, exemplified by d-cis diltiazem and verapamil.*

In displacement studies it had already been illustrated that d-cis diltiazem and verapamil interacted with the [ $^3\text{H}$ ] PN 200-110 binding site in rat cerebral cortex through a complex mechanism. That the inhibitory effects of verapamil and d-cis diltiazem were similar under these conditions was surprising, since it had been widely established previously (e.g. Glossmann & Ferry, 1985 ) that these agents interacted with the [ $^3\text{H}$ ] DHP site in a positive and negative allosteric manner, and yet as illustrated in Table 3.2 the effect of the d-cis diltiazem in displacement studies was to cause inhibition of specific binding. Although this inhibitory action was partial, and both compounds inhibited specific binding

incompletely, the interactions were the same on the basis of these displacement experiments alone.

At DHP binding sites in rat cerebral cortex, labelled by [ $^3\text{H}$ ] PN 200-110, the regulation of binding by class II calcium antagonists was shown to be very temperature dependent. At 0°C, 25°C and 37°C, the effect of verapamil was inhibitory, and the affinity and percent of displaceable binding was unaffected. In contrast, at 37°C, a stimulatory effect of d-cis diltiazem was observed whereby an enhancement of specific binding was observed, but this effect became inhibitory as the temperature was reduced, thus at 25°C and 4°C displacement of [ $^3\text{H}$ ] PN 200-110 was observed. At 4°C and 25°C the potency of d-cis diltiazem was similar but a greater amount of specific binding was displaceable at the lower temperature.

Table 3.6	VERAPAMIL		D-CIS DILTIAZEM	
	pIC <sub>50</sub>	nH ( % inhibition)	pIC <sub>50</sub>	nH ( % inhibition)
TEMP				
37°C	7.42	0.72 (41)	17% maximal increase in binding	
25°C	7.69 ± 0.09	0.92 (42)	7.58 ± 0.13	1.00 (37)
0°C	7.64	0.60 (49)	7.23 ± 0.23	1.01 (68)

**Table 3.6** The effect of temperature on the displacement of 0.03 nM [ $^3\text{H}$ ] PN 200-110 from rat cerebral cortex. At 37°C diltiazem caused an increase in the amount of specific binding but this % increase was not sufficient to reliably evaluate an EC<sub>50</sub> for the effect. % inhibition is the maximal inhibition of specific binding up to a concentration of 10  $\mu\text{M}$ . Values represent the mean  $\pm$  s.e. mean of 2-5 experiments, each performed in duplicate.

An important observation in relation to the inhibition of binding observed at 25°C, was that the rate of dissociation of [ $^3\text{H}$ ] PN 200-110 was decreased compared to control under identical experimental conditions (Control  $0.0078 \pm 0.0008 \text{ min}^{-1}$ , and  $0.002 \pm 0.0007 \text{ min}^{-1}$  in the presence of 10  $\mu\text{M}$  d-cis diltiazem), whereas an increase in the dissociation rate was observed in the presence of 10  $\mu\text{M}$  verapamil ( $0.017 \pm 0.002 \text{ min}^{-1}$ ).

The overall inhibition of specific binding caused by d-cis diltiazem in competition experiments must therefore have resulted from an action other than a reduction in the dissociation rate constant, otherwise a net reduction in specific binding would not be observed. This must imply an effect on association rate. The effect of diltiazem in displacement experiments with [ $^3\text{H}$ ] PN 200-110 in rat cortex at 25°C was not consistent with previously reported findings since, with other [ $^3\text{H}$ ] DHP ligands only a stimulatory effect had been reported (Glossmann & Ferry, 1985), with diltiazem only becoming inhibitory at very low temperatures (Mir & Spedding, 1987). To examine if this effect was a property of diltiazem alone, rather than differing assay conditions, a series of experiments was conducted to evaluate the properties of d-cis diltiazem and verapamil under parallel experimental conditions with different ligands, tissues and temperatures. The results of these experiments are shown in Figure 3.5. It can be seen that the degree of positive allosterism exhibited by diltiazem was dependent on all three experimental variables. Thus a greater positive allosteric effect was observed with [ $^3\text{H}$ ] nitrendipine than with [ $^3\text{H}$ ] PN 200-110 under identical experimental conditions in cerebral cortex at 37°C, whilst at 25°C, an enhancement of [ $^3\text{H}$ ] PN 200-110 binding was observed in rabbit skeletal muscle membranes but under the same conditions, d-cis diltiazem caused incomplete inhibition of binding in cerebral cortex.

The extent to which d-cis diltiazem regulates [ $^3\text{H}$ ] DHP binding through an allosteric interaction appeared to be dependent on many factors and the results indicated that the susceptibility of the DHP binding site to allosteric regulation by other non DHP calcium antagonists may differ between tissues, an important consideration when defining the interaction of any given agent. Since the positive heterotropic effect of diltiazem resulting in an enhancement of specific [ $^3\text{H}$ ] DHP binding appeared to be most evident in skeletal muscle, the effects of cis- and trans-diclofurime were examined at the [ $^3\text{H}$ ] PN 200-110 site in skeletal muscle membranes. Diclofurime isomers were suitable candidates to examine these differences in allosteric control, since the molecular site of action of this agent has shown to be the same as diltiazem in that the regulation of [ $^3\text{H}$ ] nitrendipine binding to brain by trans-diclofurime is thought to be through an allosteric mechanism similar to

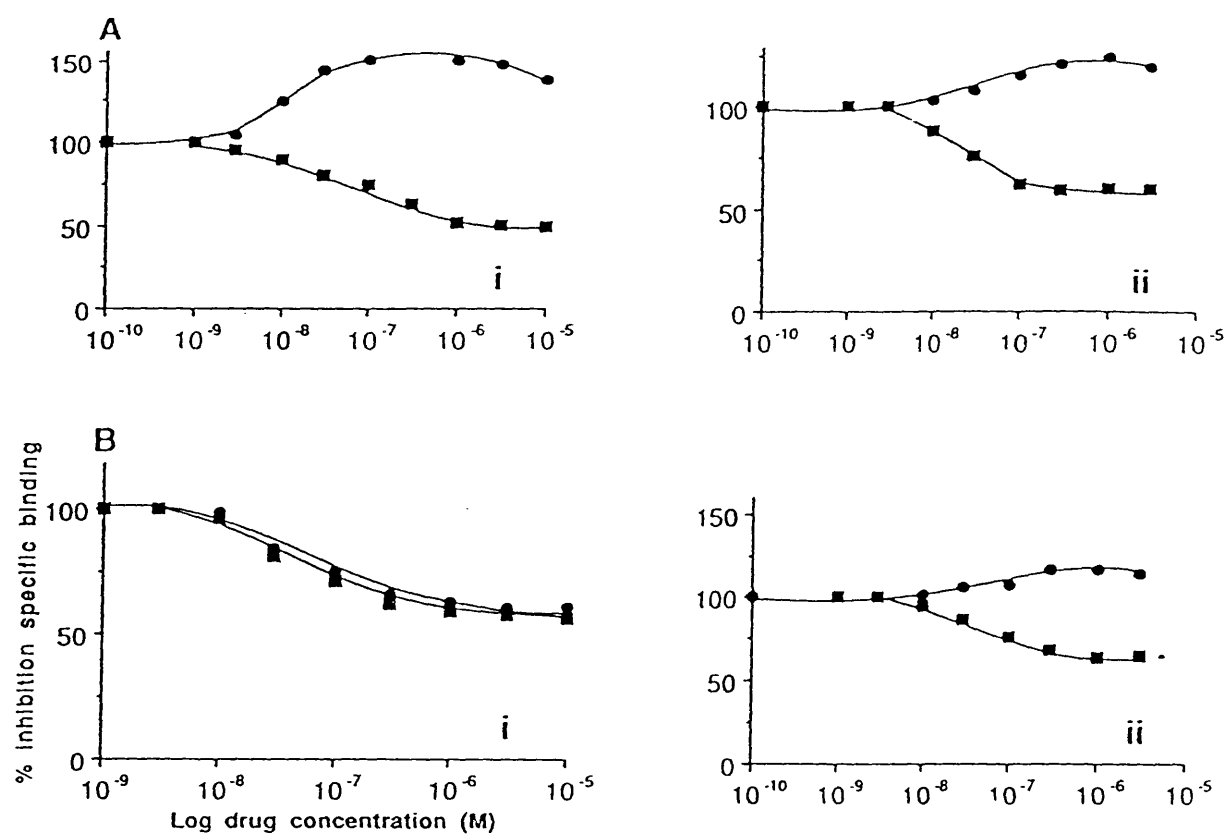


**Figure 3.5.**

Comparative allosteric properties of verapamil (■) and d-cis-diltiazem (●).

A. Comparative competition experiments carried out in rat cerebral cortex at 37°C (for 30 min) with i) 0.2 nM [ $^3$ H] nitrendipine and ii) 0.03 nM [ $^3$ H] PN 200-110.

B. Comparative inhibition of [ $^3$ H] PN 200-110 binding at 25°C from i) rat cerebral cortex (ligand concentration 0.2 nM) and ii) rabbit skeletal muscle membranes (ligand concentration 0.2 nM). Representative data of 3 experiments is shown.

diltiazem. Moreover, the compound is a potent and stereoselective inhibitor of [ $^3\text{H}$ ] diltiazem binding in cerebral cortex membranes, and on this basis, has been claimed to be a potent class II calcium antagonist (Mir & Spedding, 1987).

The effect of *cis*- and *trans*-diclofurime at the [ $^3\text{H}$ ] PN 200-110 site are shown in Figure 3.6. These data show that the interaction of diclofurime was different to its previously reported effects at the [ $^3\text{H}$ ] nitrendipine site in cerebral cortex, where an inhibitory effect only became apparent at low temperatures. In contrast, in skeletal muscle *trans* diclofurime, the active isomer, inhibited the binding of [ $^3\text{H}$ ] PN 200-110 at 40°C and 37°C with similar affinity. The *cis*-isomer of diclofurime was inactive at 37°C, but became inhibitory at 40°C. The potency of *trans*-diclofurime ( $\text{IC}_{50}$  based on maximal inhibition) was  $0.84 \pm 0.14 \mu\text{M}$  at 37°C and  $0.91 \pm 0.25 \mu\text{M}$  at 40°C ( $n=3$ ).

### **3.2. Interaction of class III calcium antagonists with [ $^3\text{H}$ ] DHP and $\text{Na}^+$ channel binding sites.**

#### ***3.2.1. pH effects at the [ $^3\text{H}$ ] PN 200-110 site in rat cerebral cortex***

As shown in Table 3.2 class III calcium antagonists interact with the [ $^3\text{H}$ ] PN 200-110 binding site with a range of affinities and different Hill slopes. Inhibition of binding was incomplete with some compounds and the affinity of these agents was lower than that of class I and II agents. The interactions of flunarizine and lidoflazine were investigated over a wider pH range to examine the possibility that a more favourable ionic species could be promoted at lower assay pH. This was easily achieved in this series of experiments because control [ $^3\text{H}$ ] PN 200-110 binding to rat cerebral cortex membranes was maximal and stable over the pH range 6.5 - 7.4, such that drug affinities could be directly compared to control as the binding of the [ $^3\text{H}$ ] DHP ligand would not be compromised at lower pH. Table 3.7 illustrates that under conditions of reduced assay pH the affinity for the [ $^3\text{H}$ ] PN 200-110 binding site in rat cerebral cortex was increased for all class III compounds tested. The potency of flunarizine showed a six fold increase at pH 6.5 compared to pH 7.4. The

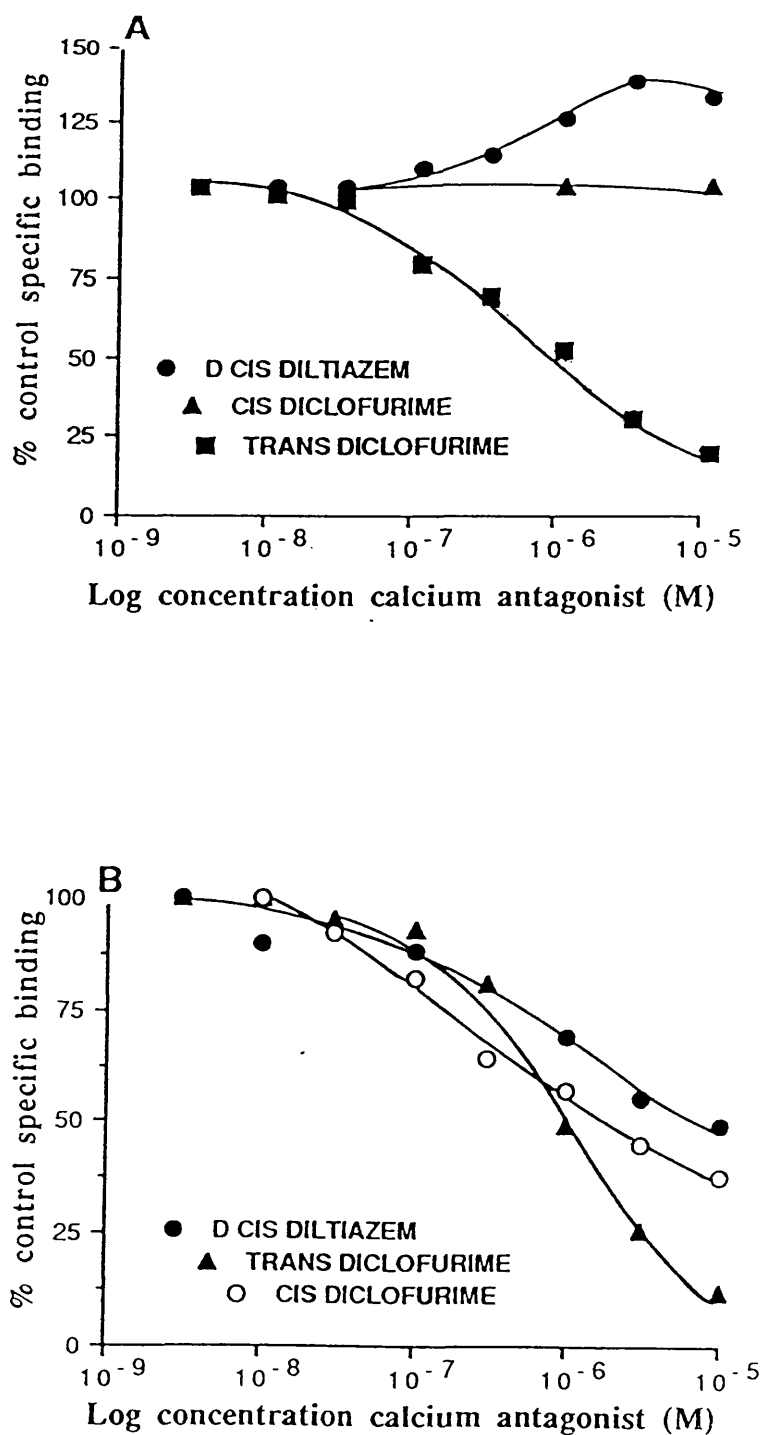


**Figure 3.6.** Allosteric regulation of [ $^3\text{H}$ ] PN 200-110 binding in rabbit skeletal muscle membranes by d-cis-diltiazem, *cis*-diclofurime and *trans*-diclofurime. Competition experiments were carried using 0.2 nM [ $^3\text{H}$ ] PN 200-110 incubated at A) 37°C for 30 min and B) 40°C for 180 min.

CALCIUM ANTAGONIST			
	pH 7.4	pH 7.0	pH 6.5
	IC <sub>50</sub>		
Nitrendipine ( <i>nM</i> )	0.32 ± 0.08	0.31 ± 0.07	0.35 ± 0.08
Flunarizine ( <i>μM</i> )	0.46 ± 0.08	0.22 ± 0.03	0.08 ± 0.01
Lidoflazine ( <i>μM</i> )	0.31 ± 0.06	0.16 ± 0.04	0.08 ± 0.01
RS 87476 ( <i>μM</i> )	1.05 ± 0.14	0.87 ± 0.2	0.43 ± 0.08

**Table 3.7.** The effect of decreasing pH (H<sup>+</sup> supplemented Tris-HCl buffer) on calcium antagonist potency at the [<sup>3</sup>H] PN 200-110 binding site in rat cerebral cortex. Values represent mean ± s.e.mean *μM* IC<sub>50</sub> (nM for nitrendipine) for 3-4 separate determinations, with each experiment run in parallel at all pHs against nitrendipine as control.

Concentration of competitor in saturation experiment	Kd	Bmax
<b>i</b>		
Control	$0.03 \pm 0.009$	$221 \pm 20$
0.5 nM nifedipine	$0.045 \pm 0.007$	$219 \pm 15$
5.0 nM nifedipine	$0.16 \pm 0.02$	$196 \pm 6$
<b>ii</b>		
Control	$0.03 \pm 0.007$	$224 \pm 21$
10nM fluspirilene	$0.06 \pm 0.01$	$211 \pm 21$
100 nM fluspirilene	$0.13 \pm 0.03$	$138 \pm 21$

**Table 3.8** Comparative shifts in saturation parameters of [ $^3\text{H}$ ] PN 200-110 binding in rat cerebral cortex produced by i) nifedipine and ii) fluspirilene. Values represent Kd (nM) and Bmax (fmol/mg protein) as mean  $\pm$  s.e.mean for 4 experiments, compared against control for each determination.

potency of lidoflazine and RS-87476 was also increased, but to a lesser degree. The affinity of nitrendipine was not affected across the pH range, and the control level of [ $^3\text{H}$ ] PN 200-110 was constant throughout.

### *3.2.2. Effects on [ $^3\text{H}$ ] PN 200-110 saturation binding parameters.*

To further characterise the interaction at the [ $^3\text{H}$ ] PN 200-110 binding site, the effect of fluspirilene on [ $^3\text{H}$ ] PN 200-110 equilibrium binding parameters was tested. Fluspirilene was chosen in this series of experiments because it was found to be relatively potent in competition experiments and displaced [ $^3\text{H}$ ] PN 200-110 from rat cerebral cortex membranes with a low Hill slope. It seemed unlikely that these effects resulted from a competitive interaction. Results from saturation experiments carried out in the presence of fluspirilene were consistent with the interaction being non-competitive (Table 3.8). Fluspirilene caused a decrease in both the equilibrium dissociation constant ( $K_d$ ) and receptor density ( $B_{\text{max}}$ ). That fluspirilene also decreased  $K_d$  in these experiments indicated an allosteric interaction, the coupling between the sites being negative. The low Hill slope for fluspirilene in competition studies at the [ $^3\text{H}$ ] DHP site would be consistent with the interaction of fluspirilene being negatively co-operative. In contrast, similar saturation experiments carried out in the presence of nifedipine indicated that the compound caused a change in the affinity of [ $^3\text{H}$ ] PN 200-110 but had no effect on  $B_{\text{max}}$ . These findings were indicative of a competitive interaction.

### *3.2.3. Effects on [ $^3\text{H}$ ] PN 200-110 dissociation kinetics.*

It has so far been established that the effects of class II and III calcium antagonists at the [ $^3\text{H}$ ] DHP site in brain tissue are non-competitive and saturation studies have indicated that some of these effects might also be negatively allosteric. Such effects can be readily assessed by characterisation of the interaction of a compound at the [ $^3\text{H}$ ] DHP binding site by an examination of dissociation binding kinetics. When dissociation is

Calcium antagonist	Dissociation rate (min <sup>-1</sup> )
<b>CONTROL</b>	0.0078 ± 0.0008
<b>CLASS I</b>	
NIFEDIPINE (10nM)	0.0086 ± 0.001
<b>CLASS II</b>	
D CIS DILTIAZEM (10μM)	0.002 ± 0.0007**
VERAPAMIL (10μM)	0.017 ± 0.002*
<b>CLASS III</b>	
FLUSPIRILENE (1μM)	0.014 ± 0.001**
LIDOFLAZINE (10μM)	0.016 ± 0.003*
RS 87476 (10μM)	0.012 ± 0.001*
FLUNARIZINE (10μM)	0.015

**Table 3.9** The effect of calcium antagonists on the rate of dissociation of [<sup>3</sup>H] PN 200-110 from rat cerebral cortex membranes at 25°C. Dissociation was initiated by the addition of 1 μM nitrendipine alone (control) or in the presence of the indicated concentration of calcium antagonist. Single values are the mean of 2 separate determinations, others represent the mean ± s.e.mean of 3-4 determinations. In all experiments a control dissociation rate was established in parallel with any other determination. \*p<0.05 \*\*p<0.01 compared to control.

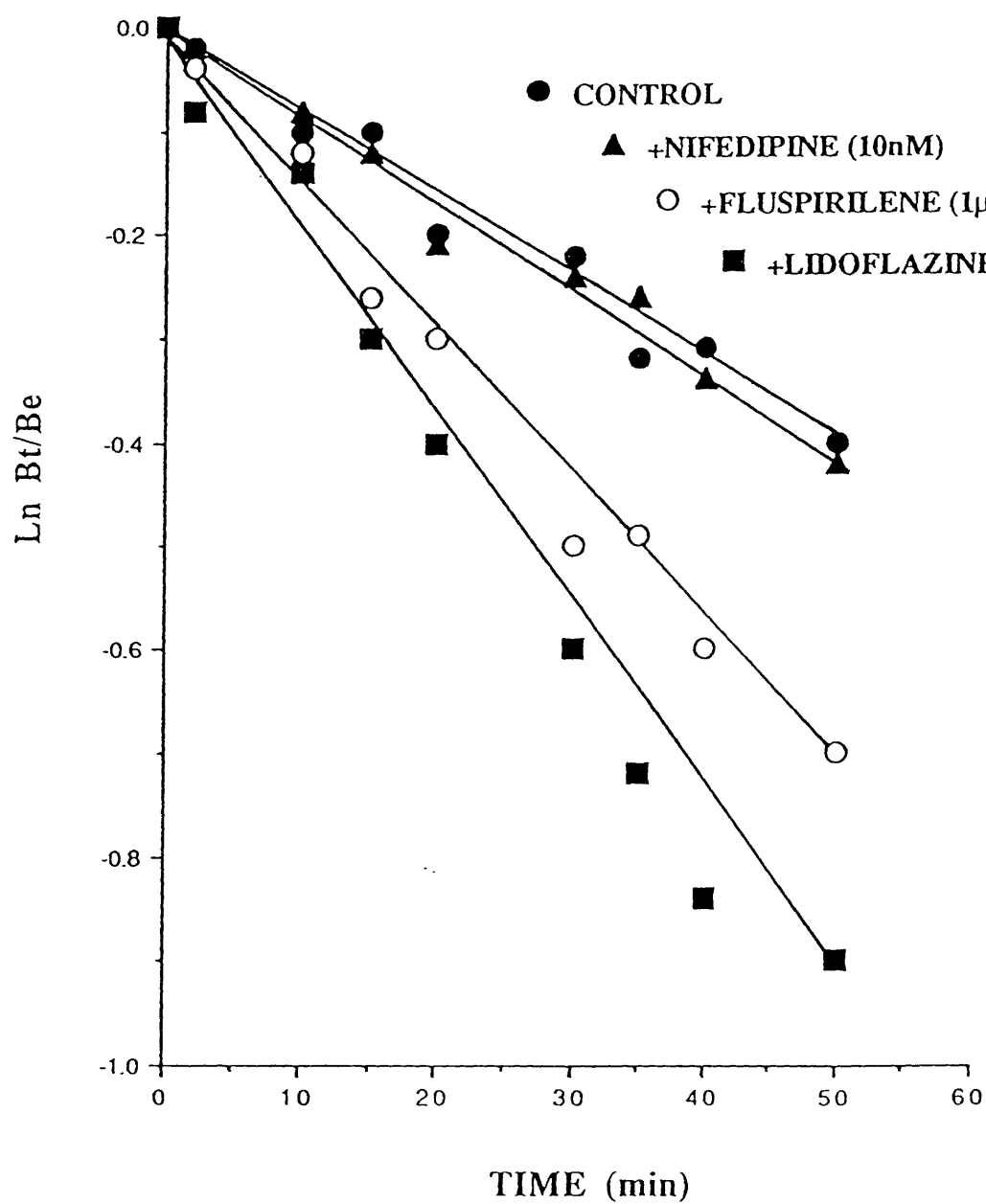


**Figure 3.7.** The effect of calcium antagonists on the rate of dissociation of [ $^3\text{H}$ ] PN 200-110 from rat cerebral cortex membranes. Following attainment of equilibrium (100 min), dissociation was initiated by the addition of 1  $\mu\text{M}$  nitrendipine alone (control) or in the presence of fluspirilene, lidoflazine or nifedipine. Data is representative of three similar experiments, mean data as in text.

initiated at steady state binding by an excess of unlabelled DHP, any change in the rate of dissociation that occurs in the presence of another compound indicates that the affinity of the receptor for the radioligand is reduced through an interaction of the compound at a site other than directly at the receptor. The concentration of agent used in these experiments should be sufficient to cause an effect relative to its affinity for the site, more than ten fold higher than  $IC_{50}$  or  $K_i$ , although inappropriately high concentrations should not be used to avoid other effects other than directly at the receptor under study. This could be a problem for less selective compounds, however, only an effect at the labelled receptor would be detected in this system. Thus, a competitive agent would not change the rate of dissociation if acting directly at the receptor site, since dissociation has been initiated by a large excess of a competitive compound, the added presence of another competitive agent will be ineffective. The effects of a variety of calcium antagonists on the rate of [ $^3H$ ] PN 200-110 dissociation from rat cerebral cortex membranes at 25°C is shown in Table 3.9 and illustrated in Figure 3.7. It can be seen that the rate of dissociation of the ligand-receptor complex from equilibrium was significantly increased in the presence of all class III agents tested indicative of a non-competitive, negatively allosteric mechanism for this group of compounds. Nifedipine, a competitive dihydropyridine, was ineffective. The class II agents, d-cis diltiazem and verapamil caused a significant decrease and increase in the rate of dissociation, indicating that these agents are coupled to the DHP site in a positive and negative manner respectively.

#### *3.2.4. Affinity of class III calcium antagonists for rat striatal dopamine $D_1$ and $D_2$ receptors.*

Affinity values were established for a range of calcium antagonists at the [ $^3H$ ] spiperone and [ $^3H$ ] SCH 23390 are shown in Table 3.10. The  $D_1$  and  $D_2$  sites were characterised with a range of selective antagonists. The dopamine  $D_2$  site displayed high affinity for the drugs spiperone and haloperidol, and stereospecificity was shown for (+)

COMPOUND	DOPAMINE D <sub>2</sub>		DOPAMINE D <sub>1</sub>	
	pKi	nH	pKi	nH
SCH 23390	-		9.71 ± 0.08	1.01
Spiperone	9.80 ± 0.10	1.02	6.83 ± 0.15	0.98
(+) Butaclamol	9.38 ± 0.02	0.89	8.77 ± 0.14	1.06
(-) Butaclamol	<5		<5	
Haloperidol	9.10 ± 0.09	0.93	7.26 ± 0.19	0.99
Pimozide	9.37 ± 0.09	1.07	6.18 ± 0.08	1.02
Fluspirilene	9.38 ± 0.13	1.39	7.13 ± 0.06	1.13
Flunarizine	7.30 ± 0.12	0.74	6.21 ± 0.09	1.06
Cinnarizine	7.14 ± 0.05	1.01	-	
Lidoflazine	7.10 ± 0.06	0.94	6.34 ± 0.11	1.05
Prenylamine	6.03 ± 0.03	1.29	-	
Trifluoperazine	9.21 ± 0.03	0.89	-	
Verapamil	6.22 (n=1)	0.90	-	
D-cis diltiazem	<5		-	

**Table 3.10.** The affinity of Class III calcium antagonists for dopamine D<sub>2</sub> receptors determined with 0.06 nM [<sup>3</sup>H] spiperone in rat striatal membranes and dopamine D<sub>1</sub> receptors determined with 0.2 nM [<sup>3</sup>H] SCH 23390 also in rat striatal membranes. Values represent mean ± s.e. mean (n=3-4).

butaclamol, with the (-) isomer completely ineffective. The dopamine D<sub>1</sub> site showed high affinity for SCH 23390 and (+) butaclamol, but only moderate affinity for spiperone and haloperidol. Class III calcium antagonists displayed a range of affinities for dopamine D<sub>2</sub> sites, all compounds showed at least moderate affinity with several compounds having nM affinities comparable with the characterised D<sub>2</sub> antagonists. Furthermore, two of the more potent compounds, pimozide and fluspirilene, were more than one hundred fold selective for dopamine D<sub>2</sub> compared to D<sub>1</sub> receptors. The steep Hill slope for fluspirilene may be indicative of a positively cooperative mechanism. None of the compounds tested showed any appreciable affinity for dopamine D<sub>1</sub> sites.

### *3.2.5. Interaction of class III calcium antagonists with synaptosomal Na<sup>+</sup> channels labelled by [<sup>3</sup>H] batrachotoxinin-A-20- $\alpha$ -benzoate.*

Saturation experiments indicated that in the presence of scorpion toxin and tetrodotoxin [<sup>3</sup>H] Batrachotoxinin-A-20- $\alpha$ -benzoate ([<sup>3</sup>H] BTX) labelled a single population of binding sites in rat cortical (P2 fraction) synaptosomes with a K<sub>d</sub>  $22.3 \pm 3$  nM and a density of binding sites  $1.18 \pm 0.2$  pmol/mg protein (n=3). The alkaloid neurotoxins aconitine and veratridine completely inhibited specific [<sup>3</sup>H] BTX binding, with low  $\mu$ M affinity and Hill slopes close to unity. Under the described conditions, in the presence of scorpion toxin (0.1 mg/ml) to allosterically increase binding through an interaction at site 3 on the sodium channel and tetrodotoxin which is active at site 1 and prevents ion flux through the channel, the specific binding defined by veratridine amounted to more than 80% of the total binding, allowing the interaction of compounds with site 2 on the Na<sup>+</sup> channel to be characterised (see Postma & Catterall, 1984). On examination of the affinity for class III calcium antagonists for the [<sup>3</sup>H] BTX site, a marked trend amongst this group of agents was found, with all agents showing high affinity, K<sub>i</sub> values for all compounds was in the range 20-70 nM. The separation of affinities within the group of compounds was narrow (Table 3.11), although all compounds were more potent than the anticonvulsant phenytoin (pK<sub>i</sub>  $4.69 \pm 0.13$ ). Other classes of calcium antagonist were less

COMPOUND	Na <sup>+</sup> channel affinity	
	pKi	nH
Aconitine	5.78 ± 0.05	1.04
Veratridine	5.07 ± 0.03	1.06
Phenytoin	4.69 ± 0.13	1.15
Pimozide	7.73 ± 0.09	1.16
Fluspirilene	7.43 ± 0.05	1.02
Flunarizine	7.43 ± 0.05	0.99
Cinnarizine	7.13 ± 0.12	1.27
Lidoflazine	7.25 ± 0.12	1.27
Prenylamine	7.12 ± 0.08	1.10
RS 87476	7.23 ± 0.10	0.97
Verapamil	6.02 ± 0.03	0.75
SR 33557	6.67 ± 0.08	0.98
(+) MK 801	5.32 ± 0.06	0.78
Nifedipine	<5	-

**Table 3.11.** The affinity of calcium antagonists at the Na<sup>+</sup> channel in rat cortical synaptosomes labelled with 2 nM [<sup>3</sup>H] BTX. Affinities represent the mean ± s.e. mean of 3-4 experiments.

potent however. Dihydropyridines were inactive at this site ( $pIC_{50}$  for nitrendipine  $<5.0$ ).

To examine the specificity of the [ $^3H$ ] BTX binding displaced by these agents experiments were carried out on crude P2 and sucrose gradient prepared synaptosomes. In P2 synaptosomal preparations, flunarizine displaceable binding was completely eliminated by carrying out the experiment in the absence of toxins. In purified synaptosomes the effect of toxin removal was similar. Membrane integrity, with respect to the difference in potential across the membrane, was established as being necessary for flunarizine displaceable [ $^3H$ ] BTX binding. Synaptosomes will undergo lysis when subjected to hypotonic solutions and consequently release organelles within the synaptosome. Rupturing the synaptic plasma membrane will eliminate the potential difference across the synaptosomes (see Gordon-Weeks, 1987). This was achieved by resuspending freshly prepared P2 synaptosomal fractions in 5 mM Tris HCl, containing 50  $\mu M$   $Ca^{2+}$ , pH 8.1. Lysis of the fraction resulted in a total loss of all flunarizine-displaceable [ $^3H$ ] BTX binding. Only residual non-specific binding was observed. Taken together, these results confirmed the toxin dependence and structural integrity necessary for high affinity [ $^3H$ ] BTX binding associated with the voltage-dependent  $Na^+$  channel. Furthermore, they have also shown that the lipophilic class III calcium antagonists are amongst the most potent group of agents known for this site in comparison to previously characterised compounds.

### *3.2.6. Interaction of class III calcium antagonists with spirodecanone binding sites labelled by [ $^3H$ ] spiperone in rat hippocampus.*

In previously reported data (see Howlett *et al.*, 1979) it had been shown that several neuroleptic agents were capable of displacing [ $^3H$ ] spiperone from non-dopaminergic, non-serotonergic sites in rat hippocampal membranes. Amongst the compounds that showed marked affinity for this site were spiperone and fluspirilene. Given that many of the class III antagonists displaced [ $^3H$ ] spiperone with high affinity from dopamine  $D_2$  sites, and fluspirilene appeared to be a prototypical compound of this class (see this results section, [ $^3H$ ] fluspirilene binding) the interaction of other class III

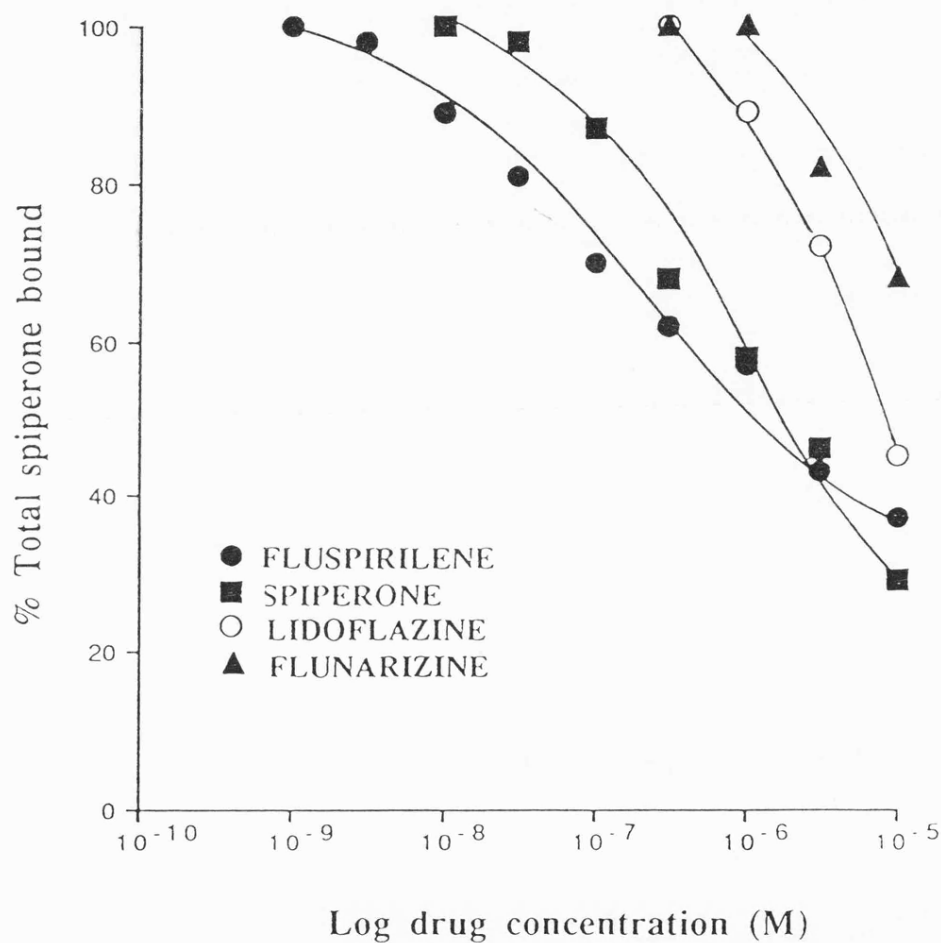


**Figure 3.8** Displacement of [<sup>3</sup>H] spiperone from rat hippocampal spirodecanone binding sites. Incubations with 0.2 nM [<sup>3</sup>H] spiperone were carried out at 25°C for 45 min in Tris-HCl washed hippocampal membrane homogenates. Spirodecanone sites were revealed by performing the experiment in the presence of 1 μM (+) butaclamol and 0.1 μM ketanserin to exclude binding of [<sup>3</sup>H] spiperone to dopamine D<sub>2</sub> or 5-HT<sub>2</sub> receptors. A representative experiment is shown, mean data as in text.

antagonists at this site were investigated. In the presence of (+) butaclamol and ketanserin (to exclude the possibility of binding to dopamine D<sub>2</sub> or 5-HT<sub>2</sub> receptors) and in agreement with previously reported data, [<sup>3</sup>H] spiperone was displaced from these sites in hippocampal membranes by spiperone (IC<sub>50</sub> 91 ± 5 nM, n=3) and fluspirilene (IC<sub>50</sub> 12 ± 3 nM, n=3) with no displacement of binding observed for the dopamine D<sub>2</sub> antagonist sulpiride. However, as illustrated in Figure 3.8, little or no affinity was shown for any of the class III calcium antagonists examined (lidoflazine, flunarizine and bepridil). It therefore seemed that this was a specific recognition site for spirodecanone butyrophenone compounds, such as fluspirilene, rather than a receptor site for a broader spectrum of agents.

### ***3.2.7. Comparative interaction of class III and other calcium antagonists at [<sup>3</sup>H] PN 200-110 and [<sup>3</sup>H] fluspirilene binding sites in skeletal muscle membranes.***

As fluspirilene appeared to possess characteristics of other class III calcium antagonists at [<sup>3</sup>H] DHP sites in brain, the availability of [<sup>3</sup>H] fluspirilene provided a means to investigate the interaction of calcium antagonists at potential [<sup>3</sup>H] fluspirilene binding sites. Experiments were carried out in an attempt to label specific binding sites in brain membrane homogenates. However, under a variety of different experimental protocols in cerebral cortex, specific binding could not be demonstrated. These experiments included the use of 0.5 mM EDTA throughout membrane preparations and assay incubations in case the binding was inhibited by divalent cations. Similarly, other experiments attempted to measure binding in the presence of divalent cations (Mg<sup>2+</sup> and Ca<sup>2+</sup> up to 5 mM) but were without success. In two preliminary experiments, in view of the high affinity expressed for striatal dopamine D<sub>2</sub> receptors, attempts were made to label dopamine D<sub>2</sub> receptors in rat striatal membranes under similar conditions to those used for [<sup>3</sup>H] spiperone. It was somewhat surprising that no specific binding of [<sup>3</sup>H] fluspirilene could be detected despite its high affinity for these sites. High affinity binding of [<sup>3</sup>H]

fluspirilene was, however, detected in rabbit skeletal muscle membranes. Examination of the pharmacology of this site with other calcium antagonists is shown in Table 3.12 and Figure 3.9. Fluspirilene displayed high affinity ( $pK_i$  9.04) for the site in agreement with the equilibrium dissociation constant 0.35 nM determined independently in saturation experiments ( $n=2$ ). The binding of [ $^3H$ ] fluspirilene was not inhibited by  $Cd^{2+}$  ions up to concentrations of 1mM. Dihydropyridine antagonists displayed low affinity for this site compared to their affinity for [ $^3H$ ] DHP sites, and the interaction appeared to be complex (Figure 3.9). The Hill slope for nitrendipine was consistently low (0.49,  $n=4$ ) with 92 % of the binding maximally inhibited at 10  $\mu$ M. The interaction appeared to be reciprocally similar to that of fluspirilene at the [ $^3H$ ] DHP in brain membranes. The low Hill slope was not significantly better fitted to a two site model and therefore suggested complex binding phenomena rather than heterogeneity of binding sites. The novel indolazine calcium antagonist, SR 33557, displayed nM affinity for this site and it displaced specific binding maximally with a Hill slope close to unity. All class III calcium antagonists examined displayed a much higher affinity for the [ $^3H$ ] fluspirilene site in skeletal muscle than at the [ $^3H$ ] DHP site in brain (Table 3.12). This higher affinity was nearly two log orders of magnitude for all compounds. Specific binding was maximally inhibited with Hill slopes close to unity for all class III compounds. These agents also showed higher affinity at the [ $^3H$ ] PN 200-110 site in skeletal muscle compared to brain, and fluspirilene was also more potent but displaced binding with a Hill slope close to unity. This observation with class III antagonists possibly reflects the differing extent to which the sites are coupled between tissues, such that the degree of allosteric control by other compounds is different between tissues at sites labelled by the same [ $^3H$ ] DHP ligand. All compounds studied (lidoflazine, flunarizine, bepridil, fluspirilene and RS 87476) displayed a similar rank order of potency for affinity at the various sites ([ $^3H$ ] fluspirilene / skeletal muscle > [ $^3H$ ] PN 200-110 / skeletal muscle > [ $^3H$ ] PN 200-110 / cerebral cortex; Figure 3.10). A feature of the interaction at the [ $^3H$ ] PN 200-110 binding site in skeletal muscle was the low Hill slopes displayed by all class III antagonists (with the exception of fluspirilene), all of which were not fitted significantly better to a two site model.

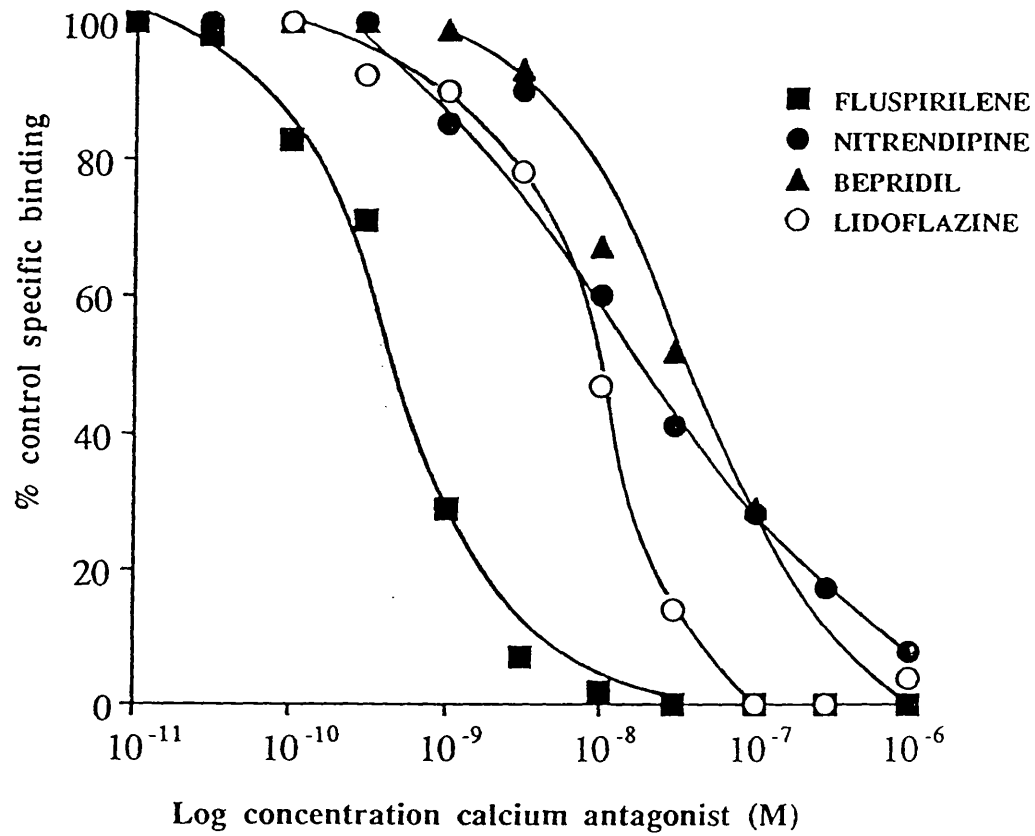


**Figure 3.9** Displacement of 0.1 nM [ $^3$ H] fluspirilene from rabbit skeletal muscle membranes by fluspirilene, nitrendipine, bepridil and lidoflazine.

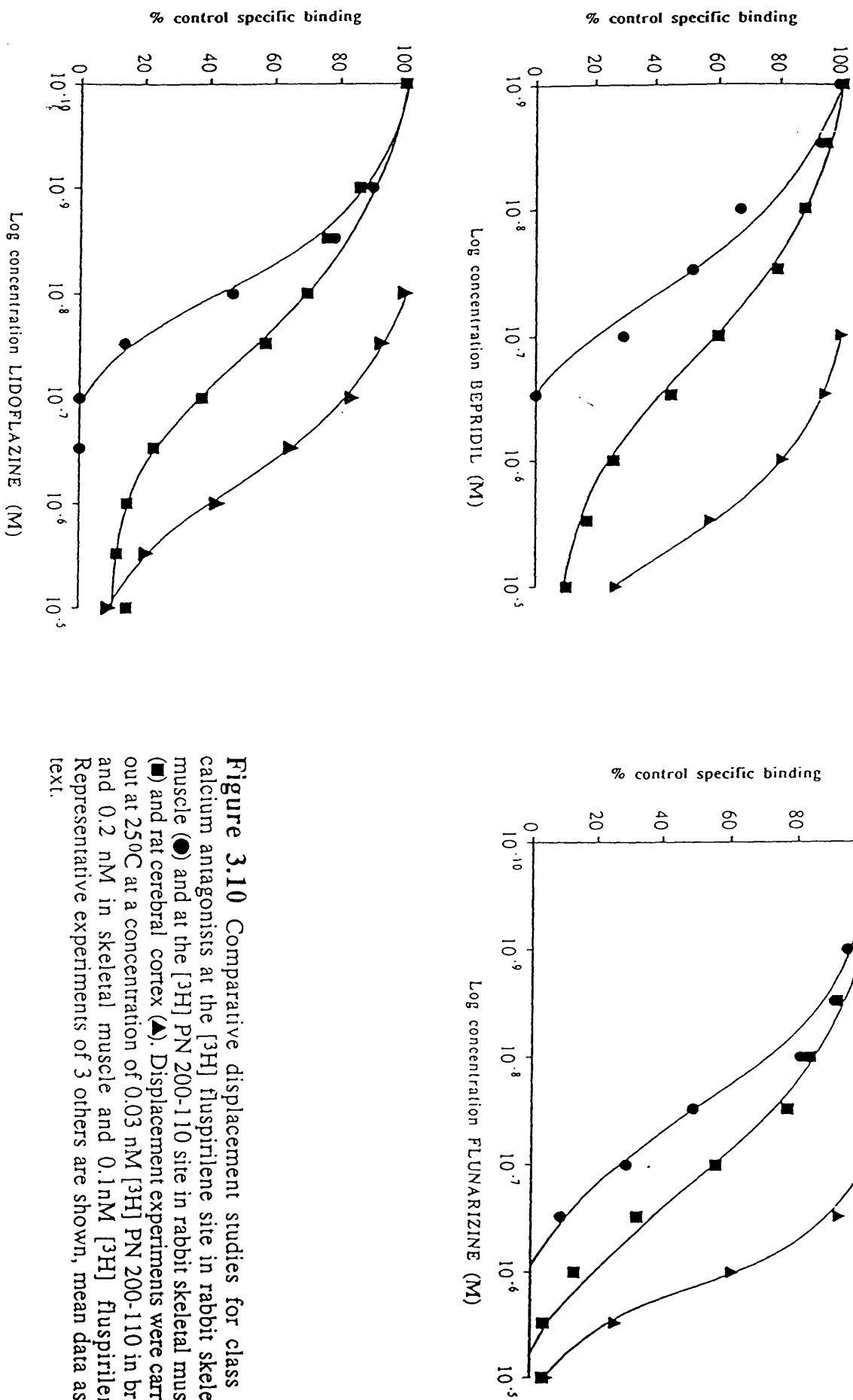


**Figure 3.10** Comparative displacement studies for class III calcium antagonists at the [ $^3\text{H}$ ] fluspirilene site in rabbit skeletal muscle (●) and at the [ $^3\text{H}$ ] PN 200-110 site in rabbit skeletal muscle (■) and rat cerebral cortex (▲). Displacement experiments were carried out at 25°C at a concentration of 0.03 nM [ $^3\text{H}$ ] PN 200-110 in brain and 0.2 nM in skeletal muscle and 0.1 nM [ $^3\text{H}$ ] fluspirilene. Representative experiments of 3 others are shown, mean data as in text.

COMPOUND	[ <sup>3</sup> H] PN 200-110		[ <sup>3</sup> H] fluspirilene	
	pKi	nH	pKi	nH
Nitrendipine	8.28 ± 0.13	1.02	6.53 ± 0.26	0.49 (*92)
SR 33557	9.31 ± 0.06	1.05	8.40 ± 0.20	0.92
Fluspirilene	8.29 ± 0.10	1.09	9.04 ± 0.1	1.12
Flunarizine	6.97 ± 0.05	0.84 (*95)	7.39 ± 0.19	0.99
Lidoflazine	6.99 ± 0.07	0.71 (*85)	7.92 ± 0.21	1.14
Bepridil	6.92 ± 0.24	0.69 (*67)	7.42 ± 0.08	0.96
RS 87476	6.82 ± 0.11	0.70 (*95)	7.63 ± 0.03	1.11

**Table 3.12.** Calcium antagonist affinity values at the [<sup>3</sup>H] PN 200-110 and [<sup>3</sup>H] fluspirilene binding sites in rabbit skeletal muscle membranes. Values represent pKi (mean ± s.e. mean of 3-4 determinations), nH is the Hill slope. Assays were carried out using 0.2 nM [<sup>3</sup>H] PN 200-110 and 0.1nM [<sup>3</sup>H] fluspirilene. (\*) is the maximal amount of displaceable specific binding at 10 μM.

### 3.3. Characterisation and identification of a novel high affinity binding site in rat cerebral cortex for [<sup>3</sup>H] SR 33557.

#### 3.3.1. *Effects at the [<sup>3</sup>H] PN 200-110 binding site in rat cerebral cortex*

In competition experiments SR 33557 inhibited [<sup>3</sup>H] PN 200-110 binding from rat cortical membranes with very high affinity ( $pK_i$   $9.60 \pm 0.10$ ,  $n=5$ ) and with a Hill slope close to unity. This potency was comparable to unlabelled dihydropyridines (Table 3.13). In the presence of  $Ca^{2+}$  the affinity of SR 33557 for the DHP site was reduced more than five fold ( $pK_i$  control  $9.54 \pm 0.04$ , and in the presence of 5 mM  $Ca^{2+}$   $pK_i$   $8.82 \pm 0.01$ ,  $n=4$ ). The potency of nitrendipine was not affected by this concentration of  $Ca^{2+}$  ( $pK_i$  values of 9.48 and 9.53 respectively). [<sup>3</sup>H] PN 200-110 saturation experiments in cerebral cortex carried out in the presence and absence of SR 33557 (Figure 3.11) indicated that the compound caused a decrease in binding affinity ( $K_d$ ) without any effect on binding density ( $B_{max}$ ). Similar findings were found with the unlabelled DHP nifedipine (control values  $K_d$   $0.029 \pm 0.008$  nM,  $B_{max}$   $221 \pm 20$  fmol/mg protein, and in the presence of 5.0 nM nifedipine  $K_d$   $0.17 \pm 0.02$  nM,  $B_{max}$   $196 \pm 6$  fmol/mg protein). These data are indicative of a competitive interaction at the [<sup>3</sup>H] PN 200-110 binding site for both classes of agent. Further confirmation of a competitive interaction at the [<sup>3</sup>H] DHP site was obtained from kinetic experiments as the rate of dissociation of [<sup>3</sup>H] PN 200-110 was not changed by the presence of SR 33557 at concentrations more than ten fold in excess of its  $K_i$  value (Figure 3.12). It has already been established earlier in this section that this is not the case for other classes of calcium antagonist at this site.

#### 3.3.2. *Comparative reversal of calcium antagonism by d-cis diltiazem*

The ability of d-cis diltiazem to allosterically increase the amount of specific [<sup>3</sup>H] DHP binding under certain experimental conditions (see Table 3.6 and Figure 3.6)

Figure 3.11

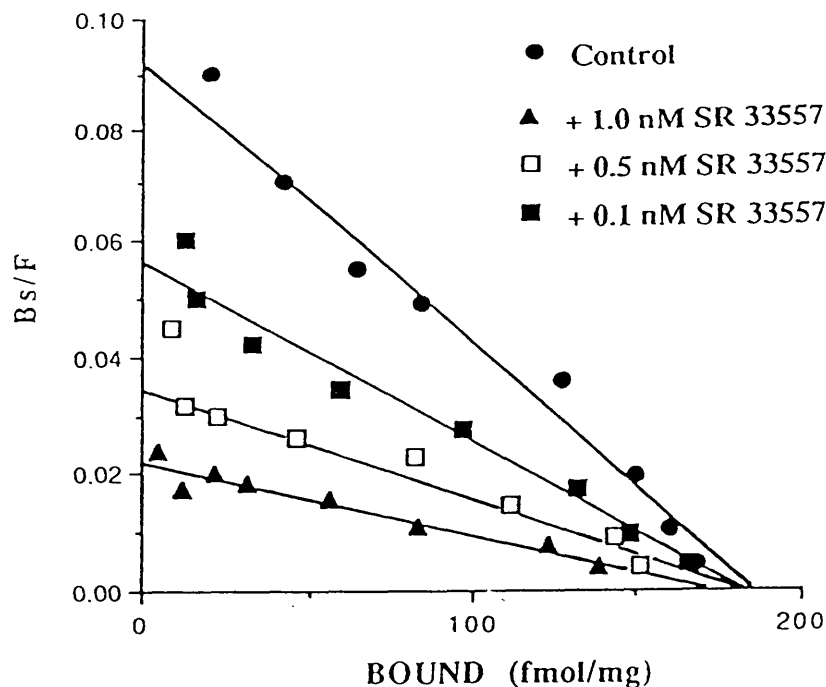
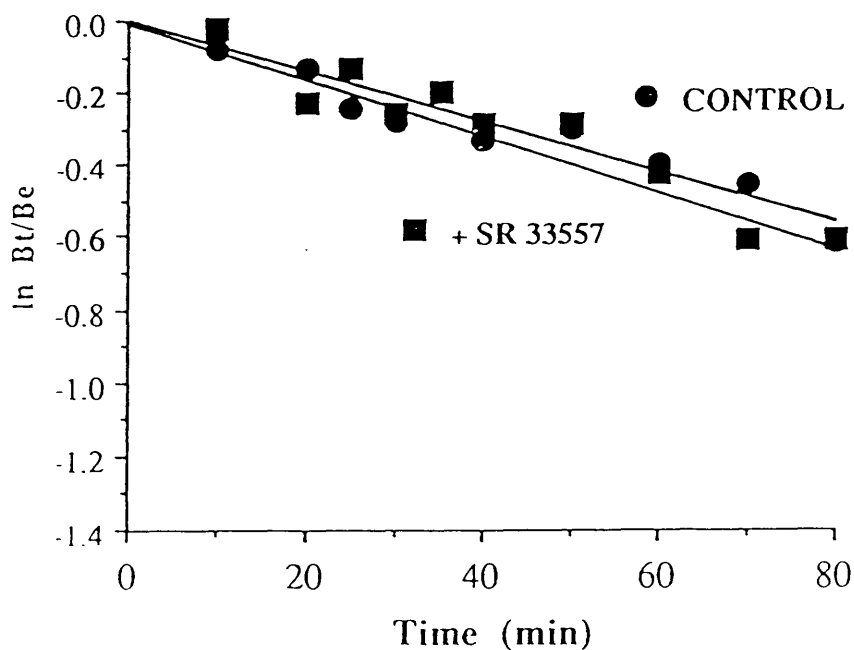


Figure 3.12



**Figure 3.11.** Scatchard transformation of [ $^3\text{H}$ ] PN 200-110 binding to rat cerebral cortex in the presence of SR 33557. Data from 4 experiments: control (●)  $K_d$   $0.04 \pm 0.006$  nM,  $B_{\text{max}}$   $186 \pm 5$  fmol/mg, (■) SR 33557 0.1 nM,  $K_d$   $0.09 \pm 0.004$ ,  $B_{\text{max}}$   $192 \pm 11$ , (□) SR 33557 0.5 nM,  $K_d$   $0.15 \pm 0.02$ ,  $B_{\text{max}}$   $193 \pm 16$ , (▲) SR 33557 1 nM,  $K_d$   $0.24 \pm 0.03$ ,  $B_{\text{max}}$   $188 \pm 12$ .

**Figure 3.12.** The effect of SR 33557 on the rate of [ $^3\text{H}$ ] PN 200-110 dissociation from rat cortex initiated by  $1 \mu\text{M}$  nitrendipine alone (control) or in the presence of 5 nM SR 33557. Data from 3 experiments. Control  $0.007 \pm 0.0009$   $\text{min}^{-1}$ , + SR 33557 (5 nM)  $0.006 \pm 0.001$   $\text{min}^{-1}$ .

provides a useful means of assessing the nature of the displacement [ $^3\text{H}$ ] DHPs resulting from other non-DHP calcium antagonists. In this series of experiments concentration effect curves were generated to d-cis diltiazem in rat cerebral cortex at 25°C using [ $^3\text{H}$ ] nitrendipine in the presence of other calcium antagonists. Figure 3.13 illustrates that the ability of d-cis diltiazem to reverse the inhibitory effects of calcium antagonism varied considerably across the range of antagonists studied. When examined at a single concentration of antagonist, it appeared that the inhibitory effects of SR 33557 were more readily reversed than those of fluspirilene and flunarizine. The inhibitory effects of nifedipine were not reversed (see Figure 3.14). A simple conclusion from these experiments would be that the reversal produced by d-cis diltiazem was dependent on the concentration of antagonist present throughout the experiment, and hence the initial amount of displaced binding. To test this hypothesis, experiments were carried out to compare the relative reversal produced by d-cis diltiazem using a range of concentrations of flunarizine and SR 33557. The results of these experiments are shown in Figure 3.14. The interaction of SR 33557 clearly differs from that of flunarizine on the basis of these experiments. Across a range of different concentrations causing different initial degrees of inhibition of [ $^3\text{H}$ ] DHP binding, it appeared that the extent to which the inhibition of specific binding was reversed by d-cis diltiazem was independent of the concentration of flunarizine used, such that the degree of reversal was the same regardless of the amount of binding initially displaced. In contrast, the reversal produced by diltiazem in the presence of SR 33557 was maximal at all concentrations, with reversal curves displaying a rightward shift with increasing concentrations of SR 33557. The results of these experiments suggested that the site of action of SR 33557 was different to those of DHPs. If SR 33557 exerted its effects directly at the DHP site, then diltiazem would be ineffective at reversing the inhibitory effects of SR 33557, as seen with nifedipine. Additional evidence that the effect of SR 33557 was not directly at the DHP site was the inhibitory effect of  $\text{Ca}^{2+}$  on the ability of SR 33557 to displace [ $^3\text{H}$ ] PN 200-110. However, as the interaction of SR 33557 was indistinguishable from competitive antagonism in a number of different tests, it would appear that the coupling between the two sites is very close.

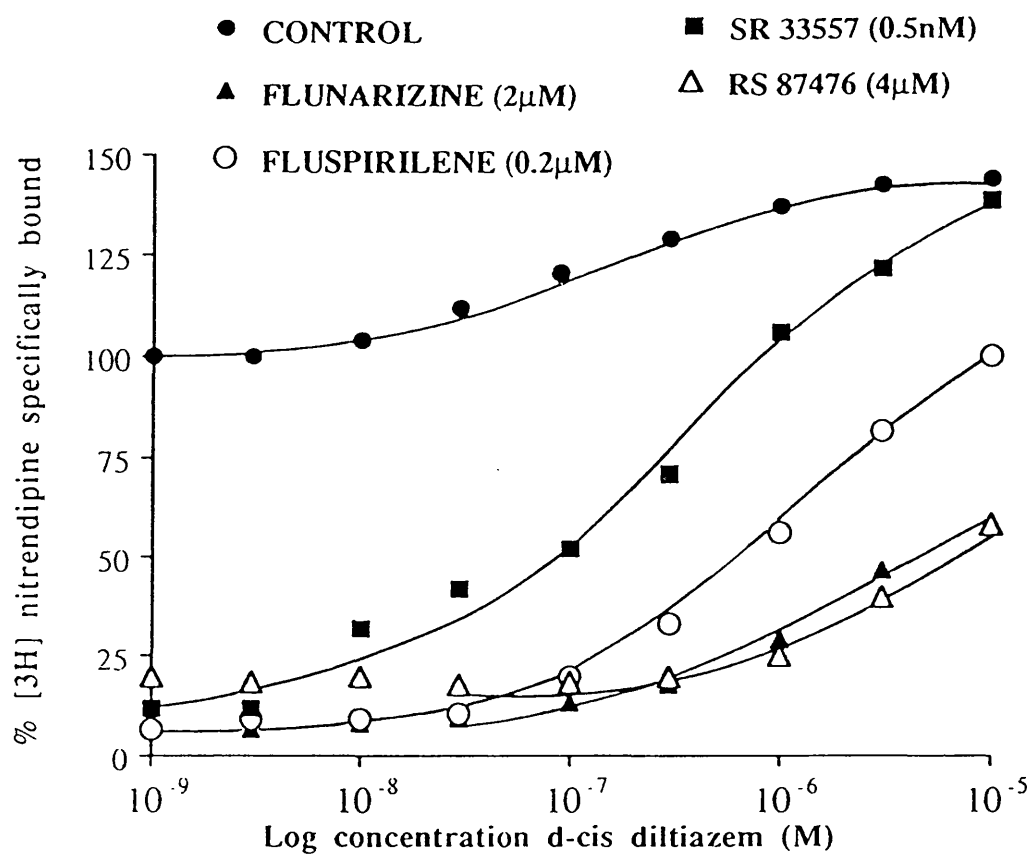


**Figure 3.13.** Comparative reversal by d-cis diltiazem of the inhibition of [3H] nitrendipine binding produced by flunarizine, fluspirilene, RS 87476 and SR 33557. Assays were carried out in rat cerebral cortex at 25°C and a representative experiment is shown.

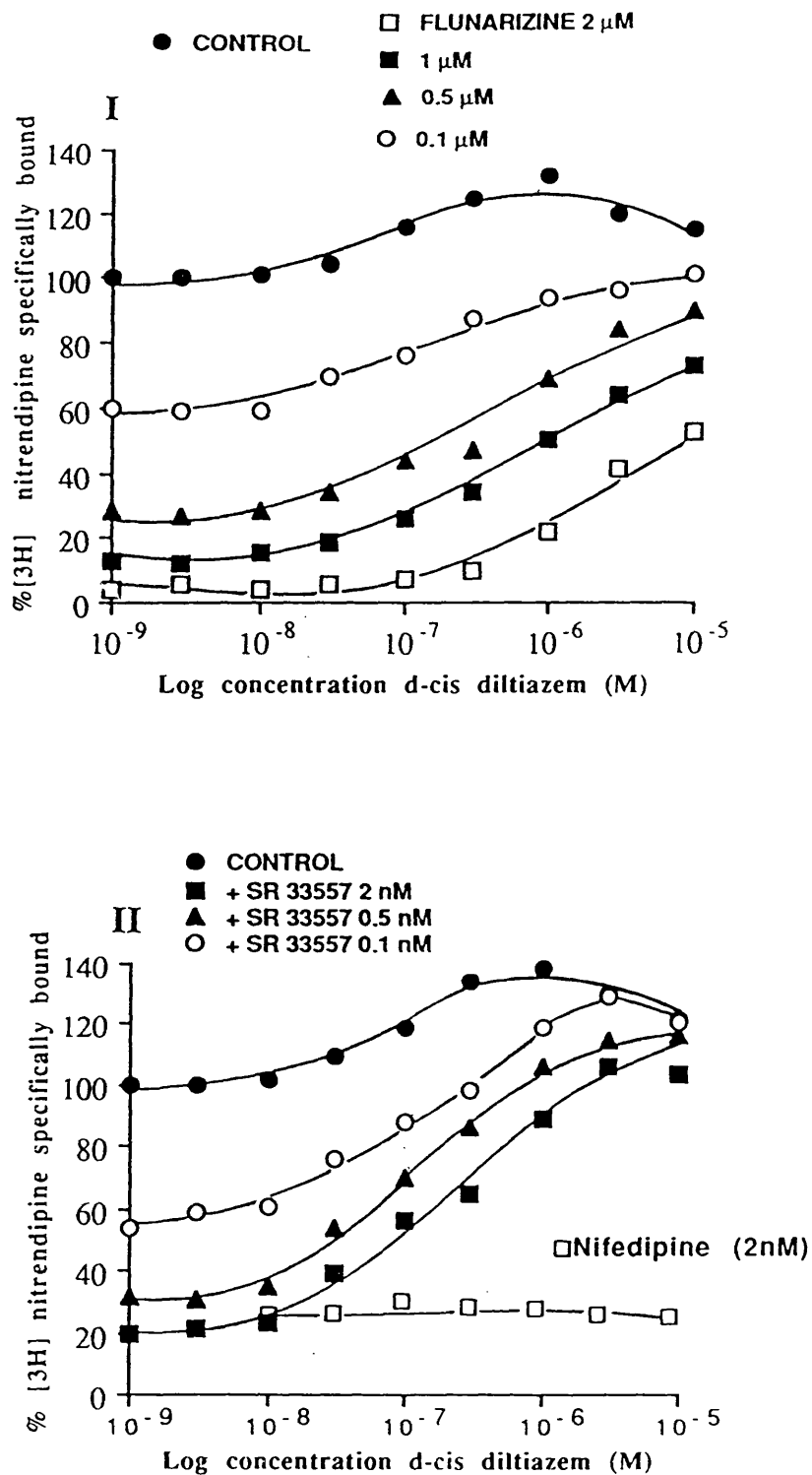


**Figure 3.14.** Comparative reversal by diltiazem of the inhibition of [3H] nitrendipine binding produced by I) flunarizine and II) SR 33557. Experiments were carried out in rat cortex at 25°C. A representative experiment of two others is shown.

### 3.3.3. [ $^3\text{H}$ ] SR 33557 binding to rat cerebral cortex membranes.

Initial saturation experiments carried out with [ $^3\text{H}$ ] SR 33557 (0.01-0.8 nM) indicated that the ligand labelled a single population of binding sites in rat cerebral cortex with high affinity ( $B_{\text{max}}$   $222 \pm 20$  fmol/mg protein,  $K_d$   $0.12 \pm 0.01$  nM,  $n=5$ ). Specific binding was saturable and reversible and at a ligand concentration equivalent to  $K_d$  amounted to 65-70 % of the total binding. Failure to include bovine serum albumin in the assay buffer and to pre-treat filters with polyethylenimine resulted in a very poor level of specific binding.

Kinetic studies of [ $^3\text{H}$ ] SR 33557 binding to rat cerebral cortex membranes indicated that when dissociation was initiated from equilibrium by the addition of  $1 \mu\text{M}$  SR 33557 the resulting first order dissociation rate was very rapid ( $K_{-1}$   $0.052 \pm 0.014 \text{ min}^{-1}$ ) in comparison to the observed pseudo first order association rate ( $K_{\text{obs}}$   $0.013 \pm 0.001 \text{ min}^{-1}$ ,  $n=4$ ) thus making a kinetic derivation of  $K_d$  impossible under this experimental protocol since:-  $K_1 = (K_{\text{obs}} - K_{-1}) / [L]$ , where  $[L]$  represents the total assay radioligand concentration.

These data indicated the presence of complex binding phenomena for [ $^3\text{H}$ ] SR 33557 since on the basis of dissociation data from the above experiments, specific binding would not be observed if  $K_{-1} \gg \text{true } K_{\text{obs}}$ . In light of these findings, preliminary saturation isotherms ( $n=2$ ) were carried out with [ $^3\text{H}$ ] SR 33557 over a wider range of ligand concentrations. Transformation of these data resulted in the detection of curvilinear Scatchard plots. The upwardly concave nature of these plots indicated several possibilities ; displaced non-specific binding, heterogeneity or the presence of multiple binding sites, or negative co-operativity between the sites. The fast dissociation rate induced by unlabelled SR 33557 would indicate negative co-operativity. To characterise this effect in more detail, the dissociation rate of [ $^3\text{H}$ ] SR 33557 was monitored under conditions where dissociation of the receptor complex was dissociated from equilibrium by infinite dilution. In these experiments a much slower rate of dissociation was observed than in the chase experiments

(Figure 3.15). In a non co-operative system it would be expected that using a protocol of infinite dilution, if the receptor sites bound the radioligand in question independently of each other, then the occupation of empty receptor sites occurring in the presence of excess unlabelled ligand would not influence the rate of dissociation of the radioligand. However, as can be seen in Figure 3.15 a marked difference was observed between the rate of dissociation in experiments where dissociation was initiated by infinite dilution alone, and those where infinite dilution was carried out in the presence of excess unlabelled SR 33557. These data strongly support the contention that negative co-operativity between the sites exists, since occupation of the sites with unlabelled ligand has the effect of decreasing the overall affinity of the receptor population resulting in an apparently rapid dissociation rate.

#### ***3.3.4. Pharmacological specificity for other calcium channel activators and antagonists***

Results from competition studies carried out with a range of calcium antagonists at the [ $^3\text{H}$ ] SR 33557 site in rat cerebral cortex are shown in Table 3.13. High affinity for this site is shown by SR 33557, although the Hill slope of 0.82 may be a reflection of the negative co-operativity observed in previous experiments. Both DHP activators and antagonists showed high affinity for the site, and the affinity and rank order for a range of calcium antagonists including benzothiazepines, phenylalkylamines and diphenylbutylpiperidines was remarkably close in comparison to that at the [ $^3\text{H}$ ] PN 200-110 binding site in the same tissue. A positive allosteric effect of diltiazem (comparative to its effects against [ $^3\text{H}$ ] nitrendipine in rat cortex under similar conditions) was not observed, and in all cases (with the exception of flunarizine) all agents displaced specific binding maximally.

#### ***3.3.5. Effect of inorganic ions.***

In contrast to the lack of effect on [ $^3\text{H}$ ] PN 200-110 binding in rat cerebral cortex

(low concentrations of divalent cations being a requisite for high affinity binding) all divalent cations tested appeared to inhibit [ $^3\text{H}$ ] SR 33557 binding in a concentration dependent manner.  $\text{Cd}^{2+}$  was a potent inhibitor of [ $^3\text{H}$ ] SR 33557 binding with an  $\text{IC}_{50}$  of  $0.026 \pm 0.015 \text{ mM}$  and the rank order of the other ions was  $\text{Cd}^{2+} > \text{Ca}^{2+} > \text{Mn}^{2+} > \text{Mg}^{2+}$ . The monovalent ion  $\text{Na}^+$  was inactive up to a concentration of 100 mM. The interactions of the cations was further evidence that the site for [ $^3\text{H}$ ] SR 33557 was distinct from other calcium antagonist binding sites, although the reciprocal coupling between the DHP and SR 33557 sites appeared to be very close.

Figure 3.15

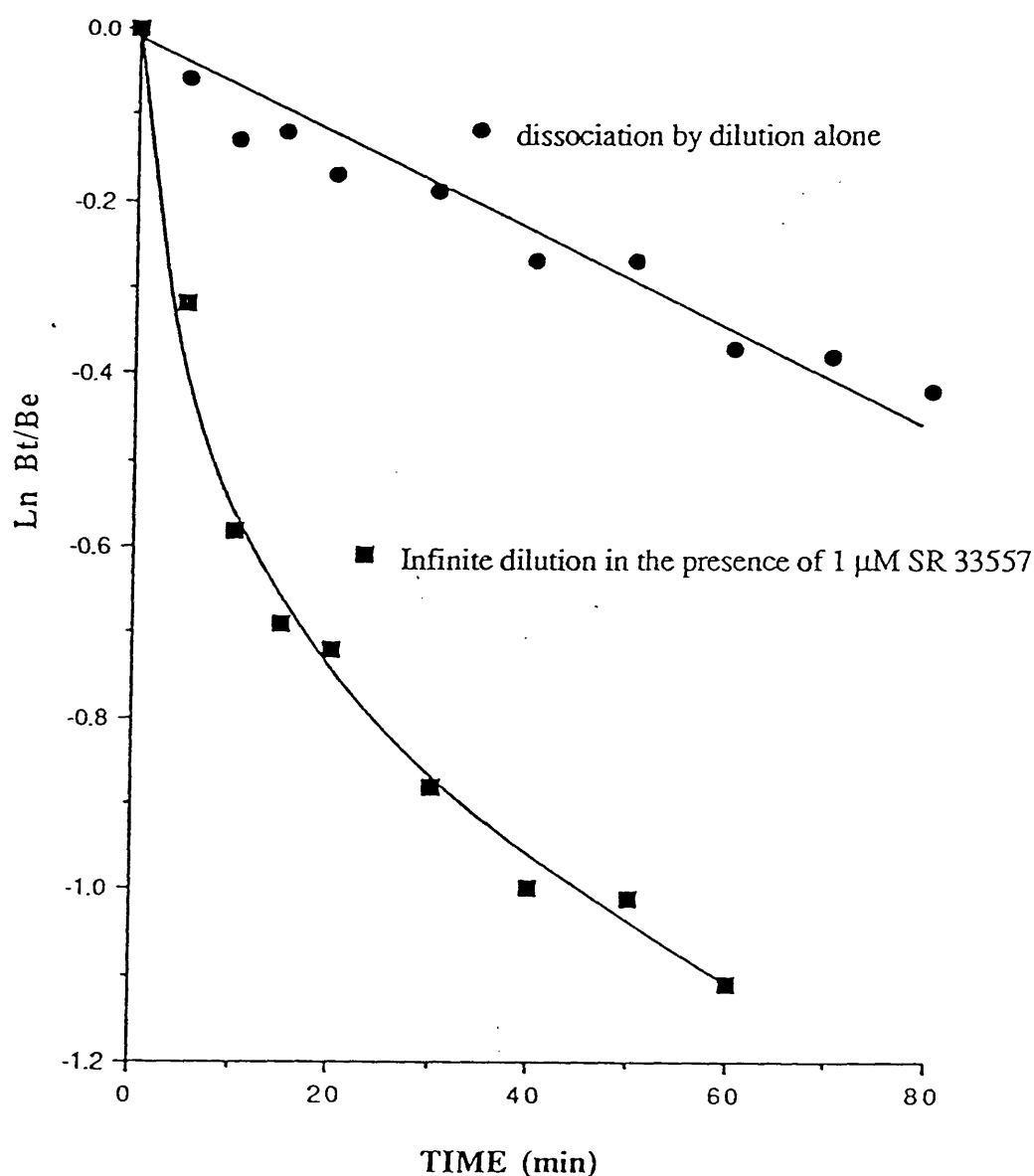


**Figure 3.15.** Comparative dissociation of  $[^3\text{H}]$  SR 33557 from rat cerebral cortex membranes at  $25^\circ\text{C}$  by different experimental protocols. Dilution was achieved by "infinite" dilution of a pre-equilibrated 30 ml assay volume (0.1 nM  $[^3\text{H}]$  SR 33557) into 3 litres of the same assay buffer. A parallel experiment was performed with the dilution buffer containing 1  $\mu\text{M}$  unlabelled SR 33557. Specific binding was determined by carrying out the same experiments with a non-specific pre-equilibrated mixture, which was subtracted from the total binding for each assay time point. To determine the binding at each time point 50 ml samples were removed from the diluted assay mixture and individually filtered over pre-treated Whatman GF/B filters (see methods). The experiment shown is representative of two others.

**i**

	<b>[<sup>3</sup>H] SR 33557</b>		<b>[<sup>3</sup>H] PN 200-110</b>	
<b>COMPOUND</b>	<b>pKi</b>	<b>nH</b>	<b>pKi or pIC<sub>50</sub></b>	<b>nH</b>

COMPOUND	pKi	nH	pKi or pIC <sub>50</sub>	nH
SR 33557	9.60 ± 0.10	0.82	9.54 ± 0.04	1.00
Nitrendipine	9.48 ± 0.14	0.90	9.67 ± 0.15	0.94
BAY K 8644	8.23 ± 0.17	0.87	8.43 ± 0.20	0.96
Fluspirilene	8.13 ± 0.17	0.87	7.69 ± 0.02	0.66*
D-600	8.09 ± 0.02	0.92	not determined	
Verapamil	7.97 ± 0.03	0.98	7.69 ± 0.09	0.92(*42)
D-cis-diltiazem	7.47 ± 0.09	0.93	7.58 ± 0.13	1.00 (*37)
Flunarizine	7.15 ± 0.14	1.06 (*92)	6.10 ± 0.20	1.28 (*92)
Lidoflazine	7.14 ± 0.11	0.82	6.44 ± 0.06	0.84 (*90)

**ii**

	<b>IC<sub>50</sub> (mM)</b>
--	-----------------------------

Cd <sup>2+</sup>	0.026 ± 0.015
Ca <sup>2+</sup>	2.09 ± 0.48
Mn <sup>2+</sup>	5.01 ± 0.7
Mg <sup>2+</sup>	11.06 ± 1.1
Na <sup>+</sup>	>100

**Table 3.13. i)** Comparative affinity values at the [<sup>3</sup>H] DHP and [<sup>3</sup>H] SR 33557 site in rat cerebral cortex for a range of calcium antagonists. Values represent the mean ± s.e. mean of 4-6 experiments. Competition curves were generated using at least 12 concentrations of competing drug in duplicate. Experiments were performed as described in methods using 0.03nM [<sup>3</sup>H] PN 200-110 and 0.1 nM [<sup>3</sup>H] SR 33557. Values represent pKi or \*pIC<sub>50</sub> where inhibition of binding is incomplete or nH <1.0 (\*maximal inhibition at 10 μM).

**ii)** Affinity values for inorganic cations at the [<sup>3</sup>H] SR 33557 site. Ions were present as their chloride salts and values represent mean ± s.e.mean of 3 separate experiments.

### 3.4 Discussion.

#### 3.4.1. Allosteric aspects of [ $^3\text{H}$ ] DHP binding.

In this chapter, high affinity binding of several [ $^3\text{H}$ ] calcium antagonists has been demonstrated and the interaction of a range of calcium antagonists at these sites has been characterised to provide a differentiation between these agents on an *in vitro* basis. The binding of [ $^3\text{H}$ ] DHP ligands to brain tissue homogenates is now well documented (Yamamura *et al.*, 1982; Murphy *et al.*, 1983; Lee *et al.*, 1984; Supavilai & Karobath., 1984; Glossmann *et al.*, 1985) and these findings have been confirmed in the present work using [ $^3\text{H}$ ] PN 200-110.

This ligand has been used because it binds with very high affinity to the inactivated state of the channel, and it exhibits low levels of non-specific binding. In rat brain membrane homogenates, the hippocampus and cerebral cortex showed the highest density of sites, and previous autoradiography studies with [ $^3\text{H}$ ] PN 200-110 have confirmed this in detail, with particular high binding densities associated with neuronal sites (demonstrated by colchicine lesioning) detected in the molecular layer of the dentate gyrus, CA1 and CA3 regions of hippocampus, and neo and frontoparietal areas of the cerebral cortex (Cortes *et al.*, 1984). Radioligand binding studies with various [ $^3\text{H}$ ] DHP ligands have demonstrated that binding properties differ between tissues (Ferry *et al.*, 1985). Thus, skeletal muscle homogenates have been demonstrated to possess the highest density of [ $^3\text{H}$ ] DHP sites yet reported (Glossmann & Ferry, 1985; Lazdunski *et al.*, 1988), however the sites are labelled with lower affinity than in brain by [ $^3\text{H}$ ] DHP antagonists. The results in this study are also consistent with such findings, as the affinity of [ $^3\text{H}$ ] PN 200-110 was ten fold lower in skeletal muscle than in brain tissues. Thus, a spectrum of affinities exists for different [ $^3\text{H}$ ] DHP ligands: different ligands have different affinities for apparently the same site, and the affinity of these sites differs between different tissue homogenates. How do these effects occur?

The affinity of any radioligand (the equilibrium dissociation constant) ultimately depends on the rate of association and the rate of dissociation of a radioligand from the

receptor. For [ $^3\text{H}$ ] DHP antagonists to have different affinities, these constants must vary between tissues. Based on data obtained in the present studies, differences in these constants may have a significant effect on the relative allosterism of [ $^3\text{H}$ ] DHP ligands by class II calcium antagonists (diltiazem, verapamil and diltiazem). That these agents modify [ $^3\text{H}$ ] DHP binding is well documented (Yamamura *et al.*, 1982; Galizzi *et al.*, 1984; Glossmann & Ferry, 1985; Mir & Spedding, 1987). Some conflicting results have been obtained in that the binding of diltiazem and verapamil might be to a single site (Murphy *et al.*, 1983; Galizzi *et al.*, 1986a) or different sites, although kinetic studies (Ferry *et al.*, 1985; Balwierczak *et al.*, 1987) clearly demonstrated that these receptors are distinct, but allosterically coupled to the DHP site (Glossmann *et al.*, 1985; Schoemaker & Langer, 1989). The respective sites for verapamil and diltiazem are also coupled to each other negatively (Galizzi *et al.*, 1985; Ferry *et al.*, 1985; Mir & Spedding, 1987; Schoemaker & Langer, 1989) but they modify [ $^3\text{H}$ ] DHP binding in a negative and positive manner. Thus occupation of one site causes a conformational change in other sites as originally proposed (Glossmann *et al.*, 1982) and now well established.

In competition experiments, verapamil inhibits binding incompletely and it has been shown that d-cis diltiazem can enhance or increase the amount of specific binding. In brain tissue homogenates this has been explained on the basis that diltiazem decreases the dissociation rate constant, thereby increasing the affinity of the radioligand. In some tissues, notably with radioligands of lower affinity, this effect has been attributed to a change in Bmax (Glossmann & Ferry, 1985). In the present work, verapamil has been demonstrated to be negatively allosteric under a variety of experimental conditions with different ligands, different tissues and different temperatures. However, data obtained with d-cis diltiazem in the present study is not entirely consistent with previously reported findings (e.g. Yamamura *et al.*, 1982; Lee *et al.*, 1984; Glossmann & Ferry, 1985; Mir & Spedding, 1987). That the effect of diltiazem is positively allosteric is suitably explained on the basis of a decrease in the dissociation rate constant, where in nearly all reported cases an enhancement of specific binding had occurred. However, the present studies have demonstrated an inhibition of specific [ $^3\text{H}$ ] PN 200-110 binding at 25°C in rat cerebral

cortex. Similar inhibitory findings for other ligands have been reported on the basis of thermodynamic properties, such that inhibitory effects of diltiazem predominated only at low (40°C) temperatures (e.g. Mir & Spedding, 1987). How is it then that under conditions where d-cis diltiazem decreased the dissociation rate constant, inhibition of binding was still observed? In this case the effect of diltiazem cannot be explained on the basis of dissociation rates alone, and an interaction with the association rate must be implied. Thermodynamically, such effects appear to be balanced, so that in cases where an enhancement of binding occurs, effects of dissociation might predominate, with effects on association increasing at lower temperatures, causing a net decrease in binding in competition studies. Thus, as association and dissociation rates also differ for ligands between tissues, and these effects are also thermodynamically dependent, inhibitory effects of diltiazem were observed against [<sup>3</sup>H] PN 200-110. Furthermore, in this series of experiments it was possible to demonstrate inhibitory effects with trans-diclofurime at all temperatures with [<sup>3</sup>H] PN 200-110 in skeletal muscle, when previously these had only been demonstrated with other [<sup>3</sup>H] DHP ligands in brain at low temperatures (Mir & Spedding, 1987). Clearly in this case, effects on association predominate. Overall, it seems apparent that [<sup>3</sup>H] DHP ligands appear to be more susceptible to allosteric control when bound with low affinity, a property that can be illustrated experimentally with different tissues (see Figure 3.5).

It is noteworthy that whilst the effects of these compounds can be differentiated on the basis of allosteric interactions, functional correlates are poor, since the effects of diltiazem, verapamil and diclofurime appear to be functionally similar. Similar potency is expressed in cardiac and K<sup>+</sup> depolarised smooth muscle (Spedding, 1983; Fleckenstein, 1988). Differentiation between calcium antagonists based on surface charge effect, when measured against Ca<sup>2+</sup> dependent contractions in partially depolarised taenia are also similar (Spedding, 1985a). Only two reported studies have shown that diltiazem can enhance the activity of DHPs. The compound has been claimed to enhance the antiseizure activity of nimodipine (Moron *et al.*, 1989) and potentiate the negative inotropic effect of nimodipine in the heart (Depover *et al.*, 1983).

### 3.4.2. Activators at the [ $^3\text{H}$ ] DHP site.

DHP activators and antagonists have been reported to exert their effect from an interaction at the same site as demonstrated in functional studies (Schramm *et al.*, 1983; Spedding & Berg, 1984) electrophysiological studies (Sanguinetti *et al.*, 1986) and radioligand binding studies (Janis *et al.*, 1984; Sarmiento *et al.*, 1987; Rampe *et al.*, 1987; Triggle & Rampe, 1989.). Some possible differences in their mechanism of interaction may exist based on thermodynamics (Maan & Hosey, 1987) and the affinity state according to membrane potential (Kokubun *et al.*, 1986). Other studies, restricted to cardiac membrane preparations or intact cardiac cells, have demonstrated the binding of [ $^3\text{H}$ ] Bay K 8644 directly, consistent with an interaction at the DHP site (Janis *et al.*, 1984, Maan & Hosey, 1987; Ferrante *et al.*, 1989). It has been claimed that a lower affinity state for Bay K 8644 may exist (Lee *et al.*, 1987), although other workers have claimed that lower affinity sites are not related to  $\text{Ca}^{2+}$  channels (Sarmiento *et al.*, 1987)

In electrophysiological experiments, previous studies have indicated that the inhibitory effects of DHP antagonists on  $\text{Ca}^{2+}$  currents were found to be converted to agonist-like responses in the presence of GTP analogues (Scott & Dolphin, 1987), thus implying a role for G proteins in the regulation of DHP mediated interactions at the L channels. These findings are not entirely consistent, as other experiments have not confirmed a pertussis toxin-sensitive G protein involvement in the inotropic response mediated by Bay K 8644 in cardiac myocytes (Anderson *et al.*, 1990), although differences may exist between these channels in neurones and the myocardium.

In the present studies, GppNHp (a stable, non-hydrolysable GTP analogue) or GTP *per se* did not modify the affinity of the nature of the interaction of Bay K 8644 with the [ $^3\text{H}$ ] DHP antagonist binding site. Modifications of the interaction of Bay K 8644 with the [ $^3\text{H}$ ] DHP antagonist binding site in the presence of GTP analogues has been reported (Bergamaschi *et al.*, 1988) in that the ability of Bay K 8644 to displace [ $^3\text{H}$ ] DHP binding from synaptosomal preparations was potentiated in the presence of GppHHp, an

effect that was pertussis toxin-sensitive. This conclusion was based on an increased displacement of [ $^3\text{H}$ ] DHP binding caused by Bay K 8644 at two selected data points, and no evidence was presented by the authors of a change in affinity or nature of interaction of the agonist. Such an effect could arise from the chelation of divalent cations by GTP analogues as described (Glossmann *et al.*, 1982), and this alone would decrease [ $^3\text{H}$ ] DHP binding such that the observed increase in displaced binding in the presence of these analogues could be misinterpreted. It has been reported that differences in membrane potential have marked effects on [ $^3\text{H}$ ] DHP antagonist binding properties (Lee *et al.*, 1987) and a lesser effect on agonist binding (Lee *et al.*, 1987 ; Triggle & Rampe, 1989). These findings do not account for the proposed effects of Bay K 8644, as synaptosomal preparations will exist in a more polarised state than membrane fractions, and under such conditions activator DHPs have been shown to potentiate [ $^3\text{H}$ ] DHP antagonist binding (Kokubun *et al.*, 1986). The ability of G protein analogues to cause a decrease in the affinity of Bay K 8644, as demonstrated at the [ $^3\text{H}$ ] nimodipine site in smooth muscle (Higo *et al.*, 1988), might therefore be a reflection of relative agonist/antagonist properties of [ $^3\text{H}$ ] nimodipine compared to [ $^3\text{H}$ ]PN 200-110. (Ferry *et al.*, 1985) .

#### 3.4.3. *Endogenous activators*

There is now considerable evidence that L-type  $\text{Ca}^{2+}$  channels can be activated by endogenously occurring substances. The best characterised of these is the lipid metabolite, palmitoyl carnitine. This naturally occurring metabolite shows a seventy fold accumulation in the cytosol and sarcolemma of hearts following myocardial ischaemia (Corr *et al.*, 1984; Knabb *et al.*, 1986). In myocyte preparations, accumulation of acyl carnitines produce marked electrophysiological changes following experimentally induced hypoxia (Knabb *et al.*, 1986) and in functional myocytes, palmitoyl carnitine has been shown to resemble the ionotropic effect of Bay K 8644 in causing an enhancement of edge movement in beating aggregates (Patmore *et al.*, 1989a). In these latter experiments, palmitoyl carnitine was capable of selectively reversing the negative inotropic effects of Class I and II calcium

antagonists, consistent with other *in vitro* actions of Bay K 8644 (Spedding & Berg, 1984; Spedding, 1985a; 1985b), thus providing evidence for a direct action on calcium channel function mediated by the DHP site. Furthermore, also consistent with an action similar to Bay K 8644, palmitoyl carnitine has been shown to activate calcium channels in smooth muscle directly (Spedding & Mir, 1987). At high concentrations, acyl carnitines have detergent properties (Adams *et al.*, 1979), although the interaction of palmitoyl carnitine at VOCs has been considered selective, firstly, because it interacts with [ $^3\text{H}$ ] calcium antagonist binding sites at concentrations lower than at other receptor sites, and secondly, because other surface active molecules did not mimic the effects of palmitoyl carnitine in smooth muscle (Spedding & Mir, 1987).

The results from the present experiments strongly suggest that the apparent activation of VOCs does not arise from an interaction at the DHP site. Displacement experiments with palmitoyl carnitine at the [ $^3\text{H}$ ] PN 200-110 site in rat cortex revealed a higher potency than previously described (Spedding & Mir, 1987), although the inhibition of binding did not appear to be competitive. Hill slopes for all acyl carnitines were steep and the apparent affinity increased as a function of chain length. This would be consistent with the inhibition of binding arising due to a disturbance in membrane integrity rather than direct inhibition of binding. These effects would have a tendency to be all or none, thus resulting in steep Hill slopes. Further confirmation of these effects was obtained in kinetic experiments, where palmitoyl carnitine at a concentration similar to that producing 50% effectiveness in other experiments (Spedding & Mir, 1987; Patmore *et al.*, 1989a) caused immediate and complete inhibition of the [ $^3\text{H}$ ] DHP receptor complex at equilibrium. This finding may explain the inhibitory effects of palmitoyl carnitine at other types of [ $^3\text{H}$ ] calcium antagonist binding site, especially the increased potency against [ $^3\text{H}$ ] verapamil (Spedding & Mir, 1987) as this site is susceptible to changes in membrane integrity caused by a variety of modulatory factors (Spedding, 1984; Galizzi *et al.*, 1985; Glossmann & Ferry, 1985). The finding that the interaction of palmitoyl carnitine is not directly at the VOC is consistent with more recent findings (see Spedding & Patmore, 1990) in which it has been demonstrated that the inotropic effects of the agent resulted from the mobilisation

of intracellular  $\text{Ca}^{2+}$ . This interaction would appear to be at the level of the sarcoplasmic reticulum since this effect of palmitoyl carnitine was blocked by ryanodine.

However, since deleterious effects on calcium channel function may be a consequence of accumulation of acyl carnitines in cells following ischaemia, and that exposure to palmitoyl carnitine was without effect on [ $^3\text{H}$ ] DHP receptor binding parameters was surprising. This was particularly so for myocardial sites, since previous studies had shown that both [ $^3\text{H}$ ] verapamil sites (Dillon & Nayler, 1987) and [ $^3\text{H}$ ] DHP sites (Nayler *et al.*, 1985; Gu *et al.*, 1988; Van Amsterdam *et al.*, 1990) were modified following myocardial ischaemia. Myocardial  $\alpha_1$  adrenoceptors are also modified following ischaemia associated with increased levels of long chain acyl carnitines (Heathers *et al.*, 1987; Corr *et al.*, 1987). Might the lack of effect on [ $^3\text{H}$ ] DHP sites be due to inappropriate conditions ? This would not appear to be the case, as results from this work have shown that up-regulation of  $\alpha_1$  adrenoceptors does occur following exposure to relatively low concentrations of palmitoyl carnitine. That the effect was selective for myocardial  $\alpha_1$  adrenoceptors (with no effect on  $\beta_1$  or other  $\alpha_1$  adrenoceptor populations) suggests that this effect may be consequent to a change in sarcolemmal fluidity exposing cryptic  $\alpha_1$  sites, since other studies from our laboratory have shown that  $\alpha_1$  adrenoceptors increase in the same tissue following *in vivo* ischaemia (Allely & Brown, 1988). Such a mechanism does not appear to regulate the density of [ $^3\text{H}$ ] DHP sites *in vitro*.

#### 3.4.4. Interactions of class III antagonists

The interaction of antagonists not belonging to class I and II groups were initially characterised at [ $^3\text{H}$ ] DHP binding sites by Murphy *et al.* (1983). It was concluded that a common site existed for these agents, allosterically coupled to the DHP site, since these compounds increased the rate of [ $^3\text{H}$ ] DHP dissociation and D-600 and verapamil were capable of reversing their inhibitory effects at the [ $^3\text{H}$ ] DHP binding site. Thus a unified model for the regulation of [ $^3\text{H}$ ] DHP binding was proposed.

It has been discussed above that the binding sites for class II agents appear to be

distinct but allosterically coupled. The interaction of class III agents is generally less well defined. Identification of this group of agents as calcium antagonists was made almost as early as the concept itself, and the agents were classified separately because they were less potent and less specific as calcium antagonists (Spedding, 1982; Fleckenstein, 1983) although several neuroleptics of this class were subsequently identified as potent inhibitors of [ $^3\text{H}$ ] DHP binding (Gould *et al.*, 1983; Quirion *et al.*, 1985). *In vitro* studies have shown that, unlike all other calcium antagonists, the effects of class III agents are not reversed by Bay K 8644 (Spedding & Berg, 1984; Spedding, 1985a; Patmore *et al.*, 1989b). If Bay K 8644 exerts its effect through the DHP site, the effects of these agents must be through potent antagonism of Bay K 8644 or through an action at another site, closely coupled to the calcium channel, such that their antagonistic effects are not readily reversed by DHP activators.

Results from the present work indicates that the site of action of class III antagonists is distinct from the DHP site, but results in the DHP site becoming less susceptible to allosteric regulation from other sites as observed with diltiazem. Previously, a precise definition of the interaction of these agents has been precluded because it has not been possible to identify a binding site directly with [ $^3\text{H}$ ] class III drugs. It was therefore of interest that a postulated fourth site on the channel was identified in skeletal muscle membranes for fluspirilene (Galizzi *et al.*, 1986b; Qar *et al.*, 1987), as this diphenylbutylpiperidine molecule is closely related to other class III compounds (Spedding, 1985).

Based on *in vitro* experiments (Fraser *et al.*, 1988), fluspirilene has been shown to be a weak antagonist of  $\text{Ca}^{2+}$  induced contractions in smooth muscle and a potent non-competitive antagonist of Bay K 8644. Furthermore, we were able to demonstrate selective inhibition of the activator effects of Bay K 8644 and CGP 2390 by fluspirilene, without any effect on the tissue sensitivity to calcium or the inhibitory effects of DHP antagonists (Kenny *et al.*, 1990). At the [ $^3\text{H}$ ] DHP site in rat cortex, the low Hill slope in competition experiments, the effects on  $B_{\text{max}}$  and  $K_d$  in saturation studies, and the increase in dissociation rate in kinetic studies indicated a non-competitive, negatively allosteric

interaction of fluspirilene. Some aspects of this non-competitive interaction of fluspirilene have been reported (Qar *et al.*, 1987). Taken together these data indicate that the site for fluspirilene is distinct from the DHP site. The conclusion drawn from functional and binding data is that the site for fluspirilene is allosterically linked to the DHP-site, but tightly coupled to the channel, perhaps inducing a conformation such that the effects of calcium channel activators are more readily suppressed than antagonists. It is unlikely that fluspirilene prevents the binding of Bay K 8644 but not other DHPs as evidence suggests that all agents in this class bind to the same site but stabilise different states of the channel. Furthermore, the binding site for Bay K 8644 responsible for antagonist effects appears to be to the inactivated state (Bellmann, 1984; Lee *et al.*, 1987). It has been reported that the mechanism of agonist and antagonist interaction may be different (Maan & Hosey, 1987). However, the interaction of fluspirilene with [<sup>3</sup>H] DHP activators has not been described to date.

Under a range of experimental conditions, a binding site for fluspirilene could not be detected in cortical membranes, although specific binding has been demonstrated in skeletal muscle and cardiac sarcolemmal membranes (Galizzi *et al.*, 1986b; Qar *et al.*, 1987; King *et al.*, 1989) consistent with a distinct but allosterically coupled binding site. If the stoichiometry of all these sites is 1:1 (King *et al.*, 1989; Garcia *et al.*, 1990) it would be expected to label the same sites in brain, as the density of other sites is sufficient to be labelled by other [<sup>3</sup>H] calcium antagonists (e.g. Mir & Spedding, 1987). However, only the three prototypical binding sites for DHPs, phenylalkylamines and benzothiazepines have thus far been demonstrated in brain tissue, and in skeletal muscle and sarcolemmal membranes a complicated picture is emerging with at least six specific sites having been claimed (Lazdunski *et al.*, 1988; King *et al.*, 1989; Garcia *et al.*, 1990), although the site for bepridil, diltiazem and verapamil has been suggested to be the same based on competitive interactions (Galizzi *et al.*, 1986a).

In the present work, all class III antagonists displayed high affinity for the [<sup>3</sup>H] fluspirilene site in skeletal muscle. This affinity has previously been confirmed for bepridil and pimozide (Galizzi *et al.*, 1986b; Lazdunski *et al.*, 1988). Fluspirilene would therefore appear to be a prototypical agent for this class of drug. The effects of DHP compounds at

the [<sup>3</sup>H] fluspirilene site has not been previously reported, although the data in the present work indicates that the sites are weakly and negatively coupled. It is interesting to note that some class III agents have previously been shown to possess lower affinity for DHP sites in the heart compared to brain (Quirion *et al.*, 1985) whilst in this work higher affinity (albeit with a complex interaction) has been shown for the DHP site in skeletal muscle compared to brain. Furthermore, all compounds show a very similar profile at the [<sup>3</sup>H] DHP and [<sup>3</sup>H] fluspirilene site in brain and skeletal muscle (see Figure 3.10). Do these findings represent differences in absolute affinity?

Class III antagonists are lipophilic agents (Rodenkirchen *et al.*, 1982; Spedding, 1985b; Carvalho *et al.*, 1989). *In vitro* studies have shown that these agents are susceptible to membrane surface charge effects and the slow onset time for these agents *in vitro* and *in vivo* may be representative of membrane accumulation effects, such that the observed effects might be due to interactions with calmodulin or membrane stabilisation properties (Spedding, 1985b). Spedding (1985a) suggested that membrane accumulation effects may account for the selectivity of some of these agents for small rather than large artery preparations. It has also been shown (Pang & Sperelakis, 1983) that some calcium antagonists accumulate inside cardiac and smooth muscle cells. The same group (Pang & Sperelakis, 1984) also demonstrated that this effect was directly related to lipid solubility. The uptake of these compounds may be particularly high in smooth muscle preparations since Carvalho *et al.* (1989) demonstrated that the presence of membrane proteins increases the amount of membrane accumulation of these compounds. It might be anticipated that such differences exist in different membrane preparations. Calcium antagonists display a range of K<sub>p</sub>s (membrane partition coefficients). For flunarizine in cortical synaptic plasma membranes, this value is 23,000 and thus for most calcium antagonists the relevant concentration in the membrane phase effective at the binding site may be many orders of magnitude higher than in the aqueous phase (see Mason *et al.*, 1991) and this interaction may also represent ionic interactions in the membrane phase (Mason *et al.*, 1989). Thus, the concentrations of drug in the membrane measured at apparent nM K<sub>d</sub> values may be closer to 1 μM, and for some compounds with extremely

high  $K_p$  values, such as amlodipine, the apparent  $K_d$  might be even higher (Mason *et al.*, 1991). Glossmann and co-workers (Boer *et al.*, 1989) have postulated that true  $K_d$  values may be inversely proportional to  $K_p$  for DHP compounds, since partitioning into the plasma membrane bilayer depletes the active drug available for receptor binding (presumably by an aqueous route). However for DHP compounds, Rhodes *et al.* (1985) demonstrated that the membrane approach was three orders of magnitude higher than the aqueous approach for receptor binding. Therefore, it is possible that higher affinity is shown by lipophilic class III agents for DHP binding sites in skeletal muscle compared to brain membranes due to a larger amount of membrane accumulation.

Furthermore, in this series of experiments, an ionic interaction for this class of agent was demonstrated (see Table 3.7). Spedding (1984; 1985a, 1985b) demonstrated that inhibitory aspects of this group of compounds were increased with the use of salicylate to increase the negative surface charge on membrane. In this work, it has been demonstrated that under conditions of increased protonation induced by a reduction in assay pH, an increase in affinity was shown for class III antagonists at the DHP site. This finding would be consistent with some previous data (e.g. Valdivia & Coronado, 1988) who demonstrated that the affinity of charged calcium antagonists increased, with uncharged compounds unaffected, by an increase in the phospholipid charge in the membrane. Such an increase in membrane accumulation and associated ionic effects may result in some selective effects. Thus, amlodipine shows a marked difference in its interaction at L-type  $Ca^{2+}$  channels in ventricular cells, and results in a greater degree of block, at depolarised potentials under conditions where pH is reduced and a greater proportion of ionised drug is available (Kass *et al.*, 1989). Such effects may have important implications in cells under pathological conditions and this is discussed in more detail in Chapter 4 with respect to the effects of calcium antagonists in cerebral ischaemia.

If a [ $^3H$ ] calcium antagonist exists in equilibrium between aqueous, membrane and receptor site phases, it is perhaps not surprising that differences exist in affinity for different DHPs between tissues (e.g. Glossmann & Ferry, 1985; Lazdunski *et al.*, 1988) as the overall  $K_d$  will be an expression of several different association and dissociation rates. This

may also explain the different allosteric effects of other agents between tissues observed in this study, if the interactions are due to an effect on association and dissociation kinetics. In addition to these physiochemical interactions, there is now evidence for L channel tissue isoforms, in that the amino acid sequence may vary along the length of the  $\alpha_1$  subunits (McKenna *et al.*, 1990) which may explain the presence of [ $^3$ H] fluspirilene sites in skeletal muscle (Qar *et al.*, 1987) and sarcollemal membranes (King *et al.*, 1989) but not brain (Kenny *et al.*, 1990).

The probability that the low affinity of flunarizine and other low affinity class III antagonists did not result from a direct interaction at the DHP site was confirmed in diltiazem reversal experiments. The ability of diltiazem to reverse the inhibitory effects of flunarizine on [ $^3$ H] nitrendipine binding was relatively poor, in contrast to other agents proposed to modulate [ $^3$ H] DHP binding allosterically (Nokin *et al.*, 1986; Nokin *et al.*, 1989). Furthermore, the degree of reversal was independent of the concentration of flunarizine used (i.e. different amounts of initial inhibition), indicating that flunarizine induces a change in the DHP site making it less susceptible to allosteric control from other sites. These effects, however, are not apparent unless a range of concentrations of antagonist are used against diltiazem and in the majority of cases only the effect of one antagonist concentration has been reported (e.g. Murphy *et al.*, 1983; Nokin *et al.*, 1986; Chatelain *et al.*, 1991). However, a more realistic possibility for diltiazem being ineffective against flunarizine is that these concentrations of flunarizine have non-specific effects on the membrane rather than at the [ $^3$ H] DHP binding site, such that the occupation of all compounds to their respective sites is affected.

#### 3.4.5. *Interactions of class III agents with neuronal Na<sup>+</sup> channels*

In physiological media flunarizine and similar compounds are low affinity calcium antagonists (Godfraind *et al.*, 1986; Fleckenstein, 1983; Spedding 1985a; Fleckenstein, 1988). Higher affinity is revealed in calcium free media (Spedding, 1985b) and *in vitro* binding experiments to vascular smooth muscle (Morel & Godfraind, 1988) indicate that

flunarizine has some selectivity for the DHP site under depolarised conditions associated with the inactivated high affinity binding state. The selectivity of these agents for L-type  $\text{Ca}^{2+}$  channels has largely been questioned because some of these agents have been shown to interact with  $\text{Na}^{+}$  channels labelled by [ $^3\text{H}$ ] BTX at similar concentrations (Pauwels *et al.*, 1986; Grima *et al.*, 1986; Velly *et al.*, 1987). In this work, it has been shown that all class III antagonists inhibit [ $^3\text{H}$ ] BTX in rat cortical synaptosomes with high affinities although there did not appear to be much separation in the range of affinities.

[ $^3\text{H}$ ] BTX binds to site 2 on the  $\text{Na}^{+}$  channel (Catterall *et al.*, 1981; Willow & Catterall, 1982) and in the presence of scorpion toxin or sea anemone toxin at site 3, causes persistent activation of  $\text{Na}^{+}$  channels. The water soluble toxin, tetrodotoxin acts at site 1 to prevent ionic passage through the channel. Ion flux studies have indicated similar properties for  $\text{Na}^{+}$  channels in synaptosomes and nerve cells (Tamkun & Catterall, 1981). Compounds whose pharmacological properties are thought to be mediated through an interaction with  $\text{Na}^{+}$  channels, including antiarrhythmic, anticonvulsant and local anaesthetic compounds, have been shown to have affinity for the [ $^3\text{H}$ ] BTX site (Willow & Catterall, 1982; Postma & Catterall, 1984; Grima *et al.*, 1986). Cardiac and neuronal  $\text{Na}^{+}$  channels labelled by [ $^3\text{H}$ ] BTX have similar properties (Sheldon *et al.*, 1986; Velly *et al.*, 1987) although the affinity for a range of compounds, although of similar rank order, was approximately one log order higher for synaptosomal sites (Grima *et al.*, 1986). Several anticonvulsant compounds have moderate affinity for the [ $^3\text{H}$ ] BTX site, and are thought, at least in part, to be effective *in vivo* through an interaction with voltage-dependent  $\text{Na}^{+}$  channels.

Phenytoin and carbamazepine have previously been reported to have high affinity for [ $^3\text{H}$ ] BTX labelled  $\text{Na}^{+}$  channels in synaptosomes (Willow & Catterall, 1982) and the  $\text{pK}_i$  of 4.69 obtained in this study is in close agreement with the previously reported  $\text{IC}_{50}$  of 40  $\mu\text{M}$ . Furthermore, phenytoin has been demonstrated to inhibit BTX induced  $\text{Na}^{+}$  flux in neuroblastoma cells (Catterall, 1981) and synaptosomes (Willow *et al.*, 1984). The effectiveness of these compounds *in vivo*, without causing massive general depression of CNS response, is explained on the basis of their interaction with  $\text{Na}^{+}$  channels, i.e.

blockade is more effective if the cell is depolarised prior to the activating stimulus (Willow *et al.*, 1985) or the cell is repeatedly pulsed (Schwartz & Grigat, 1989). Phenytoin also causes a slowing of cell recovery from inactivation following hyperpolarisation (Schwartz & Grigat, 1989), suggesting that phenytoin binds to the inactivated or closed state of the channel, giving an aspect of use dependence (Matsuki *et al.*, 1984; Rogawski & Porter, 1990). However phenytoin also produces similar frequency- and voltage-dependent inhibition of T-type  $\text{Ca}^{2+}$  currents (Twombly *et al.*, 1988). An involvement with other VOC types has also been shown as phenytoin decreases both  $\text{Ca}^{2+}$  uptake and release in brain slices (Pincus & Hsiao, 1981) and at high concentrations inhibits [ $^3\text{H}$ ] DHP binding in brain membranes (Greenberg *et al.*, 1984). Given that the class III antagonists are markedly more potent at the [ $^3\text{H}$ ] BTX site than phenytoin, does this have the same implication for neuronal  $\text{Na}^+$  channels?

Flunarizine potently displaces [ $^3\text{H}$ ] BTX and has an anticonvulsant profile similar to phenytoin (see Ashton *et al.*, 1986; Rogawski & Porter, 1990) suggesting a common mechanism of action. Indeed, like phenytoin, low concentrations of flunarizine ( $<1 \mu\text{M}$ ) block neuronal  $\text{Na}^+$  currents use-dependently (see Rogawski & Porter, 1990). Similarly Tytgat *et al.* (1988) demonstrated effects of flunarizine on T channels in the heart, with effects also reported on T channels in hypothalamic neurones (Akaike *et al.*, 1989). RS 87476 displaces [ $^3\text{H}$ ] BTX from rat cortical synaptosomes with comparable affinity to flunarizine and interacts with neuronal  $\text{Na}^+$  currents in neuroblastoma cells in a mechanism similar to that outlined for phenytoin (Sheridan *et al.*, 1991). Carbamazepine also shows voltage- and frequency- dependence, such that inhibition is greater at depolarised potentials (Willow *et al.*, 1985) and an attempt has been made to demonstrate this at the [ $^3\text{H}$ ] BTX site (Willow & Catterall, 1982), with the affinity of carbamazepine (but not phenytoin) shown to increase with depolarisation. However, in this assay, the binding of scorpion toxin is decreased with depolarisation (Catterall *et al.*, 1981) and as this allosterically regulates [ $^3\text{H}$ ] BTX binding, the increased levels required under these conditions to maintain maximal binding also suggests an interaction of carbamazepine with the toxin.

The similar affinity shown for all class III agents must question the specificity of

this assay, especially for lipophilic agents. A correlation between lipophilicity and the ability to inhibit [ $^3\text{H}$ ] BTX binding has been suggested (Pauwels *et al.*, 1986) although this did not apply to flunarizine. Furthermore, it has been shown that [ $^3\text{H}$ ] TPP $^+$  accumulation (a lipophilic ion, sensitive to changes in membrane potential) could be evoked by veratridine and scorpion toxin, an effect that was blocked by flunarizine with similar affinity to inhibition of [ $^3\text{H}$ ] BTX binding (Pauwels & Laduron, 1986). In contrast, all other classes of calcium antagonist were inactive, implying that the ability of class III agents to alter Na $^+$  channel function may result from an interaction in the bilayer, for which their lipophilic and ionic interactions might be important under conditions of excessive neuronal activity and depolarisation. The relevance of the interaction of class III antagonists at Na $^+$  channels is discussed more extensively in Chapter 4.

The affinity of class III antagonists for dopamine D $_2$  receptors was variable, although all compounds showed at least moderate affinity, with several compounds selective for D $_2$  over D $_1$  receptors. A recent report (Ambrosio & Stefanini, 1991) has confirmed the selective D $_2$  affinity for flunarizine. It is likely that the affinity for D $_2$  receptors accounts for some properties of these compounds unrelated to their affinity for VOCs.

#### ***3.4.6. Identification and characterisation of a site for SR 33557 in rat cortex***

Data in this chapter has demonstrated a putative fourth binding site for [ $^3\text{H}$ ] SR 33557 in brain membranes. The site appears to be highly coupled to the DHP site, to the extent that the interaction between the sites appears competitive under several experimental approaches.

In functional studies SR 33557 has been shown to be a potent calcium antagonist, potently inhibiting Ca $^{2+}$ - and Bay K 8644-induced contractions in smooth muscle (Nokin *et al.*, 1989; Polster *et al.*, 1990). Initial studies indicated that SR 33557 had high affinity for other [ $^3\text{H}$ ] calcium antagonist binding sites (Nokin *et al.*, 1989), proposed to result

from an interaction at a distinct, but allosterically coupled site. Schmid *et al.* (1989) first demonstrated specific binding of [<sup>3</sup>H] SR 33557 in skeletal muscle membranes to a site on the same protein as other [<sup>3</sup>H] calcium antagonist sites. This site was distinct but allosterically coupled to the other sites. Further characterisation of [<sup>3</sup>H] SR 33557 binding was carried out by Chatelain's group (Chatelain *et al.*, 1991) who confirmed a distinct but allosterically coupled site for SR 33557, such that the observed interaction with DHP, phenylkylamine and benzothiazepine ligands was through an allosteric, non-competitive interaction. This work, however, is the first to demonstrate high affinity binding of [<sup>3</sup>H] SR 33557 to brain membranes. Thus far, binding sites for other calcium antagonists such as [<sup>3</sup>H] bepridil (Lazdunski *et al.*, 1988; Janis & Triggle, 1990), [<sup>3</sup>H] fluspirilene (Galizzi *et al.*, 1986b; King *et al.*, 1989) and [<sup>3</sup>H] HOE 166 (Grassegger *et al.*, 1989) have only been shown in cardiac or skeletal muscle membranes, although an uncharacterised site for [<sup>3</sup>H] fluspirilene has been reported in purified rat brain synaptic plasma membranes (King *et al.*, 1989).

The site characterised in this work appears to be novel, with similar properties to the site reported in sarcolemmal membranes (Chatelain *et al.*, 1991). On the basis of interactions at the [<sup>3</sup>H] PN 200-110 site in cerebral cortex, the DHP and SR 33557 sites would appear to be distinct but very tightly coupled, to the extent that the interaction of SR 33557 appears competitive under several experimental approaches. Previous studies (Nokin *et al.*, 1989) indicated a non-competitive interaction for SR 33557 at the [<sup>3</sup>H] DHP site on the basis of an increase in the dissociation rate, and whilst these workers showed no affinity for SR 33557 for a variety of different receptors, the concentration of 10  $\mu$ M required to cause a change in the dissociation rate cannot be described as specific with respect to its  $K_i$  for the DHP site. This work has confirmed a distinct site for SR 33557 based on the reversal produced by d-cis diltiazem. This work has already shown that when flunarizine is employed across a range of concentrations, the ability of d-cis diltiazem to reverse the inhibition of binding is similar, irrespective of the concentration of flunarizine in the experiment. In contrast, the inhibition of [<sup>3</sup>H] nitrendipine by SR 33557 could be fully reversed by d-cis diltiazem in agreement with other observations (Nokin *et al.*, 1989),

although the present work has shown that the inhibitory effect of SR 33557 could be reversed in a surmountable fashion, such that a rightward shift was observed for the reversal potency of d-cis diltiazem. These experiments indicated that although the reversal was dependent on the concentration of SR 33557, unlike fluspirilene, allosteric modulation of DHP binding was still possible from other calcium antagonist sites. Quantitative interpretation of these data should not be made however, as SR 33557 displaces both phenylalkylamines and benzothiazepines from their binding sites with high affinity (Nokin *et al.*, 1990). Nevertheless, that this effect is observed is strong evidence that SR 33557 is not a competitive DHP antagonist, since reversal by d-cis diltiazem is completely ineffective with this type of compound.

Further evidence that the sites for SR 33557 and DHPs are tightly coupled was obtained in competition experiments with a specific site labelled by [ $^3\text{H}$ ] SR 33557 in rat cortical membranes. The rank order and affinity for a larger number of calcium antagonists was similar to that observed at the DHP site. These affinities were similar to that reported at the [ $^3\text{H}$ ] SR 33557 site in sarcolemmal membranes (Chatelain *et al.*, 1991) and skeletal muscle (Schmid *et al.*, 1989; Sol-Rolland *et al.*, 1991). The potency and maximal inhibition of binding observed with verapamil and diltiazem would be consistent with SR 33557 having mutually high affinity for both sites (Nokin *et al.*, 1990). The potency of SR 33557 being reduced more than five fold at the DHP site in the presence of  $\text{Ca}^{2+}$  would appear to be an effect at the binding site rather than a surface charge effect, as a range of divalent cations inhibit [ $^3\text{H}$ ] SR 33557 binding with an interaction similar to that described for its interaction at other sites (e.g. Chatelain *et al.*, 1991), with  $\text{Cd}^{2+}$  showing the highest potency. Similar inhibitory properties of divalent cations have been demonstrated at the verapamil and diltiazem binding sites (Galizzi *et al.*, 1985; Balwierczak & Schwartz, 1985), in contrast to the enhancement and requirement at the DHP site (Bolger & Skolnick, 1986). The effect of  $\text{Cd}^{2+}$  at the SR 33557 is in contrast to the stimulatory effect of the ion at the [ $^3\text{H}$ ] fluspirilene site in sarcolemmal membranes providing further evidence of tissue variation in the regulation of non DHP binding sites.

In summary, this chapter has demonstrated that [ $^3\text{H}$ ] DHP binding sites can be

modified by a variety of experimental factors, however, unlike other receptor sites, they are not modified by exposure to palmitoyl carnitine.  $[^3\text{H}]$  DHP sites show tissue-, temperature- and ligand-dependence in their regulation by other calcium antagonists. The  $[^3\text{H}]$  fluspirilene site in skeletal muscle appears to be prototypical for class III calcium antagonists and some of these compounds may have selective effects against calcium channel activators *in vitro*. The selectivity of this group of agents is poor, however, in comparison to the affinity expressed for other receptor types (e.g. dopamine  $\text{D}_2$ ) and ion channels as assessed by  $[^3\text{H}]$  BTX binding in rat cortical synaptosomes. The affinity for  $\text{Na}^+$  channels may be important in the mechanism whereby these agents are neuroprotective *in vivo*, which is addressed in the next two chapters of this thesis. In contrast, however,  $[^3\text{H}]$  SR 33557 appears to be a high affinity ligand for calcium channel binding sites in brain membranes. This chapter has shown that these sites appear to be distinct, but tightly coupled to other sites (Figure 3.16).

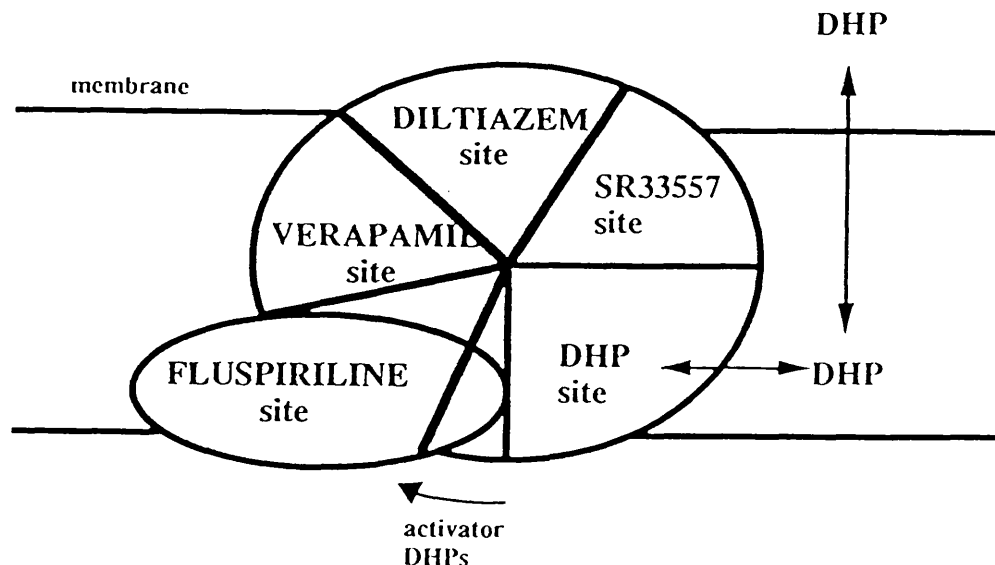


**Figure 3.16.** A proposal for distinct but allosterically coupled binding sites for calcium antagonists in brain membranes. Access to the binding sites is likely to be via the membrane phase. A site for fluspirilene, which allosterically regulates  $[^3\text{H}]$  DHP binding in brain, is illustrated. Binding sites for  $[^3\text{H}]$  fluspirilene per se exist in skeletal muscle membranes. This compound may have selective effects against calcium channel activators *in vitro*.

---

## **Chapter Four.**

***In Vivo* models of cerebral ischaemia: Effects on calcium channels and an assessment of calcium antagonists as potential neuroprotective agents.**

#### ***4.1. The effect of forebrain ischaemia on [<sup>3</sup>H] DHP antagonist binding parameters.***

##### ***4.1.1. The effect of 5 min forebrain ischaemia and 7 days recovery in the Mongolian gerbil on [<sup>3</sup>H] PN 200-110 binding***

All tissues in these studies were taken from animals that fulfilled the isoelectric criteria for acceptance as an ischaemic insult. Saturation analysis of [<sup>3</sup>H] PN 200-110 binding to gerbil brain homogenates indicated a single population of high affinity binding sites, the affinity and density of which were comparable to that previously measured in rat brain (Chapter 3). The effect of brief forebrain ischaemia and recovery in the Mongolian gerbil, induced by occlusion of right and left common carotid arteries, on [<sup>3</sup>H] PN 200-110 binding parameters is shown in Table 4.1. Ischaemia and 7 days recovery had no effect on the density or affinity of [<sup>3</sup>H] PN 200-110 binding sites in cerebral cortex, hippocampus or striatal membrane homogenates.

Autoradiograms of [<sup>3</sup>H] PN 200-110 binding to coronal gerbil brain sections following ischaemia and 7 days reperfusion are shown in Figure 4.1. Sections from non-ischaemic animals revealed the highest density of binding sites in the hippocampus, cerebral cortex and thalamus. The level of non-specific binding was very low, almost to the level of film background. Autoradiographic parameters determined from these experiments are shown in Table 4.2. Analysis of gerbil brain sections labelled with [<sup>3</sup>H] PN 200-110 binding indicated that ischaemia with recovery produced a slight reduction in the level of binding sites in CA1, cortical and thalamic areas, and a slight increase in the density of sites in the dentate gyrus, but based on the number of animals used in these experiments, none of these changes reached the level of significance.

TREATMENT		CEREBRAL CORTEX	HIPPOCAMPUS	STRIATUM
SHAM CONTROL	<b>B<sub>max</sub></b> (fmol/mg)	296 ± 25	331 ± 17	198 ± 16
	<b>K<sub>d</sub></b> (nM)	0.05 ± 0.002	0.04 ± 0.01	0.04 ± 0.006
ISCHAEMIA + 7 DAY RECOVERY	<b>B<sub>max</sub></b> (fmol/mg)	289 ± 35	274 ± 17	196 ± 30
	<b>K<sub>d</sub></b> (nM)	0.06 ± 0.002	0.05 ± 0.007	0.04 ± 0.01

**Table 4.1.** The effect of 5 min forebrain ischaemia followed by 7 days recovery on [<sup>3</sup>H] PN 200-110 binding parameters in gerbil brain.

Values represent the mean ± s.e. mean for 4-5 separate experiments.

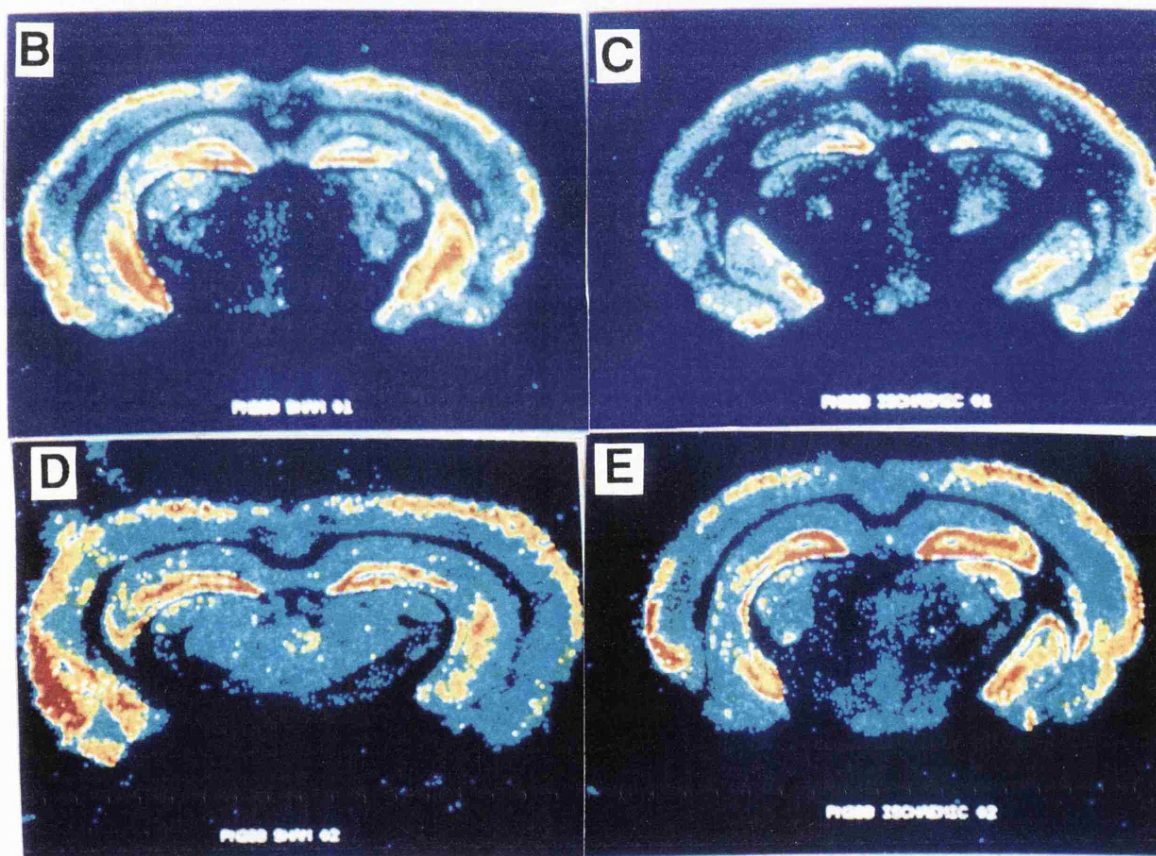
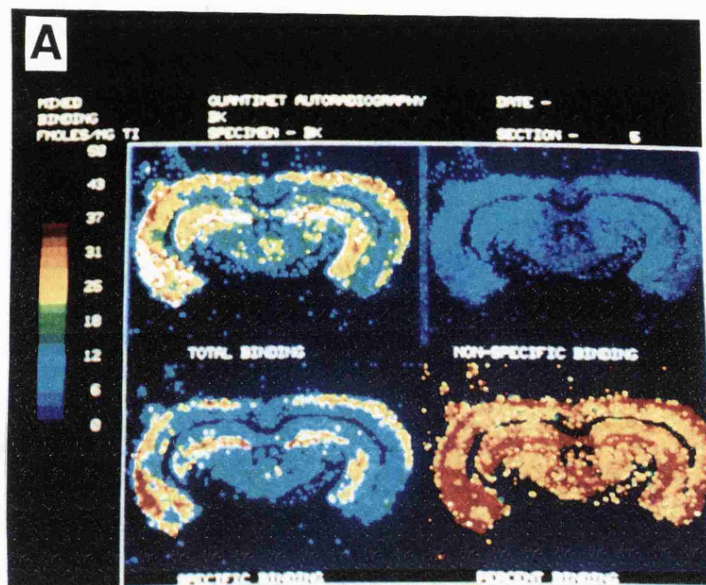


**Figure 4.1.** The effect of 5 min forebrain ischaemia on [ $^3\text{H}$ ] PN 200-110 (0.2 nM) binding to gerbil 20  $\mu\text{m}$  coronal brain sections (A-E). A. Binding to a sham control section illustrating total, non-specific, specific and percentage binding. B & D, specific binding to sections from two different sham controls, and C & E, specific binding to corresponding sections from two different gerbils after 5 min forebrain ischaemia and 7 days reperfusion.

**Table 4.2.**

## BINDING SITE DENSITY

BRAIN AREA	SHAM CONTROL	ISCHAEMIC
Hippocampal CA1	13.63 $\pm$ 1.24	10.71 $\pm$ 1.11
Dentate gyrus	28.13 $\pm$ 6.5	35.40 $\pm$ 4.82
Parietal cortex	26.30 $\pm$ 4.14	21.25 $\pm$ 1.95
Ventrolateral thalamus	18.13 $\pm$ 4.48	14.40 $\pm$ 2.55

**Table 4.2.** Autoradiographic [ $^3\text{H}$ ] PN 200-110 (0.2 nM) binding parameters to 20  $\mu\text{m}$  gerbil brain sections. Specific binding was determined by incubating parallel sections in 1  $\mu\text{M}$  nitrendipine to define non-specific binding. Binding parameters (fmol/mg tissue) were determined from duplicate measurements of total and non-specific binding from at least six sections for each animal, consisting of at least three animals per group. Specific binding represented >90% of the total binding. Values represent mean  $\pm$  s.e.mean.

#### 4.1.2. [ $^3\text{H}$ ] nitrendipine binding to ischaemic gerbil brain.

Identical experiments were carried out on tissue homogenates to examine the effect of forebrain ischaemia with a 7 day reperfusion period on [ $^3\text{H}$ ] nitrendipine binding parameters as described for [ $^3\text{H}$ ] PN 200-110 binding studies. This was to ensure that changes in binding parameters were not dependent on the radioligand used (with the possibility that the use of a higher affinity ligand may mask changes in receptor affinity). The effect of 5 min forebrain ischaemia and 7 days recovery is shown in Table 4.3. It can be seen that as with brain tissues assayed with [ $^3\text{H}$ ] PN 200-110, ischaemia with recovery had no effect on the density or affinity of DHP sites in cerebral cortex or hippocampus labelled by [ $^3\text{H}$ ] nitrendipine. Therefore, the inability to detect changes in these sites using this ischaemic protocol did not appear to be dependent on the affinity or type of [ $^3\text{H}$ ] DHP ligand employed.

#### *4.1.3. Effects of reperfusion periods on [<sup>3</sup>H] PN 200-110 binding parameters.*

Having established that a brief period of forebrain ischaemia with 7 days recovery was without effect on [<sup>3</sup>H] DHP binding parameters, similar experiments were carried out to examine the effects of reperfusion on [<sup>3</sup>H] PN 200-110 binding site parameters. Table 4.4. shows that reperfusion has a significant effect on binding parameters in the cerebral cortex, without any effect on hippocampal or striatal binding parameters. It was found that in cerebral cortex, the density of sites was increased from control,  $207 \pm 16$  fmol/mg (i.e. ischaemia with no reperfusion) to  $259 \pm 10$  fmol/mg after 1 hr reperfusion, and this density of sites decreased to a level not significantly different from control after a 72 hr reperfusion period,  $173 \pm 24$  fmol/mg. Reperfusion did not induce a change in binding site affinity in any brain area examined.

#### *4.1.4. Effects of 10 min forebrain ischaemia and various reperfusion times on the density of [<sup>3</sup>H] PN 200-110 binding sites.*

As a brief period of forebrain ischaemia and 7 days recovery only had a small effect on [<sup>3</sup>H] DHP binding parameters, a period of 10 min forebrain ischaemia was employed. Using this model, the effect of a more severe ischaemic insult could be examined on [<sup>3</sup>H] PN 200-110 binding parameters. In this extensive series of experiments a detailed profile of the effects of reperfusion was used to examine a more precise time course for any changes in binding site parameters that may have occurred as a result of the ischaemic period or from subsequent reperfusion. Data from this series of experiments are shown in Table 4.5. It was found that a 10 min period of forebrain ischaemia per se (i.e. ischaemia with no reperfusion) did not produce a significant change in the density or affinity of [<sup>3</sup>H] PN 200-110 binding sites in membrane homogenates derived from either frontal cortex or hippocampus. At the first reperfusion

TREATMENT		CEREBRAL CORTEX	HIPPOCAMPUS
SHAM CONTROL	<b>B<sub>max</sub></b> (fmol/mg)	220 ± 19	173 ± 10
	<b>K<sub>d</sub></b> (nM)	0.19 ± 0.009	0.15 ± 0.01
ISCHAEMIA + 7 DAY RECOVERY	<b>B<sub>max</sub></b> (fmol/mg)	205 ± 20	163 ± 11
	<b>K<sub>d</sub></b> (nM)	0.18 ± 0.012	0.16 ± 0.009

**Table 4.3.** The effect of 5 min forebrain ischaemia followed by 7 days recovery on [<sup>3</sup>H] nitrendipine binding parameters in gerbil brain.

Values represent the mean ± s.e. mean for 4-5 separate experiments.

TREATMENT	CEREBRAL CORTEX	HIPPOCAMPUS	STRIATUM
CONTROL			
Ischaemia + <u>0 min</u> reperfusion.	<b>Bmax</b> 207 ± 16 (fmol/mg)	208 ± 24	151 ± 16
	<b>Kd</b> 0.03 ± 0.004 (nM)	0.03 ± 0.005	0.03 ± 0.01
Ischaemia + <u>1 hr</u> reperfusion.	<b>Bmax</b> 259 ± 10*	198 ± 11	129 ± 10
	<b>Kd</b> 0.04 ± 0.01 (nM)	0.04 ± 0.005	0.03 ± 0.003
Ischaemia + <u>72 hr</u> reperfusion.	<b>Bmax</b> 173 ± 24 (fmol/mg)	187 ± 13	125 ± 17
	<b>Kd</b> 0.03 ± 0.002 (nM)	0.05 ± 0.017	0.03 ± 0.005

**Table 4.4.** The effect of reperfusion on [<sup>3</sup>H] PN 200-110 binding parameters in gerbil brain following 5 min forebrain ischaemia. Values represent the mean ± s.e.mean of 4 separate experiments.

\*p<0.05 compared to control value, unpaired t-test.

TREATMENT		FRONTAL CORTEX	HIPPOCAMPUS
NON-ISCHAEMIC SHAM CONTROL	Bmax (fmol/mg) Kd (nM)	210 ± 14 0.053 ± 0.003	200 ± 8 0.064 ± 0.009
ISCHAEMIA+ NO REPERFUSION	Bmax Kd	196 ± 11 0.06 ± 0.003	163 ± 10 0.08 ± 0.014
ISCHAEMIA+ 1 HR. REPERFUSION	Bmax Kd	165 ± 13 0.054 ± 0.005	141 ± 13* 0.08 ± 0.02
ISCHAEMIA+ 4 HR. REPERFUSION	Bmax Kd	162 ± 25 0.06 ± 0.006	132 ± 7** 0.086 ± 0.016
ISCHAEMIA+ 12 HR. REPERFUSION	Bmax Kd	155 ± 14 0.07 ± 0.01	149 ± 10* 0.07 ± 0.015
ISCHAEMIA+ 24 HR. REPERFUSION	Bmax Kd	178 ± 5 0.06 ± 0.003	152 ± 13* 0.085 ± 0.016
ISCHAEMIA+ 72 HR. REPERFUSION	Bmax Kd	158 ± 14 0.06 ± 0.007	114 ± 9** 0.075 ± 0.02

**Table 4.5.** The effect of ischaemia and various reperfusion periods on [<sup>3</sup>H] PN 200-110 binding parameters in gerbil brain following 10 min forebrain ischaemia.

Values represent the mean ± s.e.mean of 3-5 separate experiments.

\*p<0.05, \*\*p<0.01 compared to sham control using analysis of variance for multi sample comparison and the application of Dunnet's t-test.

time point measured (1 hr post-ischaemia) the density of binding sites was significantly reduced in hippocampus. The level of sites was also reduced in the frontal cortex, but to a lesser and non-significant level. Further periods of reperfusion (4-24 hr) did not result in a marked change in the level of binding sites compared to the level at 1 hr post-ischaemia. However, in hippocampal membranes at a 72 hr post-ischaemia, the level of [ $^3\text{H}$ ] PN 200-110 binding sites was reduced further, to a level of 50 % of control. The level in frontal cortex was still reduced at 72 hr post-ischaemia, but not to a significant level. The affinity of binding sites was unaffected at all time points post-ischaemia in both frontal cortex and hippocampal homogenates by this ischaemic protocol.

#### **4.2. [ $^3\text{H}$ ] PK 11195: Pharmacological characterisation.**

Prior to the use of this ligand as a marker of ischaemic damage, the characterisation of this ligand was carried out in gerbil, mouse and rat brain. PK 11195 and RO 5-4864 are peripheral type benzodiazepine (PTB) compounds. The sites for these agents have been proposed to be distinct from the sites of centrally acting agents in terms of pharmacological specificity, subcellular and anatomical distribution, and have been termed  $\omega_3$  to distinguish them from the site of action of centrally acting benzodiazepines (Langer & Arbilla, 1988 ).

##### **4.2.1. High affinity neuronal binding sites exist for [ $^3\text{H}$ ] PK 11195.**

In membrane homogenates derived from rat, gerbil and mouse brain, iterative non-linear analysis of the saturation data indicated that [ $^3\text{H}$ ] PK 11195 bound to a single population of high affinity binding sites in cerebral cortex and hippocampal membranes in all species. Binding was saturable, reversible and rapid. In rat and gerbil cerebral cortex, the  $T_{1/2}$  for association was <2 min. Transformations of [ $^3\text{H}$ ] PK 11195 saturation binding data to cerebral cortex from rat, gerbil and mouse are shown in Figure 4.2. It can be seen that whilst sites are labelled with similar affinity ( $0.21 \pm 0.05$

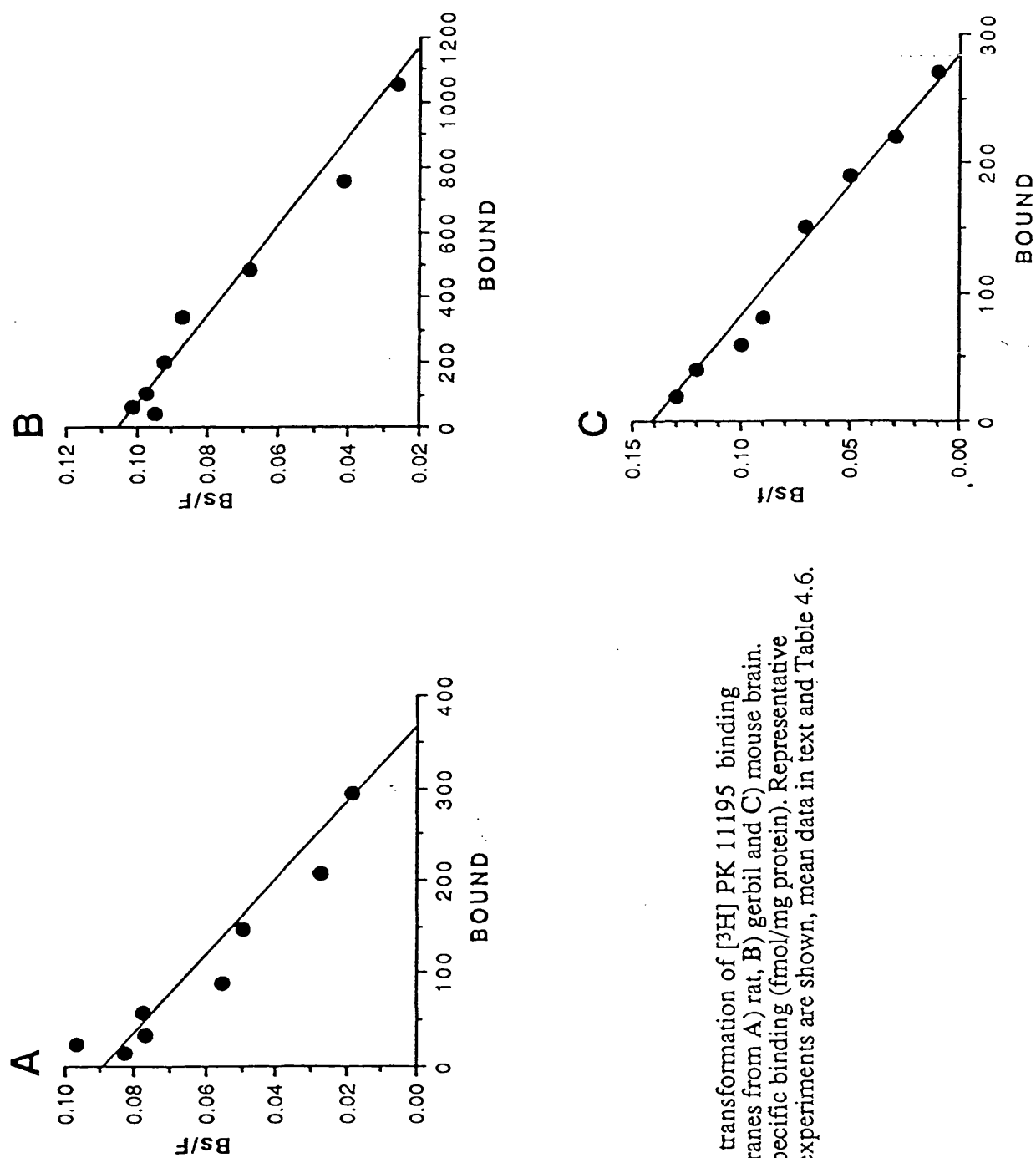


**Figure 4.2.** Scatchard transformation of  $[^3\text{H}]$  PK 11195 binding to cerebrocortical membranes from A) rat, B) gerbil and C) mouse brain. Bound axis represents specific binding (fmol/mg protein). Representative plots of at least 3 other experiments are shown, mean data in text and Table 4.6.

	HIPPOCAMPUS		CEREBRAL CORTEX	
	Kd (nM)	Bmax (fmol/mg protein)	Kd	Bmax
RAT	0.26 ± 0.03	196 ± 31	0.21 ± 0.05	254 ± 21
GERBIL	0.31 ± 0.02	1430 ± 111	0.17 ± 0.02	1360 ± 71

**Table 4.6.** Saturation binding parameters for [<sup>3</sup>H] PK 11195 to rat and gerbil brain membranes. Values represent mean ± s.e. mean (n=4).

nM,  $0.17 \pm 0.02$  nM and  $0.22 \pm 0.04$  nM in rat, gerbil and mouse cortex respectively) a much higher density of sites was labelled in gerbil cortex compared to rat and mouse. To examine if this was a property of cortical membranes alone, similar experiments were carried out in hippocampal membranes. It can be seen from data in Table 4.6 that, similarly, a much higher density of binding sites was measured in gerbil hippocampus compared to rat. The high density of binding sites detected in gerbil brain appeared to be species rather than tissue specific.

#### 4.2.2. *Selectivity of peripheral and non-peripheral benzodiazepines for $\omega_3$ sites*

The specificity of [ $^3\text{H}$ ] PK 11195 binding to brain tissues was examined with a range of peripheral-type benzodiazepine (PTB) and non-PTB compounds in rat, gerbil and mouse brain membranes. Competition experiments were carried out in both cortical and hippocampal homogenates, as saturation data had indicated differences between species. In displacement studies carried out in cerebral cortex membranes (Table 4.7. ii) the [ $^3\text{H}$ ] PK 11195 binding site in all tissues showed high affinity for PK 11195 and similar selectivity for the adenosine uptake blocker dipyridamole. The structurally related compound RO 5-4864, also an  $\omega_3$  selective ligand, showed high affinity for sites in rat and mouse cortex, but much lower affinity for the site in gerbil cortex ( $\text{pK}_i$   $8.48 \pm 0.02$  in rat,  $8.46 \pm 0.07$  in mouse and  $6.70 \pm 0.12$  in gerbil cortex). Similarly, a range of centrally acting benzodiazepines (diazepam, flunitrazepam and clonazepam) also displayed higher affinity for the [ $^3\text{H}$ ] PK 11195 site in rat and mouse cortex compared to gerbil cortex. All compounds examined appeared to displace [ $^3\text{H}$ ] PK 11195 from a single binding site. In hippocampal membranes (Table 4.7. i) all compounds displayed a similar profile to that observed in cerebral cortex. High affinity was displayed by PK 11195, but as in cortical membranes, the [ $^3\text{H}$ ] PK 11195 site in gerbil cortex displayed low affinity for RO 5-4864 ( $\text{pK}_i$   $6.57 \pm 0.02$ ) compared to rat ( $8.16 \pm 0.07$ ) or mouse (7.80). Lower affinity was also expressed for centrally acting compounds at the site in

## HIPPOCAMPUS

i						
	RAT		GERBIL		MOUSE	
COMPOUND	pKi	nH	pKi	nH	pKi	nH
PK 11195	8.90 ± 0.06	0.83	9.06 ± 0.11	1.05	8.50	0.98
RO 5 4864	8.16 ± 0.07	0.96	6.57 ± 0.02	0.97	7.80	0.60
Dipyridamole	7.24 ± 0.06	0.93	6.64 ± 0.05	1.11	6.70	1.20
Diazepam	6.90 ± 0.09	1.06	5.44 ± 0.10	1.10	6.60	0.85
Flunitrazepam	6.55 ± 0.03	1.26	5.44 ± 0.08	1.05	6.70	0.98
Nitrazepam	5.27 ± 0.01	0.86	5.88 ± 0.01	1.32	5.20	1.10
Clonazepam	5.22 ± 0.16	1.24	5.25 ± 0.05	0.96	5.20	1.20
Lorazepam	5.58 ± 0.16	0.93	5.46 ± 0.08	0.83	5.10	0.85

## CEREBRAL CORTEX

ii						
	RAT		GERBIL		MOUSE	
COMPOUND	pKi	nH	pKi	nH	pKi	nH
PK 11195	9.28 ± 0.08	1.02	9.38 ± 0.15	1.13	9.57 ± 0.04	0.98
RO 5 4864	8.48 ± 0.02	0.92	6.70 ± 0.12	0.83	8.46 ± 0.07	0.79
Dipyridamole	7.19 ± 0.12	0.92	7.55 ± 0.10	1.02	7.56 ± 0.05	1.14
Diazepam	7.25 ± 0.15	0.90	5.45 ± 0.11	0.90	7.44 ± 0.17	0.88
Flunitrazepam	6.95 ± 0.09	0.93	5.42 ± 0.03	0.87	7.12 ± 0.02	0.92
Clonazepam	<5		5.28	0.77	5.38 ± 0.08	0.83
Bay K 8644	-		5.05	1.39	-	
Nitrendipine	-		5.74	1.24	-	
Flunarizine	-		4.63	0.60	-	
MK 801	-		<5		-	
D-cis-diltiazem	-		<5		-	

**Table 4.7.** Affinities of central and peripheral type benzodiazepine compounds for the [ $^3$ H] PK 11195 binding site in rat, gerbil and mouse i) hippocampus and ii) cerebral cortex membranes. Displacement experiments were carried out with 0.2 nM [ $^3$ H] PK 11195 and affinity values (pKi) are represented as mean  $\pm$  s.e. mean for 3-5 experiments (nH, Hill slope). Single values represent a single or mean of 2 determinations.

gerbil hippocampus. At the site in gerbil hippocampus, low  $\mu\text{M}$  affinity was shown by dihydropyridines (nitrendipine and Bay K 8644) and flunarizine. MK 801 and d-cis diltiazem were ineffective. Thus, the  $\omega_3$  site in rat and mouse brain showed a similar strict structure-activity requirement for affinity at the site, with high affinity only shown by  $\omega_3$  type ligands. The low affinity shown by RO 5-4864 in gerbil brain appeared to be species-dependent.

#### *4.2.3. Effects of RO 5-4864 on [ $^3\text{H}$ ] PK 11195 saturation binding parameters in cortical membranes.*

To determine whether the low affinity expressed by RO 5-4864 in gerbil brain was a reflection of a non-competitive interaction, the nature of the interaction of RO 5-4864 with the [ $^3\text{H}$ ] PK 11195 binding site was determined by examining its effect on [ $^3\text{H}$ ] PK 11195 saturation binding parameters in cortical membranes from rat and gerbil. Linear transformation of the saturation data (Table 4.8.) are shown in Figure 4.3.

**Table 4.8.**

RAT CORTEX	Bmax (fmol/mg protein)	Kd (nM)
CONTROL	303 $\pm$ 42	0.23 $\pm$ 0.02
+ 5.0 nM RO 5-4864	269 $\pm$ 31	0.72 $\pm$ 0.09
+ 10.0 nM RO 5-4864	287 $\pm$ 46	1.07 $\pm$ 0.04
GERBIL CORTEX	Bmax (fmol/mg protein)	Kd (nM)
CONTROL	1102 $\pm$ 72	0.24 $\pm$ 0.02
+ 0.1 $\mu\text{M}$ RO 5-4864	935 $\pm$ 75	0.41 $\pm$ 0.06
+ 0.5 $\mu\text{M}$ RO 5-4864	960 $\pm$ 44	0.77 $\pm$ 0.05

**Table 4.8.** The effect of RO 5-4864 on [ $^3\text{H}$ ] PK 11195 saturation binding parameters in rat and gerbil cortex at 25°C. Values represent mean  $\pm$  s.e. mean for four experiments performed in triplicate against control.

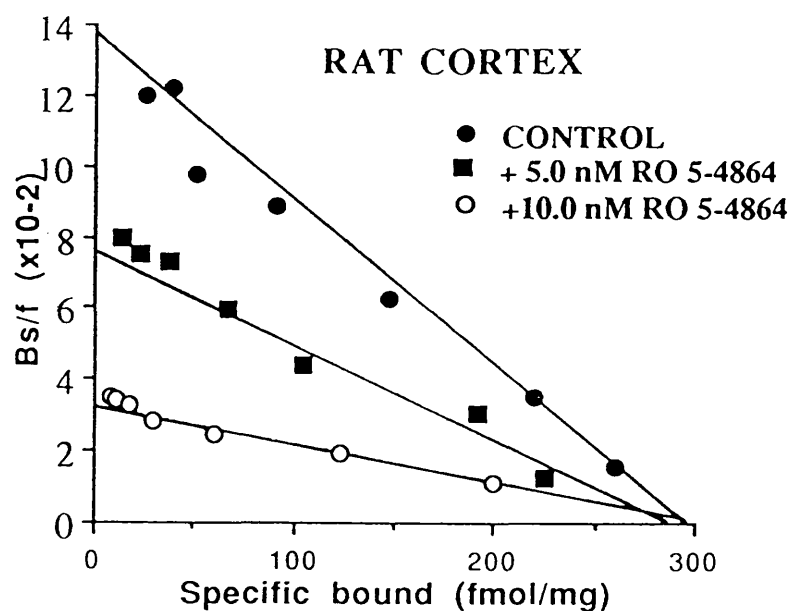
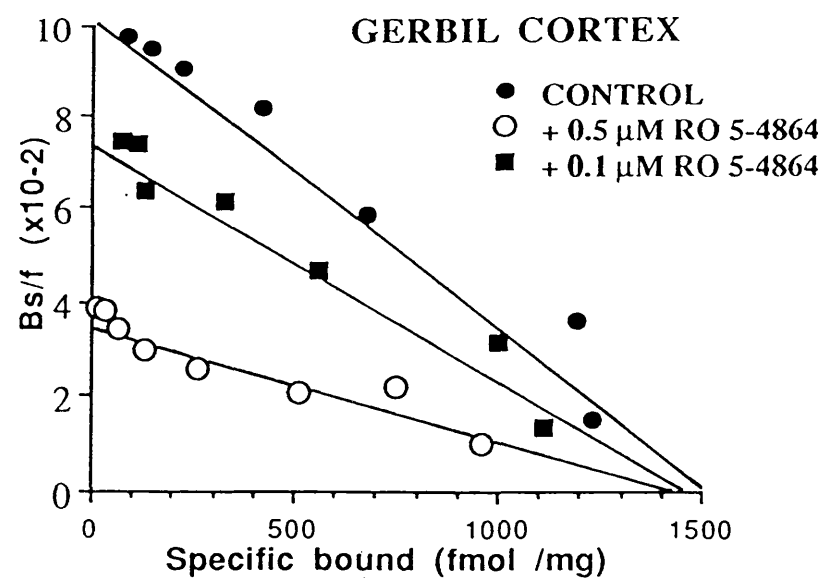


**Figure 4.3.** Scatchard transformation of [ $^3\text{H}$ ] PK 11195 saturation binding to rat and gerbil cortex in the presence of RO 5-4864. The graphs are representative plots of 3 other experiments. The mean data for binding parameters is given in the results section.

The presence of RO 5-4864 in [ $^3\text{H}$ ] PK 11195 saturation shift experiments, at concentrations respective to  $K_i$  to give similar quantifiable shifts in binding parameters, caused a change in affinity without any change in receptor density. These data indicated that the interaction of RO 5-4864 was competitive at  $\omega_3$  sites in rat and gerbil cortex.

#### 4.2.4. Effects of RO 5-4864 on [ $^3\text{H}$ ] PK 11195 dissociation kinetics.

On account of the rapid rate of dissociation that occurred at  $25^\circ\text{C}$  in gerbil cortical membranes ( $0.262\text{min}^{-1}$ ,  $n=2$ ) the effect of RO 5-4864 was examined on [ $^3\text{H}$ ] PK 11195 dissociation kinetics at  $40^\circ\text{C}$ . Preliminary experiments established that the affinity of RO 5-4864 for [ $^3\text{H}$ ] PK 11195 sites was unaffected by this reduction in temperature ( $\text{pK}_i$  in gerbil cortex 6.79,  $\text{nH}$  1.16,  $\text{pK}_i$  in mouse cortex 8.53,  $\text{nH}$  0.99). The effect of RO 5-4864 on dissociation rate kinetics is shown in Figure 4.4. In gerbil, rat and mouse cortical membranes, after the establishment of equilibrium (100 min), the presence of excess RO 5-4864 (at similar concentrations with respect to  $K_i$ ) did not change the rate of dissociation of [ $^3\text{H}$ ] PK 11195 compared to control in either rat, gerbil or mouse cortical membranes. Dissociation rate data is shown in Table 4.9.

**Table 4.9**

DISSOCIATION RATE ( $\text{min}^{-1}$ )

RAT CORTEX CONTROL	$0.014 \pm 0.0015$
+ 0.1 $\mu\text{M}$ RO 5-4864	$0.015 \pm 0.004$
GERBIL CORTEX CONTROL	$0.015 \pm 0.0017$
+ 10 $\mu\text{M}$ RO 5-4864	$0.014 \pm 0.002$
MOUSE CORTEX CONTROL	$0.014 \pm 0.002$
+ 0.1 $\mu\text{M}$ RO 5-4864	$0.015 \pm 0.003$

**Table 4.9.** The effect of RO 5-4864 on [ $^3\text{H}$ ] PK 11195 dissociation rate at  $40^\circ\text{C}$  in cortical membranes. Values represent mean  $\pm$  s.e.mean of four experiments performed in duplicate against parallel controls.

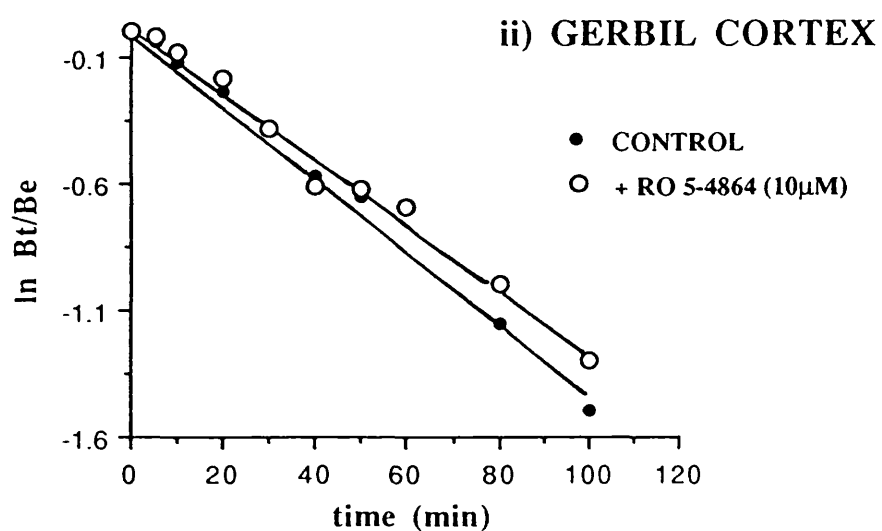
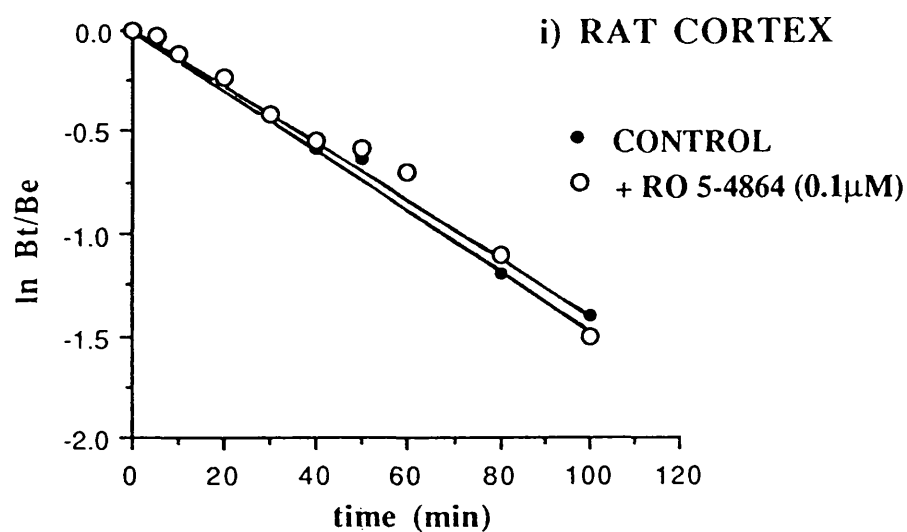


**Figure 4.4.** The effect of RO 5 4864 on the rate of dissociation of [ $^3\text{H}$ ] PK 11195 from i) rat and ii) gerbil cortex membranes at 4  $^{\circ}\text{C}$ . Dissociation was initiated by the addition of 1  $\mu\text{M}$  PK 11195 alone (control) or in the presence of 0.1  $\mu\text{M}$  RO 5 4864 in rat cortex and 10  $\mu\text{M}$  RO 5 4864 in gerbil cortex. Mean data is shown in results text.

The lack of effect of RO 5-4864 on [ $^3\text{H}$ ] PK 11195 dissociation rate kinetics in these experiments was further evidence for a competitive interaction for RO 5-4864. Therefore, the difference in affinity for gerbil brain sites did not reflect a difference in the nature of the interaction at these sites in comparison to rat and mouse where the interaction was of higher affinity. Furthermore, under the described conditions, no evidence could be found for heterogeneity of binding sites based on the interaction of RO 5-4864.

#### ***4.2.5. [ $^3\text{H}$ ] PK 11195 labelled subcellular fractions***

Due to the very high density of [ $^3\text{H}$ ] PK 11195 binding sites detected in gerbil brain in comparison to other species examined, the characteristics of [ $^3\text{H}$ ] PK 11195 binding were compared in rat and gerbil subcellular fractions.

Crude P2 mitochondrial (and synaptosomal) pellets from rat and gerbil cortex were assayed for [ $^3\text{H}$ ] PK 11195 binding parameters. The affinity and density of binding sites was similar to that found in membrane homogenates. In rat cortical P2 fractions the density of sites was  $230 \pm 17$  fmol/mg protein and the affinity was 0.21 nM. In gerbil cortical P2 fractions the density was 1530 fmol/mg and the affinity was 0.16 nM. These data are close to the binding parameters in membrane homogenates ( $254 \pm 21$  fmol/mg and  $0.21 \pm 0.05$  nM in rat,  $1360 \pm 71$  fmol/mg and  $0.17 \pm 0.02$  nM in gerbil). Binding studies were also carried out on sucrose gradient purified fractions from the crude P2 pellet in an attempt to characterise the binding of [ $^3\text{H}$ ] PK 11195 to purified mitochondria.

#### ***4.2.6. Distribution of binding sites.***

The distribution of subcellular binding sites (Figure 4.5.) demonstrated that, in both rat and gerbil cortex homogenates, enrichment of binding was found in the crude mitochondrial/synaptosomal P2 pellet. Differences were found upon separation of the

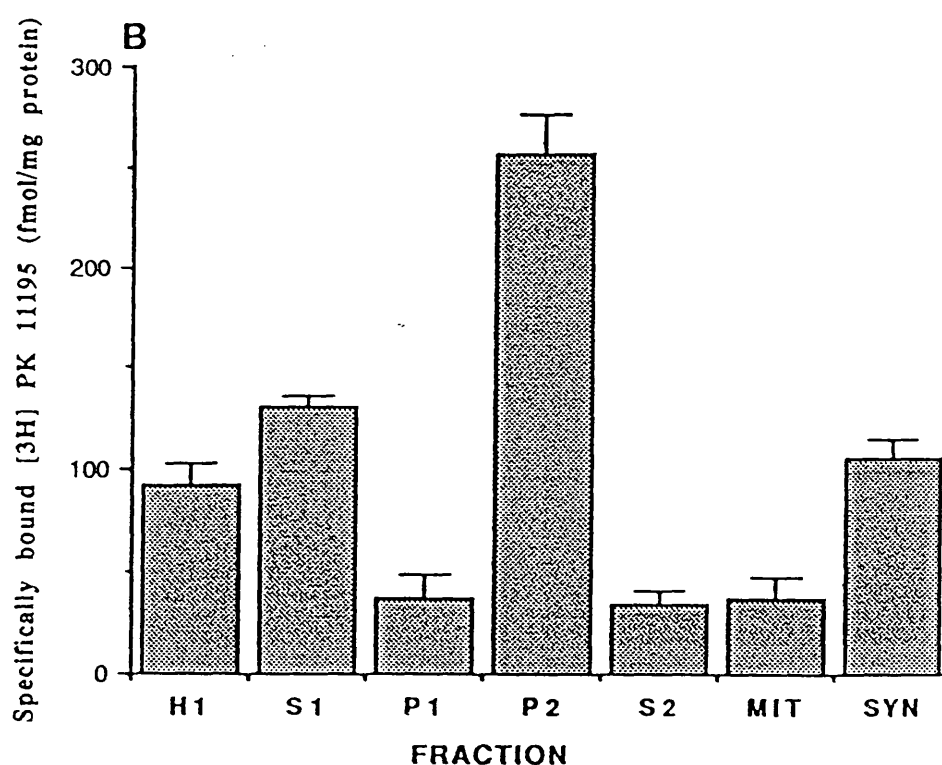
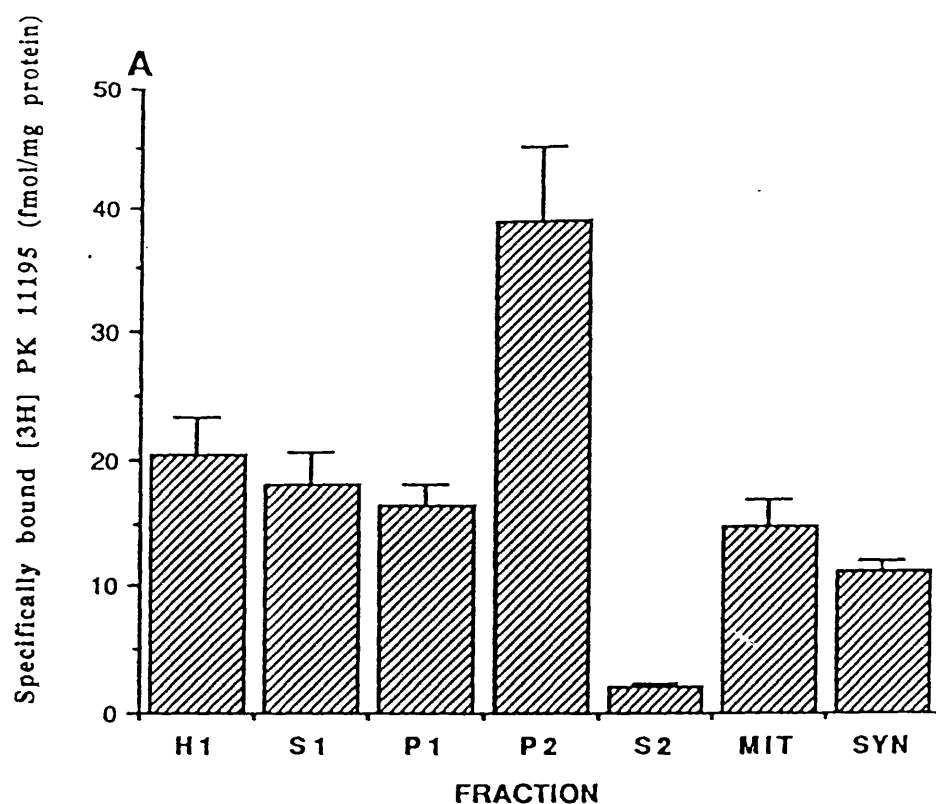


**Figure 4.5.** Subcellular distribution of [ $^3\text{H}$ ] PK 11195 binding sites to A) rat and B) gerbil brain homogenate. S1 and P1 are the resulting supernatants and pellets from the initial 1,000g spin. Centrifugation of the S1 fraction at 17,000g yielded the P2 fraction. Fractionation of the P2 pellet over a sucrose gradient at 100,000g yielded a mitochondrial pellet (MIT) and synaptosomal fraction (SYN) at the 1.2/1.0 M sucrose interface. Values represent mean  $\pm$  s.e. mean for the specific binding of 0.1 nM [ $^3\text{H}$ ] PK 11195 to each fraction.

COMPOUND	RAT		GERBIL	
	pKi	nH	pKi	nH
PK 11195	9.12 ± 0.15	1.04	9.56 ± 0.26	1.21
RO 5-4864	8.58 ± 0.04	1.11	6.64 ± 0.06	1.19
Dipyridamole	6.82 ± 0.24	0.96	7.32 ± 0.08	1.02
Flunitrazepam	6.71 ± 0.15	1.20	5.38 ± 0.12	1.13

**Table 4.10.** Displacement of 0.2 nM [<sup>3</sup>H] PK 11195 from rat and gerbil purified mitochondrial membranes from cerebral cortex. Assays were carried out in a final volume of 1.0 ml in 50 mM Tris-HCl buffer for 30 min at 25°C. Non-specific binding was determined in the presence of 10 μM RO 5-4864. Values represent mean ± s.e. mean (n=3).

crude P2 pellet with a higher enrichment of binding in purified mitochondria from rat cortex compared to gerbil cortex. However, in both cases there was no enrichment in these fractions compared to the initial P2 pellet. Purified synaptosomes from rat and gerbil cortex were found to contain relatively high densities of binding sites, and in the gerbil cortex a greater enrichment was found in synaptosomal than the mitochondrial fraction with a large degree of residual binding in the S2 fraction (which would mainly be composed of microsomes). Although the relative purity and yield of the various fractions were not assessed in this series of experiments, the data clearly indicated that [ $^3\text{H}$ ] PK 11195 binding sites, particularly in gerbil brain, were not exclusively associated with mitochondrial fractions.

#### 4.2.7. [ $^3\text{H}$ ] PK 11195 binding to purified mitochondria.

The pharmacological specificity of [ $^3\text{H}$ ] PK 11195 binding sites has largely been characterised and shown to be associated with mitochondrial membranes in a number of tissues (e.g. Anholt *et al.*, 1986). In competition experiments similar to those carried out on membrane fractions, the nature of the binding site in purified mitochondria from rat and gerbil brain tissue was examined, since these sites did not appear to be enriched in comparison to other well characterised peripheral tissues. However, it can be seen in Table 4.10 that the selectivity and affinity shown for PK 11195, RO 5-4864, dipyridamole and flunitrazepam was identical to that in crude membrane homogenates. The low affinity of RO 5-4864 (and flunitrazepam) in gerbil membrane homogenates in comparison to other species was therefore consistent in both crude membranes and purified mitochondrial fractions in this species.

#### 4.3. [ $^3\text{H}$ ] PK 11195 as a marker of ischaemic damage following forebrain ischaemia.

The density and affinity of [ $^3\text{H}$ ] PK 11195 binding was assessed after 5 min forebrain ischaemia in the gerbil. The experiments were carried out and analysed as described for [ $^3\text{H}$ ] PN 200-110 binding with the important exception that EEGs were not monitored during the occlusion period. Ischaemia with 7 days recovery resulted in a significant increase ( $p < 0.01$ ) in the density of [ $^3\text{H}$ ] PK 11195 binding sites in hippocampal membranes from ischaemic animals compared to non-ischaemic controls (Table 4.11.). Ischaemia and recovery had no effect on receptor binding site affinity in either brain area. There was no change in the density of [ $^3\text{H}$ ] PK 11195 binding sites in the cerebral cortex following ischaemia and recovery.

**Table 4.11.**

TISSUE	NON-ISCHAEMIC		ISCHAEMIC	
	Kd	Bmax	Kd	Bmax
	(nM)	(fmol/mg protein)		
Hippocampus	$0.32 \pm 0.02$	$1430 \pm 111$	$0.29 \pm 0.10$	$2160 \pm 170^*$
Cerebral cortex	$0.18 \pm 0.07$	$1560 \pm 70$	$0.22 \pm 0.05$	$1740 \pm 150$

**Table 4.11.** The effect of 5 min forebrain ischaemia on [ $^3\text{H}$ ] PK 11195 binding parameters in gerbil brain. Forebrain ischaemia was induced by occlusion of right and left common carotid arteries for 5 min. followed by recovery for 7 days. Saturation experiments ( $n=4-5$ ) were carried out as described in methods and statistical significance

( $p < 0.01$ , unpaired t-test) is given for ischaemic against non-ischaemic controls.

Autoradiographic analysis of [ $^3\text{H}$ ] PK 11195 binding to 20  $\mu\text{m}$  coronal brain sections taken from control and ischaemic animals showed that 5 min forebrain ischaemia, followed by 7 days recovery, resulted in an increase in binding density in CA1 and CA3 regions of hippocampus, and parietal cortex (I-II) compared to sham controls, but this increase was only consistent and significant in the CA1 region (Table 4.12.). In a total of 7 ischaemic animals used for several different [ $^3\text{H}$ ] PK 11195 autoradiographic experiments, the extent to which binding increased following ischaemia in other brain areas was variable. Figure 4.6. illustrates the ischaemic induced variation in binding density for two different animals subjected to identical procedures and demonstrates the involvement of other brain areas in animals showing a large increase in binding in CA1 of the hippocampus.

**Table 4.12.**

BRAIN REGION	SHAM CONTROL	ISCHAEMIC
Hippocampal CA1	152 $\pm$ 42	314 $\pm$ 43*
Hippocampal CA3	202 $\pm$ 28	231 $\pm$ 30
Parietal cortex (I-II)	191 $\pm$ 28	247 $\pm$ 18

**Table 4.12.** Autoradiographic [ $^3\text{H}$ ] PK 11195 (1.0 nM) binding parameters (fmol/mg tissue) were determined from duplicate measurements of total and non-specific binding (defined by 10  $\mu\text{M}$  RO 5-4864) from at least six sections for each animal, consisting of at least three animals per group. The specific binding represented 85-90 % of the total binding and values represent mean  $\pm$  s.e.mean. \* $p < 0.05$  against non-ischaemic sham control, unpaired t-test.

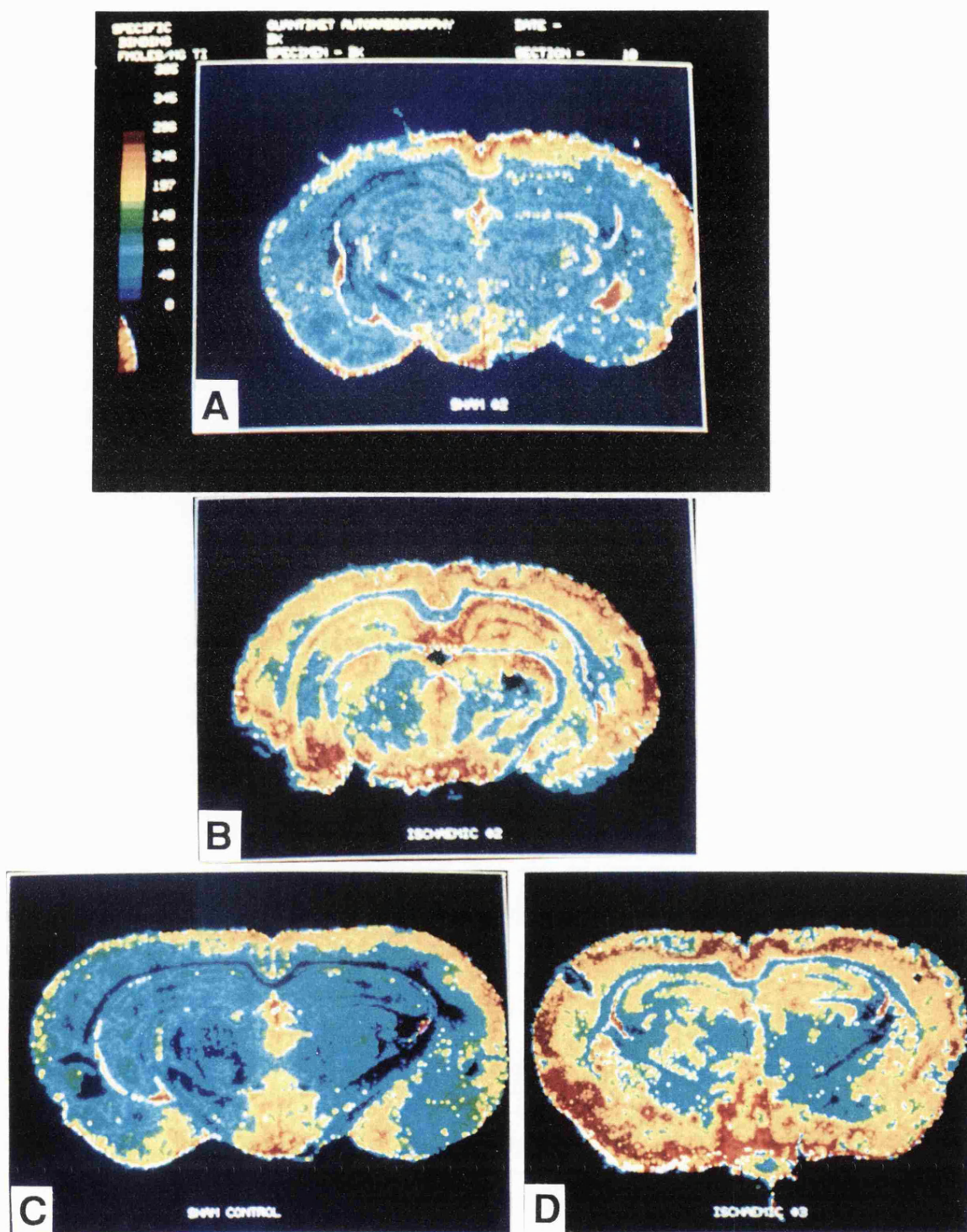


**Figure 4.6.** Autoradiographic changes in  $[^3\text{H}]$  PK 11195 (1.0 nM) binding to 20  $\mu\text{m}$  coronal gerbil brain sections following 5 min forebrain ischaemia and 7 days reperfusion. A and C represent control sections from sham controls, B and D represent sections taken from two different ischaemic animals. Note the ischaemia-induced increase in binding in areas other than hippocampal CA1 regions.

#### ***4.4.1. [<sup>3</sup>H] PK 11195 as a marker of neuronal damage in a mouse model of focal ischaemia.***

Permanent occlusion of the middle cerebral artery in the mouse, induced by electrocoagulation, resulted in a reproducible and similar cortical infarct, even though the precise anatomy of the middle cerebral artery differed markedly between animals in relation to the zygomatic arch and the foramen on the overlying cranium. When visualised microscopically 7 days after occlusion, the infarcted area appeared as a distinct necrotic core surrounded by a pale penumbra. This core and penumbra was routinely taken for binding analysis, and for uniformity and consistency between experiments, only cortical tissue was used, although lateral aspects of the caudate putamen could possibly be damaged in this model. Middle cerebral artery occlusion did not appear to be associated with obvious behavioural symptoms, and there was no evidence that mortality was increased as a direct result of operative procedures. As the increase in [<sup>3</sup>H] PK 11195 binding has been proposed to result from reactive changes in non-neuronal cells, ischaemia-induced changes in binding parameters were analysed at several time points post-ischaemia to determine the optimal post-ischaemic reperfusion period prior to analysis of ischaemic tissue samples.

*Some of the experimental analysis of ischaemic tissue samples in this and some of the following experiments were also carried out by co-workers in this laboratory (Dr. Christine Brown, Alison MacKinnon, Michael Stewart). However, the methods used were identical to those already established.*

#### ***4.4.2. Post-ischaemic changes in cortical [<sup>3</sup>H] PK 11195 binding parameters following middle cerebral artery occlusion in the mouse.***

Changes in the density of [<sup>3</sup>H] PK 11195 binding to ischaemic cortical tissue samples at various time points post-ischaemia are shown in Table 4.13. and Figure 4.7.

Preliminary experiments indicated that short post-ischaemic time periods (1 and 2 hrs) had no effect on the density of  $\omega_3$  binding sites in the ischaemic left cortex. The increase at 24 hrs (n=5) was small and not significant and whilst at 72 hrs the density of sites had increased by 171%, ( $p < 0.01$ , n=6 ANOVA, Dunnet's t-test) the maximal increase was detected at 7 days and represented an increase of 301% (n=5,  $p < 0.001$ ) compared to the control (corresponding right cortex) level. The density of sites in non-ischaemic right cortical tissues was similar at all time points and did not differ from the level in sham operated animals. An important observation in this series of experiments was that the level of sites in the non-ischaemic right cortex from left MCA occluded animals was similar and not significantly different to the level in the right or left cortex from non-occluded control animals.

To examine the reproducibility of these experimental procedures, in a subsequent separate series of experiments similar data were obtained following occlusion of the left MCA and 7 days recovery. These data are shown in Table 4.14.

**Table 4.13.**

	n	Kd (nM)	Bmax (fmol/mg protein)
<b>ISCHAEMIC (LEFT)</b>			
24hr	5	$0.15 \pm 0.13$	$208 \pm 60$
72hr	6	$0.18 \pm 0.13$	$462 \pm 49^*$
168hr	5	$0.20 \pm 0.08$	$746 \pm 50^{**}$
168hr SHAM	5	$0.21 \pm 0.05$	$170 \pm 28$
<b>NON-ISCHAEMIC (RIGHT)</b>			
24hr	5	$0.27 \pm 0.11$	$152 \pm 42$
72hr	6	$0.20 \pm 0.10$	$238 \pm 34$
168hr	5	$0.18 \pm 0.07$	$186 \pm 25$
168hr SHAM	5	$0.20 \pm 0.07$	$154 \pm 32$

**Table 4.13.** Temporal [ $^3\text{H}$ ] PK 11195 binding changes in cortical brain tissues following left MCA occlusion in the mouse. Saturation binding parameters represent mean  $\pm$  s.e. mean.

\* $P < 0.05$  \*\* $P < 0.01$  (ANOVA, Dunnet's t-test).

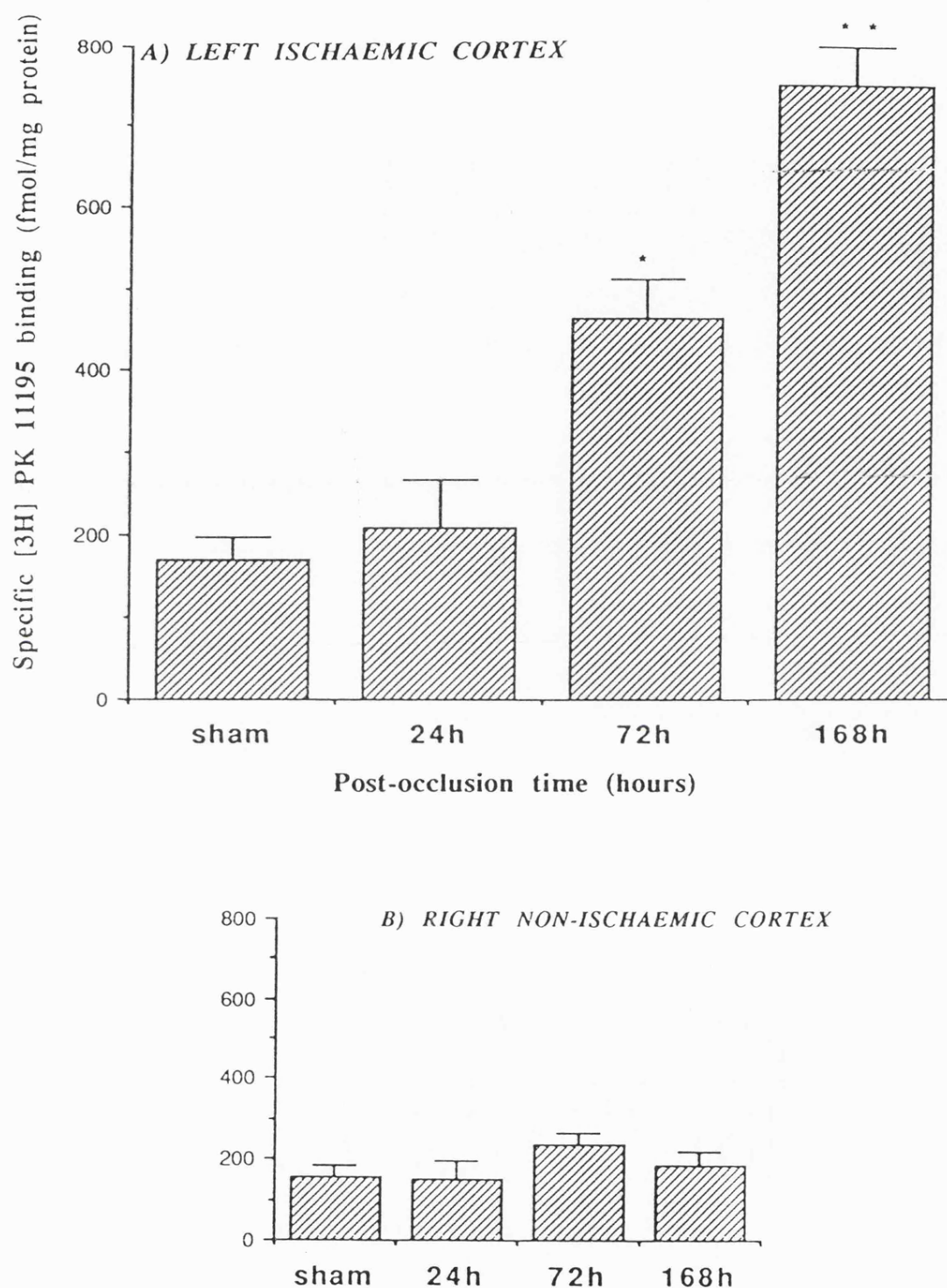


**Figure 4.7.** Temporal increase in the density of [ $^3\text{H}$ ] PK 11195 binding sites in mouse cortical tissue homogenates (A: left and B: right) following left middle cerebral artery occlusion. Values represent mean  $\pm$  s.e. mean of 5-6 determinations. (\* $p < 0.05$  \*\* $p < 0.01$  using ANOVA and application of Dunnet's t-test compared to sham control group)

**Table 4.14.**

NON-ISCHAEMIC RIGHT CORTEX		ISCHAEMIC LEFT CORTEX	
Kd (nM)	Bmax (fmol/mg)	Kd	Bmax
0.22 ± 0.04	289 ± 70	0.18 ± 0.03	1157 ± 89

**Table 4.14.** Ischaemia-induced increases in cortical  $\omega_3$  sites assessed by [ $^3\text{H}$ ] PK 11195 binding after left MCA occlusion in the mouse. Saturation binding parameters represent mean  $\pm$  s.e. mean of 6-8 separate determinations. The change in binding in left cortical tissue represents an increase of 300 % of the control non-ischaemic right cortex.

The localised nature of the infarcted area in this model was confirmed in preliminary experiments using 20  $\mu\text{m}$  coronal sections cut from the brains of ischaemic and non-ischaemic animals and the [ $^3\text{H}$ ] PK 11195 binding sites qualitatively assessed on autoradiograms. Figure 4.8. illustrates that the density of  $\omega_3$  sites is highly localised and markedly increased in the parietal cortex of the ischaemic hemisphere compared to the corresponding area in non-ischaemic controls.

#### ***4.4.3. MK-801 and RS 87476 attenuate the ischaemia-induced increase in $\omega_3$ sites following left MCA occlusion in the mouse.***

To validate the use of MCA occlusion in the mouse as a model of focal ischaemia, the neuroprotective potency of MK 801 was assessed, as other studies have shown this compound to be neuroprotective in other models of focal ischaemia (e.g. Park *et al.*, 1988a; 1988b; McCulloch, 1991). The effect of MK 801 in comparison with RS 87476 and nimodipine is shown in Table 4.15 and Figure 4.9. Cumulative data for vehicle control animals (n=30) indicated that, as in previous experiments, occlusion of the left MCA caused an increase in the density of  $\omega_3$  sites in the left ischaemic hemisphere without any effect on density in the non-ischaemic hemisphere from the same

**Figure 4.8.** [ $^3\text{H}$ ] PK 11195 autoradiography in mouse brain after left middle cerebral artery occlusion and 7 days recovery. Representative total binding to 20  $\mu\text{m}$  coronal sections labelled with 0.2 nM [ $^3\text{H}$ ] PK 11195 are illustrated. The ischaemia-induced increase in  $\omega_3$  sites is highly localised in the parietal cortex.

**Ischaemic**



**Non-Ischaemic**



group of animals. This increase represented 226 % of the level in the non-ischaemic right cortex. Table 4.15. and Figure 4.9. illustrate that both MK 801 and RS 87476, administered 500 µg/kg i.p. 30 min pre-occlusion, with follow up dosing every 8 hrs for 7 days (t.i.d.) significantly reduced the ischaemia-induced increase in  $\omega_3$  sites in the left ischaemic hemisphere compared to vehicle control animals.

LEFT ISCHAEMIC CORTEX	n	Kd (nM)	Bmax (fmol/mg protein)
SHAM CONTROL	5	0.20 ± 0.04	170 ± 28 **
LEFT MCA LIGATED	30	0.18 ± 0.02	858 ± 68
MK 801 (2)	6	0.11 ± 0.02	302 ± 21 **
NIMODIPINE (2)	5	0.30 ± 0.06	1229 ± 224
RS 87476 (1)	6	0.23 ± 0.03	382 ± 114 *
RS 87476 (2)	6	0.12 ± 0.01	348 ± 51 *
RS 87476 (3)	5	0.23 ± 0.02	187 ± 40 **
RIGHT NON-ISCHAEMIC CORTEX			
SHAM CONTROL	5	0.20 ± 0.03	154 ± 32
LEFT MCA LIGATED	30	0.18 ± 0.02	263 ± 21
MK 801 (2)	6	0.14 ± 0.01	240 ± 9
NIMODIPINE (2)	5	0.23 ± 0.04	325 ± 71
RS 87476 (1)	6	0.20 ± 0.03	226 ± 46
RS 87476 (2)	6	0.16 ± 0.01	242 ± 26
RS 87476 (3)	5	0.23 ± 0.04	185 ± 49

**Table 4.15.** Effect of MK-801, RS-87476 and nimodipine on the increase in the density of  $\omega_3$  sites in mouse cortical tissues following left MCA occlusion. Values represent mean ± s.e.mean for n determinations. All drugs were administered i.p. at 500 µg/kg. (1) single dose, 30 min pre-occlusion, (2) 30 min pre-occlusion + t.i.d. and (3) 15 min post-occlusion + t.i.d. Statistical significance for the decrease in ischaemic cortex (\* p<0.01, \*\*p<0.001, ANOVA, Dunnet's t-test) is given in comparison against left MCA ligated group.

As the above table shows, nimodipine was ineffective when administered under the dosing regimen used for MK 801. Conversely, RS 87476 was found to significantly attenuate the increase in  $\omega_3$  sites in the left cortex under a variety of different dosing

regimens, and potent neuroprotection was still conferred on post-occlusion administration. Whilst the comparative data in Table 4.15. gives an index of neuroprotection, it is difficult to assess drug potency in a quantitative manner. Some workers have attempted to circumvent this problem by an assessment of the % increase in the left ischaemic hemisphere against the corresponding increase in the right, i.e. as its own control (e.g. Gotti *et al.*, 1990), similar to the way in which control data has been expressed in the present experiments (Table 4.14.). This is not an appropriate way to quantify a drug effect when only the drug effect on the ischaemia-induced increase is to be measured. If the data in the next series of experiments is considered (see Table 4.16.), such analysis can lead to misleading interpretation of results. Consider the data with SR 33557. The control left ligated value is 849, the corresponding right value, i.e. its own non-ischaemic control, is 221. This represents an increase of 284%. For SR 33557 (1) the corresponding values are 775 and 320 representing an increase of 142%. These data imply SR 33557 to be effective although the ischaemic levels are not different. Thus, a small drug effect on the basal level of  $\omega_3$  sites in the corresponding non-ischaemic right hemisphere has a pronounced effect on the difference when expressed as % increase for left compared against corresponding right in the same animal, but it does not represent the drug effect on the ischaemia-induced increase. Therefore, transformation of the data representing a drug effect has been calculated in terms of % damage, calculated below:-

For the left MCA ligated group a 100% damage level was calculated as that due to ischaemia, thus:-

LEFT ISCHAEMIC (mean Bmax for group) - CORRESPONDING RIGHT (mean Bmax for group) = 100 % damage.

The % damage in the drug treated group could be expressed relative to this 100% level,

$$\frac{\text{DRUG GROUP(LEFT Bmax - RIGHT Bmax)}}{\text{LEFT MCA GROUP (LEFT Bmax - RIGHT Bmax)}} = X \%$$

For the data above this would correspond to  $(775-320)/(849-221)=0.72$  or 72% damage compared to control as 100%. By representation of the data in this way, as opposed to a direct comparison between the % change in  $\omega_3$  sites in ischaemic hemispheres and drug treated hemispheres, the attenuation of ischaemia-induced increases in  $\omega_3$  levels is apparent only for the drug effect on ischaemic related increases, rather than any change in basal levels that the drug may cause. However, such a representation does not lend itself to statistical analysis although it gives an indication of drug related changes occurring in the control level of sites if the efficacy of a compound appears to be different when the data is assessed by the two different approaches.

#### ***4.4.4. Comparative neuroprotection by other CEBs in the mouse MCA occlusion model.***

Having established potent neuroprotective properties for RS 87476 in the above series of experiments, the properties of flunarizine and SR 33557 were also examined. In this series of experiments, nimodipine was also examined at a ten fold lower dose than that used in the previous experiments, and administered post-occlusion, similar to other calcium antagonists, as the previous experiments indicated that neuroprotection could still be conferred with compounds on post-occlusion administration. Table 4.16 and Figure 4.9 illustrate that flunarizine (at 500  $\mu\text{g/kg}$ ) caused a significant reduction in the ischaemia-induced increase in  $\omega_3$  sites whilst SR 33557 was ineffective at both 50 and 500  $\mu\text{g/kg}$ . Nimodipine, however, in contrast to the previous experiments (at 500  $\mu\text{g/kg}$  pre-ischaemia) caused a significant reduction in the increase in  $\omega_3$  sites when administered at a dose level of 50  $\mu\text{g/kg}$  post-ischaemia. To test whether the effect of flunarizine may be due to its moderate dopamine  $D_2$  affinity, the selective dopamine  $D_2$  antagonist (+) butaclamol was examined at 500  $\mu\text{g/kg}$ , but was without effect at this dose.

LEFT ISCHAEMIC CORTEX	n	Kd	Bmax (fmol/mg protein)
LEFT MCA LIGATED	12	0.35 ± 0.03	849 ± 85
FLUNARIZINE (1)	5	0.21 ± 0.05	402 ± 21 *
SR 33557 (1)	6	0.32 ± 0.04	775 ± 75
SR 33557 (2)	6	0.34 ± 0.03	862 ± 126
NIMODIPINE (2)	5	0.31 ± 0.04	373 ± 68 *
(+) BUTACLAMOL (1)	6	0.36 ± 0.03	847 ± 82
<b>RIGHT NON-ISCHAEMIC CORTEX</b>			
LEFT MCA LIGATED	12	0.29 ± 0.04	314 ± 60
FLUNARIZINE (1)	5	0.21 ± 0.01	206 ± 29
SR 33557 (1)	6	0.29 ± 0.04	320 ± 21
SR 33557 (2)	6	0.35 ± 0.04	382 ± 36
NIMODIPINE (2)	5	0.31 ± 0.05	241 ± 69
(+) BUTACLAMOL (1)	6	0.29 ± 0.04	403 ± 47

**Table 4.16.** Effect of flunarizine, SR 33557, nimodipine and (+) butaclamol on the ischaemia-induced increase in  $\omega_3$  sites following left MCA occlusion in the mouse. Values represent mean  $\pm$  s.e. mean for n determinations. Compounds were administered i.p. at (1) 500  $\mu$ g/kg and (2) 50  $\mu$ g/kg 15 min post-occlusion with t.i.d. Statistical significance for the decrease in ischaemic cortex (\* $p$ <0.01, ANOVA, Dunnet's t-test) is given in comparison to the left MCA occluded group.

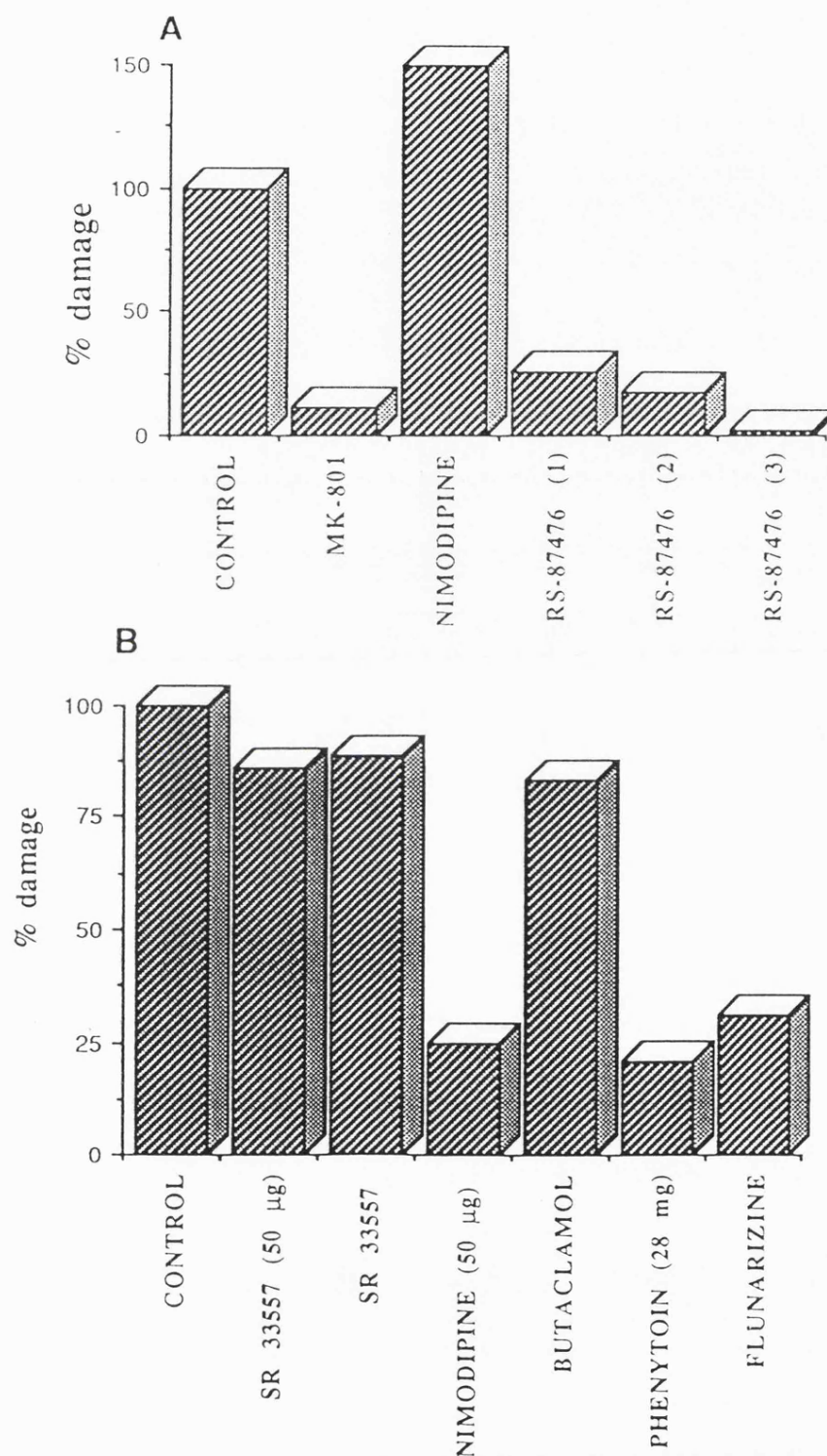
#### ***4.4.5. Phenytoin is a potent neuroprotective agent in the mouse MCA occlusion model.***

Data in the previous chapter showed that both RS 87476 and flunarizine interacted with neuronal Na<sup>+</sup> channels labelled by [<sup>3</sup>H] BTX with high affinity, with both compounds showing relatively low affinity for neuronal DHP sites labelled by [<sup>3</sup>H] PN 200-110. To examine the possible relevance of this affinity, phenytoin was examined in the mouse MCA occlusion model as this agent is thought to be an effective anti-convulsant through an interaction with voltage-dependent Na<sup>+</sup> channels (Rogawski &

Porter, 1990). On this basis, a dosing regimen was selected to match an effective anticonvulsant dose in other experimental models, and a dose of 28 mg/kg administered i.v. through the tail vein was chosen. The drug was administered 30 min post-occlusion with one further dose given 24 hrs later. The brain tissues from this series of experiments were not analysed by full saturation analysis, but at a single saturating concentration of [<sup>3</sup>H] PK 11196 (1.0 nM), although it was possible to express the % damage in the same way as described for the previous series of experiments. The effect of phenytoin on the ischaemia-induced increase in  $\omega_3$  sites is shown in Figure 4.10. and it can be seen that the compound produced a highly significant reduction in the density of  $\omega_3$  sites following left MCA occlusion compared to vehicle control.

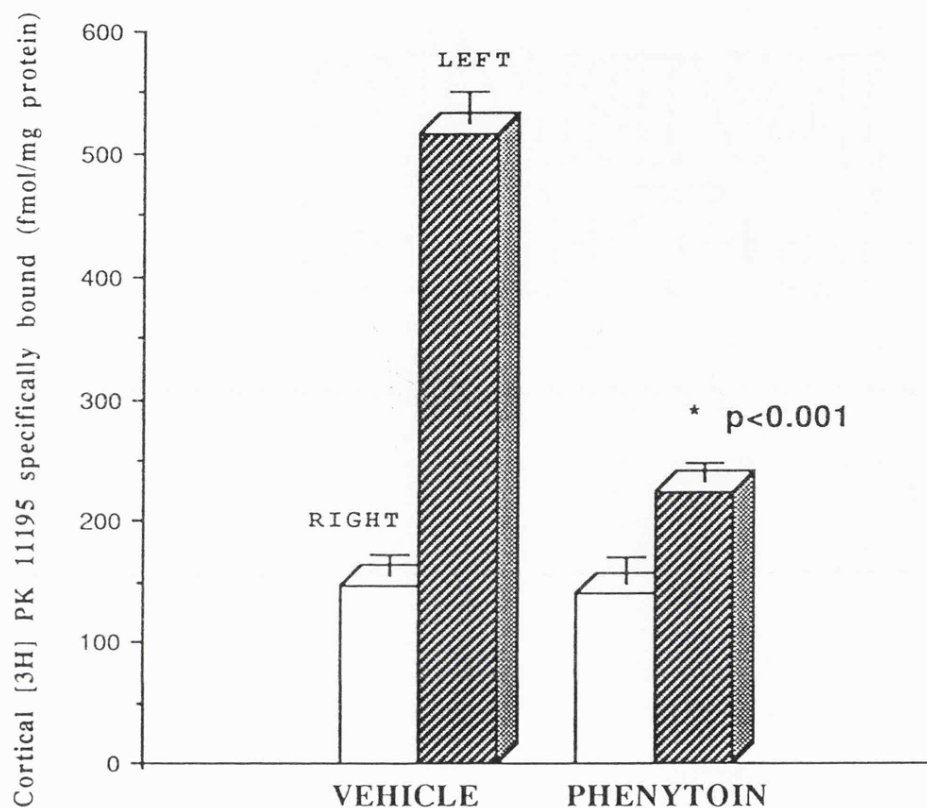
Thus, [<sup>3</sup>H] PK 11195 has been shown to be a sensitive indirect marker of neuronal damage due to the increase in  $\omega_3$  sites following forebrain and focal ischaemia. The mouse MCA model provided a useful and sensitive means of detecting potential neuroprotective agents. In this model, neuroprotection has been conferred for a range of compounds. RS 87476, flunarizine and MK 801 were all effective at the doses examined. SR 33557 and (+) butaclamol were ineffective, and nimodipine showed dose-dependent protection, being efficacious at lower, rather than higher doses.

Figure 4.9. Comparative neuroprotective potency of calcium antagonists in mouse MCA model of focal ischaemia



**Figure 4.9.** A. All drugs were administered at 500 µg/kg i.p. 30 min pre-ischaemia + t.i.d. dosing for 7 days, except RS 87476 (1), 500 µg/kg i.p. single dose pre-ischaemia and RS 87476 (3), 500 µg/kg i.p. 15 min post-ischaemia and t.i.d. dosing for 7 days. B. All drugs were administered 15 min post-ischaemia + t.i.d. dosing at 500 µg/kg i.p. unless indicated.

**Figure 4.10.** The protective effect of phenytoin in mouse MCA occlusion model



**Figure 4.10.** Phenytoin, 28 mg/kg i.v. (n=6 animals) or vehicle (0.1 ml, n=6) was administered via the tail vein 30 min post-ischaemia followed by one single dose 24 hrs later. Specifically bound [<sup>3</sup>H] PK 11195 was determined on individual cortical samples at a ligand concentration of 1.0 nM. The comparative protective effect of phenytoin, expressed in terms of % damage, is shown in Figure 4.9 (B). Statistical significance (\*p<0.001) for the level of binding sites in the ischaemic cortex from phenytoin treated group vs vehicle treated group (unpaired t-test) is shown.

## 4.5. Discussion

### 4.5.1. [ $^3\text{H}$ ] DHPs as neuronal markers ?

A unified hypothesis (Siesjo, 1981) that  $\text{Ca}^{2+}$  is the common mediator of cell death (Hass, 1981; Rothman, 1984) indicates a critical role for  $\text{Ca}^{2+}$  producing neuronal damage as a result of cerebral ischaemia; consequently, attenuation or a modification of this transmembranal flux into ischaemic cells with calcium antagonists may reduce the extent of ischaemic injury. If so, does neuronal protection result purely from an interaction with VOCs ?

Certainly evidence suggests a role for  $\text{Ca}^{2+}$  in ischaemic models *in vivo* (focal and forebrain models) and *in vitro*. Extracellular ionic measurements have indirectly implicated a large increase in intracellular  $\text{Ca}^{2+}$  during experimental ischaemia (Nicholson *et al.*, 1977; Harris *et al.*, 1981; Hansen, 1985). This phenomenon is well documented in cerebral ischaemia (see Siesjo, 1988; Siesjo & Bengtsson, 1989a). However, Yamaguchi *et al.* (1986) demonstrated that intracellular  $\text{Ca}^{2+}$  increased to a similar extent in a variety of different brain regions following forebrain ischaemia, although it is well established that these areas are clearly different in their selective vulnerability (Kirino, 1982; Suzuki *et al.*, 1983). This finding prompted several studies (Simon *et al.*, 1984; Dux *et al.*, 1987) which indicated a tendency for  $\text{Ca}^{2+}$  to normalise after ischaemia, with  $\text{Ca}^{2+}$  accumulation associated with longer post-ischaemic periods. Thus, both tissue and mitochondrial  $\text{Ca}^{2+}$  levels have been shown to be increased following ischaemia/reperfusion (Hossmann *et al.*, 1985; Deshpande *et al.*, 1987) although the exact temporal relationship between the influx of  $\text{Ca}^{2+}$  and apparent selective morphological injury is not unequivocal.

Evidence does however suggest that the secondary increase in cellular  $\text{Ca}^{2+}$  precedes morphological (CA1 neurone) changes (Deshpande *et al.*, 1987; Siesjo, 1988) such that the time course for tissue  $\text{Ca}^{2+}$  accumulation is closely related to the period of delayed neuronal death (Martins *et al.*, 1988). Observations with  $^{45}\text{Ca}^{2+}$  in gerbil forebrain ischaemia (Ikeda *et al.*, 1989) have demonstrated that  $\text{Ca}^{2+}$  accumulation was temporally associated with histological cell changes and showed that selectively vulnerable

(hippocampal CA1) brain areas showed an abnormally high uptake after the disappearance of the pyramidal neurones, possibly indicating a different mechanism for  $\text{Ca}^{2+}$  accumulation in selectively vulnerable areas. In models of focal ischaemia, changes in  $\text{Ca}^{2+}$  are dependent on the reduction of cerebral blood flow to the ischaemic tissue such that extracellular levels fall (Harris *et al.*, 1981; Harris & Symon, 1984) associated with increased intracellular levels (Rappaport *et al.*, 1987). This results partially from intracellular components releasing  $\text{Ca}^{2+}$  (Raichle, 1983) with intracellular levels becoming particularly elevated following reperfusion (Greenberg *et al.*, 1991).

*In vitro* models of ischaemia have demonstrated a marked dependence on extracellular  $\text{Ca}^{2+}$  for the production of neuronal injury (Rothman, 1983; Choi, 1988b) and consistent with *in vivo* findings, neuronal injury in tissue culture has been shown to be associated with delayed  $\text{Ca}^{2+}$  accumulation (Marcoux *et al.*, 1990). Given this overwhelming evidence of a role for  $\text{Ca}^{2+}$  in the ischaemic process, how will attenuation of cellular  $\text{Ca}^{2+}$  entry be beneficial?

It has been outlined in the introduction to this work that of the three types of VOC (L, T and N; Nowycky *et al.*, 1985), sites labelled by [ $^3\text{H}$ ] DHPs in brain tissue represent L-type VOCs (Miller, 1987). Brain ischaemia is associated with increased levels of extracellular  $\text{K}^+$  (Hansen, 1985; Siesjö & Bengtsson, 1989b) such that a possible route of  $\text{Ca}^{2+}$  entry under such conditions could be through L-type VOCs. There is a vast amount of evidence suggesting a role for glutamate (and associated  $\text{Ca}^{2+}$  entry through NMDA gated ion channels) as a mediator of ischaemic damage (Simon *et al.*, 1984; Choi, 1985; Rothman & Olney, 1986; Choi, 1988a; 1988b) although further  $\text{Ca}^{2+}$  entry via VOCs may result from cellular depolarisation following NMDA receptor activation (Siesjö, 1988).

This work has attempted to examine indirectly a role of L channels in ischaemia using [ $^3\text{H}$ ] DHP ligands. If these neuronal binding sites represent L channels, do they show plasticity or loss following ischaemia/reperfusion similar to other situations? A reduction in brain [ $^3\text{H}$ ] DHP sites has been demonstrated following kainic acid induced lesions in striatum (Sanna *et al.*, 1986; Skattebol *et al.*, 1988) and colchicine lesions in hippocampus (Cortes *et al.*, 1983). Other workers (Bolger *et al.*, 1987) have demonstrated

increases in hippocampal [ $^3\text{H}$ ] DHP binding following 6-OH dopamine lesions. Furthermore, neuronal DHP sites show plasticity in other disease states such as hypertension (Ishii *et al.*, 1983) and human brain [ $^3\text{H}$ ] DHP sites are decreased in areas associated with neuronal loss (Nishini *et al.*, 1986). DHP sites are also modified following experimental myocardial ischaemia (Nayler *et al.*, 1985; Gu *et al.*, 1988).

In the present studies no evidence was found for a change in [ $^3\text{H}$ ] DHP binding in membrane homogenates from cerebral cortex, striatum or hippocampus following brief (5 min) forebrain ischaemia and 7 days recovery regardless of the [ $^3\text{H}$ ] DHP used to label the sites, although a reversible reperfusion-induced change was detected in the cerebral cortex. Forebrain ischaemia in the rat following unilateral carotid artery occlusion has been claimed to cause a selective and reversible increase in hippocampal binding (Magnoni *et al.*, 1988). [ $^3\text{H}$ ] DHP binding sites are associated with CA1 neurones (Cortes *et al.*, 1984), and at this time hippocampal neurone loss is selective for CA1 and some neurones in the hilus (Kirino, 1982; Schmidt-Kastner & Freund, 1991). The failure to observe a change in binding parameters in hippocampal homogenates following 5 min forebrain ischaemia and 7 days recovery reflects the selective loss of only certain neurones in the total hippocampal homogenate which is unlikely to be detected.

The reversible increase observed in cerebral cortex at 24 hrs post-ischaemia is unclear, although  $^{45}\text{Ca}^{2+}$  autoradiography studies have implicated an involvement of brain areas other than the hippocampus following 5 min forebrain ischaemia in this model (Ikeda *et al.*, 1989) and the increase in cortical [ $^3\text{H}$ ] nimodipine sites observed following focal ischaemia in the rat is partially reversible (Hogan *et al.*, 1991). The observed change in cerebral cortex may therefore be indicative of other neuronal changes, since brief forebrain ischaemia has been shown to induce changes in muscarinic receptors and adenosine uptake sites in areas with minimal neuronal damage (Onodera *et al.*, 1987). Furthermore, 5 min forebrain ischaemia in the gerbil produces a significant decrease in 5-HT<sub>2</sub> binding sites in frontal cortex (Brown *et al.*, 1988). On account of those observations, and the relatively minor effect in whole cortex and other brain areas following a 5 min period of ischaemia, analysis of [ $^3\text{H}$ ] DHP sites in this work was restricted to frontal cortex for the examination

of longer periods of ischaemia.

It is worth emphasising, however, that the use of a 5 minute isoelectric period to verify a standard ischaemic insult in these experiments avoided some of the experimental artifacts that can attenuate neuronal injury from an ischaemic insult such as temperature (Kuroiwa *et al.*, 1990; Welsh *et al.*, 1990) and anaesthetic (Clifton *et al.*, 1989), especially as core temperature may not reflect variations in brain temperature during an ischaemic insult (Ginsberg & Busto, 1989). The failure, however, to detect a significant reduction in CA1 binding sites from autoradiographic studies after 5 min forebrain ischaemia is a reflection of the residual CA1 binding and the poor autoradiographic distinction of the CA1 pyramidal cell layer in these relatively small brain sections. Other studies of forebrain ischaemia in the rat have detected decreased binding as a function of pyramidal neurone loss, accompanied by the loss of apical dendrites and thus [ $^3\text{H}$ ] DHP binding sites in stratum radiatum have been shown to be reduced as a function of cell loss in stratum pyridamole (Onodera & Kogure, 1990).

In the present study, the finding that a more severe (10 min) period of ischaemia significantly lowered site density in hippocampus (with a lesser effect in frontal cortex) as soon as 4 hours post-ischaemia, with a further reduction at 72 hours, does demonstrate the presence of L channel VOCs in neuronal tissue. Previous studies have indicated an involvement of other structures following longer periods of ischaemia including damage to hippocampal CA3, hilar, caudate putamen, neocortical, thalamic and some cerebellar neurones (see Ginsberg & Busto, 1989; Schmidt-Kastner & Freund, 1991). Initial preliminary studies from these laboratories using gerbils that appeared to be inherently different in their susceptibility to neuronal damage (C. Calder, personal communication) demonstrated reversible changes in [ $^3\text{H}$ ] nitrendipine binding in whole cerebral cortex homogenates following 10 min forebrain ischaemia (Kenny *et al.*, 1986) although these findings were not confirmed in the present work with [ $^3\text{H}$ ] PN 200-110 in frontal cortex.

The loss of hippocampal binding sites following 10 min, but not 5 min ischaemia, would be consistent with effects of forebrain ischaemia on [ $^3\text{H}$ ] PN 200-110 binding sites in the rat (Onodera & Kogure, 1990) where it was found that the density of hippocampal

CA1, CA3 and dentate gyrus binding sites decreased as a function of reperfusion. In the present study it was found that the density of hippocampal sites was further reduced with longer periods of reperfusion, probably reflecting the loss of those neurones presenting as histologically abnormal post-ischaemia, and eventually becoming fully necrotic and lost with longer reperfusion periods (Kirino, 1982; Gill *et al.*, 1987). A decrease after longer reperfusion periods has been reported for a number of receptor types including hippocampal DHP, muscarinic, adenosine A<sub>1</sub> and 5-HT<sub>1A</sub> sites (Onodera *et al.*, 1987; Onodera & Kogure, 1990; Kenny *et al.*, 1991).

#### 4.5.2. [<sup>3</sup>H] PK 11195 as a marker of $\omega_3$ sites in forebrain ischaemia

From the above discussion it is apparent that radioligand binding assays to specific receptor sites, histological staining for specific neurone loss (or the use of specific enzyme assays for certain neurone types) can be a suitable approach for the quantification of ischaemia-induced cell loss. Thus, loss of pyramidal CA1 neurones (in gerbil forebrain ischaemia) and the graded loss of other neuronal types following forebrain ischaemia in other rodents has been extensively characterised (Pulsinelli & Brierley, 1979; Kirino, 1982; Pulsinelli & Buchan, 1988; Ginsberg & Busto, 1989), the protection of which has been attributed to a variety of putative neuroprotective agents including NMDA antagonists (Gill *et al.*, 1987) and calcium antagonists (Deshpande & Wieloch, 1986; Alps *et al.*, 1988; Beck *et al.*, 1988). However, cerebral ischaemia is heterogeneous in nature consisting of a multiple series of biochemical dysfunctions, with a cascade of metabolic and functional changes beyond the simple phenomenon of cell loss. As a consequence, some specific cell loss or necrosis can go undetected experimentally because of the lack of specific receptor ligands or enzyme markers. Certainly changes in [<sup>3</sup>H] DHP binding parameters were not sufficient to assess neuroprotective agents quantitatively. To this end, the present study has attempted to quantify ischaemic damage, in both forebrain and focal ischaemia, using an indirect approach, ultimately aimed at establishing a means whereby potential neuroprotective agents can be quantifiably assessed without measuring the attenuated loss

of selective neuronal populations. For these studies, the ligand [ $^3\text{H}$ ] PK 11195 has been successfully used.

PK 11195 is a peripheral-type benzodiazepine ligand, so called because the sites for these agents differ from the centrally acting benzodiazepine binding sites in terms of their anatomical and subcellular distribution (Benavides *et al.*, 1983; Anholt *et al.*, 1986). However, whilst termed peripheral, sites for these agents are found in the CNS (Basile & Skolnick, 1986) where a classification for them as  $\omega_3$  has been proposed to distinguish them from the sites of action of the centrally acting compounds such as diazepam and RO 15-1788 (Langer & Arbilla, 1988).

As a consequence of neuronal cell loss following cerebral ischaemia there is proliferation of astrocytes and glia (reactive gliosis) and an invasion of macrophages into ischaemic tissue (Dolman, 1986). Characteristic of  $\omega_3$  sites is their abundance on non-neuronal cell types, in particular microglia (Syapin & Skolnick, 1979; Zavala & Lenfant, 1987; Benavides *et al.*, 1988). Such criteria would appear to make [ $^3\text{H}$ ] PK 11195 an ideal candidate to quantify ischaemic damage and considerable evidence has accumulated to support this view. Thus, excitotoxic lesions have been shown to increase  $\omega_3$  site density following intra-striatal injection of excitatory amino acids (Schoemaker *et al.*, 1982; Benavides *et al.*, 1987; Benavides *et al.*, 1988) with the associated changes in the density of  $\omega_3$  sites more sensitive to detection using  $\omega_3$  ligands than assessing neuronal damage with neuronal marker enzymes. The density of  $\omega_3$  sites has been shown to be elevated following focal ischaemia in the cat and rat (Dubois *et al.*, 1988). More pertinently, these ligands have been postulated to be sensitive indicators of neuronal disease states in the human brain, as the density of sites is elevated in senile dementia of the Alzheimer's type (Owen *et al.*, 1983) and Huntington's disease (Schoemaker *et al.*, 1982). In the human,  $\omega_3$  sites are also greatly elevated in the infarcted brain regions of stroke patients, with a seven fold elevation in binding sites in the periphery of the infarcted area compared to normal brain tissue (Benavides *et al.*, 1988). The same workers have shown similar increases in  $\omega_3$  sites in the periphery of active plaques in multiple sclerosis patients, and in both cases this correlates well with the extent of the histological lesion (Benavides *et al.*,

1988).

The high affinity [ $^3\text{H}$ ] PK 11195 binding to rat brain tissues observed in this chapter is consistent with the pharmacology of  $\omega_3$  sites (Benavides *et al.*, 1983; Doble *et al.*, 1987; Langer & Arbilla, 1988). Thus, the affinity of  $\omega_3$  and non- $\omega_3$  compounds for this site is in agreement with previously reported data with the rank order of potency PK 11195 > RO 5-4864 > diazepam > flunitrazepam (LeFur *et al.*, 1983). Thus far,  $\omega_3$  sites have not been characterised in gerbil brain even though this species is extensively used as an ischaemic model, and on the basis of data in the present studies they have been shown to be different from those in rat and mouse brain. A previous study has reported species differences in the density and affinity of RO 5-4864 for  $\omega_3$  sites labelled in the cerebral cortex of various species (Awad & Gavish, 1987). The results from this study confirm those finding, with RO 5-4864, a structurally related  $\omega_3$  ligand, having an affinity in gerbil brain comparable to that in human brain tissues (Doble *et al.*, 1987). Despite the low affinity of RO 5 4864 in gerbil brain, the compound still maximally displaced [ $^3\text{H}$ ] PK 11195 binding to the same level as that by unlabelled PK 11195, and thus RO 5-4864 was still a suitable compound for defining non-specific binding in gerbil brain membranes.

Furthermore, the present studies have shown these differences to be highly species specific as opposed to tissue specific, as the properties in gerbil hippocampus are similar to those in cerebral cortex. Some previous studies have indicated differences between [ $^3\text{H}$ ] RO 5-4864 and [ $^3\text{H}$ ] PK 11195 based on thermodynamic binding studies (LeFur *et al.*, 1983). In the present studies there was no evidence of heterogeneity of binding sites based on the interaction of RO 5-4864 in competition studies as previously reported (Awad & Gavish, 1987), since Hill slopes did not deviate significantly from unity and a competitive interaction of RO 5-4864 was confirmed in saturation and kinetic experiments. However, the relatively low affinity of RO 5-4864 expressed for  $\omega_3$  sites in gerbil brain is an important finding as both [ $^3\text{H}$ ] PK 11195 and [ $^3\text{H}$ ] RO 5-4864 have been used as markers of neuronal damage (Owen *et al.*, 1983; Benavides *et al.*, 1987). The density and affinity of  $\omega_3$  sites in gerbil brain was examined 7 days after forebrain ischaemia to achieve maximal changes in [ $^3\text{H}$ ] PK 11195 binding due to reactive gliosis, astrocyte proliferation and

infiltration of macrophages following ischaemic cell loss. A similar time course for the loss of specific receptor sites ( $D_1$  receptors labelled by [ $^3H$ ]SCH 23390) and an increase in  $\omega_3$  sites labelled by [ $^3H$ ] PK 11195 binding has been shown previously (Dubois *et al.*, 1988).

Forebrain ischaemia and 7 days recovery significantly increased the level of  $\omega_3$  sites in hippocampus when binding was measured in brain homogenates, however autoradiograms of [ $^3H$ ] PK 11195 binding to ischaemic gerbil brain sections indicated a variability in the extent to which other brain areas showed elevated levels of  $\omega_3$  sites, although the increase was only consistent and significant in the CA1 subfield. Why should differences be noted?

Previous studies of forebrain ischaemia have indicated that gerbils are more resistant to unilateral than bilateral carotid artery occlusion (Ito *et al.*, 1975) probably due to the completeness of the circulus arteriosus (Berry *et al.*, 1975) such that those animals surviving single carotid occlusion with minor outcome had a prominent anastomoses between the proximal portion of the anterior cerebral arteries forming a midline azygous vessel. It has been further demonstrated (Alps *et al.*, 1985) that the level of neurotransmitter depletion following single artery occlusion was dependent on the extent to which the anterior artery connections were complete. It is thus possible that small differences in collateral blood supply (although normally considered negligible from the vertebral supply) could be an important factor in the degree of ischaemia resulting from bilateral carotid artery occlusion in a small population of animals. It has been noted above that some cortical receptor changes have been observed in this model at a time when there is no apparent evidence for histological cell changes (Kirino & Sano, 1984), although other workers have indicated an involvement of other brain areas in this model, on the basis of histological observations, only in those animals severely symptomatic of the ischaemic insult i.e. complete loss of CA1 neurones (Alps *et al.*, 1988). It is therefore possible that changes in [ $^3H$ ] PK 11195 binding, being a sensitive and indirect marker of ischaemic damage, might be indicative of cell change resulting from ischaemia, as cortical cell injury assessed by histological means appears to be associated with prolonged unilateral occlusion (Ito *et al.*, 1975) or longer periods of forebrain ischaemia (Pulsinelli *et al.*, 1982b; Wieloch, 1985).

Thus, in the present work, [ $^3\text{H}$ ] PK 11195 autoradiographic analysis indicated consistent damage in CA1, with an involvement of other brain areas only in those animals demonstrating the largest changes in CA1.

The above discussion has been based on indirect evidence that [ $^3\text{H}$ ] PK 11195 binding sites are elevated after neuronal damage due to glial proliferation (Benavides *et al.*, 1987). However, the increase in  $\omega_3$  density is less pronounced in gliotic dementia disease states (Schoemaker *et al.*, 1982; Owen *et al.*, 1983) than in ischaemic cerebrovascular disease and multiple sclerosis (Benavides *et al.*, 1988). Such conclusions are complicated by *in vitro* findings. Zavala *et al.* (1984) demonstrated that  $\omega_3$  sites were associated with macrophages, although lesion induced microglia retain similar surface properties to macrophages (Perry & Gordon, 1988). An attempt to correlate  $\omega_3$  sites with specific cell types following experimental cortical infarction has recently been made (see Myers *et al.*, 1991), and it was found that lesioned increased  $\omega_3$  sites correlated well with the spatial localisation and appearance of macrophages (marked by ED-1) whereas reactive astrocytes (stained by glial fibrillary acid protein) were outside the region defined by [ $^3\text{H}$ ] PK 11195.

The enrichment of [ $^3\text{H}$ ] PK 11195 binding sites in mitochondrial/synaptosomal P2 fractions is consistent with previous reports (eg. Basile & Skolnick, 1986) however the binding to synaptosomal fractions requires further characterisation, as many studies have shown that [ $^3\text{H}$ ] PK 11195 binding co-purifies with mitochondrial markers (Anholt, 1986; Anholt *et al.*, 1986; Basile & Skolnick, 1986; Doble *et al.*, 1987) with binding sites located on the outer mitochondrial membrane (Anholt *et al.*, 1986). Despite any differential labelling of subcellular components, however, the selectivity and affinity of a range of compounds was the same in purified mitochondria and crude membranes from rat and gerbil cortex, indicating that in rat brain the site in purified mitochondria is similar to that characterised in other peripheral tissues. In gerbil brain, even this purified mitochondrial site still retains a marked species difference. However, the association of  $\omega_3$  sites with mitochondrial membranes has largely been derived from experiments in peripheral tissue and there is no corresponding increase in mitochondrial markers in brain areas with elevated densities of  $\omega_3$  sites (Dubois *et al.*, 1988).

In this respect, gerbil brain tissue appears to be similar to that of human (Doble *et al.*, 1987) and cat (Benavides *et al.*, 1984) with high densities of binding sites associated with synaptosomal fractions and relatively low affinity expressed for  $\omega_3$  sites by RO 5-4864, possibly indicating a preferential neuronal location in these tissues. The use of specific cell markers (e.g. Petito *et al.*, 1989) would establish if the abundance of  $\omega_3$  sites in gerbil brain is due to a preponderance of particular cell types. On this basis, the high basal levels in gerbil brain may result in the elevation of  $\omega_3$  sites appearing less striking than in other animal models following ischaemia, and whilst the present work is the first to examine changes in  $\omega_3$  sites following forebrain ischaemia, a recent report (Benavides *et al.*, 1990), although not characterising these changes, has confirmed an increase in  $\omega_3$  sites in selectively vulnerable brain areas. In view of the lower basal levels of  $\omega_3$  sites in rat brain, this may prove to be a more useful species in quantifying  $\omega_3$  changes and their attenuation by potential neuroprotective compounds.

#### 4.5.3. $\omega_3$ sites following focal ischaemia in the mouse

Changes in  $\omega_3$  density following occlusion of the MCA in the mouse however is a robust and reliable model for the quantification of neuroprotective agents. Experimental determination of ischaemia-increased  $\omega_3$  density in ischaemic samples was reproducible and consistent between different experimental groups. During the progress of this work, a similar model has been independently characterised by another group (Benavides *et al.*, 1990; Gotti *et al.*, 1990). These workers have confirmed the temporal increase in  $\omega_3$  density following MCA occlusion, however the increase in binding density in ischaemic cortical tissue samples was less than that found in the present studies. Consistent with previous reports (e.g. Dubois *et al.*, 1988) these workers found that the density of  $\omega_3$  sites following MCA occlusion in the mouse was greatest in the border or penumbra of the infarcted area, with a more diffuse increase across the ipsilateral cortex. Thus, in the reported studies (Benavides *et al.*, 1990) all ipsi and contralateral cortical tissue were assayed. In these laboratories, tissue taken for assay was restricted to that in the ischaemic

zone and outlying penumbra, resulting in a more favourable increase in  $\omega_3$  density in ischaemic samples compared to corresponding controls. In most experiments, this increase was 250-350 % of the control value allowing a more accurate quantification of potential neuroprotective compounds. This is further enabled because of the low basal level of  $\omega_3$  sites in mouse cortex, similar to the rat and comparable to that in rabbit and guinea pig (Awad & Gavish, 1987). Similarly, the selectivity for  $\omega_3$  sites by peripheral and centrally acting benzodiazepines was comparable to that in the rat.

In this model, potent neuroprotective properties have been established for MK 801. This compound has previously been shown to be neuroprotective following focal ischaemia induced by occlusion of the MCA in rat and cat, the compound reducing infarct volume at all stereotaxic co-ordinates examined (Iversen *et al.*, 1989; McCulloch, 1991; Park *et al.*, 1988a; 1988b). The compound was effective when administered up to several hours post-ischaemia although these findings are not entirely consistent as other groups (see Simon, 1989) could find no protective effect of MK 801 under several dosing regimens. In the present studies MK 801 was found to be neuroprotective at a dose of 0.5 mg/kg when administered i.p. 30 min pre-ischaemia and t.i.d. dosing for 7 days. Similar levels of protection in this model with MK 801 (0.1 and 1.0 mg/kg i.p, dosed 5 min post-ischaemia with less maintenance) have also been found independently (Gotti *et al.*, 1990). The use of MK 801 has previously been thought to be favourable on the basis of use dependency since its interaction at the NMDA site is enhanced by the presence of glutamate (Kemp *et al.*, 1987), although the interaction of non-competitive (but not competitive) NMDA antagonists with NMDA receptors is voltage-dependent and their affinity is decreased with depolarisation (MacDonald *et al.*, 1987) and therefore the potency of these agents may be reduced during ischaemia.

Other agents which interact at other regulatory sites on the NMDA channel complex such as the polyamine site (Carter *et al.*, 1989) are also neuroprotective (Gotti *et al.*, 1990). An account of the neuroprotective properties for compounds acting at the NMDA channel complex has been described earlier (see 1.3.6.). Thus, in the present studies, MK 801 has verified the use of the mouse MCA model.

#### 4.5.4. Calcium antagonists as neuroprotective agents following MCA occlusion in the mouse

In initial experiments, no protection was conferred with nimodipine when the drug was administered at a dose of (500 µg/kg) pre-ischaemia with maintainance. However, a significant attenuation of the ischaemia-induced increase in  $\omega_3$  sites was observed when administered with a lower dose (50 µg/kg ) post-occlusion. A considerable variation in the effectiveness of nimodipine is also apparent based on the findings of other groups. Nimodipine has been reported to decrease infarct volume following MCA occlusion in the rat in some studies (Obana *et al.*, 1985; Germano *et al.*, 1987) but not others (Mohamed *et al.*, 1985; Kobayashi *et al.*, 1988). Such differences have been attributed to relative changes in cerebral blood flow (CBF), such that with similar infusion rates of nimodipine, a change in CBF was not found when the drug was administered post-occlusion (Gotoh *et al.*, 1986) but was increased when given pre- and during the occlusion period (Mohamed *et al.*, 1985). It is difficult to resolve the data obtained in the present study on this basis, as nimodipine was more effective when dosed post- rather than pre-ischaemia, and post-ischaemic administration has been reported to be dose-dependent, with significant protection only afforded at high concentrations in this model (Gotti *et al.*, 1990). Nevertheless, DHPs have been reported to be effective in focal ischaemia when administered post-occlusion (see Ginsberg *et al.*, 1991). It is possible that a fine balance exists for these agents when protection is a direct consequence of favourable changes in local CBF. Indeed whilst the majority of studies have attributed the beneficial effects of nimodipine to increases in CBF (see Wauquier *et al.*, 1988) other studies have shown that nimodipine causes hypofusion in some brain areas and hyperfusion in others (Smith *et al.*, 1983). At doses similar to those effective in the present study, nimodipine did not change local CBF in rat hippocampal subfields (Nuglisch *et al.*, 1990), although this effect may be different in the territory of the MCA in mouse cortex and it would be anticipated that such

effects would be dose-dependent. In models of global ischaemia extensive investigations with nimodipine (see Hossmann, 1989) have shown essentially no protection of neuronal populations (eg Vibulsresth *et al.*, 1987; Alps *et al.*, 1988; Pashen *et al.*, 1988). On the other hand, nicardipine, which belongs to the same group of calcium antagonists as nimodipine is effective in forebrain ischaemia models (Alps & Hass, 1987; Alps *et al.*, 1988). This latter point is well illustrated with flunarizine.

Flunarizine is well documented to protect neuronal populations in models of forebrain ischaemia (Deshpande & Wieloch, 1986; Van Reempts *et al.*, 1987; Alps *et al.*, 1988) although the study by Beck *et al.* (1988) showed that whilst cortical CBF increased post-ischaemia this was not the case in the hippocampus where protection was conferred. As outlined in the introduction to this thesis, such results indicate that protective effects conferred by this class of drug result from a direct interaction with ischaemic brain tissue. Similar findings have also been reported with RS 87476 in a 4 vessel occlusion model of forebrain ischaemia in rat (Alps *et al.*, 1990). It is difficult to resolve some findings with calcium antagonists in models of ischaemia, since many compounds have properties at other receptor and ion channel sites, for example (S)-emopamil decreases infarct volume after MCA occlusion (Ginsberg *et al.*, 1991) although this compound also has affinity for 5-HT<sub>2</sub> receptors. In this respect, it is also difficult to resolve the potent neuroprotective properties of flunarizine and RS 87476 on the basis of their interaction as calcium antagonists.

From the results obtained in the previous chapter, RS 87476 has been demonstrated to be a relatively weak calcium antagonist, and on the basis of several *in vitro* approaches can be classified with other class III antagonists. Based on calcium antagonist affinity this class of agent, as demonstrated with flunarizine, would be unlikely to have marked haemodynamic effects at the concentration used in this work, however at the same doses used to confer protection with MK 801, RS 87476 and flunarizine were protective. Furthermore, neuroprotection was conferred with both agents when administered post-occlusion, and with RS 87476 by a single dose administered pre-ischaemia. These findings have been recently confirmed and extended (Kucharczyk *et al.*, 1991) where RS 87476 has

been found to reduce infarct size in a cat model of unilateral MCA occlusion with infarct size reduced by up to 88%. Nicardipine has also been reported to markedly reduce infarct volume in this model (Kucharczyk *et al.*, 1989).

The finding that phenytoin was effective in this model has confirmed the previous finding that neuroprotection can be achieved with agents other than NMDA antagonists or calcium antagonists. On the basis of data obtained in the present experiments, coupled with other reported findings, it would appear that affinity for L-type VOCs (as based on [<sup>3</sup>H] calcium antagonist binding studies) probably relates to likely improvements in post-ischaemic hypofusion. However, other relatively weak calcium antagonists and some high affinity dihydropyridines appear to be consistently protective, indicating that these compounds may interact with the ischaemic process directly. Thus far, there are no reported data for high affinity interactions with any NMDA receptor subtypes or L-type VOCs for phenytoin, and therefore neuroprotection with this compound would appear to result from some other mechanism. In this respect, the efficacy of phenytoin in the mouse MCA model was achieved at a dose level similar to its anticonvulsant profile (McNamara *et al.*, 1989). The same dose has been shown to be effective in reducing infarct volume following MCA occlusion in the rat (Boxer *et al.*, 1990).

Several conclusions can be made on the basis of the data obtained in this chapter. Firstly, it would appear that affinity for the L-type VOC is not a requirement for a neuroprotective compound. Secondly, a variety of compounds that show affinities for Na<sup>+</sup> channels appear to be neuroprotective, and phenytoin has been postulated to be anticonvulsant through this mechanism.

Thus, in summary, by means of a robust, focal ischaemia model in the mouse, neuroprotection has been demonstrated by compounds other than NMDA antagonists. The present studies have also demonstrated that with high affinity DHPs, efficacy is inversely dose-dependent. The potent neuroprotective properties demonstrated for several class III calcium antagonists, devoid of major haemodynamic complications, might render these agents to be effective treatments of acute ischaemic stroke.

---

## **Chapter Five.**

### **An assessment of neuroprotection in the rat *in vitro* hippocampal slice**

## 5.1. Introduction.

The data in the preceding chapter demonstrated several types of compound to be neuroprotective *in vivo*, and an interaction with ionic homeostasis was discussed in relation to the possible mechanism whereby these agents may confer protection against ischaemic damage. In this chapter neuroprotective properties will be assessed in an *in vitro* model of cerebral ischaemia, using the rat hippocampal slice preparation (Figure 5.1.). *In vitro*, brain slices retain many of the biochemical and electrophysiological properties of the intact brain, including synaptic transmission. In the present series of experiments, synaptic transmission was assessed by measuring evoked potentials in the CA1 pyramidal layer of the hippocampus in response to afferent stimulation. In the *in vitro* hippocampal slice, orthodromic stimulation of the Schaffer collateral/commisural pathway results in the synchronous firing of many CA1 pyramidal cells, and when measured extracellularly, results in the so-called 'population spike'. The sharp negativity of the response represents the summed action potentials of many CA1 pyramidal cells simultaneously firing and when prepared appropriately, such extracellular potentials measured in response to activation of apical dendritic synapses via the Schaffer collaterals are similar to potentials measured in the intact animal (Andersen, 1981). In this experimental model, ischaemic conditions can be mimicked by the use of a hypoxic, low glucose superfusate. These experimental conditions result in the rapid failure of synaptic transmission as indicated by the loss of the population spike recorded extracellularly in the hippocampal CA1 pyramidal cell layer (Lipton & Whittingham, 1984).

Several aspects of this thesis have already addressed the well documented observation that certain neuronal populations appear selectively vulnerable to experimental ischaemia or seizure states, with the CA1 region of the hippocampus being the most vulnerable (Pulsinelli *et al.*, 1982; Griffiths *et al.*, 1983; Schmidt-Kastner & Freund, 1991). During ischaemia, it has been claimed that the excessive release of glutamate is a causative factor leading to  $\text{Ca}^{2+}$  dependent neuronal death (Benveniste *et al.*, 1984; Siesjo, 1988; Garthwaite, 1989). In particular, a variety of studies have indicated a failure of  $\text{Ca}^{2+}$  homeostasis to be important in the longer term neuronal damage associated with hypoxic insults in hippocampal slices (Kass & Lipton, 1986; Lipton & Lobner, 1990). Therefore, given that the primary excitatory input into CA1 is glutamatergic (Malthe-Sorensen *et al.*,

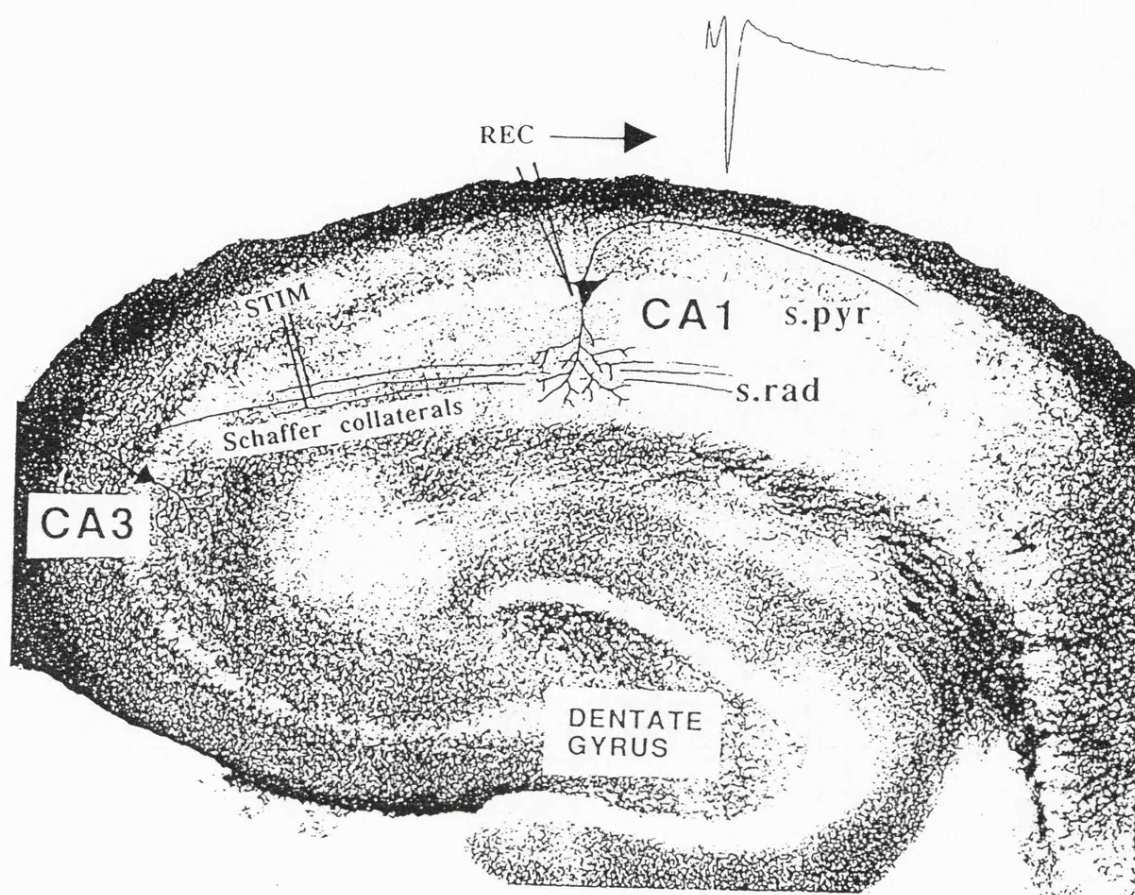


**Figure 5.1.** The *in vitro* hippocampal slice with diagrammatical illustration of stimulating and recording electrode positions in stratum radiatum (s.rad) and stratum pyramidale (s.pyr) respectively.

1979) the hippocampal slice provides an ideal means of quantifying synaptic function and its loss through hypoxic deprivation of metabolic support.

In hippocampal slices, hypoxia leads to a lack of ion homeostasis that appears to precipitate an intense neuronal depolarisation, similar to the ionic changes associated with spreading depression (Siesjo, 1988; Siesjo & Bengtsson, 1989b; Aitken *et al.*, 1991). Loss of synaptic transmission in the hippocampus is exquisitely sensitive to hypoxia and this has been attributed to the functional loss of ATP-dependent ionic pumps (Lipton & Whittingham, 1982; Kass & Lipton, 1986) and the subsequent failure of ionic homeostasis (Hansen, 1985). In this respect it is well established that decreases in the level of glucose and increases in temperature have deleterious effects on slice function compromised by hypoxia (see Lipton & Whittingham, 1984; Schurr & Rigor, 1989). Consequently, initial efforts in this chapter were aimed at establishing a standard 'ischaemic' insult resulting in non-recovery of synaptic function, constructed such that the potential protective effects of compounds could be detected.

Given that changes in ionic homeostasis and the excessive release of excitatory amino acids have been postulated to be causative in the events leading to ischaemic damage, there have been several reports of agents which reduce hypoxic injury in hippocampal slices, in that they allow the recovery of synaptic transmission following hypoxia. However, findings have not been consistent. Aitken *et al.* (1988) could find no evidence for a protective effect of competitive NMDA antagonists against the latency time to spreading depression or % slice recovery, whilst Rader & Lanthorn, (1989) have reported that NMDA antagonists shorten the total time of depolarisation. Somjen *et al.* (1990) suggested that the ability of compounds to protect against hypoxia-induced transmission failure was dependent on their ability to shorten the duration of depolarisation. However, potential and ionic changes as assessed by intracellular and ion sensitive electrodes suggest that the initial sequence of events leading to synaptic failure is not due to depolarisation (Sick *et al.*, 1987). Whilst this occurs with longer hypoxic periods, it appears that the initial synaptic failure may be due, at least in part, to neuronal hyperpolarisation with a resultant decrease of neuronal excitability. Intracellular recordings in CA3 hippocampal neurones have demonstrated a hypoxia-induced hyperpolarisation, associated with an increased K<sup>+</sup> conductance, to be a cause of synaptic transmission failure, such that Mourre *et al.* (1989) were able to demonstrate that this hyperpolarisation could be blocked by glibenclamide, a compound which blocks ATP-dependent K<sup>+</sup> channels. The time course for depolarisation

in the hippocampal slice (Sick *et al.*, 1987; Grigg & Anderson, 1990) has been shown to correlate well with the time course for changes in extracellular  $K^+$  in ischaemic brain (see Hansen, 1985). As the extent of this later depolarisation may be related to the non-recoverability of the slice, and the resemblance to the changes in ionic homeostasis during ischaemia *in vivo*, the hippocampal slice renders itself an ideal model to examine the effects of compounds in an *in vitro* model of ischaemia.

## 5.2. Methods.

### 5.2.1. Preparation of rat hippocampal slices.

The data in this series of experiments were derived from a total of 56 slices taken from 39 male Sprague-Dawley rats (200-300 g). Rats were killed by decapitation and the brain was carefully removed and placed in ice cold ( $4^{\circ}\text{C}$ ) oxygenated (95%  $\text{O}_2$  / 5%  $\text{CO}_2$ ) artificial cerebrospinal fluid (ACSF). The composition of ACSF used for slice preparation and holding the slices prior to experimental recording was (in mM): NaCl (118), KCl (3),  $\text{NaH}_2\text{PO}_4$  (1.25),  $\text{NaHCO}_3$  (25), D-glucose (10),  $\text{CaCl}_2$  (2),  $\text{MgCl}_2$  (1.3). Hippocampi were dissected from the cerebral hemispheres and mounted against agar blocks on a detachable metal platform. Hippocampi were fixed to the base of the metal platform with cyanoacrylate adhesive. The metal platform was then immersed in ice cold ACSF and 500  $\mu\text{m}$  transverse sections were cut with a Vibroslice (Campden Instruments). Slices were then immediately transferred to a holding chamber containing oxygenated ACSF at room temperature. In all experiments slices were held for at least 1 hour prior to transfer to the recording chamber. Slices were transferred to the recording chamber (5 ml volume) with a wide-bore pipette and placed on a nylon mesh mounted on a plexiglass grid. In the recording chamber slices were fully submerged in superfusate and secured by sandwiching them between the nylon mesh and a second mesh mounted on a moveable basket from above. In all experiments the slices were superfused with ACSF at a flow rate of 8-10 ml / min.

### 5.2.2. *Establishment of 'population spikes'.*

Bipolar stimulating electrodes were placed in stratum radiatum and recording electrodes (1-2 megohm, 4M NaCl) were placed directly above the CA1 pyramidal cell layer. The recording electrodes were made from glass (GC120; Clark Electromedical), pulled on a Sutter P-87 micropipette puller, with the tip broken back under microscopic control to produce an electrode with a tip diameter suitable for extracellular recording ( $\sim 1\mu\text{V}$ ). The extracellular response elicited in the CA1 pyramidal cell layer due to concentric bipolar stimulation of the Schaffer collateral pathway is a 'population spike'. Stimulating current was delivered once every 10s (pulse width 0.1-0.3 msec) and the optimal amplitude of the population spike was achieved by slowly tracking down into the CA1 pyramidal cell layer in 10  $\mu\text{m}$  steps by means of a Burleigh 6000 Micropositioning System (Burleigh Instruments). After establishment of a maximal response, the stimulus intensity was adjusted to elicit a population spike between 75 and 80% of the maximal amplitude ( $>1.5\text{ mV}$ ). The evoked population spike was monitored on an oscilloscope, digitised, and saved onto floppy disk via an analogue to digital converter (Cambridge Electronic Design 1401) controlled by software (Signal Averager, version 5.1) for later analysis. The peak negativity of the population spike amplitude was recorded via a sample and hold circuit (Firbank Electronics) and, together with the DC potential, was continuously displayed on a chart recorder for permanent record.

### 5.2.3. *Establishment of a standard 'ischaemic' protocol.*

Initial experiments were designed to establish a period of experimental hypoxia (induced by changing the superfusate to hypoxic ACSF gassed with 95%  $\text{N}_2$  / 5%  $\text{CO}_2$ ) with modifications to pre-incubation period, temperature, glucose concentration and the period of hypoxia which resulted in reproducible non-recovery of synaptic transmission in the slice after a given period in hypoxic ACSF. To maintain the slices in optimum condition in the holding chamber, in all experiments the glucose level in the ACSF for preparation and holding the slices was 10 mM. The period of hypoxia examined in this series of experiments was 10 min. As Figure 5.2. illustrates, when this period of hypoxia was examined in the presence of 10 mM glucose, with the slices maintained in the recording chamber at  $32^\circ\text{C}$ , synaptic activity returned in all slices tested ( $n=4$ ) within 10 min of

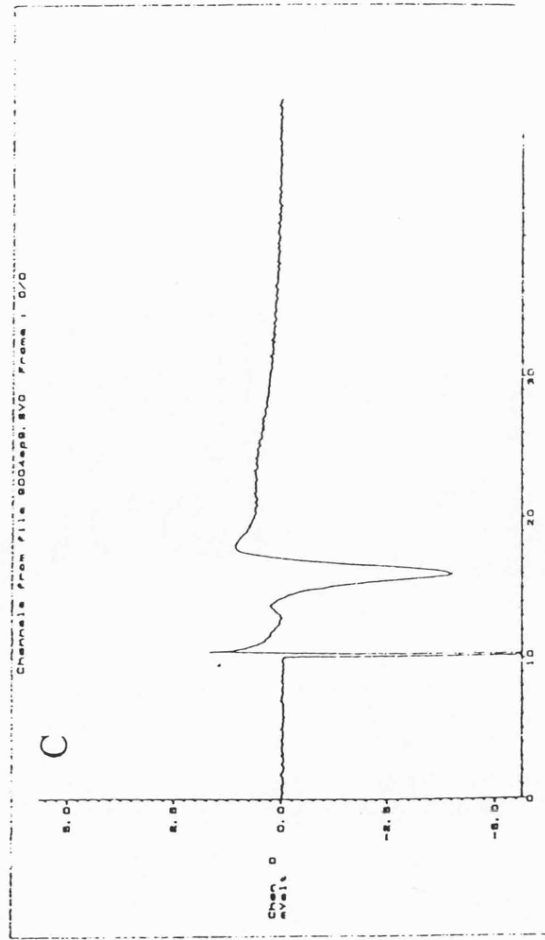
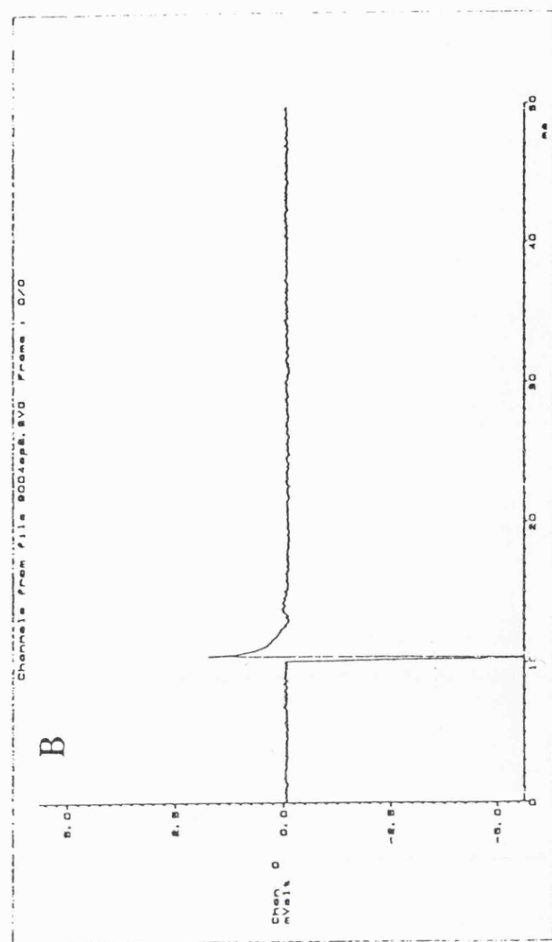
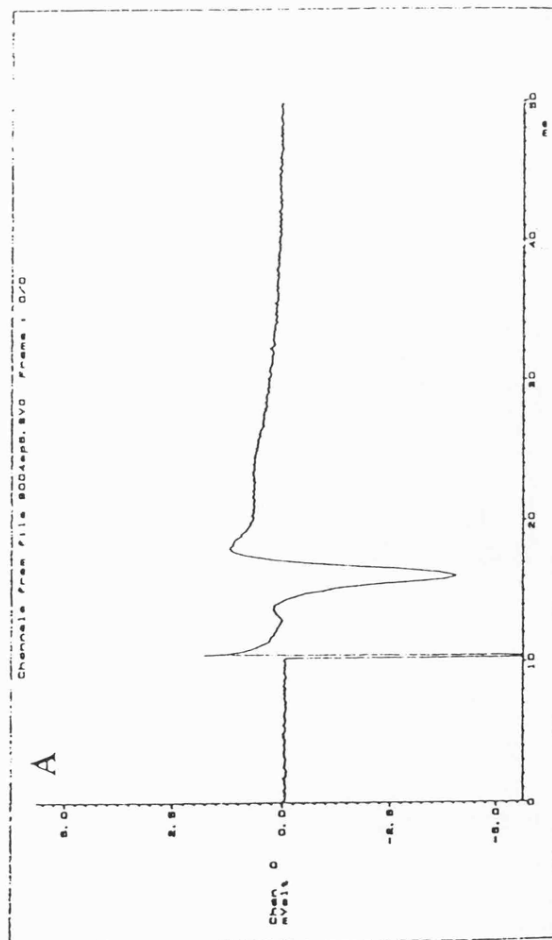


**Figure 5.2.** Hypoxic changes in the population spike at 320C with superfusates containing 10 mM glucose. A. Pre-hypoxic control. B. After 5 min hypoxia. C. Recovery of the population spike 10 min post-hypoxia.

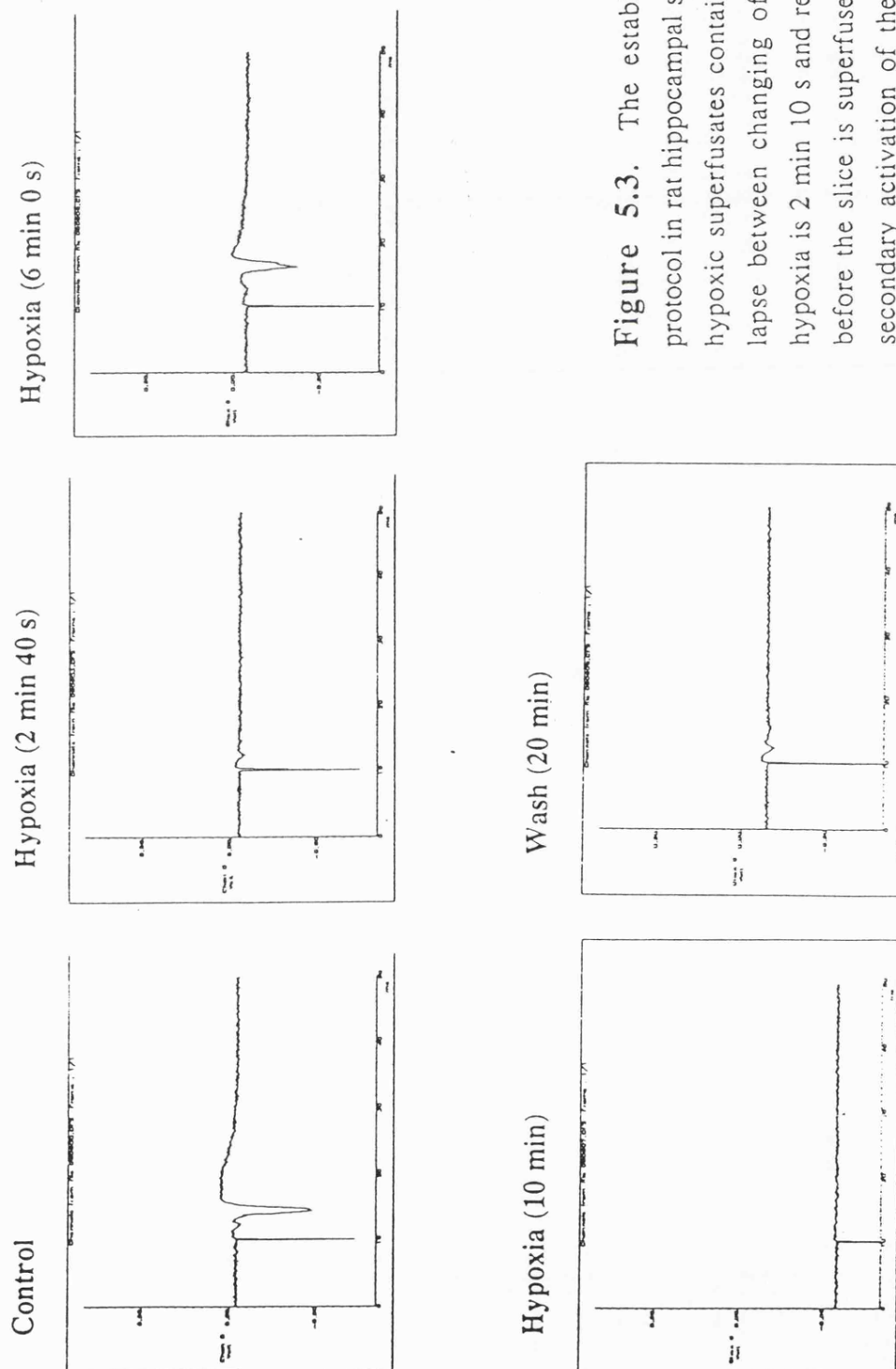


**Figure 5.3.** The establishment of a control hypoxic protocol in rat hippocampal slices at 35°C, with normoxic and hypoxic superfusates containing glucose at 4mM. The time lapse between changing of superfusates and the onset of hypoxia is 2 min 10 s and represents the tubing "dead space" before the slice is superfused with hypoxic ACSF. Note the secondary activation of the population spike at 6 min and secondary failure associated with a fall in DC potential. After 20 min post-hypoxia the DC potential returns close to control although the slice is synaptically inactive.

return to normoxic ACSF following hypoxia. In other experiments, with both normoxic and hypoxic superfusates containing a lower glucose concentration (4 mM) and with slices still maintained at 32°C, synaptic activity still recovered in all slices tested (n=5).

However as Figure 5.3. illustrates, when the temperature of the superfusate was increased to 35°C, with normoxic and hypoxic superfusates both containing 4 mM glucose (osmotically balanced with NaCl) the spike underwent a predictable sequence of events during, and after, the hypoxic period. After establishment of a stable, control response, on changing to the hypoxic superfusate, the spike initially disappeared, reappeared and then disappeared a second time. This secondary failure was not recoverable with a 20 min period in normoxic ACSF. It was also apparent from this series of experiments that secondary failure of the population spike was temporally related to a change in the extracellular DC potential which exhibited a rapid negative deflection (corresponding to intracellular depolarisation)

Thus, a reproducible hypoxic protocol was established. In all subsequent experiments, slices were cut and maintained in ACSF (10 mM glucose) for at least 1 hr as described. The slices were transferred to the recording chamber maintained at 35°C with all superfusates now containing 4 mM glucose. On establishment of a stable pre-hypoxic submaximal population spike the slice was left for 20-30 min (control or drug incubation period). The normoxic superfusate was then replaced with hypoxic ACSF for 10 min and then normoxic superfusate was returned for a 20 min period, after which the slice was then discarded.

In the following experiments, the incubation time for all drugs used was 20 min and none of the drugs examined had any effect on the amplitude of the pre-hypoxic population spike compared to control. The concentrations of the compounds examined were chosen on the basis of previously reported efficacy in various *in vitro* models. Thus, NMDA antagonists (CPP and (+) MK 801 )were examined at 10  $\mu$ M since this concentration of MK 801 has been reported to be effective in a similar hypoxic hippocampal slice model (Grigg & Anderson, 1990). The concentration of calcium antagonists used (nifedipine and fluspirilene) was also 10  $\mu$ M. Whilst this concentration is in excess of the  $K_i$  for their respective binding sites labelled by [ $^3$ H] calcium antagonists, this concentration of a DHP (nifedipine) has been shown to attenuate the slow neurotoxicity in cultured neurones induced by a depolarising agent, AMPA (Weiss *et al.*, 1990). To examine the effect of phenytoin, a concentration was chosen (20  $\mu$ M) that had previously

been shown to be active in attenuating epileptiform bursting in rat hippocampal slices through an interaction with Na<sup>+</sup> channels (Ashton *et al.*, 1986).

### 5.3. Results.

#### *5.3.1. The effect of NMDA antagonists and calcium antagonists on population spikes during and after 10 min hypoxia.*

In all control slices (n=18) the population spike underwent the sequence of events illustrated in Figure 5.3. After the primary failure, the time to secondary activation was  $185 \pm 31$  s (Table 5.1) and the duration of secondary activation was  $84 \pm 8$  s. Following secondary failure of the population spike recovery did not occur in any of the control slices examined.

In the presence of CPP (n=4, 10 $\mu$ M) it was found that the time of secondary activation was longer and significantly different ( $p < 0.05$ , unpaired t-test) compared to control (Table 5.1). In CPP treated slices, synaptic activity returned in all slices examined. When examined at 20 min post-hypoxia, the amplitude of the population spike was not significantly different from control. As Table 5.1. illustrates, in the presence of 10  $\mu$ M (+) MK-801 the sequence of events was similar to that observed with CPP, in that the period of secondary activation was longer (although not statistically significant) and synaptic activity, assessed by population spike amplitude, returned to a level of  $68 \pm 21$  % of the control spike at 20 min post-hypoxia.

However, neither 10  $\mu$ M nitrendipine (n=5) nor 10  $\mu$ M fluspirilene (n=4) allowed synaptic recovery of slices when examined up to a period of 20 min hypoxia. In the presence of nitrendipine, the secondary activation time was similar to that measured in control slices, whilst in the presence of fluspirilene secondary activation was short, and in two slices was not observed at all.

#### *5.3.2. The effect of phenytoin on population spike parameters and slice viability after 10 min hypoxia.*

Table 5.2. shows the effect of 20  $\mu$ M phenytoin (n=6) on population spike parameters compared with vehicle control (n=6, 0.1% polyethyleneglycol 300, 0.02 %

Incubation	Time to 2 <sup>o</sup> activation	Time of 2 <sup>o</sup> activation	Return of synaptic activity post-hypoxia	Slice recovery
Control	185 ± 31	84 ± 8	-	0 / 18
10 µM (+) MK 801	179 ± 30	168 ± 40	726 ± 120	4 / 4
10 µM CPP	252 ± 42	306 ± 96*	612 ± 72	4 / 4
10 µM nitrendipine	189 ± 24	83 ± 18	-	0 / 5
10 µM fluspirilene	-	< 30	-	0 / 4

**Table 5.1.** The effect of hypoxia on population spike parameters in the absence (control) and presence of various drugs. Values represent the time (s) to secondary activation of the population spike after primary failure, duration of secondary activation (s), the time taken (post-hypoxia) for the return of synaptic activity (s) and the number of slices recovering from the hypoxic insult. Data represents the mean ± s.e. mean (\*p<0.05 compared to control).

Incubation	Time to 2 <sup>o</sup> activation	Time of 2 <sup>o</sup> activation	Return of synaptic activity post-hypoxia	Slice recovery
Vehicle control	156 ± 12	78 ± 24	-	0 / 6
20 µM phenytoin	288 ± 48*	228 ± 36**	499 ± 66	4 / 6 <sup>1</sup>

**Table 5.2.** The effect of hypoxia on population spike parameters in the absence (vehicle control, n=6) and presence of 20 µM phenytoin (n=6). Values represent the time (s) to secondary activation of the population spike after primary failure, duration of secondary activation (s), the time taken (post-hypoxia) for the return of synaptic activity (s) and the number of slices recovering from the hypoxic insult. Data represents the mean ± s.e. mean (\*p<0.05, \*\*p<0.01 compared to control).<sup>1</sup> two slices exhibiting < 20% recovery, four slices exhibiting recovery >100%.

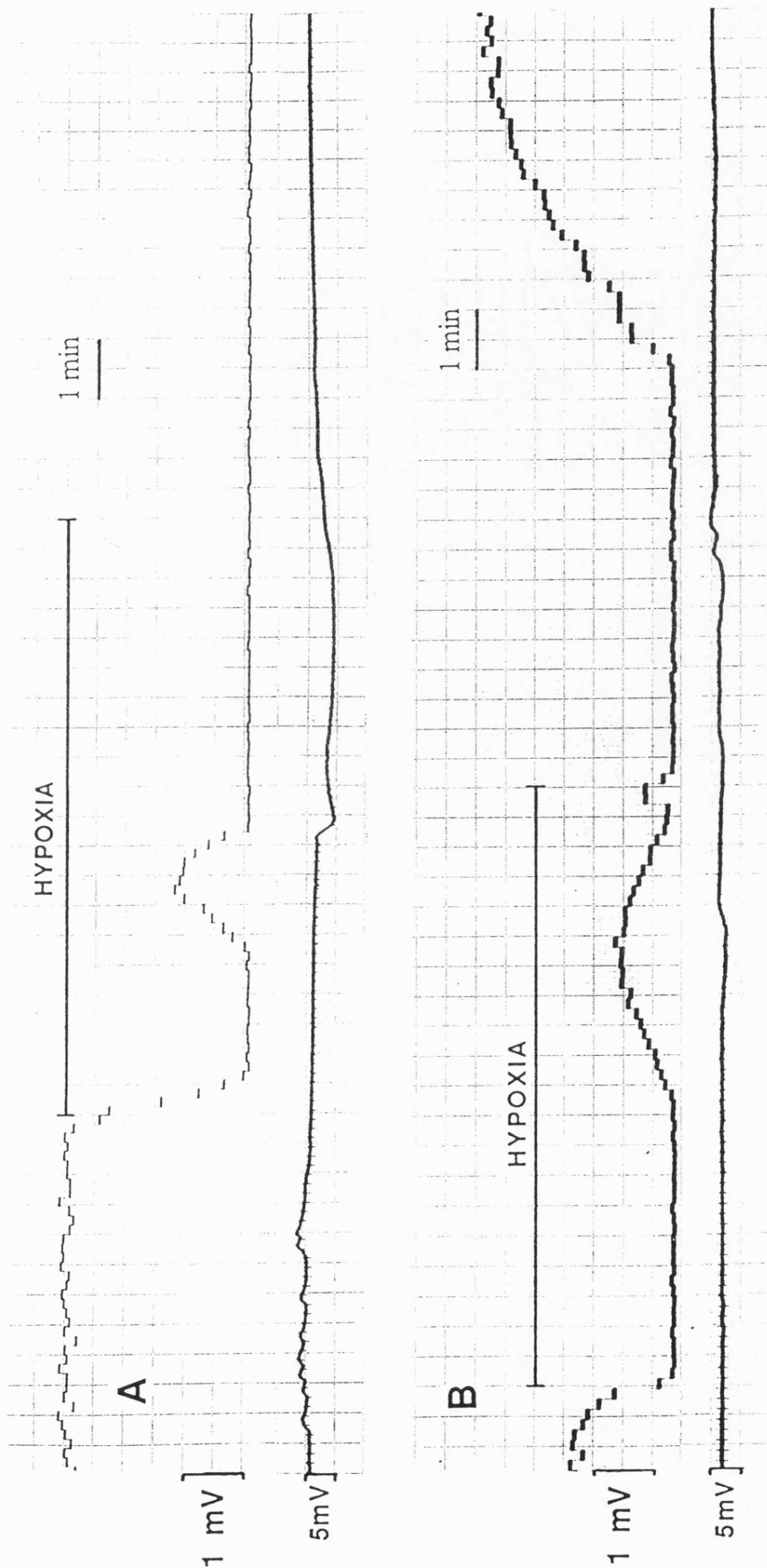


**Figure 5.4.** The effect of hypoxia in A) the absence of phenytoin (control) and B) the presence of 20  $\mu$ M phenytoin. The upper traces show the peak negativity of the population spike amplitude and the lower traces show the corresponding DC potential output from the recording electrode. Note the negative DC potential change associated with secondary failure of the population spike in the control, but not in the phenytoin treated slice.

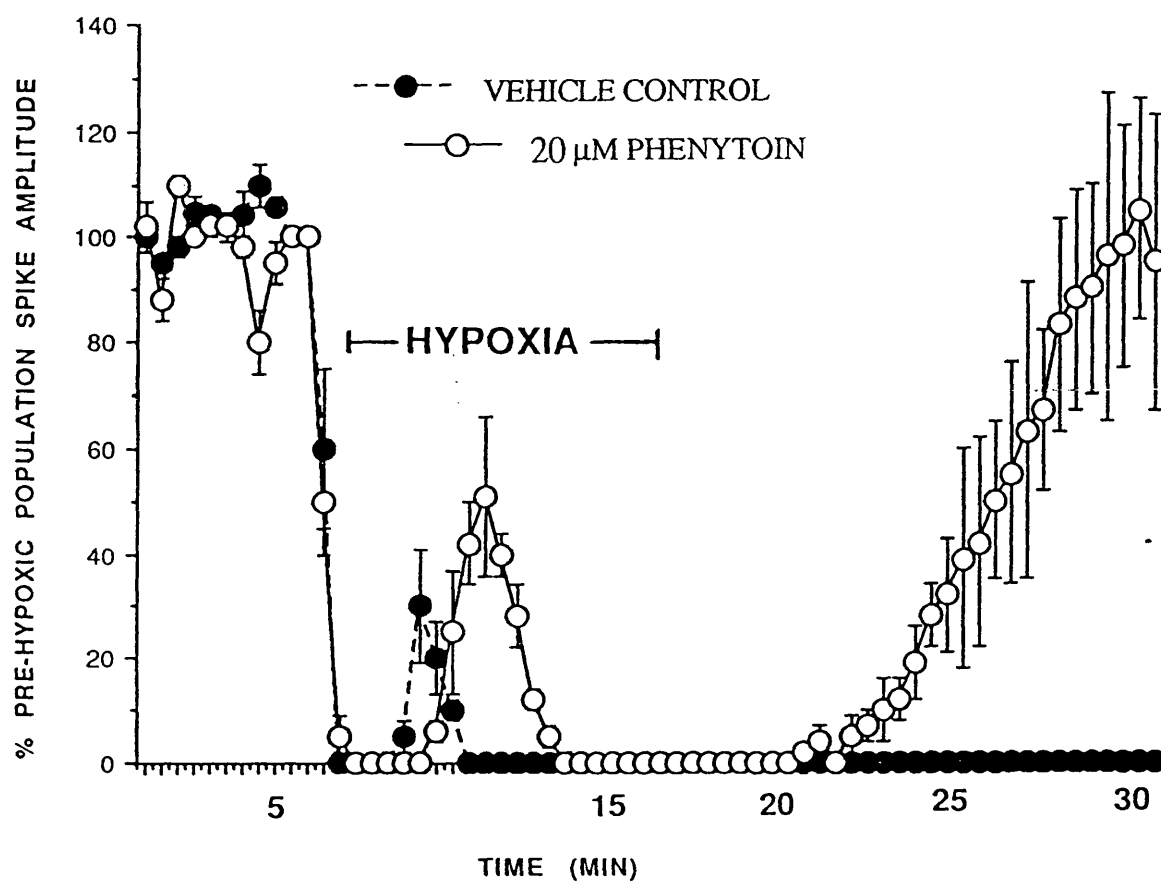


**Figure 5.5.** The effect of hypoxia on population spike amplitude in the absence (●) and presence of 20 μM phenytoin (○). Data points, expressed as a % of the pre-hypoxic control are the mean  $\pm$  s.e.mean for  $n=6$  experiments.

ethanol). Vehicle treated slices exhibited no difference in the duration of secondary activation or return of synaptic recovery after 20 min post-hypoxia compared to control slices. As Table 5.2. and Figures 5.4 and 5.5 illustrate, phenytoin significantly ( $p < 0.05$ ) increased the time to secondary activation and prevented the fall in DC potential after secondary failure compared to vehicle control and, as in previous experiments with CPP, the time of secondary activation was also increased ( $p < 0.01$ ) compared to vehicle control. Of the six slices examined, two slices showed partial recovery ( $< 20\%$ ) whilst four slices exhibited synaptic recovery with the post-hypoxic population spike amplitude greater than the pre-hypoxic control.

## 5.4. Discussion

In this chapter, having established a reproducible protocol for experimental hypoxia in the hippocampal slice, failure of the CA1 population spike has been demonstrated to be a sensitive index of hypoxia. Primary failure occurred in 100 % ( $n=56$ ) of slices examined and in all cases this was found to occur immediately in hypoxic superfusates in both control and drug treated slices. As outlined in the introduction to this chapter, evidence indicates that this primary failure is due to an activated  $K^+$  conductance (Sick *et al.*, 1987; Mourre *et al.*, 1989). Whilst in the gerbil hippocampal slice a large and sustained hyperpolarisation has been demonstrated throughout the hypoxic period when a lower temperature ( $30^{\circ}\text{C}$ ) and higher (11mM) glucose concentration were employed (Rogers *et al.*, 1990), the majority of studies have shown hypoxia to be associated with depolarisation after the initial hyperpolarisation (e.g. Sick *et al.*, 1987; Grigg & Anderson, 1990). One of the first consequences of hypoxia would be a marked lowering of ATP levels causing the opening of ATP-dependent  $K^+$  channels (e.g. Miller, 1990) and this may account for the small elevation in extracellular  $K^+$  associated with early hypoxia (see Hansen, 1985). It seems likely that initial transmission failure occurs at the dendritic level, as antidromic stimulation of CA1 neurones in the alveus has been shown to elicit population spikes in CA1 at a time when the orthodromic spike had failed (Grigg & Anderson, 1990).

The second, larger, and more sustained increase in extracellular  $K^+$  which is associated with decreased extracellular concentrations of  $\text{Ca}^{2+}$  and  $\text{Na}^+$  has been well documented (e.g. Nicholson *et al.*, 1977; Hansen & Zeuthen, 1981; Harris *et al.*, 1981; Siesjo, 1988). Such ionic changes have also been demonstrated in other energy-

compromised states in brain tissue, and the term spreading depression (SD) has been used to describe this phenomenon (see Somjen *et al.*, 1990). Indeed the ionic changes that have been reported in the hippocampal slice closely resemble *in vivo* findings (see Siesjö, 1988). The neurotransmitter hypothesis of SD (in which glutamate is implicated in hypoxic SD) is based on the probability that the early rise in extracellular  $K^+$  is associated with depolarisation of presynaptic terminals and subsequent release of transmitter. The postsynaptic actions of released excitatory neurotransmitter, associated with  $Na^+$  and  $Ca^{2+}$  entry, would depolarise postsynaptic membranes and lead to more  $K^+$  efflux, thus establishing positive feedback and initiating SD. This phenomenon has been demonstrated in the initiation of SD in slice experiments with depolarising stimuli such as the iontophoretic application of excitatory amino acids, anoxia, perfusion with high  $K^+$ , high frequency orthodromic stimulation and veratridine (Alger *et al.*, 1984; Ashton *et al.*, 1990). However, in all cases, as observed in the present studies after the secondary failure of the population spike, the response is characterised by a sudden, negative DC shift in the extracellular potential with a cessation of evoked responses. Interestingly, initial experiments in this chapter indicated that during the 10 min hypoxic period, secondary activation did not occur when the slices were incubated at lower temperatures in normal (10 mM) glucose, with synaptic transmission returning on reoxygenation, indicating that the ionic changes may be related to metabolic integrity. Similar results have been reported by Schurr & Rigor (1989) who demonstrated that more than 90% of slices recovered following a 10 min hypoxic period in ACSF containing 10 mM glucose. Grigg & Anderson (1989) also demonstrated that the use of elevated glucose reduced hypoxia-induced depolarisation and increased slice survival. This was proposed to result from a preservation of  $Na^+/K^+$  ATPase activity, therefore attenuating the build up of extracellular  $K^+$ . Other studies of *in vitro* anoxia, using the anoxic isolated rat optic nerve (Ransom *et al.*, 1990), have also demonstrated that the magnitude of the increase in extracellular  $K^+$  was attenuated with increased levels of glucose. Indeed, the effect of glucose deprivation on synaptic function in the rat hippocampal slice has been shown to be concentration related (Dong *et al.*, 1988). Such effects appear to be at odds with *in vivo* findings, at least in forebrain ischaemia where hyperglycaemia exacerbates ischaemic damage (see Ginsberg & Busto, 1989).

In hippocampal slices, however, the direct effect of elevated glucose is apparent without other longer term complications (such as oedema) that occur *in vivo*, and if the

large depolarisation that occurs following secondary failure of the population spike is mediated by  $\text{Na}^+$  and  $\text{Ca}^{2+}$  entry, then conserved levels of ATP in this model would be effective in reducing cellular build up of these ions through more efficient  $\text{Ca}^{2+}$  and  $\text{Na}^+/\text{K}^+$  ATPase pump systems. Thus, in hippocampal slices, Lipton & Lobner (1990) were able to demonstrate that cellular accumulation of  $\text{Ca}^{2+}$  during hypoxia resulted not through NMDA-gated or VOC-mediated  $\text{Ca}^{2+}$  entry, but because of reduced extrusion due to failure of the  $\text{Ca}^{2+}$  ATPase pump. Furthermore, in the present experiments there was no evidence for a protective effect with nitrendipine. Other studies of hypoxia *in vitro* (e.g. Ransom *et al.*, 1990) have also failed to demonstrate protective effects of DHPs, despite neuronal injury being dependent on extracellular  $\text{Ca}^{2+}$ . Furthermore, Weiss *et al.* (1990) have shown that nifedipine was ineffective against neurotoxicity induced by brief exposure to high concentrations of glutamate, but effective against the slow neurotoxicity elicited by low level exposure of cultured cortical neurones to AMPA. This would be consistent with  $\text{Ca}^{2+}$  entry being responsible for longer term damage in hypoxic models.

The secondary activation of the population spike during hypoxia was first reported by Sick *et al.*, (1987) and has been confirmed by other workers (e.g. Grigg & Anderson, 1990). The data obtained in the present studies are also consistent with those findings, although the mechanism whereby this occurs is unclear. However, the secondary activation was shown by Sick *et al.* (1987) to be associated with a slow rise in extracellular  $\text{K}^+$  and it may be envisaged that this reverses the initial hyperpolarisation and allows the propagation of action potentials before the secondary larger rise in extracellular  $\text{K}^+$  induced by uncontrolled depolarisation, with the subsequent failing of synaptic transmission.

The data in the present series of experiments indicated that treatment of hippocampal slices with either a competitive or a non-competitive NMDA antagonist resulted in the recovery of synaptic transmission after a period of hypoxia. This is consistent with previous findings (e.g. Clark & Rothman, 1987; Grigg & Anderson, 1990), the efficacy of these agents being related to their ability to attenuate the secondary depolarisation mediated by NMDA receptors. The lack of effect of these agents reported by other workers (e.g. Aitken *et al.*, 1988) may be a reflection of a more severe hypoxic insult occurring with the use of interfaced as opposed to fully submerged slices. However, in the report by Aitken *et al.* (1988) it was suggested that those agents which afforded protection delayed the onset of SD-like depolarisation, and whilst NMDA antagonists were ineffective in this study, in the other reports, NMDA antagonists were found to lengthen the time to

secondary failure (Clark & Rothman, 1987; Grigg & Anderson, 1990). Thus, these agents would appear to reduce the extent of neuronal depolarisation associated with secondary failure. In this respect it would be of interest to examine the effect of hypoxia in hippocampal slices sectioned at the level of the Schaffer collateral / commissural pathway (so-called 'minislices'), effectively removing the input to CA1 from CA3, since other studies have demonstrated protective effects against forebrain ischaemia in selectively vulnerable hippocampal CA1 neurones after destruction of CA3 pyramidal neurones, which effectively reduces the excitatory amino acid input (Onodera *et al.*, 1986).

In the previous chapter of this thesis it was shown that neuroprotection *in vivo* could be conferred by agents other than NMDA antagonists, presumably by a different mechanism. For some calcium antagonists, interactions with other ion channels (e.g. Na<sup>+</sup>) were implicated, and in this respect phenytoin was found to be neuroprotective *in vivo*. The data in this chapter have demonstrated the compound to be protective in the hypoxic hippocampal slice model.

The introduction to this thesis outlined a variety of experimental evidence that points to an important role for Na<sup>+</sup> influx as an early consequence of ischaemia (associated with neuronal swelling) contributed to by NMDA receptor-mediated entry and cumulative voltage-dependent entry following a reduction in the efficacy of the Na<sup>+</sup>/K<sup>+</sup> ATPase. *In vivo*, focal application of the Na<sup>+</sup> channel blocker, tetrodotoxin (TTX) in the hippocampus, has been reported to decrease neuronal damage following four vessel occlusion in the rat (Yamasaki *et al.*, 1991). TTX has also been found to improve recovery and attenuate the decrease in ATP levels following hypoxia in rat hippocampal slices (Boening *et al.*, 1989). In this latter study, the authors attributed the protective property of TTX to its ability to preserve ATP levels through decreased Na<sup>+</sup> entry, thereby reducing the effective load on the Na<sup>+</sup>/K<sup>+</sup> ATPase. Other studies have shown that phenytoin decreases the accumulation of extracellular K<sup>+</sup> and this effect may be due to an interaction with Na<sup>+</sup>/K<sup>+</sup> ATPase (Artru & Michenfelder, 1981; Meyer, 1989). In a comparative study using TTX and flunarizine in hippocampal slices (Ashton *et al.*, 1990) both agents delayed the onset and severity of SD induced by veratridine. In another study (Palmer *et al.*, 1988) it was shown that flunarizine prevented the deficit in Na<sup>+</sup>/K<sup>+</sup> ATPase following ischaemia. The interaction of flunarizine with Na<sup>+</sup> channels may be important in this respect. Indeed, both phenytoin and flunarizine have been claimed to decrease Na<sup>+</sup> currents during depolarisation and reduce epileptic burst firing in hippocampal slices (Ashton *et al.*, 1986). Under conditions of hypoxia, reverse

operation of the  $\text{Na}^+/\text{Ca}^{2+}$  exchanger will contribute to increased  $[\text{Ca}^{2+}]_i$ , and under these conditions it has been proposed that agents such as bepridil have protective effects against hypoxic damage *in vitro* by a direct inhibition of the exchanger mechanism (Stys *et al.*, 1991). However, a reduction in  $[\text{Na}^+]_i$  through blockade of  $\text{Na}^+$  channels would have the same effect, since it is the reduced  $\text{Na}^+$  gradient that results in this reversed operation.

Whilst the data in the present study indicate a protective effect of phenytoin in as much as all slices exhibited synaptic activity after the hypoxic period, the effect on DC potential, when taken in context with the findings in other studies, indicated that with those agents allowing synaptic recovery, the fall in DC potential was less marked or even absent. This implies a possible interaction with ionic homeostasis and the level of depolarisation. This is further supported by the findings in the present study that both NMDA antagonists and phenytoin increased the time of secondary activation during hypoxia.

Initial attempts were made in the present work to examine the effect of flunarizine in the hypoxic hippocampal slice protocol, although it was apparent that at concentrations above  $0.5\ \mu\text{M}$  the compound was not in solution. The poor solubility of flunarizine in ACSF has been reported by other workers, to the extent that the compound had to be applied by 'nanodrop' directly onto the CA1 region of the slice (e.g. Ashton *et al.*, 1986). It may have been possible to examine the effect of the compound using a carrier vehicle such as cyclodextrin, although time did not allow this series of experiments to be carried out. It was on this basis that fluspirilene was used since it has similar affinity for  $\text{Na}^+$  channels (as measured against  $[^3\text{H}]$  BTX), and whilst the solubility appeared to be better than that of flunarizine, the actual amount of fluspirilene dissolved in the aqueous media was uncertain. However, at an apparent concentration of  $10\ \mu\text{M}$  no protective effect was observed in the present studies despite the high affinity of the compound for the  $[^3\text{H}]$  BTX binding site. Indeed, the very brief secondary activation would indicate a rapid failure of ion homeostasis. However, as yet, there are no reported data that the interaction of fluspirilene with  $\text{Na}^+$  channels is through a mechanism similar to phenytoin.

In those slices treated with phenytoin, whilst partial recovery was observed in two slices such that the percent recovery for the experimental group was close to 100 % (Figure 5.5), in those that fully recovered it was apparent that the post-hypoxic spike was increased in amplitude compared to the pre-hypoxic control. This appears to be similar to the phenomenon of long term potentiation (LTP) in the hippocampal slice induced by tetanic

stimulation of the excitatory pathways which results in a long lasting potentiation of synaptic transmission. LTP is inhibited by NMDA antagonists (see Collingridge, 1985) indicating a role for excitatory amino acid transmission. It is possible that the same mechanisms are operative after slice recovery in the presence of phenytoin, since elevated concentrations of glutamate released during the hypoxic period would be likely to cause marked NMDA receptor activation. Interestingly, post-hypoxic augmentation of the population spike was not seen in those slices treated with either of the NMDA antagonists and this is consistent with the well documented ability of these agents to inhibit the induction of LTP (see Collingridge & Davies, 1989). On the other hand, phenytoin has been reported to be ineffective in preventing the induction of LTP in hippocampal slices (Stringer & Lothman, 1987; Birnsteil & Hass, 1991).

In conclusion, this chapter has demonstrated NMDA antagonists to be protective in an *in vitro* model of ischaemia. This might arise from a reduction in neuronal depolarisation associated with NMDA receptor activation. However, such an effect can also be demonstrated with phenytoin, possibly as a result of a decrease in neuronal excitability via an interaction with Na<sup>+</sup> channels.

## Chapter Six

### *Epilogue: Why are class III calcium antagonists neuroprotective?*

Chapters 3 and 4 have shown that class III calcium antagonists have relatively poor selectivity for the L-type VOC, such that a classification by the WHO has been proposed for these agents as group IV (Vanhoutte & Paoletti, 1987). Flunarizine is typical of this class of drug (Spedding, 1985a), and on the basis of binding data in the present studies, and recent *in vitro* evidence in smooth muscle (Fraser & Spedding, 1991), RS-87476 also fulfills these criteria. On the other hand, functional and binding experiments point to nicardipine as being a potent class I calcium antagonist, however, all three compounds have been shown to be neuroprotective. Two questions need to be addressed based on the findings of the present work. Firstly, why should there be differences between various calcium antagonists in terms of their neuroprotective potency and secondly, is affinity for L-type VOCs an absolute requisite for a neuroprotective compound?

Certainly functional data indicate that sites for this class of drug are coupled to the VOC, and taken together with binding data, this interaction appears to be of relatively low affinity and selectivity. However, even within a group of similar agents, DHPs for example, there are marked differences between compounds such as nimodipine and nicardipine as neuroprotective agents (e.g. Alps *et al.*, 1988), although they share similar affinities as calcium antagonists. One common property that this group of neuroprotective agents share is high affinity for the [<sup>3</sup>H] BTX binding site in rat cortical synaptosomes. It is significant that nicardipine is the only DHP with high affinity for this site, the affinity being comparable to other class III agents (Pauwels *et al.*, 1990). The high affinity that these agents express for this site does not appear to correlate with local anaesthetic properties (Reith *et al.*, 1987; Grima *et al.*, 1986; Pauwels *et al.*, 1986), however strong evidence suggests that they do interact with voltage-dependent Na<sup>+</sup> channels. In cultured cells this has been demonstrated with the use of veratridine (with subsequent calcium overload). Class III antagonists, and nicardipine, inhibit veratridine-induced LDH release in rat

hippocampal neurones (Pauwels *et al.*, 1990) and similarly, other previous studies have shown the same compounds to be effective in attenuating veratrine-induced  $\text{Ca}^{2+}$  overload in chick myocytes (Patmore *et al.*, 1989b). More recently (Patmore *et al.*, 1991), RS 87476 has also been shown to be effective in this model. These data indicate an interaction of these compounds with activated voltage dependent  $\text{Na}^{+}$  channels. Indeed in the study by Pauwels *et al.* (1990) a remarkably close correlation existed for the affinity of these agents at the  $[^3\text{H}]$  BTX binding site and their ability to decrease veratridine-induced LDH release.

$\text{Ca}^{2+}$  overload following exposure to veratridine in cultured cells is an effect secondary to increased cytosolic  $\text{Na}^{+}$ . In cells, the primary control mechanism for  $\text{Ca}^{2+}$  extrusion is the  $\text{Na}^{+}/\text{Ca}^{2+}$  exchange mechanism, and as the  $\text{Na}^{+}$  gradient regulates this mechanism,  $\text{Ca}^{2+}$  extrusion is decreased under conditions of increased cytosolic  $\text{Na}^{+}$ , with  $\text{Ca}^{2+}$  overload resulting. Therefore, toxicity in these cultures is dependent on extracellular  $\text{Ca}^{2+}$  (see Garthwaite, 1989). Furthermore, there is evidence that under conditions of excessive levels of cytosolic  $\text{Na}^{+}$  this exchanger may gate  $\text{Ca}^{2+}$  into the cell (Nachshen *et al.*, 1986; Stys *et al.*, 1991). Class III agents have been shown to prevent calcium overload (Patmore *et al.*, 1989b; Patmore *et al.*, 1991) and protect neuronal cell cultures following exposure to some neurotoxins (Pauwels *et al.*, 1990). However, *in vitro*, the same agents are weak against neurotoxicity induced by exposure to glutamate or kainate (Härtley & Choi, 1989; Pauwels *et al.*, 1990). Therefore, the *in vivo* efficacy of these agents in ischaemic models indicates that neuroprotection can be afforded by mechanisms other than antagonism of NMDA receptor-mediated events. *In vivo* such consequences may be secondary to these agents causing a change in the threshold or latency to depolarisation following the onset of ischaemia (see Chapter 5). Although selective lesioning of the excitatory input to CA1 neurones protects against ischaemic injury, protective effects can also be achieved with the localised application of TTX to the hippocampal CA1 subfield (Yamasaki *et al.*, 1990). In similar experiments, Prenen *et al.* (1988) demonstrated that localised application of TTX was also protective against cell injury, and the authors suggested that neurotransmission following  $\text{Na}^{+}$  influx may be a crucial factor in the development of ischaemic damage. The interaction of phenytoin with voltage-dependent

Na<sup>+</sup> channels (Willow *et al.*, 1985) is thought to mediate its effects as an anticonvulsant (Rogawski & Porter, 1990). In the present studies, phenytoin produced a highly significant reduction in the ischaemia-induced increase in  $\omega_3$  sites following MCA occlusion in the mouse. In the context of this finding, it is important to note that the administration and dose of phenytoin used in these experiments is similar to its efficacy as an anticonvulsant in experimental models (McNamara *et al.*, 1989). Further evidence that neuronal damage is due to excessive neuronal activity has also been demonstrated in the striatum, as lesioning the input from the nigro-striatal pathway attenuates ischaemic damage (Globus *et al.*, 1987).

It is interesting to note that similar to TTX, flunarizine protects the hippocampal slice *in vitro* from veratridine induced neurotoxicity through an interaction with ion homeostasis (Ashton *et al.*, 1990). Other experimental evidence also points to flunarizine causing an increase in the threshold for hypoxic cell depolarisation (Marranes *et al.*, 1989), possibly reducing excitotoxic transmitter release under such circumstances, since *in vivo*, the threshold for K<sup>+</sup> to cause depolarisation is increased in the presence of flunarizine (see Pauwels *et al.*, 1991). This effect has been postulated to be important in the ability of this type of agent to increase the latency time to the onset of spreading depression following experimental hypoxia (discussed in Chapter 5).

Previous studies have established that Ca<sup>2+</sup> flux can also occur through Na<sup>+</sup> channels under some circumstances. Na<sup>+</sup> channels activated by veratridine have been shown to gate a Ca<sup>2+</sup> current in neuroblastoma cells (Jacques *et al.*, 1981). Furthermore a TTX-sensitive Ca<sup>2+</sup> current has been demonstrated in rat hippocampal CA1 pyramidal neurones illustrating Ca<sup>2+</sup> flux through voltage-dependent Na<sup>+</sup> channels (Takahashi *et al.*, 1989) and Miller's group (Kongsamut *et al.*, 1985) demonstrated that BTX and veratridine inhibited <sup>45</sup>Ca uptake induced by Bay K 8644 in the presence of elevated K<sup>+</sup>, indicating that both BTX and veratridine could modulate the effects of DHPs. This finding is perhaps not surprising given the close homology of the Na<sup>+</sup> and Ca<sup>2+</sup> channel  $\alpha_1$  subunits (Catterall, 1986; Tanabe *et al.*, 1987) both of which have four transmembrane motifs. As in the Ca<sup>2+</sup> channel  $\alpha_1$  subunit, there appear to be distinct binding sites in the  $\alpha_1$  subunit which also shows considerable variation in Na<sup>+</sup> channels (Noda *et al.*, 1986).

The neuroprotective properties of some DHPs (nicardipine) but not others (nimodipine) has been proposed to result from a more favourable accumulation of nicardipine in ischaemic tissue (low pH) due to the pKa of the drug (see Spedding, 1989). However, this conclusion does not account for nicardipine having much higher affinity for Na<sup>+</sup> channels than other DHPs. Furthermore, it has been shown that flunarizine blocks a proton gated Na<sup>+</sup> current induced under conditions of low pH (see Pauwels *et al.*, 1991). Therefore, if it is to be believed that neuroprotective calcium antagonists exert their effects through decreased neuronal excitability due to an interaction with Na<sup>+</sup> channels, then it would be expected to demonstrate some antiseizure activity for these compounds.

Flunarizine has an anticonvulsant profile (Binnie, 1988). Similar to phenytoin, but unlike DHPs, flunarizine is inactive against pentylenetetrazole (PTZ)-induced clonic seizures (Rogawski & Porter, 1990) but is active against tonic seizures under several experimental protocols (Wauquier *et al.*, 1986).

However, in a consideration of the interaction of these compounds with ion channels, it is significant that those compounds which might be effective through an interaction with Na<sup>+</sup> channels (i.e. flunarizine, phenytoin, nicardipine) are all active at T-type calcium channels. The class III calcium antagonists (cinnarizine and flunarizine) have been shown to interact with cardiac T channels (Tytgat *et al.*, 1988). In rat hypothalamic neurones flunarizine is also a potent inhibitor of T channel Ca<sup>2+</sup> currents (Akaike *et al.*, 1989), with the block being frequency dependent. However, of the dihydropyridines, as with interactions at Na<sup>+</sup> channels, nicardipine was the most potent agent of this class inhibiting this current. Phenytoin also blocks T channels (Twombly *et al.*, 1988) in a manner similar to its interaction with Na<sup>+</sup> channels, with the block being enhanced by depolarisation and repeated activation. Anticonvulsant agents have been proposed to interact and suppress Na<sup>+</sup> and Ca<sup>2+</sup> currents participating in epileptiform burst firing, such neuronal types leading to the spread of discharge activity (Wong *et al.*, 1986). Therefore, is there experimental evidence to suggest that anticonvulsants are also neuroprotective?

Certainly the non-competitive NMDA antagonists (typified by MK 801) have been shown to be anticonvulsant on the basis of NMDA receptor blockade (Wong *et al.*, 1986),

with this class of agent showing a more favourable (100-400 fold) uptake into brain tissue compared to competitive NMDA antagonists (Chapman & Meldrum, 1989). As already noted however, the potential use of such agents is limited because of marked motor toxicity at anti-ischaemic (and anticonvulsant) doses (Leander *et al.*, 1988) and the tendency to cause vacuolisation of pyramidal neurones (Olney *et al.*, 1989). However, an interesting finding from the review of Meldrum & Swan (1989) was that there was a close correlation between anticonvulsant and neuroprotective efficacy (in global ischaemia models) for a variety of competitive and non-competitive NMDA antagonists. Effective neuroprotective doses were also less than anticonvulsant ones and the authors suggested that neuroprotection may arise from a more general reduction in the activity of a variety of neuronal systems which are activated by glutamatergic input.

Data in Chapter 4 has shown phenytoin to be active in the mouse MCA model. In the gerbil, phenytoin reduces selectively vulnerable neurone loss following temperature-regulated global ischaemia (Taft *et al.*, 1989; Clifton *et al.*, 1989). Early studies indicated that phenytoin was neuroprotective in cerebral ischaemia (Artru & Michenfelder, 1980) through a mechanism whereby the compound decreased extracellular levels of  $K^+$  (Artru & Michenfelder, 1981) and a dose-related recovery of EEG with a reduction in brain swelling has been demonstrated following global ischaemia with reperfusion (Suzuki *et al.*, 1987). Furthermore, it has been demonstrated that phenytoin decreases the accumulation of free fatty acids and lactic acid during ischaemia, and accelerated their recovery to normal levels following reperfusion (Kinouchi *et al.*, 1990). Recent evidence has also demonstrated efficacy in focal ischaemia as phenytoin was found to reduce infarct volume following MCA occlusion in the rat, comparable to the protection afforded by MK 801 (Boxer *et al.*, 1990).

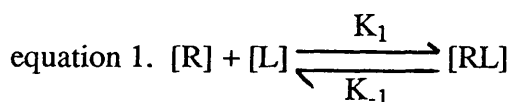
In summary, therefore, this thesis has demonstrated that calcium antagonists are potentially useful neuroprotective agents. For some of these compounds, however, their beneficial effects might be by virtue of an interaction at other ion channel types, other than at the L-type calcium channel. It cannot be concluded that affinity for any specific channel type can completely account for the efficacy of these compounds, although neuroprotection,

at least in part, can be attributed to interactions with Na<sup>+</sup> channels. Resolving the pharmacology of the T-type Ca<sup>2+</sup> channel will lead to a better understanding of this interaction. However, the present work has opened up some middle ground between the initially 'polarised' opinions that regarded neuroprotective compounds to be either NMDA antagonists or potent dihydropyridine calcium antagonists.

## Appendix.

### Theoretical basis for the direct identification of receptors in competition, kinetic and saturation radioligand binding experiments.

The simplest case of ligand-receptor interaction is given below (equation 1) for a single ligand interacting with a homogeneous receptor population.



where [R], [L] and [RL] represent the concentration of free receptor, free ligand and ligand-receptor complex at equilibrium.  $K_1$  and  $K_{-1}$  are the rate constants describing the opposing association and dissociation reactions. Thus, the equilibrium binding constant of the radioligand for the receptor can be defined as either the association binding constant ( $K_a$ , equation 2) or dissociation binding constant ( $K_d$ , equation 3).

$$\text{equation 2 } K_a = \frac{K_1}{K_{-1}} = \frac{[RL]}{[R][L]}$$

$$\text{equation 3 } K_d = \frac{K_{-1}}{K_1} = \frac{[R][L]}{[RL]}$$

This allows the determination of  $K_d$  from either saturation binding data or indirectly from kinetic experiments, although in the latter when  $K_1$  is experimentally determined to yield the pseudo first-order association rate constant ( $K_{obs}$ ), this is inherently dependent on  $K_{-1}$ , since equation 1 shows that the association of ligand to receptor is a second order reaction. The rate equation for this bimolecular reaction is

$$\frac{d[RL]}{dt} = K_a[L][R]$$

to give the following on integration,

$$K_a = \frac{2.303}{t} \log \frac{R[L-X]}{L[R-X]} \quad \text{where } R \text{ and } L = \text{unoccupied receptor and free ligand at } t_0 \text{ and } x \text{ is the amount of consumed } L \text{ and } R \text{ at time } t.$$

This equation enables  $K_a$  to be calculated from a bimolecular reaction when  $L$ ,  $R$  and  $X$  are known.  $K_{obs}$  is determined experimentally by measuring specific binding at time points ( $B_t$ ) up to equilibrium ( $B_{eq}$ ). The pseudo first-order plot of  $\ln [B_{eq}/B_{eq}-B_t]$  yields a slope  $K_{obs}$  from which  $K_1$  is determined (equation 4).

$$\text{equation 4} \quad K_1 = \frac{K_{obs} - K_{-1}}{[L]}$$

The dissociation rate is determined independently by a plot of  $\ln [B] / [B_0]$  vs time, where  $[B]$  is the bound at time  $t$  and  $B_0$  is that bound at time 0 or equilibrium. The half life for loss of specific binding is related to  $K_{-1}$  as  $0.693/t_{1/2}$ .

If binding of  $L$  to a single class of fixed affinity  $R$  is reversible, then  $K_d$  determined kinetically should be equivalent to  $K_d$  determined in saturation experiments.

$$K_d = \frac{K_{-1} \text{ min}^{-1}}{K_1 \text{ min}^{-1} \text{ M}^{-1}} = M$$

The determination of receptor density, and binding as a function of radioligand concentration is dependent on saturability of the binding reaction. Thus the maximal number of binding sites ( $B_{max}$ ) present will be  $[R] + [RL]$ . Multiplying by  $[L]$  yields equation 5.

$$\text{equation 5} \quad [RL][L] + [R][L] = B_{max}[L]$$

$$[RL][L] + \frac{[RL]}{[RL]} [R][L] = B_{max}[L]$$

$$\text{and from equation 3, } [RL]([L] + K_d) = B_{max}[L]$$

and so  $[RL] = \frac{B_{max} [L]}{[L] + K_d}$  equivalent to the hyperbolic relationship of equation 1  $y = \frac{ax}{b+x}$

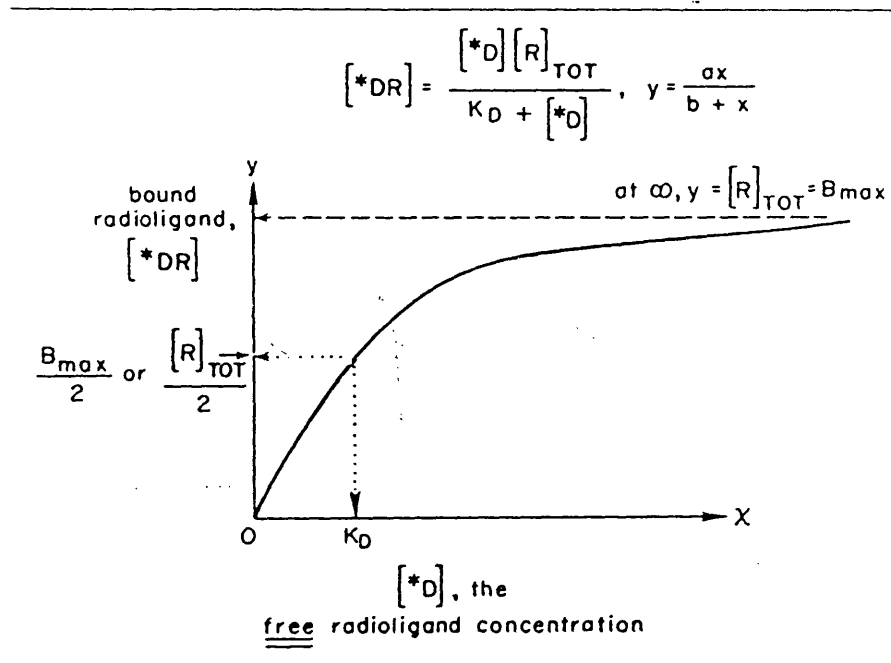


**Figure 1.** The hyperbolic relationship of mass action (from Limbird, 1986)

The definition of  $K_d$  is the concentration of ligand that half maximally occupies the receptor as in the relationship below.

$$[DR] = \frac{[R]_{total}}{2}$$

and from figure 2.1  $[R]_{total} = \frac{2 [D] [R]_{total}}{K_d + [D]}$

$$\therefore 1 = \frac{[2] [D]}{K_d + [D]}$$

$$\text{and } K_d + [D] = 2 [D], \quad K_d = [D].$$

$$K_d = [D] \text{ leading to a } [DR] = \frac{[R] \text{ total}}{2}$$

since on the rectangular hyperbola  $[DR] \Rightarrow [R] \text{ total}$  as  $[D] \Rightarrow \infty$

## References.

- Abercrombie, R.F. & Hart, C.E. (1986). Calcium and proton buffering and diffusion in isolated cytoplasm from myxicola axons. *Am. J. Physiol.*, **250**, C391-405.
- Adams, R.J., Cohen, D.W., Gupte, S., Johnson, J.D., Wallick, E.T., Wang, T. & Schwartz, A. (1979). *In vitro* effects of palmitoylcarnitine on cardiac plasma membrane Na<sup>+</sup>,K<sup>+</sup>-ATPase, and sarcoplasmic reticulum Ca<sup>2+</sup>-ATPase and Ca<sup>2+</sup> transport. *J. Biol. Chem.*, **254**, 12404-12410
- Aitken, P.G., Balestrino, M. & Somjen, G.G. (1988). NMDA antagonists: lack of protective effect against hypoxic damage in CA1 region of hippocampal slices. *Neurosci. Lett.*, **89**, 187-192.
- Aitken, P.G., Jing, J., Young, J. & Somjen, G.G. (1991). Ion channel involvement in hypoxia-induced spreading depression in hippocampal slices. *Brain Res.*, **541**, 7-11
- Akaike, N., Kostyuk, P.G. & Osipchuk, Y.V. (1989). Dihydropyridine-sensitive low-threshold calcium channels in isolated rat hypothalamic neurones. *J. Physiol.* **412**, 181-195
- Alger, A.E., Dhanjal, S.S., Dingledine, R., Garthwaite, J., Henderson, G., King, G.L., Lipton, P., North, A., Schwartzkroin, P.A., Sears, T.A., Segal, M., Whittingham, T.S. & Williams, J. (1984). Brain slice methods. In *Brain Slices*. (ed) Dingledine, R. Plenum Press. New York.
- Allely, M.C. & Brown, C.M. (1988). The effects of POCA and TGDA on the ischaemia-induced increase in  $\alpha_1$ -adrenoceptor density in the rat left ventricle. *Br. J. Pharmacol.*, **95**, 705P
- Allen, G.S., Ahn, H.S. & Preziosi, T.J. (1983). Cerebral arterial spasm- a controlled trial of nimodipine in patients with subarachnoid haemorrhage. *New Eng. J. Med.*, **308**, 619-624.
- Allen, M.C., Hoare, R.D., Fowler, C.T. & Harrison, M.J.G. (1984). Clinico-anatomic correlations in uncomplicated stroke. *J. Neurol. Neurosurg. Psychiatr.*, **47**, 1251-1254.
- Allen, M.C., Harrison, M.J.G. & Wade, D.T. (1988). In *The Management of Clinical Stroke*. (ed) Allen, M.C., Harrison, M.J.G. & Wade, D.T. Castle House Publications. England.
- Alps, B.J., Brown, C.M., Calder, C. & Kilpatrick, A.T. (1985). Striatal 5-HT levels after experimental cerebral ischaemia. *Biochem. Soc. Trans.*, **13**, 384.
- Alps, B.J., Calder, C., Hass, W.K. & Wilson, A.D. (1988). Comparative protective effects of nicardipine, flunarizine, lidoflazine and nimodipine against ischaemic injury in the hippocampus of the Mongolian gerbil. *Br. J. Pharmacol.*, **93**, 877-883
- Alps, B.J. & Hass, W.K. (1987). The potential beneficial effect of nicardipine in a rat model of transient forebrain ischaemia. *Neurology*, **37**, 809-814
- Alps, B.J., Calder, C.C., Wilson, A.D. & Pascal, J.C. (1990). Cerebral protection with a novel calcium blocker in rats. (1990). *Proc. XXth Intl. Congress (ISIM satellite)* Stockholm, Sweden.
- Ambrosio, C. & Stefanini, E. (1991). Interaction of flunarizine with dopamine D<sub>2</sub> receptors. *Eur. J. Pharmacol.* **197**, 221-223

Andersen, P. (1981). Brain slices: a neurobiological tool of increasing usefulness. *Trends Neurosci.*, **4**, 53-56.

Anderson, A.J. & Harvey, A.L. (1987).  $\omega$ -Conotoxin does not block the verapamil-sensitive calcium channels at mouse motor nerve terminals. *Neurosci. Lett.*, **82**, 177-180

Anderson, A.J., Duncan G.P., Spedding M. & Patmore L. (1990). Pertussis toxin-sensitive G-protein activation does not influence the response to Bay K 8644 in embryonic chick myocytes. *J. Cardiovasc. Pharmacol.*, **16**, 681-683

Anholt, R.H. (1986). Mitochondrial benzodiazepine receptors as potential modulators of intermediary metabolism. *Trends Pharmacol. Sci.*, **7**, 506-511

Anholt, R.H., Pedersen, E.B., de Souza, E.B. & Snyder, S.H. (1986). The peripheral-type benzodiazepine receptor. Localisation to the outer mitochondrial membrane. *J. Biol. Chem.*, **261**, 576-583.

Antiplatelet Trials Corporation (1988). Secondary prevention of vascular disease by prolonged antiplatelet treatment. *Br. Med. J.*, **296**, 320-321.

Armstrong, D. & Kalman, D. (1990). Dihydropyridines modulate  $\text{Ca}^{2+}$  channels by altering their availability to protein phosphorylation and its removal. *Biophys. J.*, **57**, 516a.

Artru, A.A. & Michenfelder, J.D. (1980). Cerebral protective, metabolic and vascular effects of phenytoin. *Stroke*, **11**, 377-382

Artru, A.A. & Michenfelder, J.D. (1981). Anoxic cerebral potassium accumulation reduced by phenytoin. Mechanism of cerebral protection. *Anesth. Analg.*, (Paris) **60**, 41-45

Ascher, P. & Johnson, J.W. (1989). The NMDA receptor, its channel and its modulation by glycine. In: *The NMDA Receptor*. (ed). Watkins, J.C. & Collingridge, G.L. pp 109-122. Oxford University Press.

Ashton, D., Reid, K., Willems, R., Marrannes, R. & Wauquir, A. (1986). Comparative actions of flunarizine, phenytoin, carbamazepine and two calcium-entry blockers on spontaneous epileptiform bursts in the low calcium hippocampal slice preparation. *Drug Dev. Res.*, **8**, 397-405.

Ashton, D., Willems, R., Marrannes, R., & Janssen, P.A.J. (1990). Extracellular ions during veratridine-induced neurotoxicity in hippocampal slices: neuroprotective effects of flunarizine and tetrodotoxin. *Brain Res.*, **528**, 212-222.

Awad, M. & Gavish, M. (1987). Binding of [ $^3\text{H}$ ] RO 5-4864 and [ $^3\text{H}$ ] PK 11195 to cerebral cortex and peripheral tissues of various species: species differences and heterogeneity in peripheral benzodiazepine binding sites. *J. Neurochem.*, **49**, 1407-1414.

Babitch, J. (1990). Channel hands. *Nature*, **346**, 321-322

Balwierczak, J.L. & Schwartz, A. (1985). Specific binding of [ $^3\text{H}$ ]-d-cis-diltiazem to cardiac sarcolemma and its inhibition by calcium. *Eur. J. Pharmacol.*, **116**, 193-194.

Balwierczak, J.L., Johnson, C.L. & Schwartz, A. (1987). The relationship between the binding site of [ $^3\text{H}$ ] d-cis-diltiazem and that of non-dihydropyridine calcium entry blockers in cardiac sarcolemma. *Mol. Pharmacol.*, **31**, 175-179.

Bamford, J.M. & Warlow, C.P. (1988). The evolution and testing of the lacunar hypothesis. *Stroke*, **19**, 1074-1082.

Bamford, J.M., Sandercock, P.A.G., Dennis, M.S., Warlow, C.P., Jones, L.N., Fowler, G., McPherson, K., Molyneux, A., Hughes, J.T., Wade, D. & Burn. (1988). A prospective study of acute cerebrovascular disease in the community: The Oxford Community Stroke Project 1981-1988. *J. Neurol. Neurosurg. Psychiatr.*, **51**, 1373-1380.

Barbaran, J.M., Snyder, S.H. & Alger, B.E. (1985). Protein Kinase C regulates ionic conductance in hippocampal pyramidal neurons: electrophysiological effects of phorbol esters. *Proc. Natl. Acad. Sci.*, **82**, 2538-2542

Barbour, B., Brew, H. & Attwell, D. (1988). Electrogenic glutamate uptake in glial cells is activated by intracellular potassium. *Nature*, **335**, 433-435.

Basile, A.S. & Skolnick, P.C. (1986). Subcellular localization of "peripheral-type" binding sites for benzodiazepines in rat brain. *J. Neurochem.*, **46**, 305-308.

Bazzi, M.D. & Nelsestuen, G.L. (1991). Proteins that bind calcium in a phospholipid-dependent manner. *Biochemistry*, **30**, 971-979.

Bean, B.P. (1984). Nitrendipine block of cardiac calcium channels: high affinity binding to the inactivated state. *Proc. Natl. Acad. Sci., USA* **81**, 6388-6392

Beck, T., Nuglish, J., Sauer, D., Bielberg, G., Mennel, H.D., Rossberg, C. & Kriegstein, J. (1988). Effects of flunarizine on post-ischaemic blood flow, energy metabolism and neuronal damage in the rat brain. *Eur. J. Pharmacol.*, **158**, 271-274.

Bellmann, P. (1984). Binding properties of a novel calcium channel activating dihydropyridine in monolayer cultures of beating myocytes. *FEBS Lett.*, **167**, 88-92.

Benavides, J., Quarteronet, D., Imbault, F., Malgouris, C., Uzan, A., Renault, C., Dubroeuq, M.C., Gueremy, C. & LeFur, G. (1983). Labelling of peripheral type benzodiazepine binding sites in the rat brain. Kinetic studies and autoradiographic localisation. *J. Neurochem.*, **41**, 1744-1750.

Benavides, J., Savaki, H.E., Malgouris, C., Laplace, C., Daniel, M., Begassat, M., Desban, M., Uzan, A., Dubroeuq, M.C., Renault, C., Gueremy, C. & Le Fur, G. (1984). Autoradiographic localisation of peripheral-benzodiazepine binding sites in the cat brain with [<sup>3</sup>H] PK 11195. *Brain Res. Bull.*, **13**, 69-77.

Benavides, J., Fage, D., Carter, C. & Scatton, B. (1987). Peripheral type benzodiazepine binding sites are a sensitive indirect index of neuronal damage. *Brain Res.*, **421**, 167-172.

Benavides, J., Cornu, P., Dennis, F., Dubois, A., Duverger, D., Fage, D., Gotti, B., MacKenzie, E.T. & Scatton, B. (1988). Imaging of human brain lesions with an  $\omega_3$  site radioligand. *Ann. Neurol.*, **24**, 708-712.

Benavides, J., Capdeville, C., Dauphin, F., Dubois, A., Duverger, D., Fage, D., Gotti B., Mackenzie, E.T. & Scatton, B. (1990). The quantification of brain lesions with an  $\omega_3$  site ligand: a critical analysis of animal models of cerebral ischaemia and neurodegeneration. *Brain Res.*, **522**, 275-289

Benveniste, H., Orejer, J., Schousboe, A. and Diemer, N.H. (1984). Elevation of the extracellular concentration of glutamate and aspartate in rat hippocampus during transient cerebral ischaemia. *J. Neurochem.*, **43**, 1369-1374.

Benveniste, H., Jorgensen, M.B., Sandberg, M., Christensen, T., Hagberg, H. & Diemer, N.H. (1989). Ischaemic damage in hippocampus CA1 is dependent on glutamate release and intact innervation from CA3. *J. Cerebral Blood Flow Metab.*, **9**, 629-639.

Bergamaschi, S., Govoni, S., Cominetti, P., Parenti, M. & Trabucchi, M. (1988). Direct coupling of a G-protein to dihydropyridine sites. *Biochem. Biophys. Res. Comm.*, **156**, 1279-1286.

Berridge, M.J. & Irvine, R.F. (1989). Inositol phosphates and cell signalling. *Nature*, **341**, 197-205.

Berry, K., Wisniewski, H.M., Svarzbein, L. & Baez, S. (1975). On the relationship of brain vasculature to production of neurological deficit and morphological changes following acute unilateral common carotid artery ligation in gerbils. *J. Neurol. Sci.*, **25**, 75-92.

Billard, W., Ruperto, V., Crosby, G., Iorio, L.C. & Barnett, A. (1984). Characterisation of the binding of [<sup>3</sup>H] SCH 23390, a selective D-1 receptor antagonist ligand, in rat striatum. *Eur. J. Pharmacol.*, **35**, 1885-1893.

Binnie, C.D. (1988). Flunarizine in epilepsy. *Ann. NY. Acad. Sci.*, **522**, 710-711

Birnstiel, S. & Hass, H. (1991). Anticonvulsants do not suppress long-term potentiation in the rat hippocampus. *Neurosci. Lett.*, **122**, 61-63.

Blaustein, M.P. (1988). Calcium transport and buffering in neurones. *Trends Neurosci.*, **11**, 438-443.

Boast, C.A., Gerhardt, S.C., Pastor, G., Lehmann, J., Etienne, P. & Liebmann, J.M. (1988). The NMDA antagonists CGS 19755 and CPP reduce ischaemic brain damage in gerbils. *Brain Res.*, **442**, 345-348.

Boening, J.A., Kass, I.S., Cottrell, J.E. & Chambers, G. (1989). The effect of blocking sodium influx on anoxic damage in the rat hippocampal slice. *Neuroscience*, **33**, 263-268.

Boer, R., Grassegger, A., Schudt, C. & Glossmann, H. (1989). (+) nifedipine binds with high affinity to Ca<sup>2+</sup> channels and a subtype of  $\alpha_1$  adrenoceptors. *Eur. J. Pharmacol.*, **172**, 131-145.

Bolger, G.T. & Skolnick, P. (1986). Novel interactions of cations with dihydropyridine calcium antagonist binding sites in brain. *Br. J. Pharmacol.*, **88**, 857-866.

Bolger, G.T., Basile, A.S., Janowsky, A.J., Paul, S.M. & Skolnick, P. (1987). Regulation of dihydropyridine calcium channel antagonist binding sites in the rat hippocampus following neurochemical lesions. *J. Neurol. Res.*, **17**, 285-290

Boxer, P.A., Cordon, J.J., Maan, M.E., Rodolosi, L.C., Vartanian, M.G., Rock, D., Taylor, C.P. & Marcoux, F.W. (1990). Comparison of phenytoin with non-competitive N-methyl-D-aspartate antagonists in a model of focal ischaemia in the rat. *Stroke*, **21**, III 47-51.

Brannan, T., Weinberger, J., Knott, P., Taff, I., Kaufmann, H., Togasaki, D., Nieves-Rosa, J. & Maker, H. (1987). Direct evidence of acute, massive striatal dopamine release in gerbils with unilateral strokes. *Stroke*, **18**, 108-110.

- Brown, A.W., Levy, D.E., Kublik, M., Harrow, J., Plum, F. & Brierely, J.B. (1979). Selective chromatolysis of neurones in the gerbil brain: a possible consequence of "epileptic" activity produced by common carotid artery occlusion. *Ann. Neurol.*, **5**, 127-138.
- Brown, C.M., Kilpatrick, A.T., Martin, A. & Spedding, M. (1988). Cerebral ischaemia reduces the density of 5-HT<sub>2</sub> binding sites in the frontal cortex of the gerbil. *Neuropharmacology*, **27**, 831-836
- Busto, R., Dietrich, W.D., Globus, M., Valides, I., Scheinberg, P & Ginsberg, M.D. (1987). Small differences in intra-ischaemic brain temperature critically determine the extent of ischaemic neuronal injury. *J. Cerebral Blood Flow Metab.*, **7**, 729-738.
- Carafoli, E. (1987). Intracellular calcium homeostasis. *Ann Rev. Biochem.*, **56**, 395-433.
- Carter, C., Rivy, J.P. & Scatton, B. (1989). Ifenprodil and SL 82. 0175 are antagonists at the polyamine site on the N-methyl-D-aspartate (NMDA) receptor. *Eur. J. Pharmacol.*, **164**, 611-612.
- Carvalho, C.M., Oliveira, C.R., Lima, M.P., Leysen, J.E. & Carvalho, A.P. (1989). Partition of Ca<sup>2+</sup> antagonists in brain plasma membranes. *Biochem Pharmacol.*, **38**, 2121-2127.
- Catterall, W.A. (1981). Inhibition of voltage sensitive sodium channels in neuroblastoma cells by antiarrhythmic drugs. *Mol. Pharmacol.*, **20**, 356-362.
- Catterall, W.A., Morrow, C.S., Daly, J.W. & Brown, G.B. (1981). Binding of batrachotoxinin-A-20- $\alpha$ -benzoate to a receptor site associated with sodium channels in synaptic nerve ending particles. *J. Biol. Chem.*, **256**, 8922-8927.
- Catterall, W.A. (1986). Voltage-dependent gating of sodium channels: correlating structure and function. *Trends Neurosci.*, **9**, 7-10.
- Cerebral Embolism Study Group. (1983). Immediate anti-coagulation of embolic stroke: a randomised trial. *Stroke*, **14**, 668-676.
- Chapman, A. & Meldrum, B.S. (1989). Non-competitive N-methyl-D-aspartate antagonists protect against sound induced seizures in DBA/2 mice. *Eur. J. Pharmacol.*, **166**, 201-211.
- Chatelain, P., Beaufort, P., Meysmans, L. & Clinet, M. (1991). Characterisation of the slow calcium channel binding sites for [<sup>3</sup>H] SR 33557 in rat sarcolemmal membranes. *Mol. Pharmacol.*, **39**, 64-71.
- Chen, Z.M., Collins, R., Peto, R. & Li, W.X. (1989). No association between serum cholesterol and stroke rates in a Chinese population. *N. Engl. J. Med.*, **321**, 1339-1340.
- Cheng, Y.C. & Prusoff, W.H. (1973). Relationship between the inhibition constant (K<sub>i</sub>) and the concentration of inhibitor which causes 50% inhibition (I<sub>50</sub>) of an enzymatic reaction. *Biochem Pharmacol.*, **22**, 3099 - 3018.
- Cheung, W.Y. (1980). Calmodulin plays a pivotal role in cellular regulation. *Science*, **207**, 19-27.
- Cheung, W.Y. (1988). Calmodulin and its activation by cadmium ion. *Ann. NY. Acad. Sci.*, **522**, 74-87.

Choi, D.W. (1985). Glutamate neurotoxicity in cortical cell culture is calcium dependent. *Neurosci. Lett.*, **58**, 293-297.

Choi, D.W. (1988a). Glutamate neurotoxicity and diseases of the nervous system. *Neuron*, **1**, 623-624.

Choi, D.W. (1988b). Calcium dependent neurotoxicity: Relationship to specific channel types and role in ischaemic damage. *Trends Neurosci.*, **11**, 465-469.

Choi, D.W., Goldberg, M.P., Monyer, H. & Weiss, J.H. (1989). Assessment of protective agents in primary central neuronal cell culture. In: *Cerebrovascular Diseases*. (ed) Ginsberg, M.D. & Dietrich, D.W. Raven Press.

Choi, D.W. & Rothman, S.M. (1990). The role of glutamate neurotoxicity in hypoxic-ischemic neuronal death. *Ann. Rev. Neurosci.*, **13**, 171-182.

Clark, G.D. & Rothman, S.M. (1987). Blockade of excitatory amino acid receptors protects anoxic hippocampal slices. *Neuroscience*, **21**, 665-671.

Clifton, G.L., Taft, W.C., Blair, R.E., Choi, S.C. & DeLorenzo, R.J. (1989). Conditions for pharmacologic evaluation in the gerbil model of forebrain ischemia. *Stroke*, **20**, 1545-1552

Collingridge, G.L. (1985). Long-term potentiation in the hippocampus: mechanisms of the initiation and modulation by neurotransmitters. *Trends Pharmacol. Sci.*, **6**, 407-411.

Collingridge, G.L. & Davies, S.N. (1989). NMDA receptors and long-term potentiation in the hippocampus. In: *The NMDA receptor*. (ed) Watkins, J.C. & Collingridge, G.L. Oxford University Press.

Corr, P.B., Gross, R.W. & Sobel, B.E. (1984). Amphipathic metabolites and membrane dysfunction in ischemic myocardium. *Circ. Res.*, **55**, 135-154.

Cortes, R., Supavilai, P., Karobath, M. & Palacios, J.M. (1983). The effects of lesions in the rat hippocampus suggest the association of calcium channel blocker binding sites with specific neuronal populations. *Neurosci. Lett.*, **42**, 249-254

Cortes, R., Supavilai, P., Karobath, M. & Palacios, J.M. (1984). Calcium antagonist binding sites in the rat brain: quantitative autoradiographic mapping using the 1,4-dihydropyridines [3H]PN200-110 and [3H]PY108-068. *J. Neural Transmission.*, **60**, 169-197.

Crompton, M., Ellinger, H. & Costi, A. (1988). Inhibition by cyclosporine A of a calcium-dependent pore activated by oxidative stress in heart mitochondria. *Biochem. J.*, **255**, 357-360.

Crompton, M.J. & Dedman, J.R. (1990). Protein terminology tangle. *Nature*, **345**, 212.

Cuatrecasas, P. & Hollenberg, M.D. (1975). Binding of insulin and other hormones to non-receptor materials: saturability, specificity and apparent "negative cooperativity". *Biochem. Biophys. Res. Comm.*, **62**, 31-41.

Depover, A., Grupp, I.L., Grupp, G., Schwartz, A. (1983). Diltiazem potentiates the negative inotropic action of nimodipine in heart. *Biochem. Biophys. Res. Comm.*, **114**, 922-929.

Deshpande, J.K. & Wieloch, T. (1986). Flunarizine, a calcium entry blocker, ameliorates ischaemic brain damage in the rat. *Anesthesiology*, **64**, 215-224.

Deshpande, J.K., Siesjo, B.K. & Wieloch, T. (1987). Calcium accumulation and neuronal damage in the rat hippocampus following cerebral ischaemia. *J. Cerebral Blood Flow Metab.*, **7**, 89-95

Diemer, N.H., Sandberg, M., Jorgenson, M.B. & Benveniste, H. (1989). Ischaemia-induced release of glutamate in the hippocampal CA1 region is decreased after removal of the excitatory input from CA3. *J. Cerebral Blood Flow Metab.*, **9**, S747.

Dillon, J.S. & Nayler, W.G. (1987). [<sup>3</sup>H]-verapamil binding to rat cardiac sarcolemmal membrane fragments; an effect of ischaemia. *Br. J. Pharmacol.*, **90**, 99-109.

Doble, A., Malgouris, C., Daniel, M., Daniel, N., Imbault, F., Basbaum, A., Uzan, A., Guermey, C. & Le Fur, G. (1987). Labelling of peripheral-type benzodiazepine binding sites in human brain with [<sup>3</sup>H] PK 11195: anatomical and subcellular distribution. *Brain Res. Bull.*, **18**, 49-61.

Docherty, R.J. (1988). Gadolinium selectively blocks a component of calcium current in neuroblastoma x glioma hybrid (NG108-15) cells. *J. Physiol.*, **398**, 33-47.

Dolin, S., Little, H., Hudspeth, M., Pagonis, C. & Littleton, J. (1987). Increased dihydropyridine-sensitive calcium channels in rat brain may underlie ethanol physical dependence. *Neuropharmacology*, **26**, 275-279

Dolman, C.L. (1986). Microglia, In: *Textbook of Neuropathology* (ed) Davis, R.L. & Robertson, D.M. pp 117-137. Williams and Wilkins, Baltimore.

Dolphin, A.C. (1991). Regulation of calcium channel activity by GTP binding proteins and second messengers. *Biochimica et Biophysica Acta.*, **1091**, 68-80.

Dong, W., Schurr, A., Reid, K., Schields, C.B. & West, C.A. (1988). The rat hippocampal slice preparation as an *in vitro* model of ischaemia. *Stroke*, **19**, 498-502.

Donnan, G. (1989). Smoking and Stroke : a case-controlled study. *Lancet* **11**, 643-647.

Dubois, A., Benavides, J., Peny, B., Duverger, D., Fage, D., Gotti, B., MacKenzie, E.T. & Scatton, B. (1988). Imaging of primary and remote ischaemic and excitotoxic brain lesions. An autoradiographic study of peripheral type benzodiazepine binding sites in the rat and cat. *Brain Res.*, **445**, 77-90.

Duverger, D. & MacKenzie, E.T. (1988). The quantification of cerebral infarction following focal ischaemia in the rat: Influence of strain, arterial pressure, blood glucose concentration and age. *J. Cerebral Blood Flow Metab.*, **8**, 449-461.

Dux, E., Mies, G., Hossmann, K.A. & Siklos, L. (1987). Calcium in the mitochondria following brief ischaemia of gerbil brain. *Neurosci. Lett.*, **78**, 295-300.

Dyken, M.L., Wolf, P.A., Barnett, H.J.M., Bergan, J.J., Hass, W.K., Kannel, W.B., Kuller, L., Kurtzke, J.F. & Thoralf, S.M. (1984). Risk factors in stroke. *Stroke*, **15**, 1105-1111.

Eklof, B. & Siesjo, B.K. (1973). Cerebral blood flow in ischaemia caused by carotid artery ligation in the rat. *Acta Physiol. Scand.*, **87**, 69-77.

Faden, A.I. (1984). Opiate antagonists in the treatment of stroke. *Stroke*, **15**, 575-578.

- Fagg, G.E. (1985). L-Glutamate, excitatory amino acid receptors and brain function. *Trends Neurosci.*, **8**, 207-210.
- Fallis, R., Fisher, M. & Lobo, R. (1984). A double-blind trial of naloxone in acute stroke. *Stroke*, **14**, 124.
- Farber, J.L. (1981). The role of calcium in cell death. *Life Sci.*, **29**, 1289-1295.
- Ferrante, J., Luchowski, E., Rutledge, A. & Triggle, D.J. (1989). Binding of the 1,4-dihydropyridine calcium channel activator, (-) S-bay K 8644, to cardiac preparations. *Biochem. Biophys. Res. Comm.*, **158**, 149-154.
- Ferrante, J. & Triggle, D.J. (1990). Drug- and disease- induced regulation of voltage-dependent calcium channels. *Pharmacol. Rev.*, **42**, 29-44.
- Ferry, D.R., Goll, A., Gadow, C. & Glossmann, H. (1984). (-)-[<sup>3</sup>H]-desmethoxyverapamil labelling of putative calcium channels in brain: autoradiographic distribution and allosteric coupling to 1,4-dihydropyridine and diltiazem binding sites. *Naunyn-Schmiedeberg's Arch. Pharmacol.*, **327**, 183-187.
- Ferry, D.R., Goll, A., Rombusch, M. & Glossmann, H. (1985). The molecular pharmacology and structural features of calcium channels. *Br. J. Clin. Pharmacol.*, **20**, 233-246S.
- Fisher, C.M. (1982). Lacunar strokes and infarcts. *Neurology*, **32**, 871-876.
- Fisher, C.M. (1985). The ascendancy of diastolic blood pressure over the systolic. *Lancet*, *ii*, 1349-1350.
- Fleckenstein, A. (1983). *Calcium Antagonism In Heart and Smooth Muscle*. New York: John Wiley.
- Fleckenstein, A. (1988). The calcium channel of the heart. *Ann. NY. Acad. Sci. USA*, **522**, 1-15.
- Foster, A.C. & Fagg, G.E. (1984). Acidic amino acid binding sites in mammalian neuronal membranes: their characteristics in relation to synaptic receptors. *Brain. Res. Rev.*, **7**, 103-164.
- Fraser, S., Kenny, B.A., Kilpatrick, A.T. & Spedding, M. (1988). Is fluspirilene a potential ligand for the site of action of class III calcium antagonists? *Br. J. Pharmacol.*, **94**, 463P.
- Fraser, S. & Spedding, M. (1991). RS 87476, a novel neuroprotective agent, antagonises the effects of calcium channel activators in guinea-pig taenia. *Br. J. Pharmacol.*, **104**, 156P.
- Galizzi, J.P., Fosset, M. & Lazdunski, M. (1984). Properties of receptors for the Ca<sup>2+</sup> channel blocker verapamil in transverse tubule membranes of skeletal muscle. *Eur. J. Pharmacol.*, **144**, 211-215.
- Galizzi, J.P., Fosset, M. & Lazdunski, M. (1985). Characterization of the Ca<sup>2+</sup> coordination site regulating binding of Ca<sup>2+</sup> channel inhibitors d-cis-diltiazem, (+)bepridil and (-)desmethoxyverapamil to their site in skeletal muscle transverse tubule membranes. *Biochem. Biophys. Res. Comm.*, **132**, 49-55.

- Galizzi, J.P., Borsotto, M., Barhanin, J., Fosset, M. & Lazdunski, M. (1986a). Characterization and photoaffinity labelling of receptor sites for the  $\text{Ca}^{2+}$  channel inhibitors d-cis-diltiazem, (+)bepridil, desmethoxyverapamil, and (+)PN200-110 in skeletal muscle transverse tubule membranes. *J. Biol. Chem.* **261**, 1393-1397.
- Galizzi, J.P., Fosset, M., Romey, G., Laduron, P. & Lazdunski, M.C. (1986b). Neuroleptics of the diphenylbutylpiperidine series are potent calcium channel inhibitors. *Proc. Natl. Acad. Sci.*, **83**, 7513-7517.
- Garcia, J.H. (1984). Experimental ischaemic stroke: A review. *Stroke*, **15**, 5-14.
- Garcia, M.L., King, F.V., Shevell, J.L., Slaughter, R.S., Suarez-Kurtz, G., Winquist, R.J. & Kaczorowski, G.J. (1990). Amiloride analogues inhibit L-type calcium channels and display calcium antagonist blocker activity. *J. Biol. Chem.*, **265**, 3763-3771.
- Garthwaite, G. & Garthwaite, J. Neurotoxicity of excitatory amino acid receptor agonists in rat cerebellar slices: dependence on calcium concentration. (1986). *Neurosci. Lett.*, **66**, 193-198.
- Garthwaite, J. (1989). NMDA receptors, neuronal development and neurodegeneration. In: *The NMDA Receptor*. (ed) Watkins, J.C & Collingridge, G.L. Oxford University Press.
- Gelmers, H.J., Gorter, K., de Weerd, C.J. & Wiezer, H.J.A. (1988). A controlled trial of nimodipine in acute ischemic stroke. *N. Engl. J. Med.*, **318**, 203-207.
- Gent, H., Blakely, J.A., Easton, J.D., Hachinski, V., Harbison, J.W., Panak, E., Roberts, R.S., Sicurella, J & Purpie, A. (1989). The Canadian and American ticlopidine study (CATS) in thromboembolic stroke. *Lancet*, **11**, 1215-1220.
- Germano, I.M., Bartowski, H.M., Cassel, B. & Pitts, L.H. (1987). The therapeutic value of nimodipine on experimental focal cerebral ischaemia. Neurological outcome and histopathological findings. *J. Neurochem.*, **67**, 81-87.
- Germano, I.M., Pitts, L.H., Meldrum, B.S., Bartowski, H. & Simon, R.P. (1988). Kynurenate inhibition of cell excitation decreases stroke size and deficits. *Ann. Neurol.*, **22**, 730-734.
- Gill, J.S., Zezuke, A.V. & Shipley, H. (1986). Stroke and alcohol consumption. *N. Eng. J. Med.*, **315**, 1041-1046.
- Gill, R., Foster, A.C. & Woodruff, G.N. (1987). Systemic administration of MK-801 protects against ischaemia-induced hippocampal neurodegeneration in the gerbil. *J. Neurosci.*, **7**, 3343-3349.
- Gill, R., Foster, A.C. & Woodruff, G.N. (1988). MK 801 is neuroprotective in gerbils when administered during the post-ischaemic period. *Neuroscience*, **25**, 847-855.
- Gill, R., Brazell, C., Woodruff, G.N. and Kemp, J.A. (1991). The neuroprotective action of dizocilpine (MK-801) in the rat middle cerebral artery occlusion model of focal ischaemia. *Br. J. Pharmacol.*, **103**, 2030-2036.
- Ginsberg, M.D. & Busto, R. (1989). Rodent models of cerebral ischaemia. *Stroke*, **20**, 1627-1642.
- Ginsberg, M.D., Lin, B., Morikawa, E., Dietrich, W.D., Busto, R. & Globus, Y.T. (1991). Calcium antagonists in the treatment of experimental cerebral ischemia. *Arzneim-Forsch/Drug Res.*, **41**, 334-337.

- Globus, M.T., Ginsberg, M.D., Dietrich, W.D., Busto, R. & Scheinberg, P. (1987). Substantia nigra lesions protect against ischaemic damage in the striatum. *Neurosci. Lett.*, **80**, 251-256.
- Glossmann, H., Ferry, D.R., Lubbecke, F., Mewes, R. & Hofmann, F. (1982). Calcium channels: direct identification in radioligand binding studies. *Trends Pharmacol. Sci.*, **3**, 431-437.
- Glossmann, H. & Ferry, D.R. (1985). Assay for calcium channels. *Methods Enzymol.*, **109**, 513-550.
- Glossmann, H., Ferry, D.R., Goll, A., Striesnig, J. & Zernig, G. (1985). Calcium channels and calcium channel drugs: recent biochemical and biophysical findings. *Arzneim-Forsch/Drug Res.*, **35**, 1917-1935.
- Godfraind, T., Miller, R.C. & Wibo, M. (1986). Calcium antagonism and calcium entry blockade. *Pharmacol. Rev.*, **38**, 321-416.
- Goldberg, M.P., Viseskul, V. & Choi, D.W. (1988). Phencyclidine receptor ligands attenuate cortical neuronal injury after N-methyl-D-aspartate exposure or hypoxia. *J. Pharmacol. Exp. Ther.*, **245**, 1081-1087.
- Gordon-Weeks, P.R. (1987). Isolation of synaptosomes, growth cones and their subcellular components. In: *Neurochemistry: A Practical Approach*. (eds) Turner, A.J. & Bachelard, H.S. IRL Press. England.
- Gotoh, O., Mohamed, A.A., McCulloch, J., Graham, D.I., Harper, A.M. & Teasdale, G.M. (1986). Nimodipine and the haemodynamic and histopathological consequences of middle cerebral artery occlusion in the rat. *J. Cerebral Blood Flow Metab.*, **6**, 321-331.
- Gotti, B., Duverger, D., Bertin, J. & Dupont, R. (1988). Ifenprodil and SL 82. 0175 as anti-ischaemic agents. 1. Evidence for efficacy in models of focal cerebral ischaemia. *J. Pharmacol. Exp. Ther.*, **247**, 1211-1222.
- Gotti, B., Benavides, J., MacKenzie, E.T., & Scatton, B. (1990). The pharmacotherapy of focal cortical ischaemia in the mouse. *Brain Res.*, **522**, 290-307.
- Gould, R.J., Murphy, K.M.M., Reynolds, I.J. & Snyder, S.H. (1983). Anti-schizophrenic drugs of the diphenylbutylpiperidine type act as calcium channel antagonists. *Proc. Natl. Acad. Sci.*, **80**, 5122-5125.
- Govoni, S., Battaini, F., Magnoni, S.M., Lucchi, L., Rius, R.A. & Trabucchi, M. (1988a). Plasticity of neuronal L-type calcium channels. *Ann. NY. Acad. Sci.*, **522**, 187-198.
- Govoni, S., Di Giovanni, S., Moresco, R.M., Battaini, F. & Trabucchi, M. (1988b). Effect of chronic calcium antagonist treatment on dopamine recognition sites in rat striatum. *Neurosci. Lett.*, **87**, 173-177.
- Grassegger, A., Strissnig, J., Wieler, M., Hans-Gunther, K. & Glossmann, H. (1989). [<sup>3</sup>H] HOE 166 defines a novel calcium antagonist drug receptor, distinct from the 1,4 dihydropyridine binding domain. *Naunyn-Schmiedeberg's Arch. Pharmacol.*, **340**, 752-759.
- Green, F.J., Farmer, B.B., Wiseman, G.L., Jose, M.J.L. & Watanabe, A.M. (1985). Effect of membrane depolarisation on binding of [<sup>3</sup>H] nitrendipine to rat cardiac myocytes. *Circ. Res.*, **56**, 576-585.

- Greenberg, D.A., Cooper, E.C. & Carpenter, C.L. (1984). Phenytoin interacts with calcium channels in brain membranes. *Ann. Neurol.*, **16**, 616-617.
- Greenberg, J.H., Uematsu, D., Araki, N. & Reivich, M. (1991). Intracellular calcium and pathophysiological changes in cerebral ischemia. *Arzneim-Forsch/Drug Res.*, **41**, 324-331.
- Griffiths, T., Evans, M.C. & Meldrum, B.S. (1982). Intracellular sites of early calcium accumulation in the rat hippocampus during status epilepticus. *Neurosci. Lett.*, **30**, 329-334.
- Griffiths, T., Evans, M.C. & Meldrum, B.S. (1983). Intracellular calcium accumulation in rat hippocampus during seizures induced by bicuculline or l-allylglycine. *Neuroscience*, **10**, 385-395.
- Grigg, J.J. & Anderson, E.G. (1989). Glucose and sulfonylureas modify different phases of the membrane potential change during hypoxia in rat hippocampal slices. *Brain Res.*, **489**, 302-310.
- Grigg, J.J. & Anderson, E.G. (1990). Competitive and non-competitive N-methyl-D-aspartate antagonists modify hypoxia-induced membrane potential changes and protect rat hippocampal slices from functional failure: A quantitative comparison. *J. Pharmacol. Exp. Ther.*, **253**, 130-135.
- Grima, M., Schwartz, J., Spach, M.O. & Velly, J. (1986). Antianginal arylalkylamines and sodium channels: [<sup>3</sup>H]-batrachotoxin-A 20- $\alpha$ -benzoate and [<sup>3</sup>H]-tetracaine binding. *Br. J. Pharmacol.*, **89**, 641-646.
- Grotta, J.C. (1987). Current medical and surgical therapy for cerebrovascular disease. *N. Eng. J. Med.*, **317**, 1505-1515.
- Grotta, J.C., Spydell, J., Pettigrew, L.C., Ostrew, P. & Hunter, D. (1986). The effect of nicardipine on neuronal function following ischaemia. *Stroke*, **17**, 213-219.
- Gu, X.H., Dillon, J.S. & Nayler, W.G. (1988). Dihydropyridine binding sites in aerobically perfused, ischaemic and reperfused hearts: effect of temperature and time. *J. Cardiovasc. Pharmacol.*, **12**, 272-278.
- Hagberg, H., Lehman, A., Sandberg, M., Nyström, B., Jacobson, I. & Hamberger, A. (1985). Ischaemia-induced shift in inhibitory and excitatory amino acids from intra to extracellular compartments. *J. Cerebral Blood Flow Metab.*, **5**, 413-419.
- Hajos, F., Garthwaite, G. & Garthwaite, J. (1986). Reversible and irreversible neuronal damage caused by excitatory amino acid analogues in rat cerebellar slices. *Neuroscience*, **18**, 417-436.
- Hansen, A.J. & Zeuthen, T. (1981). Extracellular ion concentration during spreading depression and ischaemia in rat brain cortex. *Acta Physiol. Scand.*, **113**, 437-445.
- Hansen, A.J. (1985). Effects of anoxia on ion distribution in the brain. *Physiol. Rev.*, **65**, 101-148.
- Harris, R.J., Symon, L., Branston, N.M. and Bayham, M. (1981). Changes in extracellular Ca<sup>2+</sup> activity in cerebral ischaemia. *J. Cerebral Blood Flow Metab.*, **1**, 203-209.
- Harris, R.J. & Symon, L. (1984). Extracellular pH, potassium, and calcium activities in progressive ischaemia of the rat cortex. *J. Cerebral Blood Flow Metab.*, **4**, 178-186.

Harris, R.J., Weiloach, T., Symon, L. & Siesjo, B.K. (1984). Cerebral extracellular calcium activity in severe hyperglycaemia: relation to extracellular potassium and energy charge. *J. Cerebral Blood Flow Metab.*, **4**, 187-193.

Harrison, M.J.G. (1980). Clinical distinction of cerebral haemorrhage and cerebral infarction. *Postgrad. Med. J.*, **56**, 629-632.

Hartley, D.M. & Choi, D.W. (1989). Delayed rescue of N-methyl-D-aspartate mediated neuronal injury in cortical culture. *J. Pharmacol. Exp. Ther.*, **250**, 752-758.

Hass, W.K. (1981). Beyond cerebral blood flow, metabolism and ischemic thresholds: an examination of the role of calcium in the initiation of cerebral infarction. *Cerebral vascular disease 3*. Amsterdam: Excerpta Medica 3-17.

Heathers, G.P., Yamada, K.A., Kanter, E.M. & Corr, P.B. (1987). Long chain acylcarnitines mediate the hypoxia-induced increase in alpha-1 adrenergic receptors on adult canine myocytes. *Circ. Res.*, **61**, 735-746.

Heros, R.C. & Korosue, K. (1989). Hemodilution for cerebral ischaemia. *Stroke*, **20**, 423-427.

Higo, K., Saito, H. & Matsuki, N. (1988). Characteristics of [<sup>3</sup>H] nimodipine binding to sarcolemmal membranes from rat vas deferens and its regulation by guanine nucleotide. *Jpn. J. Pharmacol.*, **48**, 213-221.

Hillered, L., Siesjo, B.K. & Arfors, A. (1984). Mitochondrial response to transient forebrain ischaemia and recirculation in the rat. *J. Cerebral Blood Flow Metab.*, **4**, 438-446.

Hirning, L.D., Fox, A.P., McCleskey, E.W., Olivera, B.M., Thayer, S.A., Miller, R.J. & Tsien, R.W. (1988.) Dominant role of N-type Ca<sup>2+</sup> channels in evoked release of norepinephrine from sympathetic neurons. *Science*, **239**, 57-60.

Hofmann, F., Nastainczyk, W., Rohrkasten, A., Schneider, T. & Seiber, M. (1987). Regulation of the L-type calcium channel. *Trends Pharmacol. Sci.*, **8**, 393-398.

Hogan, M., Gjedde, A., Hakim, A. (1991). Activity of the dihydropyridine calcium channels following cerebral ischemia. *Arzneim-Forsch/Drug Res.*, **41**, 332-333.

Hollenberg, M.D. (1985). Examples of homospecific and heterospecific receptor regulation. *Trends Pharmacol. Sci.*, **6**, 242-245.

Hossmann, K.A., Grosse Ophoff, B., Schmidt-Kastner, R. & Oschlies, V. (1985). Mitochondrial calcium sequestration in cortical and hippocampal neurons after prolonged ischaemia of the cat brain. *Acta Neuropathol. Berlin*. **68**, 230-238.

Hossmann, K.A. (1989). Calcium antagonists for the treatment of brain ischaemia: a critical appraisal. In: *Pharmacology of Cerebral Ischaemia* (ed) Kriegelstein, J. CRC Press.

Howlett, D.R., Morris, H. & Nahorski, S.R. (1979). Anomalous properties of [<sup>3</sup>H] spiperone binding sites in various areas of the rat limbic system. *Mol. Pharmacol.*, **15**, 506-514.

Hsu, C.Y., Faught, R.E. & Furlan, A.J. (1987). Intravenous prostacyclin in acute non-haemorrhagic stroke: a placebo-controlled double-blind trial. *Stroke*, **18**, 352-358.

Iacopino, A.M. & Christakos, S.C. (1990). Specific reduction of calcium-binding protein (28K calbindin D) gene expression in aging and neurodegenerative disease. *Proc. Natl. Acad. Sci.*, **87**, 4078-4082.

Ikeda, J., Nagashima, G., Nowak, T.S., Mies, G., Joo, F., Xu, S., Lohr, J., Ruetzler, C., Wagner, H.G. & Klatzo, I. (1989). Observations on accumulation of calcium in gerbils subject to cerebral ischaemia. In: *Pharmacology of Cerebral Ischaemia*. (ed) Kriegstein, J. CRC press.

Ishii, K., Kano, T., Kurobe, Y. & Ando, J. (1983). Binding of [<sup>3</sup>H] nitrendipine to heart and brain membranes from normotensive and spontaneously hypertensive rats. *Eur. J. Pharmacol.*, **88**, 277-278.

Ito, V., Spatz, M., Walker, T.J. & Klatzo, I. (1975). Experimental cerebral ischaemia in Mongolian gerbils 1. Light microscopic observations. *Acta Neuropath.*, **32**, 209-233.

Iversen, L.L., Woodruff, G.N., Kemp, J.A., Foster, A.C., McKernan, R., Gill, R. & Wong, E.H.F. (1989). Non-competitive NMDA antagonists as drugs. In: *The NMDA receptor*. (ed) Watkins, J.C. & Collingridge, G.L. Oxford University Press.

Jacques, Y., Frelin, G., Vigne, G., Romey, G., Parjari, M. & Lazdunski, M. (1981). Neurotoxins specific for the sodium channel stimulate Ca<sup>2+</sup> entry into neuroblastoma cells. *Biochemistry*, **20**, 6219-6225.

Janis, R.A., Rampe, D., Sarmiento, J.G. & Triggle, D.J. (1984). Specific binding of a Ca<sup>2+</sup> channel agonist to membranes from cardiac muscle and brain. *Biochem. Biophys. Res. Comm.*, **88**, 277-278.

Janis, R.A. & Bellmann, P., Sarmiento, J.G. & Triggle, D.J. (1985). The dihydropyridine receptors. In: *Bayer Symposium: cardiovascular effects of dihydropyridine-type calcium antagonists and agonists*. pp 140-155. Springer-Verlag Berlin Heidelberg.

Janis, R.A. & Triggle, D. (1990). Drugs acting on calcium channels. In: *The Calcium Channel: Its properties, function and clinical relevance*. (Eds) Hurwitz, L., Partridge, L.D. & Leach, J.K. Telford Press.

Johnson, J.W. & Ascher, P. (1987). Glycine potentiates the NMDA response in cultured mouse brain neurones. *Nature*, **325**, 529-531.

Kariman, K. (1985). Mechanism of cell damage in brain ischaemia: a hypothesis. *Life Sci.*, **37**, 71-73.

Kass, R.S. & Lipton, P. (1986). Calcium and long-term transmission damage following anoxia in dentate gyrus and CA1 regions of the rat hippocampal slice. *J. Physiol.*, **378**, 313-334.

Kass, R.S., Arena, J.P. & Chin, S. (1989). Cellular electrophysiology of amlodipine: probing the cardiac L-type calcium channel. *Am. J. Cardiol.*, **64**, 35-42.

Kazazoglou, T., Schmid, A., Renaud, J.F. & Lazdunski, M. (1983). Ontogenic appearance of Ca<sup>2+</sup> channels characterised as binding sites for [<sup>3</sup>H] nitrendipine during development of nervous system, skeletal and cardiac muscle systems in the rat. *FEBS Lett.*, **164**, 75-79.

Kazda, S., Hoffmeister, F., Garthoff, B. & Toward, R. (1979). Prevention of post ischaemic impaired reperfusion on the brain by nimodipine. In: *Cerebral Blood flow and Metabolism*. (ed) Gotoh, F., Nagai, H. and Tazaki, Y. pp 302-303. Munksgaard,

Copenhagen.

Kemp, J.A., Foster, A.C. & Wong, E.H.F. (1987). Non-competitive antagonists of excitatory amino acid receptors. *Trends Neurosci.*, **10**, 294-298.

Kenny, B.A., Kilpatrick, A.T. & Spedding, M. (1986). Changes in [<sup>3</sup>H] nitrendipine binding in gerbil cortex following ischaemia. *Br. J. Pharmacol.*, **89**, 858P

Kenny, B.A., Fraser, S., Kilpatrick, A.T. & Spedding, M. (1990). Selective antagonism of calcium channel activators by fluspirilene. *Br. J. Pharmacol.*, **100**, 211-216.

Kenny, B.A., Kilpatrick, A.T. & Spedding, M. (1991). Quantification of the affinity of drugs acting at the calcium channel. In: *Cellular Calcium, A Practical Approach* (ed) McCormack, J.G. & Cobbold, P.H. Oxford University Press.

Kenny, B.A., MacKinnon, A.C., Kilpatrick, A.T. & Brown, C.M. (1991). Changes in [<sup>3</sup>H] PK 11195 and [<sup>3</sup>H] 8-OH-DPAT binding following forebrain ischaemia in the gerbil. Submitted for publication approval.

Kermode, J.C. (1989). The curvilinear Scatchard plot. *Biochem. Pharmacol.*, **38**, 2053-2060.

Khan, K. (1972). The natural course of experimental cerebral infarction in the gerbil. *Neurology*, **22**, 510-515.

Khaw, K.T. & Rose, G. (1989). Cholesterol and coronary heart disease. *Br. Med. J.*, **299**, 606-607.

King, F.V., Garcia, M.L., Shevell, J.L., Slaughter, R.S. & Kaczorowski, G.J. (1989). Substituted diphenylbutylpiperidines bind to a unique high affinity site on the L-type calcium channel. *J. Biol. Chem.*, **264**, 5633-5641.

Kinouchi, H., Imaizumi, S., Yoshimoto, T. & Motomiya, M. (1990). Phenytoin affects metabolism of free fatty acids and nucleotides in rat cerebral ischaemia. *Stroke*, **21**, 1326-1332.

Kirino, T. (1982). Delayed neuronal death in the gerbil hippocampus following ischemia. *Brain Res.* **239**, 57-69.

Kirino, T. & Sano, K. (1984). Fine structural nature of delayed neuronal death following ischaemia in the gerbil hippocampus. *Acta Neuropathol. (Berlin)*. **62**, 209-218.

Kirino, T., Tamura, A. & Sano, K. (1984). Delayed neuronal death in the rat hippocampus following transient forebrain ischemia. *Acta Neuropathol. (Berl)* **64**, 139-147.

Knabb, M.T., Saffitz, J.E., Corr, P.B. & Sobel, B.E. (1986). The dependence of electrophysiological derangements on accumulation of endogenous long-chain acyl carnitine in hypoxic neonatal rat myocytes. *Circ. Res.*, **58**, 230-240.

Kobayashi, S., Obana, W., Andrews, B.T., Nishimura, M.C. & Pitts, L.H. (1988). Lack of effect of nimodipine on experimental regional cerebral ischaemia. *Stroke*, **19**, 147.

- Kokubun, S., Prod'ham, B., Becker, C., Porzig, H. & Reuter, H. (1986). Studies on  $\text{Ca}^{2+}$  channels in intact cardiac cells. Voltage-dependent effects and cooperative interactions of dihydropyridine enantiomers. *Mol. Pharm.*, **30**, 571-584.
- Kongsamut, S., Freedman, S.B., Simon, B.E. & Miller, R.J. (1985). Interactions of steroidal alkaloid toxins with  $\text{Ca}^{2+}$  channels in neuronal cell lines. *Life. Sci.*, **36**, 1493-1501.
- Koudstaal, P.J., Stibbe, J. & Vermeulen, M. (1988). Fatal ischaemic brain oedema after early thrombolysis with tissue plasminogen activator. *Br. Med. J.* **298**, 382.
- Kucharczyk, J., Chew, W. & Derugin, N. (1989). Nicardipine reduces ischaemic brain injury: an in vivo magnetic resonance imaging/spectroscopy study in cats. *Stroke*, **20**, 268-274.
- Kucharczyk, J., Mintorovitch, J., Moseley, M.E., Asgari, H.S., Sevick, R.J., Derugin, N. & Norman, D. (1991). Ischaemic brain damage: reduction by sodium-calcium channel modulator RS-87476. *Radiology*, **179**, 221-227.
- Kuroiwa, T., Bonnekoh, P. & Hossmann, K.A. (1990) Prevention of postischemic hyperthermia prevents ischemic injury of CA1 neurons in gerbils. *J. Cerebral Blood Flow Metab* **10**, 550-556.
- Langer, S.Z. & Arbilla, S. (1988). Imidazopyridines as a tool for the characterisation of benzodiazepine receptors: a proposal for a pharmacological classification as  $\omega_3$  receptor. *Biochem. Behav.*, **29**, 763-766.
- Lanier, W.L., Perkina, W.J., Karlsson, B.R., Milde, J.H., Scheithauer, B.W., Shearman, G.T., & Michenfelder, J.D. (1989). The effect of excitatory amino acid antagonist MK 801 on cerebral injury following complete ischaemia in primates. *J. Cerebral Blood Flow Metab.*, **9**, S744.
- Lazdunski, M., Barhanin, J., Borsetto, M., Cognard, C., Cooper, C., Coppola, T., Fosset, M., Galizzi, J.P., Hosey, M.M., Mourre, C., Renaud, J., Romey, G., Schmid, A. & Vandaele, S. (1988). Molecular properties of structure and regulation of calcium channels. *Ann. NY. Acad. Sci.*, **522**, 134-149.
- Leander, J.D., Rathbun, R.C. & Zimmerman, D.M.C. (1988). Anticonvulsant effects of phencyclidine-like drugs: relation to N-methyl-D-aspartate acid antagonism. *Brain Res.*, **454**, 368-372.
- Lee, H.R., Roeske, W.R. & Yamamura, H.I. (1984). High affinity specific [ $^3\text{H}$ ] (+) PN 200-110 binding to dihydropyridine receptors associated with calcium channels in rat cerebral cortex and heart. *Life Sci.*, **35**, 721-732.
- Lee R.T., Smith, T.W. & Marsh, J.D. (1987). Evidence for distinct calcium channel and antagonist binding sites in intact cultured embryonic chick ventricular cells. *Circ. Res.*, **60**, 683-690.
- Le Fur, G., Vaucher, N., Perrier, A., Flamier, A., Benavides, J., Renault, C., Dubroucq, M.C., Gueremy, C. & Uzan, A. (1983). Differentiation between 2 ligands for peripheral benzodiazepine binding sites, [ $^3\text{H}$ ] RO 5-4864 and [ $^3\text{H}$ ] PK 11195 by thermodynamic studies. *Life Sci.*, **33**, 449-457.
- Levine, S. (1960). Anoxic-ischemic encephalopathy in rats. *Am. J. Pathol.*, **36**, 1-17.
- Levine, S. & Payan, H. (1966). Effects of ischaemia and other procedures on the brain and retina of the gerbil. *Exp. Neurol.*, **16**, 255-262.

Limbird, L.E. (1986). Identification of receptors using direct radioligand binding techniques. In: *Cell Surface Receptor: A Short Course On Theory And Methods*. (ed) Limbird, L.E. Kluwer Academic Publishers, U.K.

Lipton, P. & Whittingham, T.S. (1979). The effect of hypoxia on evoked potentials in the *in vitro* hippocampus. *J. Physiol.*, **287**, 427-438.

Lipton, P. & Whittingham, T.S. (1982). Reduced ATP concentration as a basis for synaptic transmission failure during hypoxia in the *in vitro* guinea-pig hippocampus. *J. Physiol.*, **325**, 51-65

Lipton, P. & Whittingham, T.S. (1984). Energy metabolism and brain slice function. In: *Brain Slices*. (ed) Dingledine, R. Plenum Press. New York.

Lipton, P. & Lobner, D. (1990). Mechanisms of intracellular calcium accumulation in the CA1 region of rat hippocampus during anoxia *in vitro*. *Stroke*, **21**, III60-64.

Little, H.J., Dolin, S. & Halsey, M.J. (1986). Calcium channel antagonists decrease the ethanol withdrawal syndrome. *Life Sci.*, **39**, 2059-2065.

Llinas, R.R. (1988). The intrinsic electrophysiological properties of mammalian neurones: insights into central nervous system function. *Science*, **242**, 1654-1664.

Llinas, R.R., Sugimori, M. & Cherksey, B. (1989). Voltage-dependent calcium conductances in mammalian neurones: the P channel. *Ann. NY. Acad. Sci.*, **560**, 103-111.

Lodder, J. & van der Lugt, P.J.M. (1983). Evaluation of the risk of immediate anticoagulation treatment in patients with embolic stroke of cardiac origin. *Stroke*, **14**, 42-46.

Lowe, G.D.O. (1990). Drugs in cerebral and peripheral arterial disease. *Br. Med. J.*, **300**, 524-528.

Lowenstein, D.H., Miles, M.F., Hatam, F. & McCabe, T. (1991). Up regulation of calbindin-D28K mRNA in the rat hippocampus following focal stimulation of the perforant path. *Neuron*, **6**, 627-633.

Lucchi, L., Govoni, S., Battaini, F., Pasinetti, G. & Trabucchi, M. (1985). Ethanol administration *in vivo* alters ion control in rat striatum. *Brain Res.*, **332**, 376-379.

Maan, A.C. & Hosey, M.M. (1987). Analysis of the properties of binding of calcium channel activators and inhibitors to dihydropyridine receptors in chick heart membranes. *Cir. Res.*, **61**, 379-388.

MacDonald, J.F., Miljokovic, Z. & Pennefather, P. (1987). Use-dependent block of excitatory amino acid currents in cultured neurones by ketamine. *J. Neurophysiology*, **58**, 251-265.

MacDonald, J.W., Silverstein, F.S. & Johnston, M.V. (1987). MK-801 protects the neonatal brain from hypoxic-ischaemic damage. *Eur. J. Pharmacol.*, **140**, 359-361.

MacMahon, S., Peto, R. & Cutler, J. (1990). Blood pressure, stroke and coronary heart disease: effects of prolonged difference in blood pressure. *Lancet*, **ii**, 765-774.

Magnoni, M.S., Govoni, S., Battaini, F. & Trabucchi, M. (1988). L-type calcium channels are modified in rat hippocampus by short term experimental ischaemia. *J. Cerebral Blood Flow Metab.*, **8**, 96-99.

Malmgren, R., Warlow, C., Bamford, J. & Sandercock, P. (1987). Geographic and secular trends in stroke incidence : a critical review. *Lancet*, ii, 1196-1200.

Malthe-Sorensen, D., Skrede, K.K. & Fonnum, F. (1979). Calcium-dependent release of D-[<sup>3</sup>H]-aspartate evoked by selective electrical stimulation of excitatory afferent fibres to hippocampal cells in vitro. *Neuroscience*, **4**, 255-263.

Marangos, P.J., Sperelakis, N. & Patel, J. (1984). Ontogeny of calcium antagonist binding sites in chick brain and heart. *J. Neurochem.*, **42**, 1338-1342.

Marcoux, F.W., Probert, A.W. & Weber, M.L. (1990). Hypoxic neuronal injury in tissue culture is associated with delayed calcium accumulation. *Stroke*, **21**, 71-74.

Marrannes, R., De Prins, E., Fransen, J. & Wauquier, A. (1989). Comparison of the influence of calcium antagonists and NMDA antagonists on the cortical extracellular changes in ion concentration and DC-potential during ischaemia. *Acta Physiol. Scand.*, **136**, s582.

Martinez-Vila, E., Guillen, F., Villanueva, J.A., Matias-Guiu, J., Bigorra, J., Gil, P., Carbonell, A. & Martinez-Lage, J.M. (1990). Placebo-controlled trial of nimodipine in the treatment of acute cerebral infarction. *Stroke*, **21**, 1023-1028.

Martin, J.F., Hamdy, N., Nicholl, J., Lewtas, & Bergrall, U. (1985). Double-blind controlled trial of prostacyclin in cerebral infarction. *Stroke*, **16**, 386-390.

Martins, E., Inamura, K., Themner, K., Malmqvist, K.G. & Siesjo, B.K. (1988). Accumulation of calcium and loss of potassium in the hippocampus following transient cerebral ischaemia: a proton microprobe study. *J. Cerebral Blood Flow Metab.*, **8**, 531-538.

Mason, R.P., Campbell, S.F., Wang, S.D. & Herbette, L.G. (1989). Comparison of location and binding for the positively charged 1,4-dihydropyridine calcium channel antagonist amlodipine with uncharged drugs of this class in cardiac membranes. *Mol. Pharmacol.*, **36**, 634-640.

Mason, P.R., Rhodes, D. & Herbette, L.G. (1991). Reevaluating equilibrium and kinetic binding parameters for lipophilic drugs based on a structural model for drug interaction with biological membranes. *J. Med. Chem.*, **34**, 869-877.

Matsuki, N., Quant, F.N., Ten Eick, R.E. & Yeh, J.Z. (1984). Characterisation of the block of sodium channels by phenytoin in mouse neuroblastoma cells. *J. Pharmacol. Exp. Ther.*, **228**, 523-530.

Mattson, M.P., Rychlik, B., Chu, C. & Christakos, S. (1991). Evidence for calcium-reducing and excitatory-protective roles for the calcium-binding protein calbindin-D28K in cultured hippocampal neurones. *Neuron*, **6**, 41-51.

Matucci, R., Bennardini, F., Sciamarella, M.L., Baccaro, C., Stendardi, I., Franconi, F. & Giotti, A. (1987). [<sup>3</sup>H]-Nitrendipine binding in membranes obtained from hypoxic and reoxygenated heart. *Biochem. Pharmacol.*, **36**, 1059-1062.

McCormack, J.G., Halestrap, A.P. & Denton, R.M. (1990). Role of calcium ions in regulation of mammalian intramitochondrial metabolism. *Physiol. Rev.* **70**, 391-425.

McCulloch, J. (1991). Ischaemic brain damage-prevention with competitive and non-competitive antagonists of N-methyl-D-aspartate receptors. *Arzneim-Forsch/Drug Res.*, **41**, 319-323.

McKenna, E., Koch, W.J., Slish, D.F. & Schwartz, A. (1990). Toward an understanding of the dihydropyridine-sensitive calcium channels. *Biochem. Pharmacol.*, **139**, 1145-1150.

McNamara, J.O., Rigsbee, L.C., Buller, L.S., Shin, C. (1989). Intravenous phenytoin is an effective anticonvulsant in the kindling model. *Ann. Neurol.*, **26**, 675-678.

Meldolesi, J., Volpe, P. & Pozzan, T. (1988). The intracellular distribution of  $\text{Ca}^{2+}$ . *Trends Neurosci.*, **11**, 449-452.

Meldolesi, J., Madeddu, L. & Pozzan, T. (1990). Intracellular  $\text{Ca}^{2+}$  storage organelles in non-muscle cells: heterogeneity and functional assignment. *Biochimica et Biophysica Acta.*, **1055**, 130-140.

Meldrum, B.S. & Brierley, J.B. (1973). Prolonged epileptic seizures in primates in relation to icta physiologic events. *Arch. Neurol.*, **28**, 10-17.

Meldrum, B.S., Chapman, A.G., Patel, S. & Swan, J. (1989). Competitive NMDA antagonists as drugs. In: *The NMDA Receptor*. (ed) Watkins, J.C. & Collingridge, G.L. pp 207-216. Oxford University Press.

Meldrum, B.S. & Swan, J.H. (1989). Competitive and non-competitive NMDA antagonists as cerebroprotective agents. In: *Pharmacology of Cerebral Ischaemia*. (ed) Kriegelstein, J. CRC Press.

Meldrum, B.S. & Garthwaite, J. (1990). Excitatory amino acid neurotoxicity and neurodegenerative disease. *Trends Pharmacol. Sci.*, **11**, 379-387.

Meyer, F.B. (1989). Calcium, neuronal hyperexcitability and ischemic injury. *Brain Res. Rev.*, **14**, 227-243.

Michel, A.D. & Whiting, R.L. (1988). Methoctramine, a polymethylene tetraamine, differentiates three subtypes of muscarinic receptors in direct binding studies. *Eur. J. Pharmacol.*, **145**, 61-66.

Middlemiss, D.N. & Spedding, M. (1985). A functional correlate for the dihydropyridine binding site in rat brain. *Nature*, **314**, 94-97.

Mikami, A., Imoto, K., Tanabe, T., Niidome, T., Mori, Y., Takeshima, H., Narumiya, S. & Numa, S. (1989). Primary structure and functional expression of the cardiac dihydropyridine-sensitive calcium channel. *Nature*, **340**, 230-232.

Miller, R.J. (1987). Multiple calcium channels and neuronal function. *Science*, **235**, 46-52.

Miller, R.J. (1989).  $\text{Ca}^{2+}$  channels, excitatory amino acids and cerebral ischaemia, in: *Pharmacology of Cerebral Ischaemia*. (ed) Kriegelstein, J. pp 139-149. CRC press.

Miller, R.J. (1990). Glucose-regulated potassium channels are sweet news for neurobiologists. *Trends Neurosci.*, **13**, 197-199.

Mir, A.K. & Spedding, M. (1987). Calcium-antagonist properties of diclofurime isomers. II. Molecular aspects: allosteric interactions with dihydropyridine recognition sites. *J. Cardiovasc. Pharmacol.*, **9**, 469-477.

Mohamed, A.A., Gotoh, O., Graham, D.I., Osborne, K.A., McCulloch, J., Mendelow, A.D. & Teasdale, G.M. (1985). Effect of pretreatment with the calcium antagonist nimodipine on local cerebral blood flow and histopathology after middle

cerebral artery occlusion. *Ann. Neurol.*, **18**, 705-711.

Molinari, G.F. & Laurent, J.P. (1976). A classification of experimental models of brain ischaemia. *Stroke*, **7**, 14-17.

Molinari, G.F. (1988). Why model strokes? *Stroke*, **19**, 1195-1197.

Monaghan, D.T., Bridges, R.J. & Cotman, C.W. (1989). The excitatory amino acid receptors: their classes, pharmacology, and distinct properties in the function of the central nervous system. *Ann. Rev. Pharmacol. Toxicol.*, **29**, 365-402.

Morel, N. & Godfraind, T. (1988). Selective modulation by membrane potential of the interaction of some calcium channel entry blockers with calcium channels in rat mesenteric artery. *Br. J. Pharmacol.*, **95**, 252-258.

Mori, Y., Friedrich, T., Kim, M.S., Mikami, A., Nakai, J., Ruth, P., Bosse, E., Hofmann, F., Flockerzi, V., Furuichi, T., Mikoshiba, K., Imoto, K., Tanabe, T., & Numa, S. (1991). Primary structure and functional expression from complementary DNA of a brain calcium channel. *Nature*, **350**, 398-402.

Moron, M.A., Stevens, C.W. & Yaksh, T.L. (1989). Diltiazem enhances and flunarizine inhibits nimodipine's anti-seizure effects. *Eur. J. Pharmacol.*, **163**, 299-307.

Mourre, C., Ben-Ari, Y., Bernadi, H., Fosset, M. & Lazdunski, M. (1989). Antibiotic sulfonylureas: localisation of binding sites in the brain and effects on the hyperpolarisation induced by anoxia in hippocampal slices. *Brain Res.*, **486**, 159-164.

Munson, P.J. & Rodbard, S. (1980). Ligand: a versatile computerized approach for the characterization of ligand binding systems. *Anal. Biochem.*, **107**, 220-239.

Murphy, K.M.M., Gould, R.J., Largent, B.L. & Snyder, S.H. (1983). A unitary mechanism of calcium antagonist drug action. *Proc. Natl. Acad. Sci.*, **80**, 860-864.

Murphy, S.N. & Miller, R.J. (1989). A glutamate receptor regulates  $\text{Ca}^{2+}$  mobilization in hippocampal neurones. *Proc. Nat. Acad. Sci.*, **85**, 8737-8741.

Myers, R., Manji, L.G., Cullen, B.M., Price, G.W., Frackowiak, R.S.J. & Cremer, J.E. (1991). Macrophage and astrocyte populations in relation to [ $^3\text{H}$ ] PK 11195 binding in rat cerebral cortex following a local ischaemic lesion. *J. Cerebral Blood Flow Metab.*, **11**, 314-322.

Nachshen, D.A., Sanchez-Armass, S. & Weinstein, A.M. (1986). The regulation of cytosolic calcium in rat brain synaptosomes by sodium dependent calcium efflux. *J. Physiol.*, **381**, 17-28.

Nahorski, S.R. (1988). Inositol polyphosphates and neuronal calcium homeostasis. *Trends Neurosci.*, **11**, 444-448.

Nakayama, H., Dietrich, W.D., Watson, B.D., Busto, R. & Ginsberg, M.D. (1988). Photothrombotic occlusion of rat middle cerebral artery: histopathological and hemodynamic sequelae of acute recanalization. *J. Cerebral Blood Flow Metab.*, **8**, 474-485.

Nayler, W.G., Dillon, J.S. & McKelvie, M. (1985). An effect of ischaemia on myocardial dihydropyridine binding sites. *Eur. J. Pharmacol.*, **115**, 81-89.

Nedergaard, M. (1988). Mechanisms of brain damage in focal cerebral ischaemia. *Acta Neurol. Scand.*, **77**, 81-101.

Newberg, L.A., Steen, P.A., Milde, J.H. & Michenfelder, J.D. (1984). Failure of flunarizine to improve cerebral blood flow or neurological recovery in a canine model of complete cerebral ischaemia. *Stroke*, **15**, 606-671.

Nicholson, C., Bruggencate, G.T., Steinberg, R. and Stockle, H. (1977). Calcium modulation in brain extracellular microenvironment demonstrated with ion-selective micropipette. *Proc. Natl. Acad. Sci.*, **74**, 1287-1290.

Nicotera, P., Hartzell, P., Davis, G. & Orrenius, S. (1986). The formation of plasma membrane blebs in hepatocytes exposed to agents that increase cytosolic  $\text{Ca}^{2+}$  is mediated by the action of a non-lysosomal proteolytic system. *FEBS Lett.*, **209**, 139-144.

Nishini, N., Noguchi-Kuno, S.A., Sugiyama, T. & Tanaka, C. (1986). [ $^3\text{H}$ ] nitrendipine binding sites are decreased in the substantia nigra and striatum of the brain from patients with Parkinson's disease. *Brain Res.*, **377**, 186-189.

Nitsch, R., Leranth, C. & Frotscher, M. (1990). Most somatostatin immunoreactive neurones in the rat facial dentate do not contain the calcium-binding protein parvalbumin. *Brain Res.*, **528**, 327-329.

Noda, M., Ikeda, T., Suzuki, H., Takeshima, H., Takashima, T., Kuno, M. & Numa, S. (1986). Expression of functional sodium channels from cDNA. *Nature*, **322**, 826-828.

Nokin, P., Clinet, M., Swillens, S., Delisee, C., Meysmans, L. & Chatelain, P. (1986). Allosteric modulation of [ $^3\text{H}$ ] nitrendipine binding to cardiac and cerebral membranes by amiodarone. *J. Cardiovasc. Pharmacol.*, **8**, 1051-1057.

Nokin, P., Clinet, M., Polster, P., Beaufort, P., Meysmans, L., Gougat, J. & Chatelain, P. (1989). SR33557, a novel calcium-antagonist: interaction with [ $^3\text{H}$ ]-(+)-nitrendipine and [ $^3\text{H}$ ]-(-)-desmethoxy-verapamil binding sites in cerebral membranes. *Naunyn-Schmiedeberg's Arch. Pharmacol.*, **339**, 31-36.

Nokin, P., Clinet, P., Beaufort, L., Meysmans, R., Laruel, R. & Chatelain, P. (1990). SR 33557, a novel calcium entry blocker. II. Interactions with 1,4-dihydropyridine, phenylalkylamine and benzothiazepine binding sites in rat heart sarcolemmal membranes. *J. Pharmacol. Exp. Ther.*, **255**, 600-

Norris, J.W. & Hachinski, V.C. (1986). High dose steroid treatment in cerebral infarction. *Brit. Med. J.*, **292**, 21-23.

Nowycky, M.C., Fox, A.P. & Tsien, R.W. (1985). Three types of neuronal calcium channel with different calcium agonist sensitivity. *Nature*, **316**, 339-343.

Nuglisch, J., Kartoutly, J.C., Mennel, H.D., Rossberg, C. & Krieglstein, J. (1990). Protective effect of nimodipine against ischaemic neuronal damage in rat hippocampus without changing post-ischaemic blood flow. *J. Cerebral Blood Flow Metab.*, **10**, 654-659.

Obana, W.G., Bartkowski, H.M., Cassel, M.E., Nishimura, M.C. & Pitts, L.H. (1985). Nimodipine pre-treatment reduces infarct size after middle cerebral artery occlusion in the rat. *Clin. Res.* **33**, 69A.

Oczkowski, W.J., Hamchinski, V.C., Bogusslavski, J., Barnett, H.J.M. & Carruthers, S.G. (1989). A double-blind, randomised trial of PY 108-068 in acute ischaemic cerebral infarction. *Stroke*, **20**, 604-608.

Okamoto, K., Yamuri, Y. & Nagaoka, A. (1974). Establishment of the stroke-prone spontaneously hypertensive rat (SHR). *Circ. Res.*, **34**, 143-153.

Olivera, B.M., Gray, W.R., Zeikus, R., McIntosh, J.M., Varga, J., Rivier, J., deSantos, V. & Cruz, L.J. (1985). Peptide neurotoxins from fish hunting cone snails. *Science*, **230**, 1338-1343.

Olney, J.W., Labruyere, J. & Price, M.T. (1989). Phencyclidine, dizoclipine and cerbrocortical neurones. *Science*, **244**, 1360-1362.

Onodera, H., Sato, G. & Kogure, K. (1986). Lesions to Schaffer collaterals prevent ischaemic death of CA1 pyramidal cells. *Neurosci. Lett.*, **68**, 169-174.

Onodera, H., Sato, G. & Kogure, K. (1987). Quantitative autoradiographic analysis of muscarinic, cholinergic and adenosine A<sub>1</sub> binding sites after transient forebrain ischaemia in the gerbil. *Brain Res.*, **415**, 309-322.

Onodera, H. & Kogure, K. (1990). Calcium antagonist, adenosine A<sub>1</sub> and muscarinic bindings in rat hippocampus after transient ischaemia. *Stroke*, **21**, 771-776.

Osbourne, K.A., Shigeno, T., Balarsky, A.M., Ford, I., McCulloch, J., Teasdale, G.M. & Graham, D.I. (1987). Quantitative assessment of early brain damage in a rat model of focal ischaemia. *J. Neurol. Neurosurg. Psychiatry*, **50**, 402-410.

Owen, F., Poulter, M. & Waddington, J.L. (1983). [<sup>3</sup>H] RO 5-4864 and [<sup>3</sup>H] flunitrazepam binding in kainate-lesioned rat striatum and temporal cortex of brains from patients with senile dementia of the Alzheimer subtype. *Brain Res.*, **278**, 373-375.

Owen, P.J., Marriott, D.B. & Boarder, M.R. (1989). Evidence for a dihydropyridine-sensitive release of noradrenaline and uptake of calcium in adrenal chromaffin cells. *Br. J. Pharmacol.*, **97**, 133-138.

Palmer, G.C., Palmer, S.J. & Christie-Pope, B.C. (1988). Protective action of calcium channel blockers on Na<sup>+</sup>, K<sup>+</sup>-ATPase in gerbil cerebral cortex following ischemia. *J. Neurosci. Res.*, **19**, 252-257.

Pang, D.C. & Sperelakis, N. (1983). Nifedipine, diltiazem, bepridil and verapamil uptake into cardiac and smooth muscles. *Eur. J. Pharmacol.*, **87**, 199-207.

Pang, D.C. & Sperelakis, N. (1984). Uptake of calcium antagonistic drugs into muscles as related to their lipid solubilities. *Biochem. Pharmacol.*, **33**, 821-826.

Panza, G., Grebb, J.A., Sanna, E., Wright, A.G. & Hanbauer, I. (1985). Evidence for down regulation of [<sup>3</sup>H] nitrendipine recognition sites in mouse brain after long term treatment with nifedipine or verapamil. *Neuropharmacology*, **34**, 1116-1117.

Park, C.K., Nehls, G.G., Graham, D.T., Teasdale, G.M. & McCulloch, J. (1988a). Focal ischaemia in the cat: treatment with the glutamate antagonist MK-801 after induction of ischaemia. *J. Cerebral Blood Flow Metab.*, **8**, 757-762.

Park, C.K., Nehls, G.G., Graham, D.I., Teasdale, G.M. & McCulloch, J. (1988b). The glutamate antagonist MK 801 reduces focal ischaemic damage in the rat. *Ann. Neurol.*, **24**, 543-551.

Pashen, W., Hallmayer, J. and Rohn, G. (1988). Relationship between putrescine content and density of ischaemic cell damage in the brain of mongolian gerbils : Effects of nimodipine and barbiturate. *Acta. Neuropath.*, **75**, 388-394.

Paton, W.D.M. & Rang, H.P. (1965). The uptake of atropine and related drugs by intestinal smooth muscle of the guinea-pig in relation to acetylcholine receptors. *Proc. R. Soc. Lond.*, **163**, 1-44.

Patmore, L., Duncan, G.P. & Spedding, M. (1989a). Interactions of palmitoyl carnitine with calcium-antagonists in myocytes. *Br. J. Pharmacol.*, **97**, 443-450

Patmore, L., Duncan, G.P. & Spedding, M. (1989b). The effects of calcium antagonists on calcium overload contractures in embryonic chick myocytes induced by ouabain and veratrine. *Br. J. Pharmacol.*, **97**, 83-94

Patmore, L., Duncan, G.P., Kenny, B.A. & Spedding, M. (1991). RS 87476, a novel neuroprotective agent, inhibits veratrine-induced calcium overload in embryonic chick myocytes. *Br. J. Pharmacol.*, **104**, 175P.

Pauwels, P.J. & Laduron, P.M. (1986). TPP<sup>+</sup> accumulation in rat brain synaptosomes as a probe for Na<sup>+</sup> channels. *Eur. J. Pharmacol.*, **132**, 289-293.

Pauwels, P.J., Leysen, J.E. & Laduron, P. (1986). [<sup>3</sup>H] Batrachotoxinin A 20- $\alpha$ -benzoate binding to sodium channels in rat brain: characterisation and pharmacological significance. *Eur. J. Pharmacol.*, **124**, 291-298.

Pauwels, P.J., Assouw, H.P., Peeters, L. & Leysen, J.E. (1990). Neurotoxic action of veratridine in rat brain neuronal cultures: mechanism of neuroprotection by Ca<sup>2+</sup> channel-antagonists non-selective for slow Ca<sup>2+</sup> channels. *J. Pharmacol. Exp. Ther.*, **255**, 1177-1122.

Pauwels, P.J., Leysen, J.E. & Janssen, P.J. (1991). Ca<sup>2+</sup> and Na<sup>+</sup> channels involved in neuronal cell death. Protection by flunarizine. *Life Sci.*, **48**, 1881-1893.

Penniston, J.T. (1983). Plasma membrane Ca<sup>2+</sup> pumping ATPase. *Ann. NY. Acad. Sci.*, **402**, 296-302.

Perez-Reyes, E., Kim, H.S., Lacerda, A.E., Horne, W., Wei, X., Rampe, D., Campbell, K.P., Brown, A.M. & Birnbaumer, L. (1989). Induction of calcium currents by the expression of the  $\alpha_1$ -subunit of the dihydropyridine receptor from skeletal muscle. *Nature*, **340**, 233-236.

Perry, V.H. & Gordon, S. (1988). Macrophages and microglia in the nervous system. *Trends. Neurosci.*, **11**, 272-277.

Persechini, A., Moncrief, N.D. & Kretsinger, R.H. (1989). The EF-hand family of calcium-modulated proteins. *Trends Neurosci.*, **12**, 462-467.

Pert, C., & Snyder, S. (1973). Opiate demonstration in nervous tissue. *Science*, **179**, 1011-1014.

Petito, C.K., Feldmann, E., Pulsinelli, W.A. & Plum, F. (1987). Delayed hippocampal damage in humans following cardiorespiratory arrest. *Neurology*, **37**, 1281-1286.

Petito, C.K., Chung, H.M., Morgello, S., Felix, J.C. & Lesser, M.L. (1989). Post-ischaemic increases in astrocyte glutamine synthetase and intermediate filament proteins. In: *Cerebrovascular Diseases* (ed) Ginsberg, M.D & Dalton, W. Raven Press, New York.

Petruk, K.C., West, M. & Mohr, G. (1988). Effect of nimodipine on the outcome of patients with subarachnoid haemorrhage and surgery. *J. Neurosurg.*, **69**, 683-686.

- Pickard, J.D., Murray, G.D., Illingworth, R., Shaw, M.D.M., Teasdale, G.M., Foy, P.M., Humphrey, P.R.D., Lang, D.A., Nelson, R., Richards, P., Sinar, J., Bailey, S. & Skene, A. (1989). Effect of oral nimodipine on cerebral infarction and outcome after subarachnoid haemorrhage: British aneurysm nimodipine trial. *Brit. Med. J.*, **298**, 636-642.
- Pietrobon, D., DeVirgilio, F. & Pozzan, T. (1990). Structural and functional aspects of calcium homeostasis in eukaryotic cells. *Eur. J. Biochem.*, **193**, 599-622.
- Pincus, J.H. & Hsiao, K. (1981). Calcium uptake mechanisms affected by some convulsant drugs. *Brain Res.*, **217**, 119-127.
- Polster, P., Christophe, B., Van Damme, M., Houlliche, A. & Chatelain, P. (1990). SR 33557, a novel calcium entry blocker. 1. In vitro isolated tissue studies. *J. Pharmacol. Exp. Ther.*, **255**, 593-599.
- Postma, S.W. & Catterall, W.A. (1984). Inhibition of [<sup>3</sup>H] batrachotoxinin A 20- $\alpha$ -benzoate to sodium channels by local anaesthetics. *Mol. Pharmacol.*, **25**, 219-227.
- Prenen, H.M., GwanGo, K., Postema, F., Zuiderveen, F. & Korf, J. (1988). Cerebral cation shifts in hypoxic brain damage are prevented by the sodium channel blocker terotodotoxin. *Exp. Neurol.*, **99**, 118-132.
- Pulsinelli, W.A. & Brierley, J.B. (1979). A new model of bilateral hemispheric ischemia in the unanaesthetised rat. *Stroke*, **10**, 267-272.
- Pulsinelli, W.A., Waldman, S., Rawlinson, D. & Plum, F. (1982a). Moderate hyperglycaemia augments ischaemic brain damage. A neuropathologic study in the rat. *Neurology*, **32**, 1239-1246.
- Pulsinelli, W.A., Brierley, J.B. & Plum, F. (1982b). Temporal profile of neuronal damage in a model of transient forebrain ischemia. *Ann. Neurol.*, **11**, 491-498.
- Pulsinelli, W.A. (1985). Deafferentation of the hippocampus protects CA1 pyramidal neurones against ischaemic injury. *Stroke*, **16**, 144.
- Pulsinelli, W.A. & Buchan, A.M. (1988). The four-vessel occlusion rat model: Method for complete occlusion of vertebral arteries and control of collateral circulation. *Stroke*, **19**, 913-914.
- Pulsinelli, W.A. & Buchan, A.M. (1989). The utility of animal models in predicting pharmacotherapeutic response in the clinical setting. In: *Cerebrovascular Diseases*. (ed) Ginsberg, M.D. & Dietrich, W.D. Raven Press.
- Qar, J., Galizzi, J-P., Fosset, M. & Lazdunski, M. (1987). Receptors for diphenylbutylpiperidine neuroleptics in brain, cardiac, and smooth muscle membranes. Relationship with receptors for 1,4-dihydropyridines and phenylalkylamines and with Ca<sup>2+</sup> channel blockade. *Eur. J. Pharmacol.*, **141**, 261-268.
- Quirion, R., Lafaille, F. & Nair, N.P.V. (1985). Comparative potencies of calcium channel antagonists and anti-schizophrenic drugs on central and peripheral calcium channel binding sites. *J. Pharm. Pharmacol.*, **37**, 437-440.
- Rader, P.K. & Lanthorn, T.H. (1989). Experimental ischaemia induces a persistent depolarisation blocked by decreased calcium and NMDA antagonists. *Neurosci. Lett.*, **99**, 125-130.
- Raichle, M. (1983). The pathophysiology of brain ischaemia. *Ann. Neurol.*, **13**, 2-10.

- Ramkumar, V. & El-Fakahany, E.E. (1984). Increase in [ $^3\text{H}$ ]-nitrendipine binding sites in the brain in morphine tolerant mice. *Eur. J. Pharmacol.*, **102**, 371-372.
- Ramkumar, V. & El-Fakahany, E.E. (1985). Changes in the affinity of [ $^3\text{H}$ ]-nitrendipine binding sites in the brain upon chlorpromazine treatment and subsequent withdrawal. *Res. Commun. Chem. Pathol. Pharmacol.*, **48**, 463-466.
- Rampe, D., Luchowski, E., Rutledge, A., Janis, R.A. & Triggle, D.J. (1987). Comparative aspects of temperature dependence of [ $^3\text{H}$ ] 1,4-dihydropyridine  $\text{Ca}^{2+}$  channel antagonist and activator binding to neuronal and muscle membranes. *Can. J. Physiol. Pharmacol.*, **65**, 1452-1460.
- Ransom, B.R., Stys, P.K. & Waxman, S.G. (1990). The pathophysiology of anoxic injury in central nervous system white matter. *Stroke*, **21**, 52-57.
- Rappaport, Z.H., Young, W. & Flamm, E.S. (1987). Regional brain calcium changes in the rat middle cerebral artery occlusion model of ischemia. *Stroke*, **18**, 760-764.
- Rasmussen, H. & Barrett, P.Q. (1984). Calcium messenger system: an integrated view. *Physiol. Rev.*, **64**, 938-984.
- Reeves, J.P. & Hale, C.C. (1984). The stoichiometry of the cardiac sodium-calcium exchange system. *J. Biol. Chem.* **259**, 7733-7739.
- Regulla, S., Schneider, T., Nastainczyk, W., Meyer, H.E. & Hofmann, F. (1991). Identification of the site of interaction of the dihydropyridine channel blockers nitrendipine and azidopine with the calcium-channel  $\alpha_1$  subunit. *EMBO J.*, **10**, 45-49.
- Reith, M.E., Kim, S.S. & Lajtha, A. (1987). Binding sites for [ $^3\text{H}$ ] tetracaine in synaptosomal sodium channel preparations from mouse brain. *Eur. J. Pharmacol.*, **143**, 171-178.
- Reuter, H., Porzig, H., Kokubun, S. & Prod'ham, B. (1988). Calcium channels in the heart. Properties and modulation by DHP enantiomers. *Ann. NY. Acad. Sci.*, **522**, 16-24.
- Reynolds, I.J. & Miller, R.J. (1988). Multiple sites for the regulation of the N-methyl-D-aspartate receptor. *Mol. Pharmacol.*, **33**, 581-584.
- Rhodes, D.G., Sarmiento, J.G. & Herbette, L.G. (1985). Kinetics of binding of membrane-active drugs to receptor sites. Diffusion limited rates for a membrane bilayer approach of 1,4-dihydropyridine calcium channel antagonists to their active site. *Mol. Pharmacol.*, **27**, 612-623.
- Richter, C., Theus, M. & Schlegel, J. (1990). Cyclosporine A inhibits mitochondrial pyridine nucleotide hydrolysis and calcium release. *Biochem. Pharmacol.*, **40**, 779-782.
- Rius, R.A., Govoni, S. & Trabucchi, M. (1986). Regional modification of brain calcium antagonist binding after in vivo chronic lead exposure. *Toxicology*, **40**, 191-197.
- Rockoff, M.A., Marshall, L.F. & Shapiro, H.M. (1979). High dose barbiturate therapy in humans: a clinical review of 60 patients. *Ann. Neurol.*, **6**, 194-199.
- Rodenkirchen, R., Bayer, R. & Mannhold, R. (1982). Specific and non-specific calcium antagonists. A structure activity analysis of cardio-depressive drugs. *Prog. Pharmacol.*, **5**, 9-23.

- Rogawski, M.A. & Porter, R.J. (1990). Antiepileptic drugs: pharmacological mechanisms and clinical efficacy with consideration of promising developmental stage compounds. *Pharmacol. Rev.*, **42**, 223-287.
- Rogers, H., Birch, P.J. & Hayes, A.G. (1990). Effects of hypoxia and hypoglycaemia on DC potentials recorded from the gerbil hippocampus in vitro. *Naunyn-Schmiedeberg's Arch Pharmacol.*, **342**, 547-553.
- Roman, K., Bartowski, H., & Simon, R. (1989). The specific NMDA receptor antagonist AP-7 attenuates focal ischaemic brain injury. *Neurosci. Lett.*, **104**, 19-24.
- Ross Russel, R.W. (1984). Pathological changes in small cerebral arteries causing occlusion and haemorrhage. *J. Cardiovasc. Pharmacol.*, **6**, S691.
- Rothman, S.M. (1983). Synaptic activity mediates death of hypoxic neurones, *Science*, **220**, 536-537.
- Rothman, S.M. (1984). Synaptic release of excitatory amino acid neurotransmitter mediates anoxic neuronal death. *J. Neurosci.*, **4**, 1884-1891.
- Rothman, S.M. (1985). The neurotoxicity of excitatory amino acids is produced by passive chloride flux. *J. Neurosci.*, **5**, 1483-1489.
- Rothman, S.M. & Samaie, M. (1985). Physiology of excitatory synaptic transmission in cultures of dissociated rat hippocampal. *J. Neurophysiol.*, **54**, 701-713.
- Rothman, S.M. & Olney, J.W. (1986). Glutamate and the pathophysiology of hypoxic-ischemic brain damage. *Ann. Neurol.*, **19**, 105-111.
- Safer, P. (1980). Amelioration of post-ischaemic damage with barbiturates. *Stroke*, **11**, 565-568.
- Salford, L.G. & Siesjo, B.K. (1974). The influence of arterial hypoxia and unilateral carotid artery occlusion upon regional blood flow and metabolism in the rat brain. *Acta Physiol. Scand.*, **92**, 130-141.
- Sandercock, P.A.G., Molyneux, A.J. & Warlow, A.J. (1985). Value of computed tomography in patients with stroke : Oxfordshire Community Stroke Project. *Br. Med. J.*, **290**, 193-197.
- Sanguinetti, M.C. & Kass, R.S. (1984). Voltage-dependent block of calcium channel current in the calf cardiac Purkinje fibre by dihydropyridine calcium channel antagonists. *Circ. Res.*, **55**, 336-348.
- Sanguinetti, M.C., Krafte, D.S. & Kass, R.S. (1986). Bay K 8644: Voltage-dependent modulation of  $\text{Ca}^{2+}$  channel current in heart cells. *J. Gen. Physiol.*, **88**, 369-392.
- Sanna, E., Head, G.A. & Hanbauer, I. (1986). Evidence for a selective localisation of voltage sensitive  $\text{Ca}^{2+}$  channels in nerve cell bodies of corpus striatum. *J. Neurochem.*, **47**, 1552-1557.
- Sarmiento, J.G., Shrikhande, A.V., Janis, R.A. & Triggle, D.J. (1987). [ $^3\text{H}$ ] Bay K 8644, a 1,4-dihydropyridine  $\text{Ca}^{2+}$  channel activator: characteristics of binding to high and low affinity sites in cardiac membranes. *J. Pharmacol. Exp. Ther.*, **241**, 140-146.
- Schmid, A., Romey, G., Barhanin, J., Lazdunski, M. (1989). SR33557, an indolizinsulfone blocker of  $\text{Ca}^{2+}$  channels: identification of receptor sites and analysis of its mode of action. *Mol Pharmacol.*, **35**, 766-773.

Schmidt-Kastner, R. & Freund, T.F. (1991). Selective vulnerability of the hippocampus in brain ischemia. *Neuroscience*, **40**, 599-636.

Schoemaker, H., Morelli, M., Desh, M.P. & Yamamura, H.I. (1982). [ $^3\text{H}$ ] RO 5-4864 benzodiazepine binding in the kainate lesioned striatum and Huntington's diseased basal ganglia. *Brain Res.*, **248**, 396-401.

Schoemaker, H. & Langer, S.Z. (1989). Effects of  $\text{Ca}^{2+}$  on [ $^3\text{H}$ ] diltiazem and its allosteric interaction with dihydropyridine calcium channel binding sites in the rat cortex. *J. Pharmacol. Exp. Ther.*, **248**, 710-715.

Schramm, M., Thomas, G., Towart, R. & Franckowiak, G. (1983). Novel dihydropyridines with positive inotropic action through activation of  $\text{Ca}^{2+}$  channels. *Nature*, **303**, 535-537.

Schurr, A. & Rigor, B.M. (1989). Oxygen, glucose, lactate and synaptic function of cerebral tissue in vitro. In: *The Pharmacology of Cerebral Ischaemia*. (ed) Kriegelstein, J. CRC press.

Schwartz, J.R. & Grigat, G. (1989). Phenytoin and carbamazepine: potential and frequency-dependent block of  $\text{Na}^{+}$  currents in mammalian myelinated nerve fibres. *Epilepsia*, **30**, 286-294.

Scott, R.H. & Dolphin, A.C. (1987). Activation of a G protein promotes agonist responses to calcium channel ligands. *Nature*, **330**, 760-762.

Scotti, A.L. & Nitsch, C. (1991). The perforant path in the seizure-sensitive gerbil contains the  $\text{Ca}^{2+}$ -binding protein parvalbumin. *Exp. Brain Res.*, **85**, 137-143

Seagar, M.J., Takahashi, M. & Catterall, W.A. (1988). Molecular properties of dihydropyridine-sensitive calcium channels. *Ann. NY. Acad. Sci.*, **522**, 162-175.

Sharif, N.A. & Hughes, J. (1989). Neuroanatomical mapping and quantification of peptide and drug receptors by quantitative digital subtraction autoradiography. In: *Brain Imaging: Techniques and Applications*. (eds) Sharif, A. & Lewis, M.E. Ellis Horwood Ltd. Chichester.

Sheldon, R.S., Cannon, N.J. & Duff, H.J. (1986). Binding of [ $^3\text{H}$ ] batrachotoxinin A benzoate to specific sites on rat cardiac sodium channels. *Mol. Pharmacol.*, **30**, 617-623.

Sheridan, R.D., Patmore, L. & Spedding, M. (1991). The novel neuroprotective agents RS 87476 potently inhibits sodium currents in mouse neuroblastoma. *Br. J. Pharmacol.*, **104**, 25P.

Shigeno, T., Teasdale, G.M., McCulloch, J. & Graham, D.I. (1985). Recirculation model following MCA occlusion in rats. *J. Neurosurg.*, **63**, 272-277.

Shinton, R. & Beevers, G. (1989). Smoking and stroke : an overview. *Br. Med. J.*, **298**, 789-793.

Sick, T.J., Solow, E.L. & Roberts, E.L. (1987). Extracellular potassium ion activity and electrophysiology in the hippocampal slice: paradoxical recovery of synaptic transmission during anoxia. *Brain Res.*, **418**, 227-234.

Siesjo, B.K. (1981) Cell damage in the brain: a speculative synthesis. *J. Cerebral Blood Flow Metab.*, **1**, 155-185.

Siesjo, B.K. (1988). Historical overview: calcium, ischaemia, and death of brain cells. *Ann. NY. Acad. Sci.*, **522**, 638-661.

Siesjo, B.K. & Bengtsson, F. (1989a). Calcium fluxes, calcium antagonists, and calcium-related pathology in brain ischemia, hypoglycemia, and spreading depression: A unifying hypothesis. *J. Cerebral Blood Flow Metab.*, **9**, 127-140.

Siesjo, B.K. & Bengtsson, F. (1989b). Calcium, calcium antagonists and ischaemic cell death in the brain. In: *The Pharmacology of Cerebral Ischaemia*. (ed) Kriegelstein, J. CEC press.

Sila, C.A. & Furlan, A.J. (1988). Drug treatment of stroke. *Drugs*, **35**, 468-476.

Simon, R.P., Griffiths, T., Evans, M.C., Swan, J.H. & Meldrum, B.S. (1984). Calcium overload in selectively vulnerable neurons of the hippocampus during and after ischaemia: an electron microscopy study in the rat. *J. Cerebral Blood Flow Metab.*, **4**, 350-36.

Simon, R.P. (1989). Efficacy of competitive versus non-competitive NMDA antagonists in the treatment of focal brain ischaemia. In: *Cerebrovascular Diseases*. (ed) Ginsberg, M.D. & Dietrich, W.D. Raven Press. New York.

Skattebol, A., Hruska, R.E., Hawthoorn, M. & Triggle, D.J. (1988). Kainic acid lesions decrease striatal dopamine receptors and 1,4-dihydropyridine sites. *Neurosci. Lett.*, **89**, 85-89.

Sloviter, R.S., Sollas, A.L., Barbaro, N.M. & Laxer, K.D. (1991). Calcium-binding protein (calbindin-28K) and parvalbumin immunocytochemistry in the normal and epileptic human hippocampus. *J. Comp. Neurol.*, **381**, 381-396.

Smith J.L., Von Hanwehr, R. & Siesjo, B.K. (1986). Changes in extra and intracellular pH in the brain during and following ischaemia in hyperglycaemic and moderately hypoglycaemic rats. *J. Cerebral Blood Flow Metab.*, **6**, 524-583.

Smith, M-L., Kagstrom, E., Rosen, I. & Siesjo, B.K. (1983). Effect of the calcium antagonist nimodipine on the delayed hypoperfusion following incomplete ischemia in the rat. *J. Cerebral Blood Flow Metab.*, **3**, 543-546.

Smith, P.K., Krohn, R.I., Hermanson, G.T., Mallia, A.K., Gartner, F.H., Provenzano, M.D., Fujimoto, E.K., Goeke, N.M., Olson, B.J. & Klenk, D.C. (1985). Measurement of protein using bicinchoninic acid. *Anal. Biochem.*, **150**, 76-85.

Snutch, T.P., Leonard, J.P., Gilbert, M.M., Lester, H.A. & Davidson, N. (1990). Rat brain expresses a heterogeneous family of calcium channels. *Proc. Natl. Acad. Sci.*, **87**, 3391-3395.

Snyder, S.H., Pasternak, G.W. & Pert, C.B. (1975). Opiate receptor mechanisms. In : *Handbook of Psychopharmacology, Vol 5* (ed) Iversen, L., Iversen, S. & Snyder, S.H. pp 329-360. Plenum Press, New York.

Sol-Rolland, J., Joseph, M. & Rinaldi-Carmona, M. (1991). Interaction of SR 33557 with skeletal muscle calcium channel blocker receptors in the baboon: characterization of its binding sites. *J. Pharmacol. Exp. Ther.*, **257**, 595-601.

Somjen, G.G., Aitken, P.G., Balestrino, M., Herreras, O. & Kawasaki, K. (1990). Spreading depression-like depolarisation and selective vulnerability of neurones. *Stroke*, **21**, III 179-183.

Spat, A., Bradford, P.G., MacKinney, J.S., Rubin, R.P. & Putney, J.W. (1986). A saturable receptor for  $^{32}\text{P}$  inositol-1,4,5-triphosphate in hepatocytes and neutrophils. *Nature*, **319**, 514-516.

Spedding, M. (1982). Assessment of " $\text{Ca}^{++}$ -antagonist" effects of drugs in  $\text{K}^{+}$ -depolarised smooth muscle. Differentiation of antagonist sub-groups. *Naunyn-Schmiedberg's Arch. Pharmacol.*, **318**, 234-240.

Spedding, M. (1983). Direct inhibitory effects of some "calcium antagonists" and trifluoperazine on the contractile proteins in smooth muscle. *Br. J. Pharmacol.*, **79**, 225-231.

Spedding, M. (1984). Changing surface charge with salicylate differentiates between subgroups of calcium-antagonists. *Br. J. Pharmacol.*, **83**, 211-220.

Spedding, M. & Berg, C. (1984). Interactions between a "calcium agonist" Bay K 8644 and calcium antagonists differentiate calcium antagonist subgroups. *Naunyn Schmiedeberg's Arch. Pharmacol.*, **328**, 69-75.

Spedding, M. (1985a). Activators and inactivators of  $\text{Ca}^{++}$  channels: new perspectives. *J. Pharmacol., (Paris)* **16**, 319-343.

Spedding, M. (1985b). Calcium antagonist subgroups. *Trends Pharmacol. Sci.*, **6**, 109-114.

Spedding, M. & Mir, A.K. (1987). Direct activation of  $\text{Ca}^{2+}$  channels by palmitoyl carnitine, a putative endogenous ligand. *Br. J. Pharmacol.*, **92**, 457-468.

Spedding, M., Kilpatrick, A.T. & Alps, B.J. (1989). Activators and inactivators of calcium channels: effects in the central nervous system. *Fundam. Clin. Pharmacol.*, **3**, 3s-29s

Spedding, M. & Patmore, M. (1990). Acyl carnitines and myocardial ischaemia. *J. Mol. Cell. Cardiol.*, **22**, S151-152.

Spedding, M. & Kenny, B.A. (1991). Voltage-dependent calcium channels: Structure and drug binding sites. *Biochem Soc. Trans.*, in press.

Steen, P.A., Newberg, L.A., Milde, J.H. & Michenfelder, J.D. (1983). Nimodipine improves cerebral blood flow and neurological recovery after complete cerebral ischaemia in the dog. *J. Cerebral Blood Flow Metab.*, **4**, 82-87.

Steen, P.A., Gisvold, S.E., Milde, J.H., Newberg, L.A., Scheathauer, B.V., Lanier, W.L. & Michenfelder, J.D. (1985). Nimodipine improves outcome when given after complete ischaemia in primates. *Anaesthesiology*, **62**, 406-414.

Striessnig, J., Glossmann, H. & Catterall, W.A. (1990). Identification of a phenylalkylamine binding region within the  $\alpha_1$  subunit of skeletal muscle  $\text{Ca}^{2+}$  channels. *Proc. Natl. Acad. Sci.*, **87**, 9108-9112.

Stringer, J.L. & Lothman, E.W. (1987). Phenytoin does not block hippocampal long-term potentiation or frequency potentiation. *Ann. Neurol.*, **23**, 281-286.

Stys, P.K., Waxman, S.G. & Ransom B.R. (1991).  $\text{Na}^{+}$ - $\text{Ca}^{2+}$  exchanger mediates  $\text{Ca}^{2+}$  influx during anoxia in mammalian central nervous system white matter. *Ann. Neurol.*, **30**, 375-380.

Supavilai, P. & Karobath, M. (1984). The interaction of [ $^3\text{H}$ ] PY 108-068 and of [ $^3\text{H}$ ] PN 200-110 with calcium channel binding sites in rat brain. *J. Neural. Transmission*, **60**, 149-167.

Suzuki, J., Abiko, H., Mizoi, K., Oba, M. & Yoshimoto, T. (1987). Protective effect of phenytoin and its enhanced action by combined administration with mannitol and vitamin E in cerebral ischaemia. *Acta. Neurochir.*, **88**, 56-64.

Suzuki, N. & Yoshioka, T. (1987). Differential blocking action of synthetic  $\omega$ -conotoxin on components of  $\text{Ca}^{2+}$  channel current in clonal GH3 cells. *Neurosci. Lett.*, **75**, 235-239.

Suzuki, R., Yamaguchi, T., Choh-Luh, L. & Klatzo, I. (1983). The effects of 5-minute ischaemia in mongolian gerbils II. Changes of spontaneous neuronal activity in cerebral cortex and CA1 sector of hippocampus, *Acta. Neuropathol. (Berl)*, **60**, 217-222.

Swan, J.H., Evans, M.C. & Meldrum, B.S. (1988). Long term development of selective neuronal loss and the mechanism of protection by 2-amino-7-phosphonoheptanoate in a rat model of incomplete forebrain ischaemia. *J. Cerebral Blood Flow Metab.*, **8**, 64-78.

Swan, J.H. & Meldrum, B.S. (1989). Early, not late, administration of NMDA receptor antagonists protect against selective ischaemic cell loss. *J. Cerebral Blood Flow Metab.*, **9**, S558.

Syapin, P.J. & Skolnick, P. (1979). Characterisation of benzodiazepine binding sites in cultured cells of neuronal origin. *J. Neurochem.*, **32**, 1047-1051.

Taft, W.C., Clifton, G.L., Blair, R.E. & De Lorenzo, R.J. (1989). Phenytoin protects against ischaemia-produced neuronal cell death. *Brain Res.*, **484**, 143-148.

Takahashi, K., Wakamori, M. & Akaike, N. (1989). Hippocampal CA1 pyramidal cells of rats have four voltage-dependent calcium conductances. *Neurosci. Lett.*, **104**, 229-234.

Tamkun, M.M. & Catterall, W.A. (1981). Ion flux studies of voltage sensitive sodium channels in synaptic nerve-ending particles. *Mol. Pharmacol.*, **19**, 78-86.

Tamura, A., Graham, D.I., McCulloch, J. & Teasdale, G.M. (1981a). Focal cerebral ischaemia in the rat: 1. Description of technique and early neuropathological consequences following middle artery occlusion. *J. Cerebral Blood Flow Metab.*, **1**, 53-60.

Tamura, A., Graham, D.I., McCulloch, J. and Teasdale, G.M. (1981b). Focal ischaemia in the rat: 2. Regional cerebral blood flow determined by ( $^{14}\text{C}$ ) iodoantipyrine autoradiography following middle cerebral artery occlusion. *J. Cerebral Blood Flow Metab.*, **1**, 61-69.

Tanabe, T., Takeshima, H., Mikami, A., Flockerzi, V., Takahashi, H., Kangawa, K., Kojima M., Matsuo, H., Hirose, T. & Numa, S. (1987). Primary structure of the receptor for calcium channel blockers from skeletal muscle. *Nature*, **328**, 313-318.

Tanabe, T., Beam, K.G., Powell, J.A. & Numa, S. (1988). Restoration of excitation-contraction coupling and slow calcium current in dysgenic muscle by dihydropyridine receptor complementary DNA. *Nature*, **336**, 134-139.

Tanabe, T., Beam, K., Adams, B.A., Niidome, T. & Numa, S. (1990). Regions of the skeletal muscle dihydropyridine receptor critical for excitation-contraction coupling. *Nature*, **346**, 567-572.

Tang, C.M., Presser, F. & Morad, M. (1988). Amiloride selectively blocks the low threshold calcium channel. *Science*, **240**, 213-215.

Triggle, D.J. & Rampe, D. (1989). 1,4-dihydropyridine activators: structural and functional distinctions. *Trends Pharmacol. Sci.*, **10**, 507-511.

Tsien, R.W., Lipscombe, D., Madison, D.V., Bley, K.R. & Fox, A.P. (1988). Multiple types of neuronal calcium channels and their selective modulation. *Trends Neurosci.*, **11**, 431-437.

Tsien, R.W., Ellinor, P.T. & Horne, W.A. (1991). Molecular diversity of voltage-dependent calcium channels. *Trends Pharmacol. Sci.*, **12**, 349-354.

Twombly, D.A., Yoshii, M. & Narahashi, Y. (1988). Mechanisms of calcium channel block by phenytoin. *J. Pharmacol. Exp. Ther.*, **246**, 189-195.

Tyson, G.W., Teasdale, G.M., Graham, D.I. & McCulloch, J. (1984). Focal cerebral ischaemia in the rat: topography of hemodynamic and histopathological changes. *Ann. Neurol.*, **15**, 559-567.

Tytgat, J., Vereecke, J. & Carmeliet, E. (1988). Differential effects of verapamil and flunarizine on cardiac L-type and T-type Ca channels. *Naunyn-Schmiedeberg's Arch. Pharmacol.*, **337**, 690-692.

Valdivia, H. & Coronado, R. (1988). Pharmacological profile of skeletal muscle channels in plasma lipid bilayers. *Biophys. J.*, **53**, 555a.

Vanhoutte, P.M. & Paoletti, R. (1987). The WHO classification of calcium antagonists. *Trends Pharmacol. Sci.*, **8**, 4-5.

Van Amsterdam, F.T., Van Amsterdam-Magnoni, M.S., Hass, H., Punt, N.C. & Zaagsma, J. (1990). Protection by verapamil and nifedipine against ischaemic-induced loss of [<sup>3</sup>H]-(+)-PN 200-110 binding sites in the rat heart. *Naunyn-Schmiedeberg's Arch. Pharmacol.*, **341**, 137-142.

Varadi, G., Lory, P., Schultz, D., Varadi, M. & Schwartz, A. (1991). Acceleration of activation and inactivation by the  $\beta$  subunit of the skeletal muscle calcium channel. *Nature*, **352**, 159-161.

Van Reempts, J., van Deuren, B., van de Ven, M., Cornelissen, F. & Borgers, M. (1987). Flunarizine reduces cerebral infarct size after photochemically induced thrombosis in spontaneously hypertensive rats. *Stroke*, **18**, 1113-1119.

Velly, J., Grima, M., Martinak, G., Spach, M.O. & Schwartz, J. (1987). Effects of some anti-anginal and vasodilating drugs on sodium influx and on binding of [<sup>3</sup>H] batrachotoxinin-A-20- $\alpha$ -benzoate and [<sup>3</sup>H] tetracaine. *Naunyn-Schmiedeberg's Arch. Pharmacol.*, **335**, 176-182.

Vibulskresth, S., Dietrich, W.D., Busto, R. & Ginsberg, M.D. (1987). Failure of nimodipine to prevent ischemic neuronal damage in rats. *Stroke*, **18**, 210-215.

Wagner, J.A., Gugginp, S.E., Reynolds, J.F., Snowman, A.M., Biswas, A., Olivera, B.M. & Snyder, S.H. (1988). Calcium antagonist receptors. *Ann. NY. Acad. Sci.*,

522, 116-133.

Wallace, M.C., Teasdale, G.M. & McCulloch, J. (1989). Autoradiographic demonstration of increased MK 801 binding in ischaemic tissue in vivo. *J. Cerebral Blood Flow Metab.*, **9**, S745.

Watkins, J.C. (1989). The NMDA receptor concept: original development. In: *The NMDA receptor*. (ed) Watkins, J.C. & Collingridge, G.L. Oxford University Press.

Watson, B.D., Dietrich, W.D., Busto, R., Wachtel, M.S. & Ginsberg, M.D. (1985). Induction of reproducible brain infarction by photochemically initiated thrombosis. *Ann. Neurol.*, **17**, 497-504.

Wauquier, A., Ashton, D., Clincke, G., Fransen, J., Gillardin, J.M. & Janssen, P.A.J. (1986). Anticonvulsant profile of flunarizine. *Drug Dev. Res.*, **7**, 49-60.

Wauquier, A., Ashton, D. & Clincke, H.C. (1988). Brain ischaemia as a target for Ca<sup>2+</sup> entry blockers. *Ann. NY. Acad. Sci.*, **522**, 478-490.

Weiland, G.A. & Molinoff, P.B. (1981). Quantitative analysis of drug-receptor interactions. 1. Determination of kinetic and equilibrium properties. *Life Sci.*, **29**, 313-330.

Weinfeld, F.D. (1981). The national survey of stroke. *Stroke*, **12**, 1S.

Weiss, J.H., Hartley, D.M., Koh, J. & Choi, D.W. (1990). The slow channel blocker nifedipine attenuates slow excitatory amino acid neurotoxicity. *Science*, **247**, 1474-1477.

Weissmann, G. (1991). Aspirin. *Scientific American*, **264**, 58-64.

Welch, K.M.A., Wang, T.P. & Chabi, E. (1978). Ischaemia-induced seizures and cortical monoamine levels. *Ann. Neurol.*, **3**, 152-155.

Welch, K.M.A. (1982). Impairment of cerebral serotonin and energy metabolism during ischaemia-relevance to migraine. *Adv. Neurol.*, **33**, 35-40.

Welsh, F.A., Ginsberg, M.D., Rieder, W. & Budd, W.W. (1980). Deleterious effect of glucose pretreatment on recovery from diffuse cerebral ischaemia in the cat. II. Regional metabolite levels. *Stroke*, **11**, 355-363.

Welsh, F.A., Sakamoto, T., McKee, A.E. & Sims, R.E. (1987). Effect of lactacidosis on pyridine nucleotide stability during ischemia in mouse brain. *J. Neurochem.*, **49**, 846-851.

Welsh, F.A., Sims, R.E. & Harris, V.A. (1990). Mild hypothermia prevents injury in gerbil hippocampus. *J. Cerebral Blood Flow Metab.*, **10**, 557-563.

Westenbroek, R.E., Ahljianian, M.K. & Catterall, W.A. (1990). Clustering of L-type Ca<sup>2+</sup> channels at the base of major dendrites in hippocampal pyramidal neurones. *Nature*, **347**, 281-284.

White, B.C., Wiegenstein, J.G. & Winegar, C.D. (1984). Brain ischaemic anoxia. *J. Am. Med. Assoc.*, **251**, 1586-1590.

Wiebers, D.O., Adams, H.P. & Whisnant, J.P. (1990). Animal models of stroke: Are they relevant to human diseases? *Stroke*, **21**, 1-3.

Wieloch, T. (1985). Neurochemical correlates to regional selective neuronal vulnerability. *Prog Brain Res.*, **63**, 69-85

Wieloch, T., Gustafsson, I. & Westerberg, E. (1988). MK 801 does not prevent against brain damage in a rat model of cerebral ischaemia. *Neurochem. Int.*, **12**, 24.

Williams, L.T., Mullikin, D. & Lefkowitz, R.J. (1976). Identification of  $\alpha$ -adrenergic receptors in uterine smooth muscle membranes by [ $^3$ H] dihydroergotamine binding. *J. Biol. Chem.*, **251**, 6915-6923.

Willow, M. & Catterall, W.A. (1982). Inhibition of binding of [ $^3$ H] batracotoxinin A 20- $\alpha$ -benzoate to sodium channels by the anticonvulsant drugs diphenylhydantoin and carbamazepine. *Mol. Pharmacol.*, **22**, 627-635.

Willow, M., Kuenzel, E.A. & Catterall, W.A. (1984). Inhibition of voltage-sensitive sodium channels in neuroblastoma cells and synaptosomes by the anticonvulsant drugs diphenylhydantoin and carbamazepine. *Mol. Pharmacol.*, **25**, 228-235.

Willow, M., Gono, T. & Catterall, W.A. (1985). Voltage clamp analysis of the inhibitory actions of diphenylhydantoin and carbamazepine on voltage sensitive sodium channels in neuroblastoma cells. *Mol. Pharmacol.*, **27**, 549-558.

Wong R.K.S. & Prince, D.A. (1978). Participation of calcium spikes during intrinsic burst firing in hippocampal neurons. *Brain Res.*, **159**, 385-390.

Wong, E.H., Kemp, J.A., Priestly, T., Knight, A.R., Woodruff, G.N. & Iversen, L. (1986). The anticonvulsant MK 801 is a potent N-methyl-D-aspartate antagonist. *Proc. Natl. Acad. Sci.*, **83**, 7104-7108.

Wong, E.F. & Kemp, J.A. (1991). Sites for antagonism on the N-methyl-D-aspartate receptor channel complex. *Ann. Rev. Pharmacol. Toxicol.*, **31**, 401-425.

Yamaguchi, T., Wagner, H.G. & Klatzo, I. (1986). Post-ischaemic pathophysiology in the gerbil-changes in extracellular  $K^+$  and  $Ca^{2+}$ . In: *Mechanisms of Secondary Brain Damage* (ed) Baethmann, A. pp 249-258. GoKG Unterberg A. Plenum Publ. Corp.

Yamamura, H.I. & Snyder, S.H. (1974). Muscarinic cholinergic binding in rat brain. *Proc. Natl. Acad. Sci.*, **71**, 1725-1729.

Yamamura, H.I., Schoemaker, H., Boles, R.G. & Roeske, W.R. (1982). Diltiazem enhancement of [ $^3$ H] nitrendipine binding to calcium channel associated drug binding sites in rat brain synaptosomes. *Biochem. Biophys. Res. Comm.*, **108**, 640-646.

Yamasaki, Y., Kogure, K., Hara, H., Ban.H. & Akaike, N. (1991). The possible involvement of tetrodotoxin-sensitive ion channels in ischemic damage in the rat hippocampus. *Neurosci. Lett.*, **121**, 251-254.

Yamori, Y., Horie, R., Handa, H., Sato, M. & Fukase, M. (1976). Pathogenetic similarity of strokes in stroke-prone spontaneously hypertensive rats and humans. *Stroke*, **7**, 46-53.

Zavala, F., Haumont, J. & Lenfant, M. (1984). Interaction of benzodiazepine with mouse macrophages. *Eur. J. Pharmacol.*, **106**, 561-566.

Zavala, F. & Lenfant, M. (1987). Benzodiazepine and PK 11195 exert immunomodulating activities by binding on a specific receptor on macrophages. *Ann. NY. Acad. Sci.*, **496**, 240-249.